

**AN IMPROVED BUS SIGNAL PRIORITY SYSTEM FOR  
NETWORKS WITH NEARSIDE BUS STOPS**

A Dissertation

by

WONHO KIM

Submitted to the Office of Graduate Studies of  
Texas A&M University  
in partial fulfillment of the requirements for the degree of

DOCTOR OF PHILOSOPHY

December 2004

Major Subject: Civil Engineering

**AN IMPROVED BUS SIGNAL PRIORITY SYSTEM FOR  
NETWORKS WITH NEARSIDE BUS STOPS**

A Dissertation

by

WONHO KIM

Submitted to the Office of Graduate Studies of  
Texas A&M University  
in partial fulfillment of the requirements for the degree of

DOCTOR OF PHILOSOPHY

Approved as to style and content by:

---

Laurence R. Rilett  
(Co-Chair of Committee)

---

Amy Epps Martin  
(Co-Chair of Committee)

---

Donald Woods  
(Member)

---

Thomas Urbanik II  
(Member)

---

Jyh-Charn Liu  
(Member)

---

Kevin Balke  
(Member)

---

Paul Roschke  
(Interim Head of Department)

December 2004

Major Subject: Civil Engineering

## **ABSTRACT**

An Improved Bus Signal Priority System for Networks with Nearside Bus Stops.

(December 2004)

Wonho Kim, B.S., Chungbuk National University;

M.C.P., Seoul National University

Co-Chairs of Advisory Committee: Dr. Laurence R. Rilett

Dr. Amy Epps Martin

Bus Signal Priority (BSP), which has been deployed in many cities around the world, is a traffic signal enhancement strategy that facilitates efficient movement of buses through signalized intersections. Most BSP systems do not work well in transit networks with nearside bus stop because of the uncertainty in dwell time. Unfortunately, most bus stops on arterial roadways are of this type in the U.S.

This dissertation showed that dwell time at nearside bus stops could be modeled using weighted least squares regression. More importantly, the prediction intervals associated with the estimate dwell time were calculated. These prediction intervals were subsequently used in the improved BSP algorithm that attempted to reduce the negative effects of nearside bus stops on BSP operations.

The improved BSP algorithm was tested on urban arterial section of Bellaire Boulevard in Houston, Texas. VISSIM, a micro simulation model was used to evaluate the performance of the BSP operations. Prior to evaluating the algorithm, the parameters of the micro simulation model were calibrated using an automated Genetic Algorithm based methodology in order to make the model accurately represent the traffic conditions observed in the field.

It was shown that the improved BSP algorithm significantly improved the bus operations in terms of bus delay. In addition, it was found that the delay to other

vehicles on the network was not statistically different from other BSP algorithms currently being deployed. It is hypothesized that the new approach would be particularly useful in North America where there are many transit systems that utilize nearside bus stops in their networks.

## ACKNOWLEDGEMENTS

This dissertation is much richer because of many people who have contributed to my life and my research over these many years in College Station. First of all, I would like to express my deepest gratitude to Dr. Laurence R. Rilett, who has served not only as my advisor and co-chair, but also as my mentor in the preparation of this dissertation. A very special thanks goes to Dr. Amy Epps Martin who agreed in July of 2004 to sit on my committee and serve as my co-chair in order to meet the Office of Graduate Studies regulations. I appreciate her inspiration and thoughtful guidance. I would also like to express my appreciation to the other advisory committee members for their insight and fresh ideas which contributed significantly to this dissertation: Dr. Donald Wood, Dr. Thomas Urbanik II, and Dr. Jyh-Charn Liu. The special thanks is also given to Dr. Kevin N. Balke for his invaluable support from the Texas Transportation Institute during my doctoral study. Finally, I am most grateful to my family for their patience and encouragement throughout my study.

## TABLE OF CONTENTS

	Page
ABSTRACT.....	iii
ACKNOWLEDGEMENTS.....	v
TABLE OF CONTENTS.....	vi
LIST OF FIGURES.....	ix
LIST OF TABLES.....	xiv
<b>CHAPTER</b>	
<b>I INTRODUCTION.....</b>	<b>1</b>
1.1 Problem Statement.....	2
1.2 Research Objectives.....	4
1.3 Scope of Study.....	4
1.4 Structure of Dissertation.....	5
<b>II LITERATURE REVIEW.....</b>	<b>6</b>
2.1 Bus Signal Priority Systems.....	6
2.1.1 Passive BSP Strategies.....	7
2.1.2 Active BSP Strategies.....	8
2.1.3 BSP Strategies in Adaptive Signal Control Systems.....	11
2.1.4 BSP Strategies with Nearside Stops or Dwell Time.....	14
2.1.5 Effectiveness of Bus Signal Priority.....	15
2.2 Estimation of Bus Dwell Time.....	17
2.2.1 Characteristics of Dwell Time.....	17
2.2.2 Regression Models for Dwell Time Estimation.....	19
2.3.3 Probabilistic Models for Dwell Time.....	22
2.3 Summary.....	25
<b>III DATA COLLECTION AND STUDY DESIGN.....</b>	<b>27</b>
3.1 Study Site Selection and Description.....	27
3.2 Data Collection.....	30
3.2.1 Bus Dwell Time Data.....	30
3.2.2 Geometric and Traffic Data of the Intersections.....	34
3.3 Study Design.....	38
3.3.1 Prediction Algorithm for Bus Dwell Time.....	38
3.3.2 Bus Signal Priority Strategy.....	39
3.3.3 Microscopic Simulation Model.....	41
3.4 Experimental Design for Evaluation of BSP Strategies.....	42

CHAPTER	Page
3.4.1 Emulating Realistic Dwell Time Variation in the Simulation .....	42
3.4.2 Evaluation of the Improved BSP Strategy .....	45
3.5 Concluding Remarks .....	47
IV DWELL TIME ESTIMATION AND PREDICTION INTERVAL .....	49
4.1 Probabilistic Model for Estimating Dwell Time .....	49
4.1.1 Determinants of the Probabilistic Model .....	50
4.1.2 Probability Distribution for the Number of Boarding Passengers .....	51
4.1.3 Probability Distribution for the Number of Alighting Passengers .....	57
4.1.4 Marginal Alighting and Boarding Times .....	58
4.1.5 Estimation of Bus Dwell Time Using a Probabilistic Model .....	59
4.2 Determinants for Dwell Time .....	63
4.2.1 Analysis of Relations between Determinants and Dwell Time .....	63
4.2.2 Simple Linear Regression Model .....	67
4.2.3 Tests for Constancy of Error Variance .....	69
4.3 Weighted Least Squares Regression .....	71
4.3.1 Weighted Least Squares Procedure .....	72
4.3.2 Prediction Interval of Dwell Time .....	76
4.4 Concluding Remarks .....	78
V DEVELOPMENT OF IMPROVED BSP ALGORITHM CONSIDERING DWELL TIME VARIABILITY .....	80
5.1 Overview of the Improved BSP Algorithm .....	81
5.1.1 Assumptions and Constraints .....	82
5.2 Development of BSP Strategies .....	85
5.2.1 Fundamentals of Traffic Signal Operations .....	85
5.2.2 Development of BSP Strategies .....	88
5.3 Implementation of Improved BSP Strategies in VISSIM Operation Algorithm .....	101
5.3.1 Control Module .....	102
5.3.2 Priority Module .....	106
5.3.3 Restoring Module .....	110
5.4 Concluding Remarks .....	114
VI CALIBRATION OF THE MICROSCOPIC SIMULATION MODEL .....	115
6.1 Statistically Based Objective Function .....	116
6.2 Automated Calibration Procedure .....	119

CHAPTER	Page
6.2.1 Genetic Algorithm Process .....	119
6.2.2 Statistical Test Procedures .....	120
6.2.3 Calibration Procedure .....	123
6.3 Implementation of the Proposed Procedure .....	126
6.3.1 VISSIM Background.....	126
6.3.2 VISSIM Calibration Parameters .....	127
6.3.3 Analysis of Results.....	130
6.4 Concluding Remarks.....	133
VII EVALUATION AND SENSITIVITY ANALYSIS .....	134
7.1 Experimental Design.....	134
7.1.1 Simulation Design.....	134
7.1.2 Statistical Testing .....	140
7.2 Evaluation of the Improved BSP Algorithm.....	142
7.2.1 Impacts on Bus Operations .....	142
7.2.2 Impacts on Non-transit Vehicles.....	149
7.2.3 Summary of Findings.....	156
7.3 Sensitivity Analysis.....	157
7.3.1 Sensitivity Analysis of Prediction Interval .....	158
7.3.2 Sensitivity Analysis of Bus Headway.....	165
7.3.3 Sensitivity Analysis of Demand.....	172
7.3.4 Summary of Findings.....	178
7.4 Concluding Remarks.....	179
VIII CONCLUSIONS .....	180
8.1 Summary .....	180
8.1.1 Bus Dwell Time Prediction.....	180
8.1.2 The Improved Bus Signal Priority Algorithm.....	181
8.2 Conclusions.....	181
8.3 Future Research.....	182
GLOSSARY.....	184
NOTATION.....	190
REFERENCES.....	194
APPENDIX A .....	201
APPENDIX B .....	205
APPENDIX C .....	209
APPENDIX D.....	213
VITA .....	221



## LIST OF FIGURES

		Page
Figure 2-1	Bus delay without signal priority .....	7
Figure 2-2	Phase change for green extension strategy.....	9
Figure 2-3	Phase change for early green strategy .....	10
Figure 2-4	An example of phase insertion strategy .....	11
Figure 2-5	Dwell time components.....	17
Figure 3-1	Site map for Houston and test bed .....	29
Figure 3-2	Schematic route map and location of stops.....	30
Figure 3-3	Lateness to scheduled arrival during AM peak and off peak periods.....	32
Figure 3-4	Dwell time distribution for all stops.....	33
Figure 3-5	Geometry and traffic counts for Bintiff at Bellaire and Rookin at Bellaire .....	35
Figure 3-6	Signal phase plan for Bintiff at Bellaire and Rookin at Bellaire.....	35
Figure 3-7	Site detail for the intersection of Hilcroft and Bellaire .....	36
Figure 3-8	Signal phase plan for the intersection of Hilcroft and Bellaire .....	37
Figure 3-9	Conceptualization of active bus signal priority.....	40
Figure 3-10	Observed dwell time and cumulative distribution for route #2 at stop C .....	43
Figure 3-11	An example of bus headway groups for route #2 at stop C .....	44
Figure 4-1	Observed and predicted passenger arrival during peak period at stop A .....	55

	Page
Figure 4-2	Observed and predicted passenger arrival during off peak period at stop A ..... 56
Figure 4-3	Predicted and observed dwell time at stop A ..... 61
Figure 4-4	Relationship between passenger alighting and passenger loads at stop A ..... 64
Figure 4-5	Relationship between passenger boarding and bus headway at stop A ..... 65
Figure 4-6	Estimated regression line at stop A ..... 68
Figure 4-7	Residual plot of the regression model for stop A ..... 69
Figure 4-8	Absolute residual plot and regression line for stop A ..... 74
Figure 4-9	Estimated weighted and unweighted lines for stop A ..... 75
Figure 4-10	Prediction intervals and projected lines for stop A ..... 77
Figure 4-11	Prediction intervals and projected lines for stop B ..... 77
Figure 4-12	Prediction intervals and projected lines for stop C ..... 78
Figure 5-1	Concept of the improved BSP algorithm ..... 81
Figure 5-2	Functional diagram of the improved BSP algorithm ..... 83
Figure 5-3	Illustration of intervals in a phase ..... 86
Figure 5-4	Phase sequence and force-off points under coordination mode ..... 87
Figure 5-5	Example of green extension strategy under eight-phase signal operation ..... 89
Figure 5-6	Illustration of green extension strategy ..... 92
Figure 5-7	Example of early green strategy under eight-phase signal operation ..... 93

	Page
Figure 5-8	Illustration of early green strategy with priority request during green time..... 96
Figure 5-9	Illustration of early green strategy with priority request during red time ..... 96
Figure 5-10	Example of phase insertion strategy under eight-phase signal operation..... 97
Figure 5-11	Illustration of phase insertion strategy ..... 99
Figure 5-12	Architecture of improved BSP operational algorithm ..... 102
Figure 5-13	Illustration of the changes in control mode and decision factors..... 104
Figure 5-14	Functional logic of control module ..... 105
Figure 5-15	Functional diagram for the priority module ..... 107
Figure 5-16	Logic flow for strategy selection ..... 109
Figure 5-17	Examples of restoring for different BSP strategies..... 113
Figure 6-1	Observed travel time distribution for arterial section with signalized intersections ..... 117
Figure 6-2	Conceptualization of disaggregated performance measure in calibration..... 118
Figure 6-3	Overview of calibration procedure..... 124
Figure 6-4	(a) Rejected set with 1% MAER and (b) accepted set with 1% MAER ..... 131
Figure 7-1	Detector settings and stop locations on simulation network..... 136
Figure 7-2	Average person delays at the intersection of Rookin and Bellaire ..... 155
Figure 7-3	Changes in average bus travel time, MOE2, with significance levels ..... 159

	Page
Figure 7-4	Changes in bus arrival rate during green phase, MOE3, with significance levels ..... 161
Figure 7-5	Changes in average control delay per vehicle at the intersections, MOE5, with significance levels..... 163
Figure 7-6	Changes in average control delay per bus, MOE1, at the intersections with headway levels..... 166
Figure 7-7	Changes in bus arrival rate during green phase, MOE3, with headway levels ..... 168
Figure 7-8	Changes in average control delay per vehicle at the intersections, MOE5, with headway levels ..... 171
Figure 7-9	Changes in bus arrival rate during green phase, MOE3, with demand levels..... 174
Figure 7-10	Changes in average control delay per vehicle for the intersection, MOE5, with demand levels ..... 176
Figure B-1	Periods in the cycle for selecting different priority strategies..... 207
Figure B-2	Determination of bounds for implementing each priority Strategy ..... 209
Figure D-1	Predicted and observed dwell time at stop B ..... 215
Figure D-2	Predicted and observed dwell time at stop C ..... 215
Figure D-3	Relationship between passenger alighting and passenger loads at stop B ..... 216
Figure D-4	Relationship between passenger alighting and passenger loads at stop C ..... 216
Figure D-5	Relationship between passenger boarding and bus headway at stop B ..... 217
Figure D-6	Relationship between passenger boarding and bus headway at stop C ..... 217

	Page
Figure D-7 Estimated regression line at stop B .....	218
Figure D-8 Estimated regression line at stop C .....	218
Figure D-9 Residual plot of the regression model for stop B .....	219
Figure D-10 Residual plot of the regression model for stop C .....	219
Figure D-11 Absolute residual plot and regression line for stop B .....	220
Figure D-12 Absolute residual plot and regression line for stop C .....	220
Figure D-13 Estimated weighted and unweighted lines for stop B .....	221
Figure D-14 Estimated weighted and unweighted lines for stop C .....	221

## LIST OF TABLES

		Page
Table 2-1	Typical bus passenger boarding and alighting service times for selected bus types and door configurations (41).....	22
Table 3-1	Scheduled bus headway .....	28
Table 3-2	Required data for probabilistic model and regression model.....	31
Table 3-3	Schedule adherence and lateness .....	32
Table 3-4	Summary of bus dwell time .....	33
Table 4-1	Summary of statistics for passenger arrivals during 5 minute period .....	52
Table 4-2	Passenger arrivals with Poisson and negative binomial distribution during peak period (7:00~8:30 AM).....	54
Table 4-3	Passenger arrivals with Poisson and negative binomial distribution during off-peak period (8:30~10:00 AM).....	55
Table 4-4	Chi-square goodness-of-fit test for Poisson and negative binomial distributions .....	57
Table 4-5	Probability of alighting for passengers on buses at each stop (Route #2) .....	61
Table 4-6	Average absolute error and average predicted dwell time for all stops .....	62
Table 4-7	Summary of multiple regression models.....	67
Table 4-8	Summary of simple regression models .....	68
Table 4-9	Summary of the modified Levene test .....	71
Table 4-10	Comparison of AAE from probabilistic models and WLS models .....	75

	Page
Table 6-1	VISSIM calibration parameters ..... 129
Table 6-2	Summary of accepted parameter sets ..... 130
Table 6-3	Summary of bus and car MAER from accepted parameter set ..... 133
Table 7-1	Summary of measure of effectiveness used in the assessment of BSP scenarios ..... 137
Table 7-2	Average control delay per bus on the main street approach, MOE1 (sec/bus) ..... 143
Table 7-3	Results of Duncan test between scenarios (average control delay per bus, MOE1, at the intersection of Rookin and Bellaire) ..... 145
Table 7-4	Results of Duncan test between scenarios (average control delay per bus, MOE1, at the intersection of Hilcroft and Bellaire) ..... 145
Table 7-5	Average bus travel time on the eastbound main street, MOE2 ..... 146
Table 7-6	Results of Duncan test between scenarios (bus travel time on eastbound main street, MOE2) ..... 147
Table 7-7	Bus arrival rate during green phase, MOE3 ..... 148
Table 7-8	Results of Duncan test between scenarios (bus arrival rate during green phase, MOE3, at the intersection of Rookin and Bellaire) ..... 149
Table 7-9	Results of Duncan test between scenarios (bus arrival rate during green phase, MOE3, at the intersection of Hilcroft and Bellaire) ..... 149
Table 7-10	Average control delay per vehicle on non-priority approaches, MOE4 (sec/veh) ..... 150
Table 7-11	Results of Duncan test between scenarios (average control delay per vehicle on non-priority approaches, MOE4, at the intersection of Rookin and Bellaire) ..... 151

	Page
Table 7-12	Results of Duncan test between scenarios (average control delay per vehicle on non-priority approaches, MOE4, at the intersection of Hilcroft and Bellaire) ..... 151
Table 7-13	Average control delay per vehicle at the intersections, MOE5..... 153
Table 7-14	Results of Duncan test between scenarios (average control delay per vehicle, MOE5, at the intersection of Rookin and Bellaire)..... 154
Table 7-15	Results of Duncan test between scenarios (average control delay per vehicle, MOE5, at the intersection of Hilcroft and Bellaire)..... 154
Table 7-16	Comparison of average person delay at the intersections ..... 155
Table 7-17	A summary of statistical test results for all MOEs used ..... 157
Table 7-18	Width of the prediction interval for each significance level (second)..... 158
Table 7-19	Average bus travel time on the eastbound main street, MOE2..... 159
Table 7-20	Results of Duncan test between average bus travel times, MOE2, under various significance levels ..... 160
Table 7-21	Bus arrival rate during green phase, MOE3, under various significance levels ..... 161
Table 7-22	Results of Duncan test between bus arrival rate during green phase, MOE3, under various significance levels at the intersection of Rookin and Bellaire..... 162
Table 7-23	Results of Duncan test between bus arrival rate during green phase, MOE3, under various significant levels at the intersection of Hilcroft and Bellaire..... 162
Table 7-24	Average control delay per vehicle for the intersection, MOE5, under various levels of significance..... 163



	Page
Table 7-25	Results of Duncan test between average control delay per vehicle, MOE5, under various significance levels at the intersection of Rookin and Bellaire..... 164
Table 7-26	Results of Duncan test between average control delay per vehicle, MOE5, under various significance levels at the intersection of Hilcroft and Bellaire..... 164
Table 7-27	Average control delay per bus, MOE1, at the intersections with various headway levels ..... 166
Table 7-28	Results of Duncan test between average control delay per bus, MOE1, under various headway levels at the intersection of Rookin and Bellaire ..... 167
Table 7-29	Results of Duncan test between average control delay per bus, MOE1, under various headway levels at the intersection of Hilcroft and Bellaire..... 167
Table 7-30	Bus arrival rate during green phase, MOE3, under various headway levels ..... 168
Table 7-31	Results of Duncan test between bus arrival rate during green phase, MOE3, under various headway levels at the intersection of Rookin and Bellaire ..... 169
Table 7-32	Results of Duncan test between bus arrival rate during green phase, MOE3, under various headway levels at the intersection of Hilcroft and Bellaire ..... 169
Table 7-33	Average control delay per vehicle at the intersections, MOE5, under various headway levels ..... 170
Table 7-34	Results of Duncan test for percentage change in MOE5 under various headway levels at the intersection of Rookin and Bellaire..... 171
Table 7-35	Results of Duncan test for percentage change in MOE5 under various headway levels at the intersection of Hilcroft and Bellaire..... 172

	Page
Table 7-36	Average bus arrival rate during green phase for various demand levels..... 173
Table 7-37	Results of Duncan test between bus arrival rate during green phase, MOE3, under various demand levels at the intersection of Rookin and Bellaire ..... 174
Table 7-38	Results of Duncan test between bus arrival rate during green phase, MOE3, under various demand levels at the intersection of Hilcroft and Bellaire ..... 175
Table 7-39	Average control delay per vehicle at the intersections, MOE5, for various demand levels ..... 176
Table 7-40	Results of Duncan test for percentage changes in MOE5 under various demand levels at the intersection of Rookin and Bellaire ..... 177
Table 7-41	Results of Duncan test for percentage changes in MOE5 under various demand levels at the intersection of Hilcroft and Bellaire ..... 177
Table A-1	Signal control variables at the intersection of Bintiff and Bellaire ..... 203
Table A-2	Signal control variables at the intersection of Rookin and Bellaire ..... 204
Table A-3	Signal control variables at the intersection of Hilcroft and Bellaire ..... 205

## CHAPTER I

### INTRODUCTION

Both traffic congestion and commuting travel time in metropolitan areas have increased during the last decades, which has resulted in an increase in transit travel time, transit travel time variability, and transit operating cost. Transit agencies have been seeking technologies that can improve the service quality and reduce operating cost. The development of Intelligent Transportation Systems (ITS) has promoted transit-oriented technologies such as automatic fare collection, real-time traveler information, and transit signal priority. Intuitively, an improvement in transit performance provides an additional incentive for automobile based travelers to switch modes and reduce overall traffic congestion.

Bus Signal Priority (BSP), which has received considerable attention lately, is a traffic signal enhancement strategy that facilitates efficient movement of transit vehicles through signalized intersections. BSP provides preferential treatment to transit vehicles approaching an intersection by altering the normal traffic signal operations so that transit vehicle delay is reduced. BSP strategy improves transit operation and service quality, but its implementation is a sensitive issue because BSP strategies traditionally favor transit users over passenger-car drivers. Moreover most BSP systems that preempt the normal operations in the traffic controllers have a tendency to disrupt the signal coordination and this interrupts the progressive flow of vehicles along an arterial. Consequently it may unduly deteriorate overall traffic performance.

Another resistance to its implementation is that existing BSP systems do not work well with nearside bus stops. A majority of bus stops along arterials in U.S. cities are on the nearside of intersections. For example, approximately 80 percent of Metro's bus stops in Houston, Texas are nearside stops (1). The nearside stops have the potential to negate priority service at some intersections because of passenger boarding and

---

This dissertation follows the style and format of the *Transportation Research Record*.

alighting activities in advance of the traffic signal. For these reasons, BSP has not been widely deployed and still remains a challenging task. However, recent enhancements in the field of ITS including smart buses, communications, detection, optimization algorithms, and simulation modeling have created new capabilities to support BSP deployment in the traffic signal system. This dissertation presents a methodology for estimating the dwell time at nearside stops and the associated prediction interval. Subsequently a new BSP algorithm that can 1) provide adequate priority services without disrupting signal coordination, 2) work with nearside bus stops through the accommodation of the variability/randomness of dwell time, and 3) minimize a negative impact to the non-priority traffic at the intersection is developed.

## **1.1 PROBLEM STATEMENT**

The use of BSP at intersections with nearside stops has been the subject of much debate. The primary issue focuses on the variability in dwell times at nearside stops which could increase the uncertainty of the bus arrival during the priority phase. The uncertainty may cost buses the benefits of the priority treatment while adding additional delay to the non-priority movements. Therefore, the primary research question for BSP with nearside stops is when and how to activate the signal priority service. Most current BSP systems start to change the normal signal timing plan immediately after a priority request is placed. Prompt response to the request is based on the assumption that buses will arrive at the intersection after a pre-defined travel time from the point where the bus is first detected. Therefore any disturbance such as bus stop that alters the pre-defined travel time may deteriorate the efficiency of BSP operation. Without consideration of the dwell time and its variability in the bus travel time, there is a high likelihood that significant number of buses will fail to arrive at the intersection during the priority phase that is timed by an anticipated arrival of the bus. The primary objective of this research is to develop new BSP algorithm that can accommodate the bus dwell time as well as its associated variability.

The bus dwell time and its variability need to be predicted in order to be accounted for in the BSP algorithm. Most prior studies relating to estimating dwell time focused on the estimation of the service time for alighting and boarding passengers using ordinary least squares regression models. The regression models require the numbers of alighting/boarding passengers to be estimated in advance of the bus' arrival at the stop if they are employed in predicting dwell time. However, because of the absence of available technologies for detecting boarding and alighting passengers in advance, the application of these models has been limited to evaluations of route-specific performance which focuses on analyzing the bus travel time. Some progress has been made with respect to addressing the problems with the deterministic passenger demand. The probabilistic models which consider alighting/boarding passengers as random variables allow for a better representation of stochastic nature of dwell time. Once probability density functions for the number of alighting and boarding passengers are successfully defined, the dwell time can be predicted using the expectations of the probability distributions and other given quantities such as marginal service times for alighting and boarding activities. Due to the randomness of the numbers of alighting/boarding passengers and the variation of the service time for each passenger, some errors in prediction are inevitable even with well defined distributions and estimated quantities. Therefore, prediction interval is more informative than mean dwell time for the successful BSP implementation. One goal of this research is to develop a methodology for predicting the mean dwell time, and the associated prediction interval, that will be used in a new BSP methodology.

The variability in dwell time can be accommodated by integrating the prediction interval into the BSP algorithm. In order to incorporate the prediction interval of dwell time, a BSP system needs 1) to be able to re-evaluate a travel time including dwell time for each bus in real-time, and 2) to facilitate signal priority strategies that are capable of carrying out the prediction interval. The focus of the research described in this dissertation is on developing a better bus signal priority algorithm and a better bus dwell

time prediction methodology in order to improve bus operations at the intersections with nearside bus stop.

## **1.2 RESEARCH OBJECTIVES**

It is hypothesized that a BSP system that incorporates the variability of the dwell time in the signal timing will give superior results over BSP systems that do not consider the length of dwell time at nearside stops. The desirable features of a BSP system would be exploiting real-time information of buses in the priority granting process and incorporating a prediction model for bus dwell time within the local intersection level of a BSP system. The objectives of this research are 1) to develop a prediction algorithm for mean dwell time and its associated prediction interval, 2) to develop a BSP strategy that can accommodate the prediction interval of the dwell time, and 3) to conduct an experimental study to evaluate the methodology proposed.

## **1.3 SCOPE OF STUDY**

The study is intended to show that the predicted dwell time and the prediction interval can be used to intelligently adjust signal timings and phasing to provide priority treatment to buses without causing severe impacts on traffic. This study is not intended to be an exhaustive evaluation of the different methods for predicting bus dwell time, nor of the criteria for determining priority. The primary focus of this study is to illustrate that incorporating the prediction interval of dwell time could be used to make better control decision that improves bus operations. While many approaches could be used in implementing the improved BSP algorithm, only one approach was examined in this study.

In addition, the new BSP algorithm is designed to provide priority only using extension of green in the current phase, ending another phase early to give an early green to the bus, or insertion of an extra bus phase to allow the bus to pass before returning to the regular timing. Other strategies such as stretching window, skipping phase, and reordering phases are not considered. Testing of the algorithm is limited to traffic micro-

simulation model in a laboratory setting. Although the evaluation is performed on a test bed in Houston, Texas, no field testing is performed as part of this dissertation. Note that the traffic micro-simulation model is calibrated using empirical data. Testing is conducted on an arterial section with three signalized intersections under AM peak demand.

#### **1.4 STRUCTURE OF DISSERTATION**

This dissertation contains a total of eight chapters and three appendices. Chapter I summarizes the problems addressed by this study and establishes the objectives and scope of this dissertation. Chapter II provides a literature review of the state of the art of the main research. It includes an introduction to current methods and technologies for providing priority, and estimation models for bus dwell time. Chapter III provides descriptions for the study site and the data. It also contains the simulation methods for evaluation of the new BSP algorithm. A methodology for estimating dwell time and its associated prediction interval is developed in Chapter IV. Chapter V provides a detailed description of the development of a new BSP algorithm incorporated with the prediction interval of dwell time. Chapter VI presents a methodology for calibrating the microscopic traffic simulation model. The results of simulation study to assess the impacts of using the priority algorithm on traffic and bus operations are summarized in Chapter VII. The major conclusions and recommendations for future research are provided in Chapter VIII.

## CHAPTER II

### LITERATURE REVIEW

The purpose of this chapter is to review of the relevant literature pertaining to 1) the different types of transit signal priority<sup>1</sup> strategies that have been employed in the field and in the laboratory, and 2) the estimation of bus dwell time. The chapter begins with a discussion of the different type of BSP strategies, followed by a discussion of the proposed real-time BSP strategies currently being developed. This discussion is followed by a section that summarizes the estimation models for bus dwell time that have been previously studied.

#### 2.1 BUS SIGNAL PRIORITY SYSTEMS

The concept of bus signal priority (BSP) was established with experiments in the early 1960s (2). Research performed prior to 1990 provided most of the foundation for the current bus priority systems. The objective of bus signal priority is to reduce delay for buses at signalized intersections. The rationale for special treatments of buses has its basis in the high occupancy of these vehicles. One of objectives in timing traffic signals is to minimize the total delay to all vehicles at an intersection. However, minimizing vehicle delay may not be optimal if the passenger load of the vehicles is considered. Granting priority to buses, therefore, is more likely to minimize total person delay and maximize total person throughput.

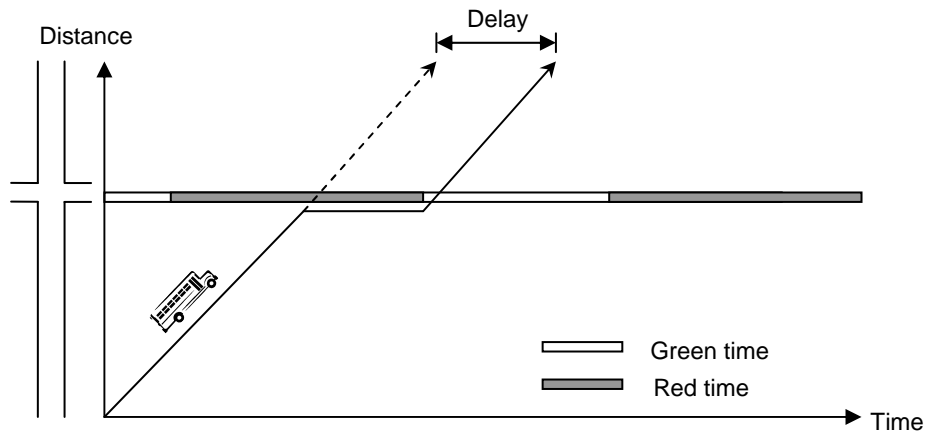
Figure 2-1 illustrates how a bus experiences delay at a traffic signal in the absence of bus signal priority. The trajectory of a bus is represented on a time-space diagram. The horizontal band in the figure represents a traffic signal. If the bus arrives during the red traffic signal, the bus is delayed until the signal turns green and the bus can proceed. Bus signal priority attempts to reduce the bus delay either by reducing the

---

<sup>1</sup> For the purpose of this dissertation transit signal priority will be referred to as Bus Signal Priority (BSP)



probability of a bus arriving during red signal or alternatively, reducing the waiting time until the green signal if the bus is stopped.



**Figure 2-1 Bus delay without signal priority**

BSP systems can be classified into three strategies; passive, active, and adaptive/real-time (3,4,5,6,7). Passive strategies operate continuously regardless of whether bus is present or not, and does not require a bus detection system. Active strategies utilize a bus detection system for sensing the buses that are qualified for priority. Adaptive/real-time strategy provides priority while simultaneously trying to optimize a given performance criteria. Each strategy will be discussed in the following section.

### **2.1.1 Passive BSP Strategies**

Passive BSP strategies (3,4,5) attempt to improve bus operations at the intersections by providing a signal timing plan designed to more frequently serve a phase that has high bus demand based on historical data. Passive priority operates regardless of whether a bus is present or not, and does not require detection of the bus on the upstream link of the signalized intersections. Thus, passive priority strategies operate independently on the buses. Passive priority strategies can be efficient when bus headways are short (i.e.

high volume of the bus), traffic volumes are low, and passenger demand is stationary (i.e. small variation in dwell time). One of the passive BSP strategies that can be considered in bus-favorable circumstances is a signal progression for buses. Because the signal timing is adjusted in order to coordinate the bus flow along an arterial, the traffic on the cross streets may experience unnecessary delay and stops. Passive BSP strategies generally are known to cause unnecessary delays to the traffic on non-priority approaches due to preferential treatment for buses every cycle regardless of whether buses are present. Other passive priority strategies that are commonly used are (3,4):

- *Adjustment of cycle length:* Under certain circumstance, reducing cycle lengths means that transit vehicles will receive service more often thus reducing delay.
- *Splitting phases:* Splitting a priority phase into multiple phases that can served more than once every cycle without necessarily reducing the cycle length.
- *Increasing phase:* Increasing green time for movements serving the transit vehicles increases the likelihood that transit vehicles will be served.
- *Metering vehicles:* Metering vehicles limits the number of vehicles allowed into the system, while it provide benefit to buses by allowing buses to bypass the metered signal.

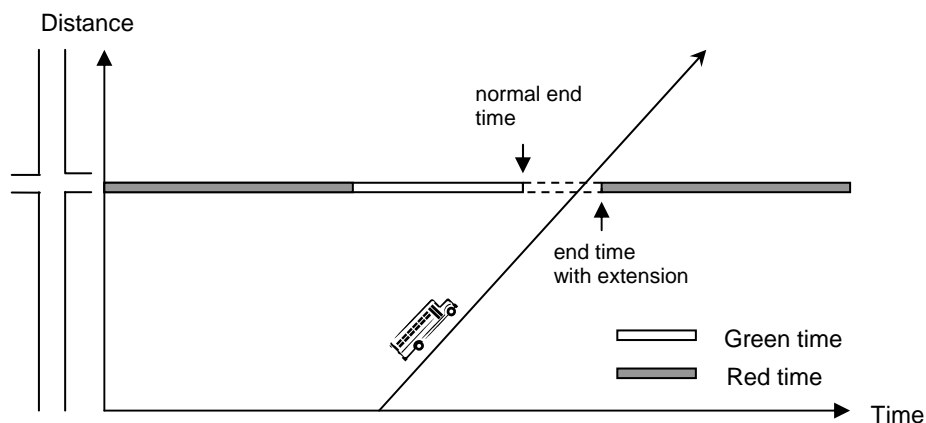
### **2.1.2 Active BSP Strategies**

Active BSP strategies (7,8) give more flexibility to the signal control system because they rely on specific information with respect to bus location. In general, active BSP strategies improve upon the passive BSP strategies in that priority is given only when a bus is present. These strategies are more infrastructure intensive than passive strategies, because they requires 1) detection devices that can sense approaching buses upstream of the intersection, and 2) advanced controllers to activate the priority strategies for granting priority. The common active strategies that a controller can perform in response to the detection of a bus are: 1) extending the green time in the current phase, 2) ending another phase early to give an early green to the bus, and 3) inserting an extra bus phase

to allow the bus to pass before returning to the regular timing. The response used will depend on when in the cycle the vehicle is detected.

### 2.1.2.1 Green extension strategy

In this strategy the green phase is extended for buses that approach the intersection during a green indication. If the bus is approaching the intersection near the end of the green interval for its approach, the current interval can be extended until the vehicle has passed through the intersection, as shown in Figure 2-2. Without extension, the vehicle would have to wait for green in the next cycle thus increasing its delay. It is considered one of the most effective BSP strategies because no clearance interval for changing phases is required.

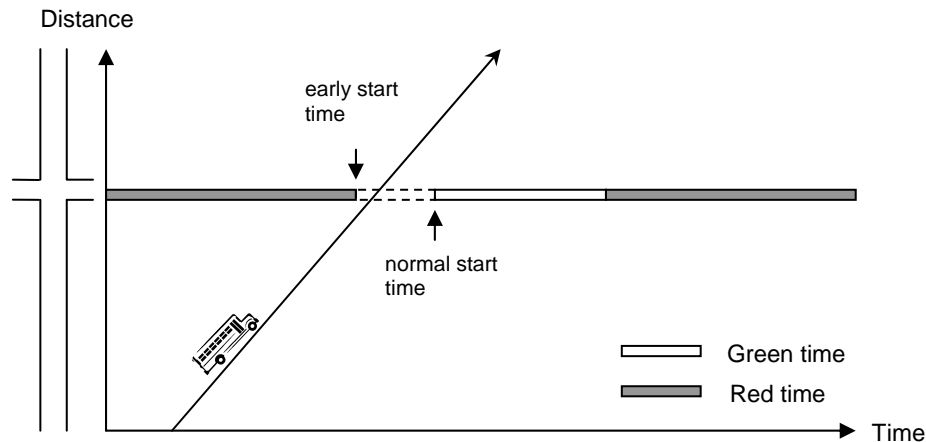


**Figure 2-2 Phase change for green extension strategy**

### 2.1.2.2 Early green strategy

When buses are detected during a red indication, the non-priority phases are truncated in order to expedite the starting phase for the bus movement. If the vehicle will arrive at the signal near the end of the red period for its approach, the current phase can be ended early to allow the green phase for the bus to be started early. This strategy is often used

in clearing queues on the bus approach so that the bus does not have to wait for queues to clear before passing through the intersection. An illustration of the early return strategy is provided in Figure 2-3.



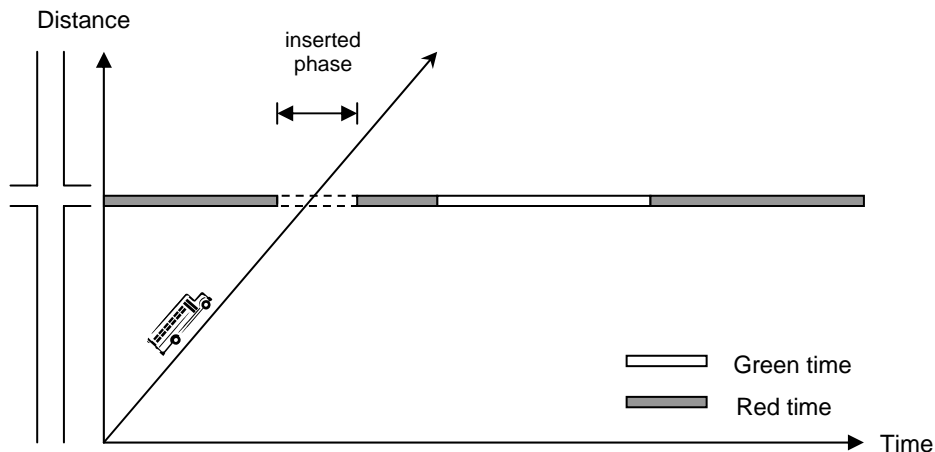
**Figure 2-3 Phase change for early green strategy**

### 2.1.2.3 Phase insertion strategy

With the phase insertion strategy, a special phase is provided when a bus is detected upstream of the intersection. If the bus will arrive at the signal in the middle of the red period for its approach, a bus phase is inserted within the normal signal sequence. The controller returns to normal operation once the bus has passed through the intersection. Figure 2-4 illustrates this strategy, where a special phase is inserted to serve the bus.

Active BSP strategy in most traffic signal controllers is frequently accomplished by preempting the normal operation in the controllers, which can cause a disruption to the system if it is operating in a coordinated mode. Some research efforts have focused on developing strategies that can keep the traffic controller in the progression while simultaneously providing a signal priority to buses (9,10). The strategies proposed from previous studies adjust the signal timing parameters within a background cycle length so as to maintain signal coordination. This constraint of a cycle length limits the amount of

time that can be allocated to a priority phase, and requires more complicated control logic in adjusting signal timing parameters within the cycle.



**Figure 2-4 An example of phase insertion strategy**

### 2.1.3 BSP Strategies in Adaptive Signal Control Systems

BSP strategies in adaptive signal control systems (11-27) are implemented by systems based on a real-time evaluation of a selective performance criterion through continuous feedback between the priority request generator (i.e. bus or detector) and the priority request server (i.e. local controller or transit management center). Some systems determine if, and how, to grant priority using optimization-based control schemes. In such schemes, total intersection delay is considered as a primary measure in evaluating the alternative timing plans or optimizing the signal timing parameters (13). Delay may be defined with respect to passenger delay, vehicle delay, weighted vehicle delay or some combination of these measures. Because common signal timing parameters such as cycle length, splits, and offset are continuously adjusted in real-time in response to the changes in traffic conditions, strategies in adaptive signal control systems do not require predefined specific priority actions. The bus priority is accomplished within most adaptive signal control systems by giving more weight to buses in the traffic signal

parameter optimization procedure. BSP strategies in adaptive signal control systems has been studied and/or implemented at both local intersection and street network level.

### *2.1.3.1 Local intersection level strategies*

Within the last several decades a number of local-intersection-based strategies have been developed. The Signal Priority Procedure of Optimization in Real-Time (SPPORT) system is based on the optimization procedure based upon generic lists of rules (including rules aimed specially at transit) that allocate different priorities to key traffic events (14,15,16,17). SPPORT evaluates several timing plans that accommodate the highest priority events from the predefined list and selects the best timing alternative. A discrete-event-based microscopic traffic simulator is used to predict the impacts of potential future switching decisions. The evaluation is accomplished using an expert system approach that considers a set of rules to select the solution. Chang, et al. (18) developed an adaptive signal system that utilizes a cellular automata traffic flow model to predict and estimate vehicle arrivals, queues, queue discharge flows and the signal control states. The provision of priority is determined based on a composite objective function consisting of estimated passenger delay, vehicle delay and schedule delay. A performance index is evaluated for each possible signal setting for the next second, and then the best signal plan is selected for implementation. In subsequent work (19,20), Automatic Vehicle Location (AVL) technology was employed to overcome shortcomings in the bus detection capability in the original design of this algorithm. It was found that the total passenger delay for the adaptive control with AVL information significantly decreased in heavy traffic volume conditions. The strategy reported by Lin et al. (21) integrates an adaptive transit operation into an adaptive signal control system. The adaptive signal control strategy is based on assessing the operating cost which is a function of passenger car delay, total number of vehicle stops, and bus delay. This strategy utilizes historic traffic patterns, current operating state, and predicted arrival to project the operating cost for a priority treatment. The analysis involves a comparison of headway versus schedule based dispatching and the effects of traffic volumes. The

authors found that a bus delay time was reduced by 55 percent and the combined operating cost was reduced by 6 percent.

### *2.1.3.2 Street-network level strategies*

Most adaptive signal control systems under operation are capable of implementing bus priority at a street-network level. The Split Cycle Offset Optimization Technique (SCOOT) is an on-line version of TRANSYT that has been adjusted to work as a real-time system (22,23). It automatically adjusts the cycle time, splits, and offsets in accordance with the change in traffic state. Transit signal priority is provided through either phase extension or early green. SCOOT provides a preferential treatment to transit through the use of weighting factors that result in favorable treatment to movements containing transit vehicles. Performance results showed that transit delay per intersection was improved by 22 percent. With low traffic volume, transit delay was significantly reduced by as much as 70 percent.

The Urban Traffic Optimization by Integrated Automation (UTOPIA) is a hierarchical real-time control system that provides absolute priority to transit vehicles at intersections (24). Performance results indicate an approximate 15%-20% increase in speed for both transit and private vehicles compared with traditional control.

PRODYN (25) is a real-time control system developed in France and implemented in several French cities. The original transit priority in PRODYN was achieved in a non-optimal way by assuming a detected bus to be worth several passenger cars in the optimization process. However, more recently a version of PRODYN has been specifically developed to provide priority to buses based on minimizing the total delay at an intersection. Coordination is provided by sharing vehicle arrival forecasts with adjacent intersections. The implementation of the revised system showed a 15% reduction in travel time for private vehicles with no increase in delay for transit vehicles.

Sydney Coordinated Adaptive Traffic System (SCATS) system is an example of both passive and active transit priority in a centralized system (26). SCATS adjusts signal plans based on traffic conditions at critical intersections. These critical

intersections control coordination within the subsystems and the subsystems coordinate with other subsystems as traffic demands vary. Transit priority is accomplished in SCATS through either phase extension or early green. Flexibility is provided allowing priority to be given depending on the time of day, tidal flow determination based on traffic flows, or congestion level of the intersection. Evaluation of the system showed a six to nineteen percent reduction of transit travel time, with benefits to passenger cars of between one and seven percent.

Duerr (27) discussed certain limitations of implementing bus priority within existing street-network level control strategies. A general problem occurs from the fact that the systems consider network-wide effects, while providing bus priority is a local intersection concern. Conflicting goals in the optimization may lead to sub-optimal results. The macroscopic models of traffic flow may result in another problem with using adaptive/real-time strategies because these models can not capture certain details of bus movements such as bus dwell time and interaction with other vehicles, consequently bus travel time may be underestimate, which can lead to inefficiencies in the system.

#### **2.1.4 BSP Strategies with Nearside Stops or Dwell Time**

It is important to note that facility design may affect the performance of the priority strategies. Nearside bus stops complicate the priority strategies because the priority green phase may be extended even if the bus is servicing passengers at the bus stop. Even if the dwell time is taken into consideration, the priority green time required will always be uncertain because of the variability in dwell time (5,9) Therefore, these green time extension may be too short and the bus is still stopped at the signal or it may be too long leading to greater delay to the non-transit vehicles.

Several studies of BSP systems have considered nearside bus stops at the local intersection level. Ngan (28) examined the impact of nearside bus stop on BSP implementation using the micro-simulation model VISSIM. Nearside bus stops were found to cause higher bus delay than far-side bus stops, all else being equal, because



uncertain dwell time at the stop lowered the BSP success rate. Another disadvantage of nearside stops is that queues from traffic signal can block the bus from reaching the nearside stop. Balke et al. (29) proposed “intelligent bus priority concept” employing AVL system that is capable of detecting a bus blocked by queues and implementing a signal priority to allow the bus to get to the bus stop. The dwell time was also taken into account when the algorithm calculates the bus arrival time at the intersection. However, the variability in dwell time was not considered. Koonce et al. (30) identified an operational deficiency with nearside stops, which effects specifically the detection range of the buses. The nearside bus stops were found to substantially reduce the detection range, which decreases the overall effectiveness of the BSP system.

The variability of bus dwell time has been addressed in predictive street-network BSP systems in which the arrival time of a bus at the intersection needs to be predicted and an advanced detection of buses is required. Head (9) addressed a difficulty with stochastic dwell times in providing anticipatory network priority that attempts to provide a bus progression band along a corridor. Because the uncertainty (i.e. randomness) of the dwell times inhibits the ability to predict the trajectory of the bus through the corridor, the prediction horizon of the bus trajectory was limited to the distance between bus stops. Wadjas and Furth (31) proposed a simulation study for the signal priority using advanced detection. The transit travel time including dwell time was predicted using a linear function of transit headway. The linear model was based on the fact that transit vehicle with longer headways are likely to have greater boarding and alighting volumes at intervening stops. Small variation in dwell time was found because the passenger model for dwell time used in the study could not consider the variation in passenger boarding and alighting times.

### **2.1.5 Effectiveness of Bus Signal Priority**

The implementation of the bus signal priority systems are generally accepted to have several benefits including the improvement of bus schedule reliability, the reduction in bus travel time, reduction in emission, and ultimately, an increased attractiveness of bus

created by an increased competitiveness to the single-occupancy automobile (32). Besides the benefits, BSP systems also have negative impacts on the traffic operation at the intersection.

BSP systems have been implemented extensively throughout Europe since 1968, generally with moderate success (33). BSP implementation under SCOOT control in London has resulted in the reduction of 32 percent in bus signal delay, with only 2.7 seconds increase in average traffic delay per vehicle during the peak periods. An installation in Angouleme, France resulted in 16 percent increase in the number of buses passing through intersection without stopping. The bus signal delay was also reduced by approximately 10 seconds per bus. The greater success in BSP implementation in Europe is attributed to the philosophy to BSP that provides a high reward for transit vehicles and passengers (33).

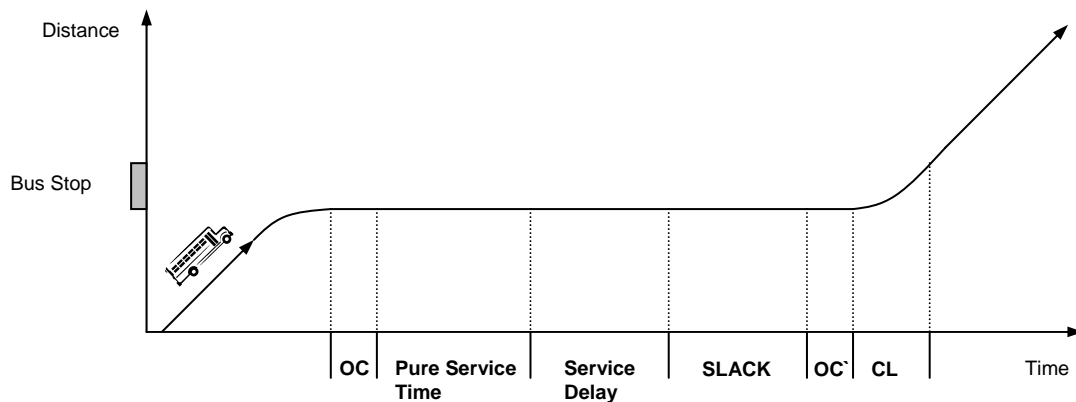
Several cities across North America have implemented BSP systems. Other cities, such as Houston, Texas, have BSP projects in the development stage or that are being planned. One of the earliest BSP installations in U.S. was the Bus Priority System (BPS) as part of the Urban Traffic Control System (UTCS) project (34,35). The field test in Washington, D.C., over a period from 1972 to 1976, resulted in a significant reduction of up to 20 percent in bus signal delay. The recent implementation of a BSP system in Los Angeles is cited as providing an 8-10 percent reduction in travel time on the lines equipped with priority, with minimal adverse impact on cross-street traffic (36). The city of Portland, Oregon has conducted field tests at fourteen intersections. By utilizing Tri-Met's AVL system, the priority can be provided to selective buses that are running behind schedule. The results indicated that bus travel times are reduced by up to 8 percent and average bus signal delay reduced by 20 percent (37). A BSP system was deployed at nine intersections along Rainier Avenue in Seattle, Washington since 2000. Before and after studies showed that BSP reduces the average bus signal delay by 34 percent for BSP-eligible buses. In addition, the signal delay for non-transit vehicles did not significantly increased (38). In Toronto the signal priority has been provided to the buses and streetcars in mixed traffic at 36 intersections. The reduction in transit signal

delay ranges from 15 to 49 percent, which has justified expansion to over 300 signalized intersections (39). BSP systems have been deployed in other cities such as Bremerton, WA; Minneapolis, MN; San Francisco, CA; and Chicago, IL. Detailed information for the effectiveness of BSP for these cities can be found elsewhere (5,29,32,40).

## 2.2 ESTIMATION OF BUS DWELL TIME

### 2.2.1 Characteristics of Dwell Time

The bus dwell time is defined by Highway Capacity Manual (HCM) as the amount of time that a bus spends while stopped to serve passengers at a specific stop (41). It is the time required to serve passengers at the busiest door, plus the time required to open and close the doors. Bus dwell time consists of several components as shown in Figure 2-5 where the amount of time that a bus spends at bus stop is divided into several time components (41). The bus trajectory and time duration were shown in time-space diagram. Each of the components is discussed further as follows:



**Figure 2-5 Dwell time components**

- $OC+OC`$  is known as “door opening and closing time” that ranges typically 2 to 5 s for normal operations.

- *Pure service time* is the minimum service time for alighting/boarding passengers. It should be less than typical passenger service times. The service time for alighting/boarding for each passenger is mainly dependent on the number of doors (42). The Highway Capacity Manual provides the service times according to the service conditions, bus types, and door configurations (i.e. conventional bus with one front door with single coin fare: 2.6 to 3.9 sec. for boarding, 1.7 to 2.0 sec. for alighting). Pure service time is the product of the number of alighting/boarding passenger and marginal service time.
- *Service delay* is a random delay associated with alighting/boarding activities. In alighting activity, passenger inertia and elderly/handicapped people delay door closing (43). The fare collecting system is most significant factor in service delay of boarding activity (44). The complexity in fare collection of the bus causes wide range of service delay.
- *Schedule slack time* is the remaining time until scheduled departure at stop if a bus is ahead of its schedule (9). Usually scheduled departure times are assigned to schedule check points that are transferring or high demand stops. The driver is required to wait until the schedule departure time at the schedule check points, otherwise slack time varies according to the driver's decision.
- *Clearance time* consists of the time for a bus to start up and travel its own length while exiting a bus stop. For bus turnout stops, the reentry delay takes account the delay associated with the wait for a sufficient gap in traffic to allow a bus to pull back into the travel lane. HCM reports that bus start-up times range from 2 to 5 s while time for a bus to travel its own length after stopping is approximately 5 to 10 s, depending on acceleration and traffic conditions. In most previous studies, clearance time was excluded because dwell time was defined the amount of time it takes for bus to serve passengers at the stop.

In the absence of other information, Highway Capacity Manual recommends that dwell time can be assumed to be 60 seconds for central business district (CBD), transit center, major on-line transfer point, or major park-and-ride stops; 30 seconds for major

outlying stops; and 15 seconds for typical outlying stops. Levinson (45) found that dwell time ranges from 20 to 60 seconds in CBD, 10 to 15 second for non-CBD stops, which accounts for up to 26 percent of travel time. However Maloney and Boyle (46) found that dwell time accounts for up to only 11 percent of travel time, representing a significant difference from previous study by Levinson. This was due to the recovery time (i.e. schedule slack time) being excluded in the measurement of dwell time.

Dwell time has been generally accepted as a major factor causing vehicle bunching, which results in variability of headways (47). Significant headway variation may result in longer average passenger waiting times and congested passenger loads in some vehicles, both of which degrade the quality of the transit service. The variability in bus dwell time is measured by the coefficient of variation (C.V.) of dwell times, which is the standard deviation of dwell time observations divided by the mean. In several U.S. cities, the C.V. of dwell times typically ranges from 40 to 80 percent (41).

### **2.2.2 Regression Models for Dwell Time Estimation**

The literature on bus dwell times has been sparse because the data collection typically involves labor-intensive works. Therefore most prior studies have focused on route-specific analyses for various issues causing bus delay, based on small samples. Most models proposed for estimating dwell time have been based on the linear relationship between number of alighting/boarding passenger and dwell time. Several ordinary least squares (OLS) regression models have been proposed for relating dwell time to passenger demand, specifically boarding and alighting passengers. Kraft and Bergen (48) found from the regression analyses that the marginal service time varied according to the time of day, service times during off-peak period were longer than those during peak period. The boarding times were found to be greater than alighting times, and service times were not different between front door and rear door. They also found that boarding times increased when a complex fare collection system, such as the cash and change fare structure, was used. Guenther and Hamet (44) studied the relationship between dwell time and fare structure using the regression models. Lin and Wilson (49)

developed several linear and non-linear regression models for estimating dwell time of light rail system. They included the number of standees in order to analyze the effect of passenger crowding on the dwell time. Adding crowding variables improved the explanatory power of most models.

With the popularization of Automatic Passenger Counter (APC) among transit agents in U.S. since 1990's, a rich set of dwell time observations can be collected at the level of individual bus stops (50). In addition, the large quantity of data allows analysis of rare events, such as lift operations. Dueker et al. (51) utilized the dwell time data from APC in estimating delay associated with bus lift use operations for passengers with disabilities in the Tri-County Metropolitan Transportation District of Oregon (TriMet). They also examined various determinants of bus dwell time, such as low floor buses, time of day, and route type effects. The passenger activity was revealed as most important determinant. Bertini and El-Geneidy (52) developed a linear regression model with the number of boarding and alighting passengers from APC of TriMet. The estimate of dwell time was used in modeling the bus trip time. It was found that when the dwell time model was incorporated into a trip time model, the results of the performance analysis were improved. Rajbhandari et. al. (47) developed several regression models relating dwell time to number of passenger boarding/alighting, achieved from onboard APC system of New Jersey Transit Corporation. The analyses revealed that the level of crowding in the bus and the time of day were not to be effective on the bus dwell time of the intercity bus service.

The literature on regression modeling of dwell time indicated that the most significant determinants of dwell time are total of boarding and alighting passengers, number of boarding passengers, number of alighting passengers, and number of standees. It was also found that marginal service time for each alighting/boarding was greater than typical values in HCM. The difference was up to 4 seconds for boarding activity and 2 seconds for alighting activity.

Similar to the regression models studied previously, a general form for estimating dwell time was proposed for the case of absence of detailed information.

Highway Capacity Manual (41) presents an additive form for estimating bus dwell time based on the linear relationship between passenger demands and passenger service times. Lost time for door opening/closing is another input variable as shown in Equation 2-1. Like the constant term in the regression models, door opening/closing time  $t_{oc}$  represents the lost time associated with bus stopping to service the passengers.

$$t_d = P_a t_a + P_b t_b + t_{oc} \quad (2-1)$$

where

- $t_d$  = bus dwell time (sec),
- $P_a$  = alighting passengers per bus through busiest door during peak 15 min (p),
- $t_a$  = passenger alighting time (sec/p),
- $P_b$  = boarding passengers per bus through busiest door during peak 15 min (p),
- $t_b$  = passenger boarding time (sec/p), and
- $t_{oc}$  = door opening and closing time (sec).

The passenger volumes in the model are required to be adjusted by the peak-hour-factor in order to reflect peak 15-min conditions. When the numbers of alighting and boarding passengers are already known, the dwell time is determined by the service time per each passenger. Boarding and alighting times for base conditions are determined by the number of doors and fare collection structure as shown in Table 2-1.

**Table 2-1 Typical bus passenger boarding and alighting service times for selected bus types and door configurations (41)**

Bus Type	Available Doors or Channels		Typical Boarding Service Times <sup>1</sup> (s/p)		Typical Alighting Service Times
	Number	Location	Prepayment <sup>2</sup>	Single Coin Fare	
Conventional (rigid body)	1	Front	2.0	2.6 to 3.0	1.7 to 2.0
	1	Rear	2.0	N/A <sup>7</sup>	1.7 to 2.0
	2	Front	1.2	1.8 to 2.0	1.0 to 1.2
	2	Rear	1.2	N/A	1.0 to 1.2
	2	Front, rear <sup>3</sup>	1.2	N/A	0.9
	4	Front, rear <sup>4</sup>	0.7	N/A	0.6
Articulated	3	Front, rear, center	0.9 <sup>4</sup>	N/A	0.8
	2	Rear	1.2 <sup>5</sup>	N/A	---
	2	Front, center <sup>3</sup>	---	---	0.6
	6	Front, rear, center <sup>3</sup>	0.5	N/A	0.4
Special single unit	6	3 double doors <sup>6</sup>	0.5	N/A	0.4

Note:

<sup>1</sup> typical interval in seconds between successive boarding and alighting passengers. Does not allow for clearance times

<sup>2</sup> also applies to pay-on-leave or free transfer situation

<sup>3</sup> one each

<sup>4</sup> less use of separated doors for simultaneous loading and unloading

<sup>5</sup> double-door rear loading with single exits, typical European design. Provides on-way flow within vehicle, reducing internal congestion. Desirable for line-haul, especially if two-person operation is feasible. May not be best configuration for busway operation

<sup>6</sup> examples: Denver 16<sup>th</sup> street mall shuttle; airport buses used to shuttle passengers to planes. Typically low-floor buses with few seats serving short, high-volume passenger trips

<sup>7</sup> no data available

### 2.3.3 Probabilistic Models for Dwell Time

As discussed in previous section, prior studies on modeling dwell time have focused on regression models relating dwell time to the passenger demand. However, the application of the regression models is limited to the situation when the exact number of alighting/boarding passengers can be observed or have been observed. Some efforts have been made for representing the number of passengers as independent random variables with given density functions. In the case of steady-state demand conditions, a binomial distribution has been known as the most suitable representation of the number of alighting passenger (48,53). When the passenger load is unknown, the distribution of



passenger alighting can be explained by Equations 2-2 and 2-3. In the case where the number of passengers on bus is known through APC system, the passenger alighting follows a binomial distribution  $Bi(L, p)$ .

$$P[\text{passenger alighting } A = x] = P[L \text{ on the bus}] \cdot P[x \text{ alighting} | L \text{ on the bus}] \quad (2-2)$$

$$= \sum_{L=x}^{\infty} f(L) \cdot \binom{L}{x} p^x (1-p)^{L-x} \quad (2-3)$$

where

- $A$  = number of passenger alighting (p),
- $L$  = total number of passengers on the bus, and
- $p$  = probability of alighting for a randomly chosen passenger on bus.

For high bus service frequency (i.e. shorter headway between buses), passenger arrivals have been frequently represented by Poisson distribution (43,48,53,54,55). When the arrival intensity rate was known, the number of boarding passengers can be expressed by Equations 2-4 and 2-5.

$$P[\text{arrivals during headway } B = x] = f(x) = \frac{m^x e^{-m}}{x!} \quad (2-4)$$

$$m = \int_a^b \lambda(t) dt \quad (2-5)$$

where

- $B$  = number of passenger arrivals during preceding headway (p),
- $a$  = departure time of previous bus,
- $b$  = arrival time of current bus, and
- $\lambda(t)$  = passenger arrival intensity (p/sec), for stationary arrival,  $m = \lambda(b - a)$ .

For better representation of the bus operations in the microscopic traffic simulation models, the schedule adherence was considered in the estimation of dwell time (56). A stochastic dwell time model was proposed as shown in Equation 2-6. The model is similar to HCM model except an additional variable for schedule slack time.

$$\begin{aligned} t_d &= P_a t_a + P_b t_b + t_{oc} + \alpha \cdot t_s && \text{when bus door} = 1 \\ t_d &= \max\{P_a t_a + P_b t_b\} + t_{oc} + \alpha \cdot t_s && \text{when bus door} > 1 \end{aligned} \quad (2-6)$$

where

$$\begin{aligned} t_s &= \text{schedule slack time (sec), and} \\ \alpha &= \text{slack time fraction, [0..1].} \end{aligned}$$

The numbers of alighting/boarding passengers at each stop are approximated by the binomial distribution and passenger arrival rate as discussed previously. The probability of alighting at each stop should be predefined using historical data. The number of passengers waiting at stop when a bus arrives is estimated by Equation 2-7. Because the number of passenger arrivals was assumed to follow a Poisson distribution, it can be estimated by a pre-defined passenger arrival rate and headway plus dwell time.

$$P_b = \lambda_p \cdot (h_{bus} + t_d) \quad (2-7)$$

where

$$\begin{aligned} \lambda_p &= \text{passenger arrival rate (p/sec), and} \\ h_{bus} &= \text{bus headway between the previous and currently arriving buses.} \end{aligned}$$

Guenthner and Sinha (57) found that negative binomial distribution was an acceptable descriptor of the number of boarding and alighting passenger, especially on higher demand routes. This result is attributed to the fact that the distribution was examined for total number of alighting/boarding passengers instead of individual

number of alighting/boarding. Adamski (43) proposed probabilistic models of passenger service processes at bus stops. He developed three density functions for boarding/alighting times based on the exponential, gamma, and erlangian probability distributions. The means and standard deviations of dwell time were calculated using moment function for each density function. The comparison with real-world observation indicated that the approximation by each distribution obtained quite good estimations for the mean and the standard deviation of dwell time.

### **2.3 SUMMARY**

Bus Signal Priority (BSP) can be classified as passive, active, and adaptive/real-time strategy. Passive priority strategies, which employ static signal settings that favor buses, are easily implemented in the field with existing hardware. Active priority and adaptive/real-time strategies, however, require specialized bus detectors and controller hardware that can respond to detected vehicle in real time. The priority service is generally provided by using adjusting signal timing plan in the manner of extension of the current green interval, starting the green interval early, and inserting an extra phase for the bus. Adaptive controllers allow more flexible logic to be defined for providing a signal priority. Buses are given more weight in optimizing the operational criteria so as to minimize the bus signal delay.

Most studies for dwell time estimation are based on the linear relationship between dwell time and alighting/boarding passengers. Ordinary least squares regression model was generally used in the explanation of the relationship. Some probabilistic models have been proposed with stochastic representations for the number of alighting/boarding passengers. Because most prior studies had focused on route-specific analyses for mainly bus operation performance, modeling passenger activity and bus operation at specific bus stop has been sparse.

The research in this dissertation aims to develop and evaluate a BSP algorithm incorporated with prediction interval of dwell time in a microscopic simulation environment. A methodology for dwell time prediction interval is developed in Chapter

IV, and a new bus signal priority algorithm is developed to improve the effectiveness of BSP at the intersections with nearside bus stops in Chapter V.

## **CHAPTER III**

### **DATA COLLECTION AND STUDY DESIGN**

The fundamentals of bus signal priority and dwell time prediction were introduced in chapter II. It was concluded that a dwell time prediction model and an improved BSP algorithm which incorporate dwell time prediction interval are needed to implement efficiently BSP at local intersections with nearside bus stops. In the first section of this chapter, the test bed for this study will be discussed. Subsequently, the methodologies used to develop these two new algorithms will be introduced. The dwell time prediction model and the improved BSP algorithm will be developed in Chapters IV and V, respectively.

The evaluation of the improved BSP strategies requires information on each vehicle whose travel behavior is stochastic. Because of the difficulty in obtaining empirical information, a microscopic simulation model that can simulate vehicles, buses, and bus passengers was utilized. The VISSIM micro-simulation model was selected. This model also provides vehicle actuated programming (VAP), an optional add-on module, for programming the user-defined traffic signal logic. Therefore, the improved BSP strategies can be implemented simultaneously with the traffic signal controller logic, using the VAP module.

#### **3.1 STUDY SITE SELECTION AND DESCRIPTION**

A study site was chosen among several candidate locations. The site was determined based on several criteria corresponding to the purposes of this dissertation:

- The site must have regular bus service routes
- The intersections must be signalized
- The intersections must be part of a coordinated system
- The site must have at least one nearside bus stop.

Careful consideration of the above criteria resulted in the selection of an arterial section of Bellaire Boulevard in Houston, Texas as shown in Figure 3-1. This arterial section is approximately 1.1km in length and is located between Bintliff Drive and Hilcroft Avenue as shown in Figure 3-2. The test bed includes four intersections, three signalized and one two-way stop-controlled intersection. Three Metro bus stops including two nearside stops are located along the eastbound approach. The improved BSP strategy will be implemented for the buses on the eastbound approach. In addition to satisfying the above criteria, this arterial was a test bed for a BSP demonstration project funded by Houston Metro in 2000.

The Bellaire Blvd is one of the major west-east arterials located in the southwest of the city of Houston. It is also a heavily traveled cross town arterial primarily traversing high-density residential areas. The southern area of Bellaire Blvd is mainly occupied by single family residences. In contrast, in the northern area, multiple family residences are dominant.

Three regular bus routes operate on the test bed. They connect suburban residential areas in the west and the Central Business District Figure 3-2 provides a schematic map of the bus routes operating in the study area. All routes stop at the far side stop near Tarnef Drive (Stop A). The nearside stop at Rookin Street (Stop B) is served by routes numbered 2 and 163. At nearside stop at Hilcroft Ave (Stop C), only route 2 operates. The service frequency (i.e. bus headway) of each route is summarized in Table 3-1. Both standard buses and articulated buses operate on these routes and all buses have two doors.

**Table 3-1 Scheduled bus headway**

	Route 17	Route 163	Route 2
Peak Hours <sup>1</sup>	20 min	8~10 min	6 ~ 8 min
Off-peak Hours	30 ~40 min	20 ~40min	10~30 min

Note:

<sup>1</sup> 7:00~8:30 AM, 5:00~6:30 PM

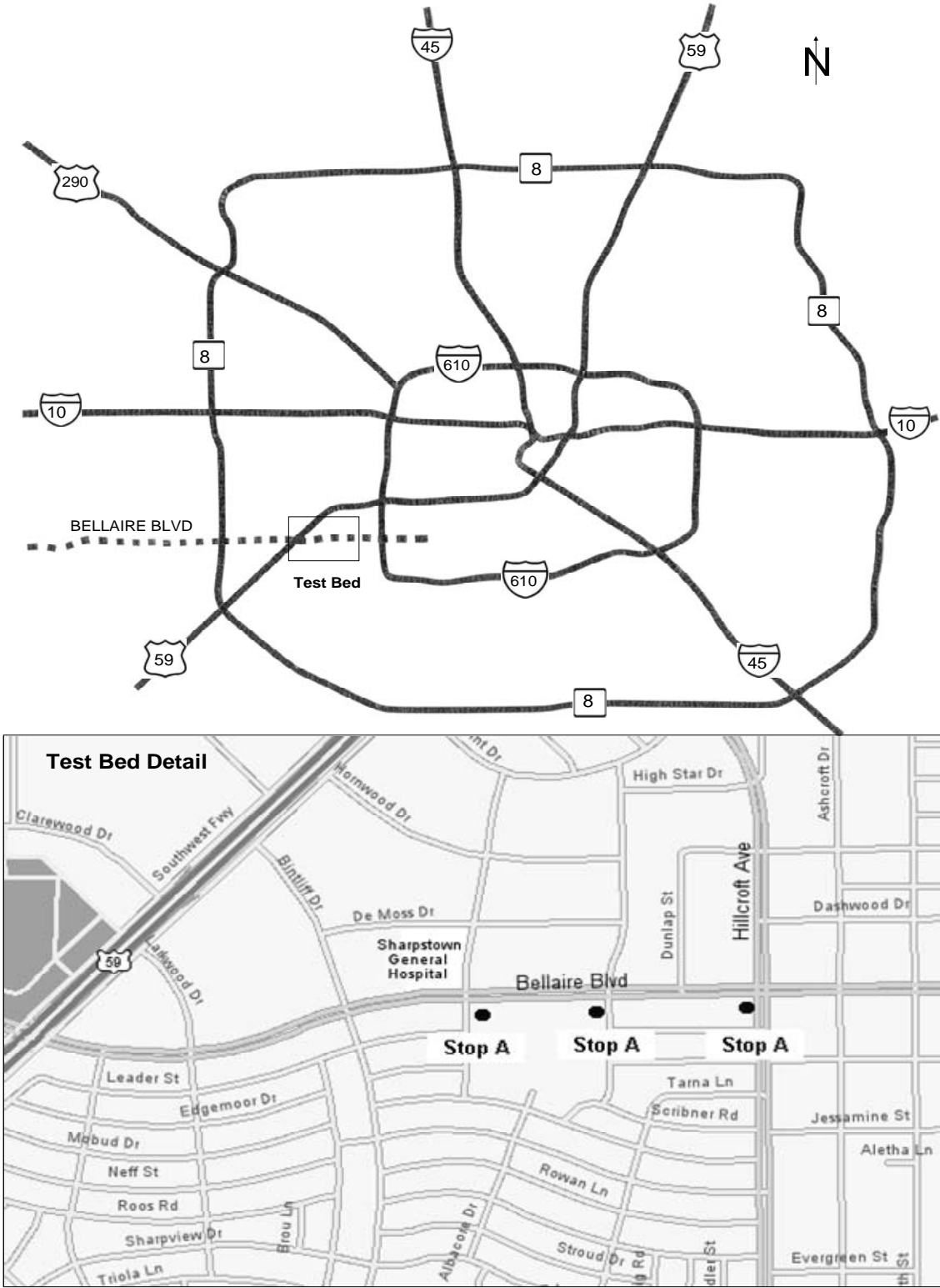
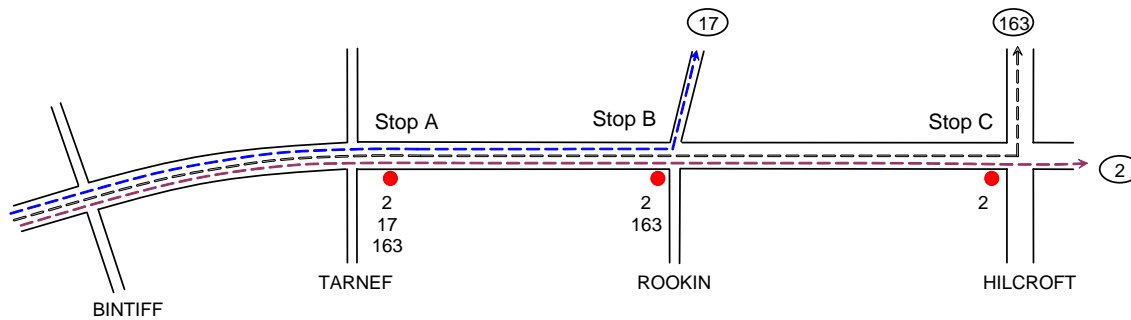


Figure 3-1 Site map for Houston and test bed



**Figure 3-2 Schematic route map and location of stops**

## 3.2 DATA COLLECTION

### 3.2.1 Bus Dwell Time Data

The data to be collected were determined by the type of the dwell time prediction model being considered. Because, in this dissertation, both a probabilistic model and a regression model will be explored for predicting dwell time at specific stop, input data for the models were collected at the level of individual bus stops. The input requirements for the probabilistic model are the probability distributions for random variables such as the number of alighting/boarding passenger and marginal alighting/boarding time. In order to define each distribution, information for both passengers and buses listed in Table 3-2 were required. For regression models, determinants of bus dwell time explored in this dissertation should be defined first. The bus dwell time can be affected by a variety of factors such as passenger demand (including transfer demand), time of day, the type of bus, schedule adherence, fare collection system, bus driver's behavior, the number of mobility-impaired passengers, etc. Because it is almost impossible to collect all data listed above, the number of determinants employed in this dissertation need to be constrained. The data used here are confined to the data that can be collected by the automatic passenger counter (APC) and automatic vehicle location (AVL) systems equipped on the buses. Because the popularity of APC and AVL systems have grown among transit agencies, it is reasonable to expect that these types of data are or will be available in many cities in North America. The retrievable data from APC/AVL system



are including the input requirements of the probabilistic model except the passenger arrival time at each bus stop as shown in Table 3-2. Additional information such as the dwell time of each bus, the schedule adherence, and the time of day can be retrieved from the bus data.

**Table 3-2 Required data for probabilistic model and regression model**

Type of Data	Data	APC/AVL
Passenger data	Passenger arrival time at each stop	
	Number of boarding passenger for each bus	√
	Number of alighting passenger for each bus	√
	Number of passenger on the bus (passenger loads)	√
Bus data	Time for which the bus doors have fully been opened	√
	Time for which the bus doors have fully closed	√

The data were collected by placing observers at each bus stop and all observers were equipped with digital timers synchronized to a reference time. The data collection was performed between 7:00 AM and 10:00 AM on five weekdays in 2003. A total of 217 buses were observed during the entire data collection period: 35 observations of route #17, 67 observations of route #163, and 115 observations of route #2.

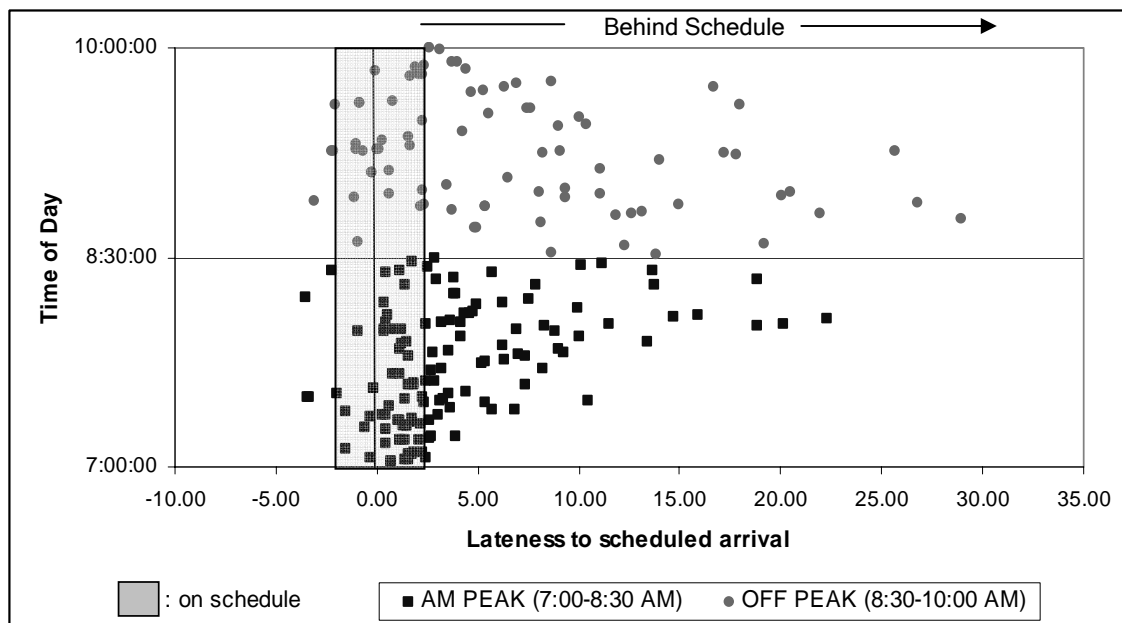
#### *3.2.1.1 Schedule adherence*

The information regarding each bus' adherence to its schedule was obtained by comparing the observed arrival times and the scheduled arrival times at each stop. It was decided that a bus is on schedule when it arrives at a specific stop within  $\pm 2$  minutes deviation from its scheduled arrival time. The analysis revealed that 33 percent of buses were on schedule during the entire study period. Approximately 36 percent of the buses were more than 5 minute late from their scheduled arrival time. It was noticed that more buses arrived on schedule during the peak period as shown in Figure 3-3. This might be because all bus routes are crossing major arterials before reaching the study site, and the delay at the intersections upstream of the study site during peak period may affect the

schedule adherence of buses at the stops of interest during off peak period. Table 3-3 summarizes the schedule adherence and the lateness for each route and time of day.

**Table 3-3 Schedule adherence and lateness**

Route #	#2		#17		#163		Overall	
	On	Late	On	Late	On	Late	On	Late
Peak	41.6 %	33.3 %	45.0 %	20.0 %	31.1 %	33.3 %	38.7 %	31.4 %
Off Peak	25.6 %	51.2 %	33.3 %	26.6 %	18.1 %	40.9 %	25.0 %	43.7 %



**Figure 3-3 Lateness to scheduled arrival during AM peak and off peak periods**

### 3.2.1.2 Dwell time

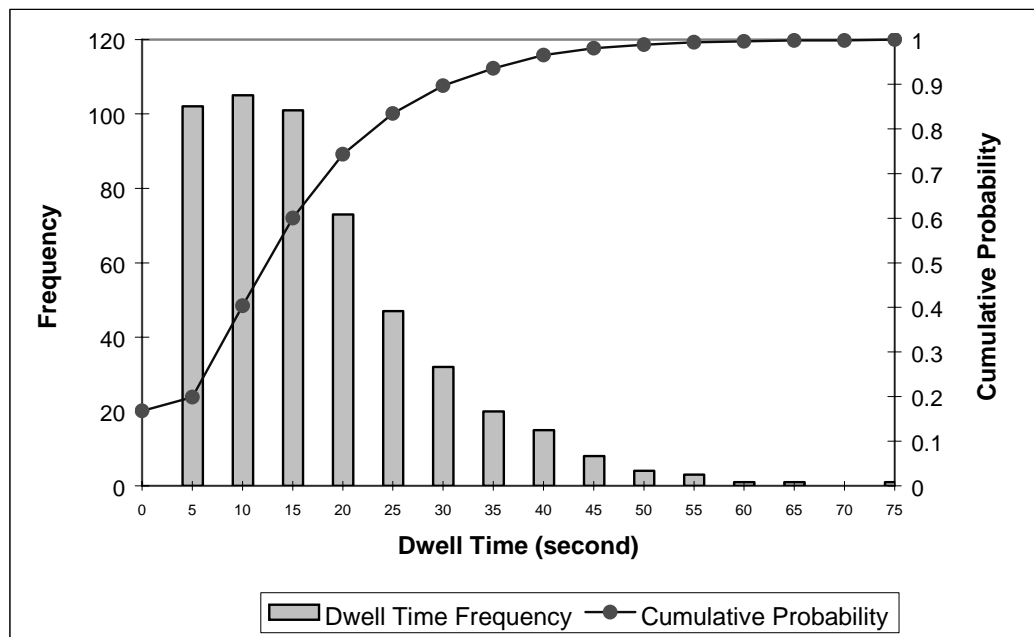
For the purpose of this dissertation, the bus dwell time was defined as the time period between the time when the doors open and time when the doors close. The average bus dwell time and its standard deviation for each bus stop are summarized in Table 3-4. Dwell times during off-peak period were longer than those during the peak period because of longer scheduled headways. However, the coefficients of variation (C.V.)

were slightly higher during peak period because of the large variation in passenger arrivals. The values of C.V. for all stop were higher than the HCM suggestion of 60%. The variance in the number of passenger arrivals during 5 minute-period was 2.0 for peak period while the variance of 1.59 was observed during off peak period.

**Table 3-4. Summary of bus dwell time**

	Peak Period ( 7:00 ~ 8:30 )			Off-Peak Period ( 8:30 ~ 10:00 )		
	Average ( sec )	S.D. ( sec )	Coefficient of Variation	Average ( sec )	S.D. ( sec )	Coefficient of Variation
Stop A	11.8	9.37	79 %	16.6	13.27	79%
Stop B	10.3	9.82	95 %	10.5	9.61	92%
Stop C	16.9	10.77	64%	19.8	11.67	59%

Figure 3-4 is a histogram of dwell time for all buses at all bus stops. There was cases of stop-skipping (i.e. 0 sec. dwell time) and the number of dwell times less than 15 seconds was 353 (i.e. 69 percent).



**Figure 3-4 Dwell time distribution for all stops**

### 3.2.2 Geometric and Traffic Data of the Intersections

The intersection data including geometrics, signal control, and traffic volume were collected at three intersections along the study site. Because the improved BSP strategies will be evaluated using a microscopic traffic simulation model, the traffic network and traffic volumes must be coded accurately in order to represent the traffic system being studied.

The intersections of Bintiff Drive at Bellaire Blvd and Rookin Street at Bellaire Blvd have identical geometric designs and signal phase plans. The geometric conditions and traffic volumes for the intersections of Bintiff Drive at Bellaire Blvd and Rookin Street at Bellaire Blvd are shown in Figure 3-5. The eastbound and westbound approaches have landscaped medians and consist of two through lanes, one through and shared right-turn lane, and one-exclusive left-turn. The northbound and southbound approaches have one through/left-turn shared lane and one through/right shared lane. The traffic demand on the eastbound approach is dominant because of the commuting traffic toward downtown during the peak hour. The north-southbound approaches experience unnoticeable congestion. Traffic volumes were collected at the intersection between 7:30 AM ~ 10:00 AM on October 16, 2003 using video cameras located on opposite corners of the intersections. The volumes were converted later into 15-minute period volumes. Traffic volume during the morning peak period (7:30 AM ~ 8:30 AM) was chosen as a representative peak volume.

The intersection signal operates in a coordinated-actuated mode with a 120-second cycle length. The coordinated phase operates on the eastbound and westbound through approaches, Bellaire Boulevard. Protected left-turn phases are provided for the eastbound and westbound approaches. These are actuated phases that can be skipped with no vehicle call. The phases for the northbound and southbound approaches are actuated and only permitted left turns are provided. The signal phase plan for the intersections of Bintiff Drive at Bellaire Blvd and Rookin Street at Bellaire Boulevard is illustrated in Figure 3-6. The signal control variables in normal mode are shown in Table A-1 and A-2 in Appendix A.

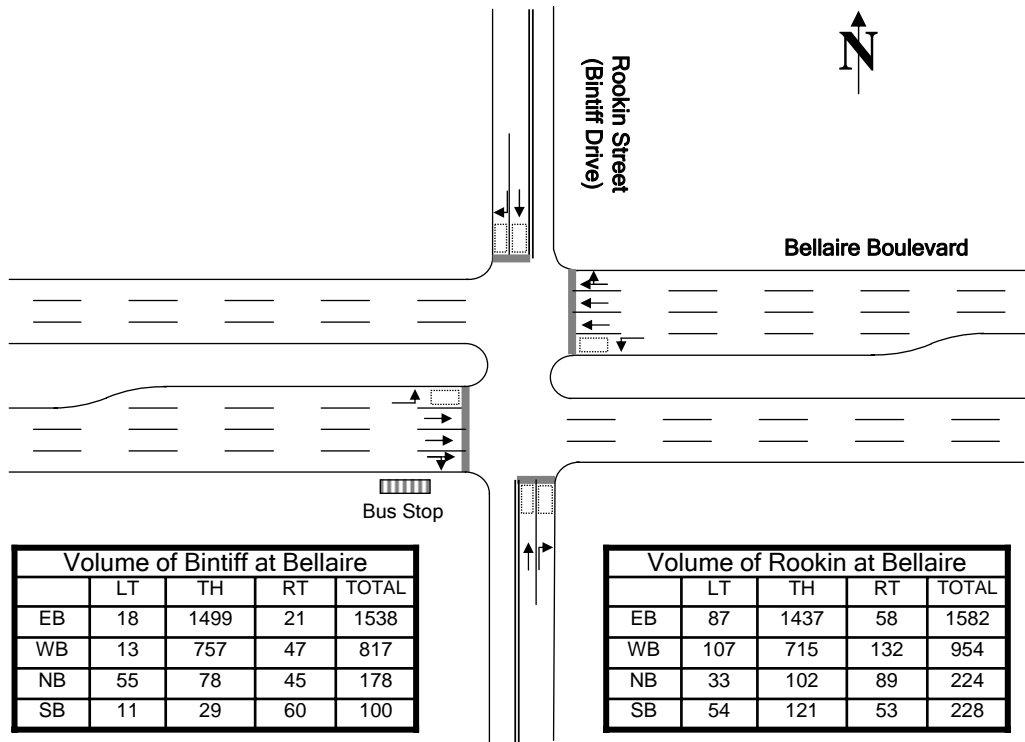


Figure 3-5 Geometry and traffic counts for Bintliff at Bellaire and Rookin at Bellaire

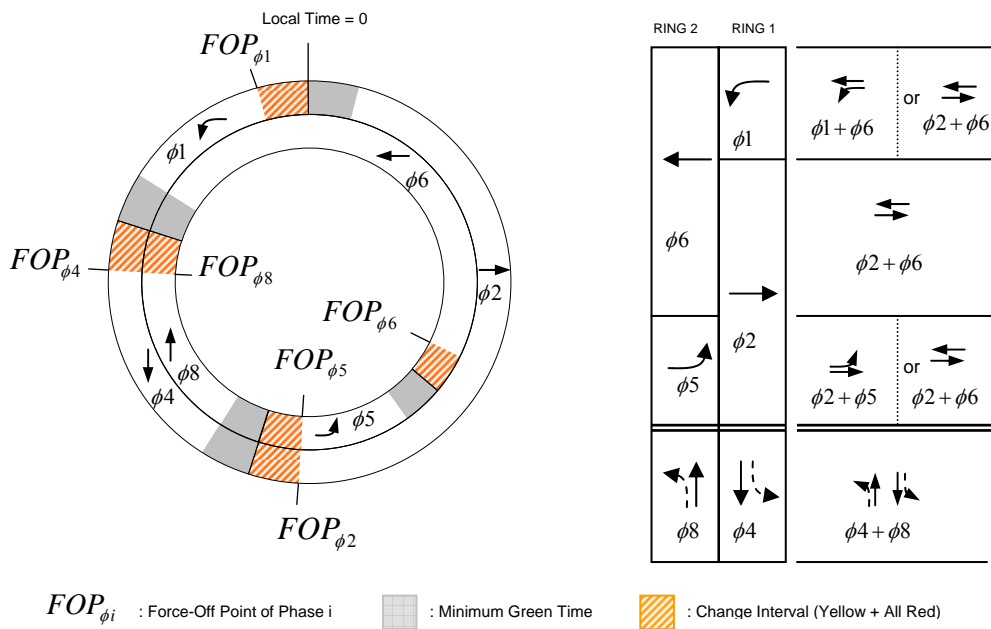
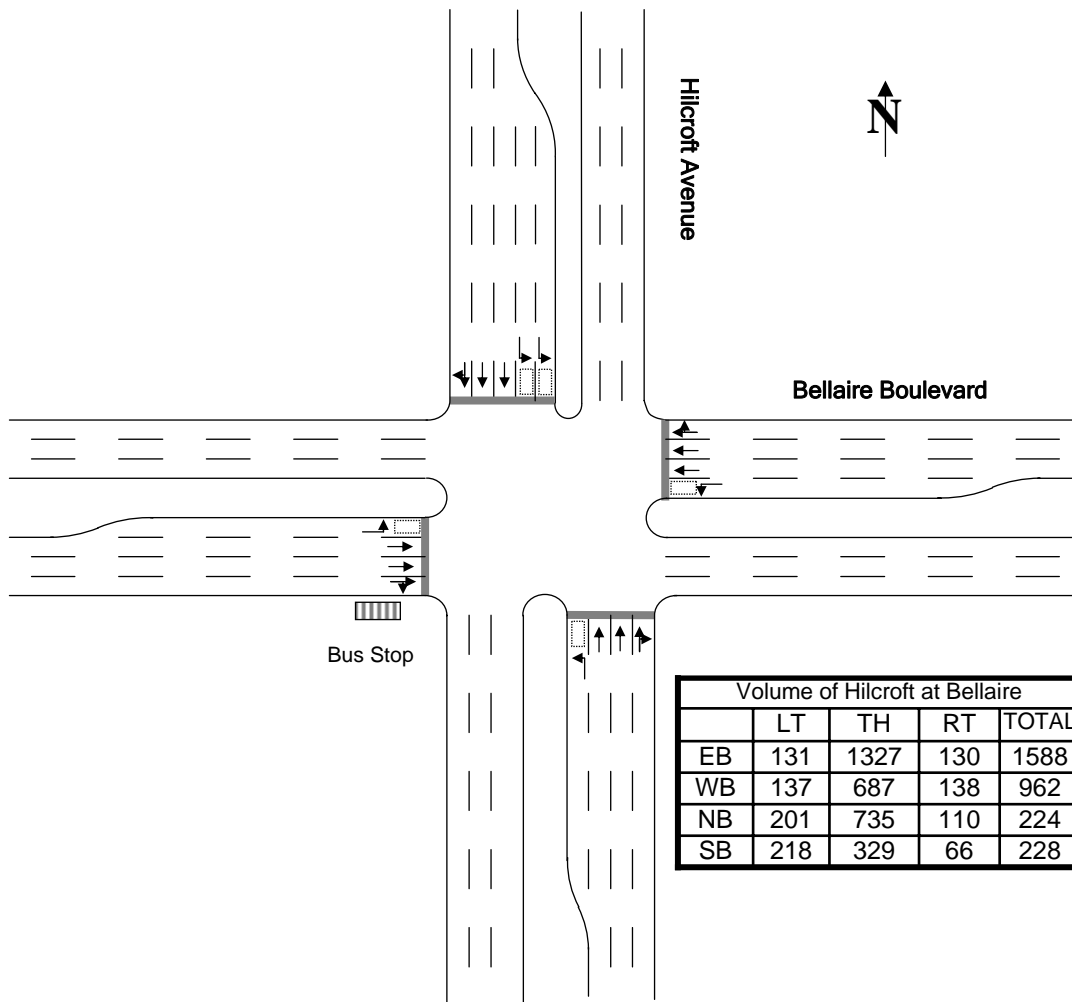


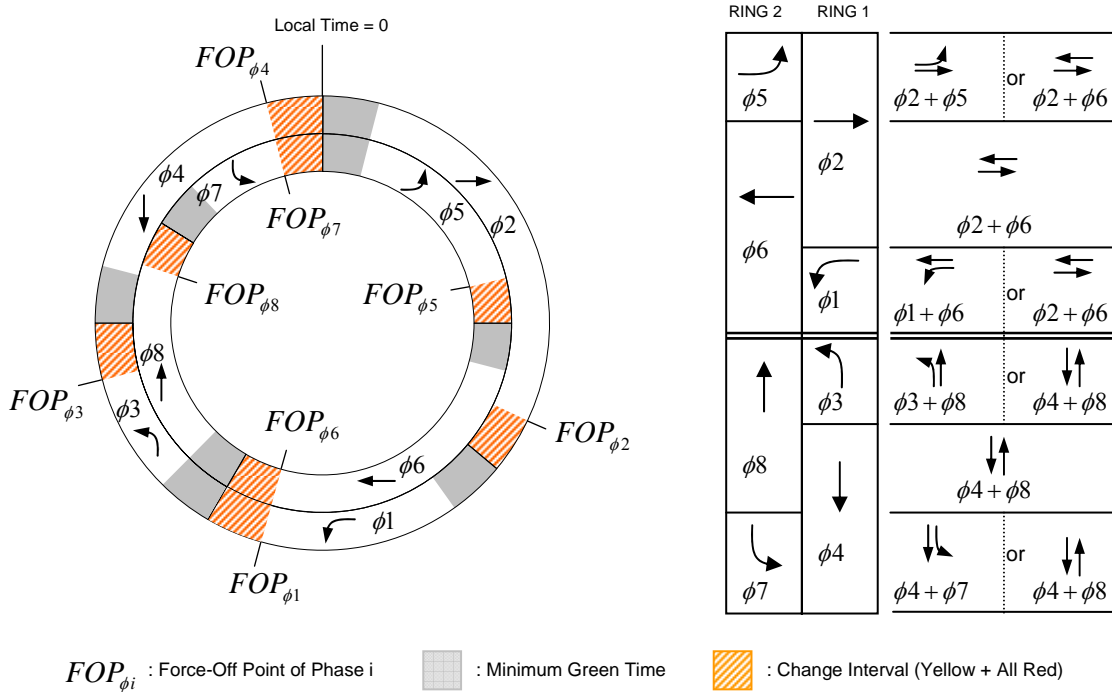
Figure 3-6 Signal phase plan for Bintliff at Bellaire and Rookin at Bellaire

The geometric conditions and traffic volumes for the intersection of Hilcroft Avenue and Bellaire Blvd are shown in Figure 3-7. Both streets have landscaped medians. The eastbound and westbound approaches have two through lanes, one through/right-turn shared lane, and one exclusive left-turn. The northbound approach has two through lanes, one exclusive left-turn lane, and one through/right shared lane. The southbound approach has two through lanes, two exclusive left-turn lanes, and one through/right shared lane. The eastbound approach (toward downtown) experiences traffic congestion during the peak hour while the north-southbound approaches have moderate traffic demand.



**Figure 3-7 Site detail for the intersection of Hilcroft and Bellaire**

Figure 3-8 illustrates a signal phase plan for the intersection of Hilcroft Avenue Street and Bellaire Boulevard. It shows the leading and lagging green phase sequences possible with the eight-phase controller. The phasing is similar to the National Electrical Manufacturers Association (NEMA) standard eight-phase controller with the addition of alternate phases where left and through movements may operate concurrently. The intersection signal operates in a coordinated-actuated mode with a 120-second cycle length. The eastbound and westbound through movements on Bellaire Boulevard are for a coordinated phase. Protected left-turn phases are provided for all approaches. These are actuated phases which could be skipped if there is no vehicle call. The through phases for northbound and southbound approaches are actuated but phase recalls are placed at every cycle (i.e. no skipping). The signal control variables operating in normal mode are shown in Table A-3 in Appendix A.



**Figure 3-8 Signal phase plan for the intersection of Hilcroft Ave and Bellaire Blvd**

### **3.3 STUDY DESIGN**

#### **3.3.1 Prediction Algorithm for Bus Dwell Time**

The use of BSP at intersections with nearside stops has been the subject of much debate. The primary issue focuses on the variability of dwell times at nearside stops that could increase the uncertainty of the bus arrival during the priority phase. The uncertainty may cost buses the benefits of the priority treatment while adding additional delay to the non-priority movements. Therefore, the primary research question for BSP with nearside stops is 1) how to predict the dwell time and its variability accurately, and 2) how to incorporate the dwell time into the BSP timing plan.

The bus dwell time depends on several characteristics of the site and the bus operations including the passenger demand at stop, the frequency of the bus service, the schedule adherence, the number of bus doors, the type of the fare collection system, and other factors. Because of the large variability in dwell time, it has been a challenging task to predict the dwell time at the level of the individual bus stop. In the context of advanced traveler information systems (ATIS), the dwell time is treated as a component of the bus travel time and predicted in conjunction with the link travel time and the intersection delay for entire bus routes or a section of the route. Therefore, for the implementation of local BSP strategy at the intersections with nearside bus stops, a prediction model for the dwell time at the level of the individual bus stop need to be developed.

In this dissertation, a probabilistic model is employed for the representation of the stochastic nature of dwell time. This is because the probabilistic model can consider all determinants as random variables and use the probability density functions as input requirements. A weighted least squares (WLS) regression model has also been developed to model the situation where the variance of dwell time is not constant. The field observation indicates that larger dwell time tends to have larger variation. WLS regression models are known to be useful for estimating the values of model parameters when the response values have differing degrees of variability over the values of the



independent variables, which violates the common assumption of the constant variance for regression modeling.

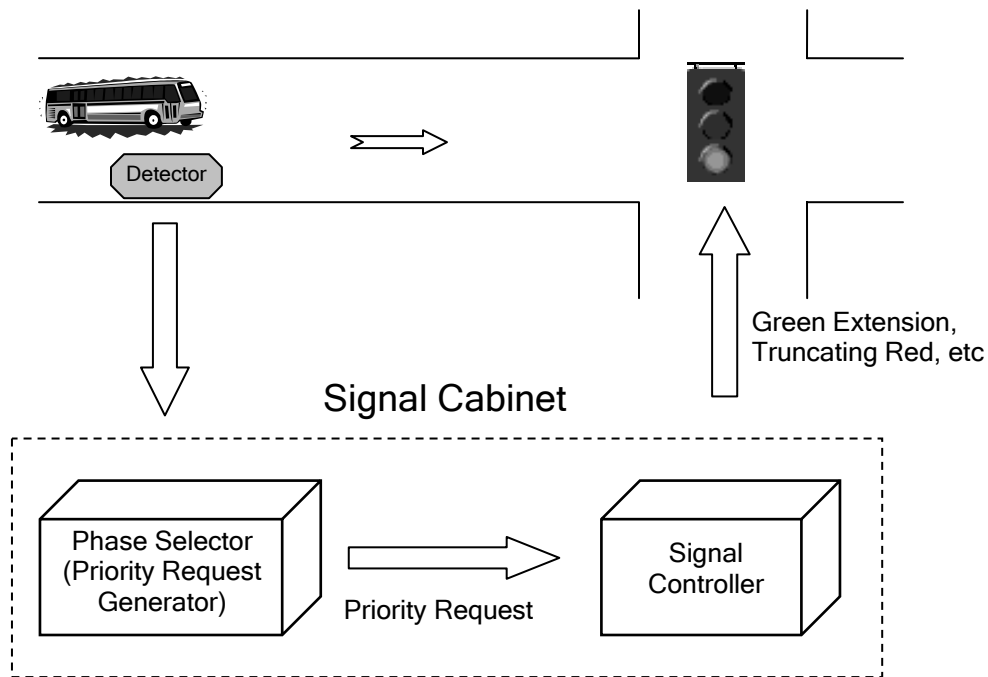
The forecasting process, including the prediction model for dwell time, is itself subject to some prediction error. Moreover, the large variations in dwell times introduce additional errors in the prediction model. In order to accommodate the variability in dwell time, the prediction error bound (i.e. prediction interval) will be incorporated into BSP algorithm. The prediction interval will be obtained from the WLS regression model. The weighting function for the variance results in non-constant prediction interval that increases as the dwell time increases. The prediction models for bus dwell time will be developed in Chapter IV.

### **3.3.2 Bus Signal Priority Strategy**

The Bus Signal Priority (BSP) is a strategy that aims to provide some priority service opportunities without significantly impacting other traffic. When a bus is detected by the detection system, the BSP system generally places a priority request immediately upon the detection of a bus. The signal controller, if not in transition or recovery mode, reacts to the priority request immediately by either extending current green phase or truncating current red phase to start the requested phase earlier. The conceptualization of the most common active BSP system is shown in Figure 3-9. As discussed in Chapters I and II, the normal BSP can operate in inefficient ways when the intersections have high utility nearside stops.

The location of the detector is based on the average bus travel time between the detector and stop line, and is selected so as to ensure that there is a green light when a bus arrives at the intersection (6,10,11). With nearside bus stops, there is a high likelihood that many of the buses will fail to arrive at the intersection during the priority phase whose timing is based upon an anticipated arrival of the bus. The effect of nearside stop in BSP implementation can be taken into account by including an average dwell time in the bus travel time. Note that this approach still assumes that the travel time including dwell time is constant (i.e. pre-defined). If the dwell time varies

significantly, the implementation of BSP may result in unnecessary stops and delay of transit vehicles at the intersection and consequently, it diminishes overall performance of the traffic signal control system.



**Figure 3-9 Conceptualization of active bus signal priority**

In order to reduce the problem of the variability in dwell time, the BSP system needs 1) to be able to re-evaluate a travel time for each bus, and 2) to facilitate signal priority strategies that are capable of accommodating the variation in dwell time. Therefore, the new bus signal priority system has to be developed so as to provide a priority phase that can accommodate the prediction interval of the dwell time without disrupting signal coordination. This improved BSP system will be developed in Chapter V.

### 3.3.3 Microscopic Simulation Model

The evaluation of the improved BSP strategy requires information on each individual unit of traffic, that is, the vehicles and buses. Therefore, a microscopic simulation model based on behavior and periodic-scan is required for this simulation study. The traffic signal logic, including BSP strategy, needs to operate in the simulation model as close as possible to the way they operate in the field. Most existing simulation models such as CORSIM do not provide traffic signal functions for implementing BSP strategies. Recently, the development of new simulation models, including the VISSIM microscopic traffic model, has increased the realism in modeling traffic signal control. VISSIM is a discrete, stochastic, time step based microscopic model, with driver-vehicle-units as single entities. It provides VAP, which is an optional add-on module for the simulation of programmable, phase-based, traffic-actuated signal control. VAP is essentially a computer program used to emulate complex control strategies such as preemption and priority system. Therefore, most functions for BSP implementations can be modeled only with traffic simulation software. All signal functions including BSP strategies and actuated-coordinated signal control can be programmed using VAP.

Prior to the evaluation of a proposed BSP algorithm, the traffic simulation model needs to be calibrated to make the model accurately represent the traffic conditions observed in the field. The calibration of a simulation model is defined as the process by which the individual parameters of the model are adjusted or tuned so that the model represents the interaction between drivers, vehicles, and the environment. The components of a simulation model that require calibration include the model parameters for traffic flow characteristics and driver's behavior. In this dissertation, an automated calibration procedure is developed based on Genetic Algorithm (GA) automated calibration program originally developed at the Texas Transportation Institute (TTI) TransLink<sup>®</sup> Research Center (58,59,60) in Perl language. The proposed procedure utilizes GA algorithm and non-parametric testing methods to find a best parameter set of VISSIM for the simulation of the test bed. The calibration parameters will be the driver behavior parameters for the car-following model and lane change behavior. Two

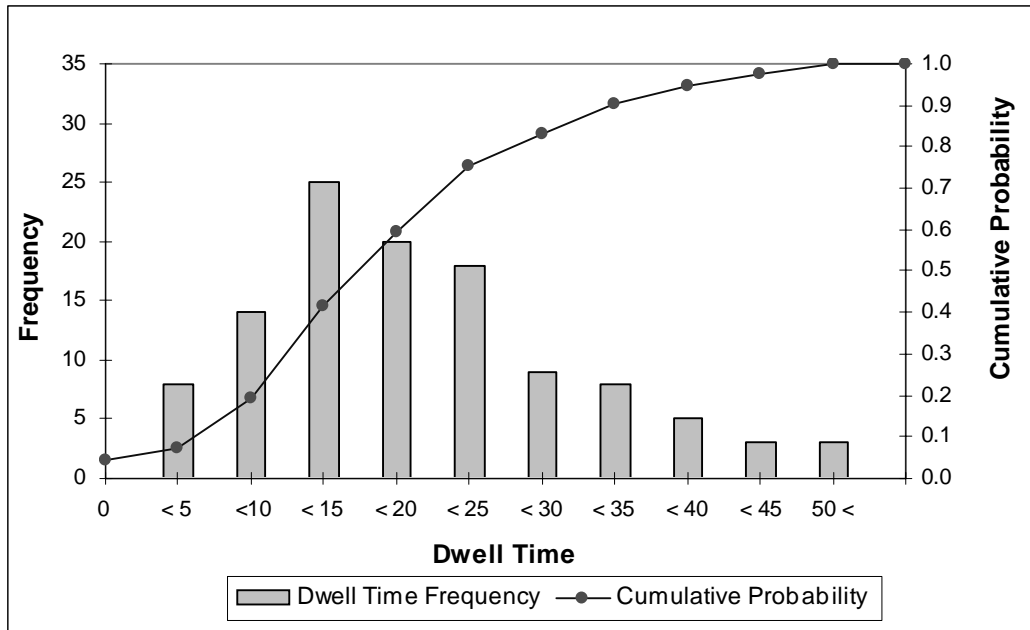
measures of performance were selected for the calibration process. The first measure will be the eastbound travel time for passenger vehicles on Bellaire Blvd. Bus travel time between stops will be used as second performance measure in order to reflect the heterogeneous characteristics of the buses in the simulation studies. The modified calibration methodology will be presented in Chapter VI.

### **3.4 EXPERIMENTAL DESIGN FOR EVALUATION OF BSP STRATEGIES**

#### **3.4.1 Emulating Realistic Dwell Time Variation in the Simulation**

As discussed previously, the improved BSP strategy aims at providing a priority phase that accommodates the variability of dwell time at nearside stops. In order to evaluate the improved BSP strategy, the variation in dwell time has to be input accurately in VISSIM.

The dwell time for each stop in VISSIM is determined by either user-defined dwell time distributions or dwell time calculation using its embedded passenger model (56). The VISSIM passenger model emulates more realistic passenger service process at each bus stop, but it cannot represent the variability in the dwell time correctly because it can only model a constant alighting or boarding time for all passengers. The method using user-defined dwell time distributions can correctly represent the expected dwell time and its associated variation. By defining the cumulative distributions for observed dwell time in VISSIM, the dwell time can be determined by selecting a cumulative percentage between 0.0 and 1.0 randomly. An example result of the computation for route #2 at stop C is shown in Figure 3-10. This would be true if all buses have the equal expectation of dwell time regardless of bus headways or passenger loads. Previous studies and field observations found that the buses with longer headway tend to have longer dwell time because of more passenger arrivals at stops. Because the dwell time distribution in VISSIM, however, cannot be altered during simulation runs, the expectation of the dwell time can not be varied according to the change in bus headways. Therefore, each simulation run can represents a specific level of dwell time and associated variability.

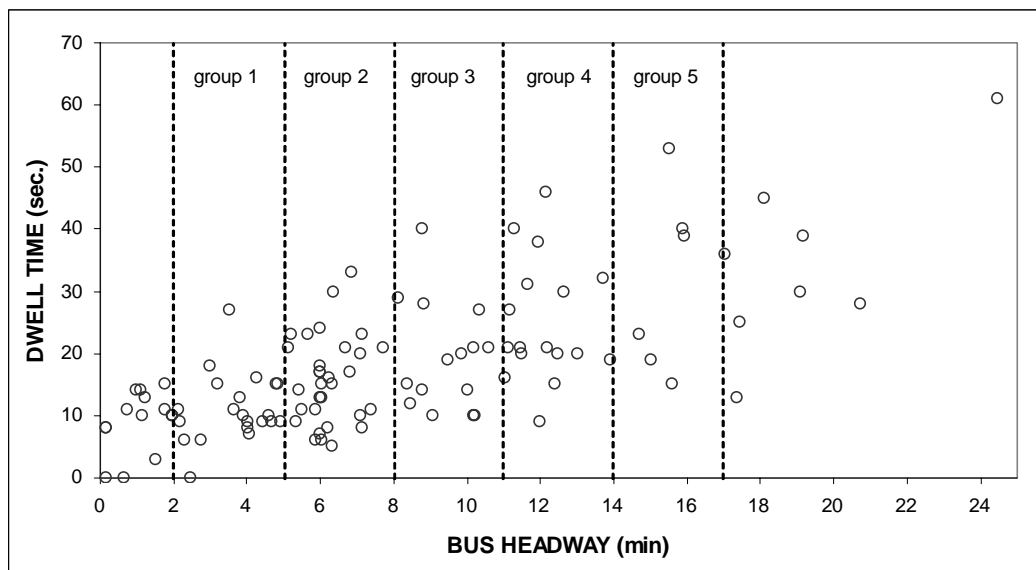


**Figure 3-10 Observed dwell time and cumulative distribution for route #2 at stop C**

For emulation of the realistic variation in dwell time in VISSIM, the bus headways are grouped into several levels and then defined based on empirical dwell time distribution for each group of headways. The simulations are performed for each group of headways, which means that buses with value of headways falling in the same group will have equal expected dwell time. The following steps illustrate an example for route #2 at stop C:

*Step 1:* Divide the bus headways into several groups. For example, the headways for route #2 at stop C are divided into five groups as shown in Figure 3-11. The headways of less than 2 minutes are excluded because the improved BSP algorithm is designed not to grant more than one priority service within a cycle (2 minutes). The headways greater than 17 minutes are excluded because the number of observations is not enough to derive a cumulative distribution.

- Step 2:* Define empirical cumulative distributions from observed dwell times for each headway group.
- Step 3:* Set the bus headway at the median of each headway group in order to generate buses with pre-defined simulation interval in VISSIM. Because the bus headway needs to vary for realistic emulation, a dummy bus stop at the dedicated dummy link is introduced. By assigning an adequate dwell time distribution to the dummy stop, the bus headway varies within the interval for each headway group.
- Step 4:* Perform the simulation for each headway group with its empirical cumulative distribution in step 2 and by using pre-defined headways from step 3 for the buses.



**Figure 3-11** An example of bus headway groups for route #2 at stop C

### **3.4.2 Evaluation of the Improved BSP Strategy**

The improved BSP strategy will be evaluated using VISSIM simulation model (with VAP). The simulation time chosen for the analyses is 1 hour and 10 minutes, including a normalization period of 10 minutes at the beginning to stabilize the traffic over the network. The traffic volume and signal timing of the base case (morning peak period) will be used for the all the simulation scenarios modeled.

The improved BSP strategy will be evaluated by comparing its performance with the following three signal operations: i) Normal operation (without BSP), ii) Basic BSP, and iii) BSP which considers average dwell time. The term ‘Normal operation’ implies the current coordinated-actuated signal logic operating in the test bed as discussed in 3.2.2. The terms ‘Basic BSP’ and ‘BSP with average dwell time’ will be discussed briefly in the following sections. The details on system architecture for BSP with average dwell time logic can be found in Appendix B. Four different VAP codes, including improved BSP strategy, were developed as parts of this dissertation.

#### *3.4.2.1 Basic BSP*

An active BSP system that is commonly implemented in practice was developed for the purposes of this dissertation. The basic BSP strategy utilizes a check-in detector which sense approaching buses upstream from the stop line. When a bus reaches the check-in detector, a priority request is immediately sent to the controller. The request is assessed based on pre-defined criteria such as number of passengers on the bus. If the request is eligible, the BSP strategy is implemented according to the current signal status at the approach of interest. A green extension strategy will be selected when a bus is detected during green time. For the bus arriving during a red period for its approach, an early green strategy is selected. The maximum green extension was set at 20 seconds and the allowance of early green was subjected to the minimum phase requirements of non-priority phases such as minimum green and change interval including yellow change interval and vehicle clearance time. Check-in detectors were located 200 meters

upstream from stop lines of the intersections. Complete details of the basic BSP strategy can be found elsewhere (5,9,10).

#### *3.4.2.2 BSP with consideration of average dwell time*

This BSP strategy incorporates the dwell time into the BSP timing plan through the addition of average dwell time in the calculation of the bus travel time from the check-in detector to the stop line. Once a bus is detected at check-in detector, the BSP algorithm assesses whether a priority service is granted through the evaluation of pre-defined criteria (i.e. number of passengers on the bus). If the bus satisfies these criteria, an adequate priority is implemented depending on when in the cycle the bus arrives at the intersection. The bus dwell time is taken into consideration in calculating bus arrival time at the intersection. The strategies used to provide priority include green extension, early green, and phase insertion strategy. Based on the bus arrival time in the cycle, multiple strategies can possibly be selected to service the bus. The algorithm examines which strategy can accommodate the approaching bus with the minimum change in the background signal plan. In other words, the selected strategy has the phase durations most closely matched with those of the background timing plan.

The traffic signal cycle can be divided into periods that define where the different strategies can be used to service the arriving buses. The time period for each strategy is determined by the variable green time (i.e. a split minus minimum green and change interval) of non priority phases adjacent to the priority phase. Through adjustments in the lower/upper bounds of the periods, the cycle can be divided into multiple periods that do not overlap each other. At any specific point of time in the cycle, only one strategy is available to be implemented. The anticipated arrival time of the bus is compared to the threshold values of the periods to determine which priority strategy is to be implemented. Figure B-1 in Appendix B shows the periods of each of the strategies in a four-phase traffic signal. A check-in detector is placed 360 meters upstream from the stop line and the observed average travel time for buses is used in calculating the bus arrival time.



The primary objective is the reduction in bus delays at the intersections. The measures of effectiveness (MOE) are the average signal delay per bus, bus travel time along the test bed, and the percentage of bus arrivals in green time. The secondary objective will be to minimize the negative impacts of non-priority movement and the MOEs will be the average delay per vehicle on non-priority approaches and the overall average delay at a given intersection. Because the performance of BSP implementation depends on traffic demand at the intersections, a sensitivity analysis will be performed. Four signal operations will be tested at various traffic volume levels, including 70%, 80%, 90%, 100%, 110%, 120%, and 130% of AM peak demand. The width of the priority window (i.e. prediction interval) in BSP strategies affects both the bus delay and the overall performance at the intersection. A wider priority window reduces bus delay but increases additional delay to non-priority traffic. The effects of the prediction interval will be assessed with different significant levels including  $\alpha=0.3$ ,  $\alpha=0.2$ ,  $\alpha=0.1$ ,  $\alpha=0.05$ , and  $\alpha=0.01$ . Ten simulation runs with different random seed numbers were performed for each scenario in order to allow a statistical analysis of whether a difference in MOE occurs as result of implementing the different BSP strategies.

### **3.5 CONCLUDING REMARKS**

The prediction models for the dwell time/interval and the improved BSP strategy were introduced in this chapter. The prediction models for dwell time will be developed using both the probabilistic model and the WLS regression model in Chapter IV. The improved BSP strategy, where the prediction interval of bus dwell time was incorporated into the BSP timing plan, will be developed in Chapter V.

The VISSIM micro-simulation model, a behavior and periodic-scan based micro-simulation model, was chosen for this study because it provides VAP (vehicle actuated programming), which is an optional add-on module for the simulation of programmable, phase-based traffic-actuated signal controls. Using VAP, BSP functions that are not provided by either vendor-specific controllers or conventional simulation models could be modeled within the simulation environment. All signal control logic in this study

including the coordinated-actuated signal control, current BSP system, and the improved BSP system, were programmed in VAP.

The test bed chosen for this study was the arterial section of Bellaire Blvd in Houston, Texas. The arterial section is approximately 1.1 km in length and is located between Bintliff Drive and Hilcroft Avenue. Three bus stops including two nearside stops were chosen for developing the dwell time prediction models. Two signalized intersections (Rookin and Bellaire, Hilcroft and Bellaire) were chosen as the test bed for the development of the improved BSP system.

## CHAPTER IV

### DWELL TIME ESTIMATION AND PREDICTION INTERVAL

Implementation of a BSP system at local intersections with nearside bus stops requires the ability to forecast bus dwell time at stops. However, because of large variability in dwell time, an accurate prediction is difficult to achieve and there can be large differences in the forecast and actual arrival time. The uncertainty in bus dwell time in the BSP system can be mitigated by employing a prediction interval instead of a predicted dwell time.

In this chapter, a probabilistic model will be examined for predicting the bus dwell time. Because probabilistic models utilize the probability distributions for both alighting and boarding passengers at each bus stop, the probability distributions for the numbers of both alighting and boarding passengers will be defined for each stop. As an alternative, a weighted least squares (WLS) regression model will be developed because WLS regression models are known to be useful for estimating the values of model parameters when the response values have differing degrees of variability over the values of independent variables. The weighting function for the variance will result in a non-constant prediction interval that increases as bus headway increases.

As discussed in Chapter III, the dwell time data were collected from three Metro bus stops along an arterial section in Houston, Texas. Dwell time and passenger counts were measured at each stop. Even though the prediction model has been developed using the bus and passenger data at specific bus stops, the methodology is applicable to any location where similar data are available.

#### 4.1 PROBABILISTIC MODEL FOR ESTIMATING DWELL TIME

The probabilistic models that consider alighting/boarding passengers as random variables allow for a better representation of the stochastic nature of dwell time (43,53). Once the probability density functions for the number of alighting and boarding

passengers are successfully defined, the dwell time can be predicted using the expectations of the probability distributions and other given quantities such as the marginal service times for alighting and boarding activities.

#### **4.1.1 Determinants of the Probabilistic Model**

The bus dwell time consists of the time needed for the following events to occur; 1) opening and closing doors, 2) passenger boarding, 3) passenger alighting, 4) schedule slack, and 5) clearance of bus from the bus stop. Note that some of these activities are sequential while others are simultaneous. Details of each of these time component were discussed in Chapter II. In the probabilistic model, all components of dwell time may be random variables. However, in this dissertation the passenger boarding and alighting times were assumed as determinants of the dwell time because dwell time is defined as a time period in which the bus doors are opened to serve passengers at a specific stop. By this definition, the schedule slack time should be included in dwell time. Because the field observation found that only two buses at stop C waited with their doors open until the scheduled departure time, it was decided that the scheduled slack time would not be considered in the model.

The probabilistic model has been defined as a function of passenger alighting time and passenger boarding time. If the numbers of passengers alighting and boarding are independent of each other, the dwell time was expressed by the sum of two random variables as shown in Equation 4-1. The marginal passenger alighting and boarding time were assumed constant.

Equation 4-1 is a reduced form that excludes the door opening and closing time, schedule slack time, and the clearance time from Equations 2-1 and 2-6. An appropriate probability distribution for each determinant (i.e. number of alighting and boarding passengers) needs to be defined to estimate the dwell time.

$$t_d = N_a \cdot t_a + N_b \cdot t_b \quad (4-1)$$

where

- $t_d$  = bus dwell time (sec),
- $N_a$  = alighting passengers per bus (p),
- $t_a$  = marginal passenger alighting time (sec/p),
- $N_b$  = boarding passengers per bus (p), and
- $t_b$  = marginal passenger boarding time (sec/p).

#### 4.1.2 Probability Distribution for the Number of Boarding Passengers

The number of boarding passengers for a specific bus can be defined as the number of passenger arrivals during the headway between buses at a specific bus stop. It has been assumed that all passengers for a given bus route that arrive in the time points between two buses (i.e. bus headway) will get aboard the following bus. In an urban environment, the bus dispatching frequency is high during peak periods in order to meet the demand. Previous studies (42,43,53,54) suggested that the Poisson distribution is an appropriate probability distribution for passenger arrivals at stops during the peak period. The Probability Mass Function (PMF) of the Poisson distribution for random variable  $X$  can be calculated according to Equations 4-2 and 4-3.

$$P[\text{arrivals during headway } N_b = x] = f(x) = \frac{m^x e^{-m}}{x!} \quad (4-2)$$

$$m = \int_a^b \lambda(t) dt \quad (4-3)$$

where

- $N_b$  = number of passenger arrivals during preceding headway,
- $a$  = departure time of previous bus,
- $b$  = arrival time of current bus, and
- $\lambda(t)$  = passenger arrival intensity (p/sec).

The preliminary evaluation of the dwell time data collected from the test bed showed that the number of passenger arrivals during a specific time period (i.e. 5-minute interval) had large variation. For example, the coefficients of variance were 77% and 94% for the peak period and off peak period, respectively. It was noted that variance during the peak period (i.e. 7:00 ~ 8:30 AM) was greater than that during off peak period. The statistics for the passenger arrivals at each stop are summarized in Table 4-1 where the units are a number of passenger arrivals during a 5-minute period.

**Table 4-1 Summary of statistics for passenger arrivals during 5 minute period**

	Stop A		Stop B		Stop C	
	Mean (pass/5 min)	Variance (pass/5 min) <sup>2</sup>	Mean (pass/5 min)	Variance (pass/5 min) <sup>2</sup>	Mean (pass/5 min)	Variance (pass/5 min) <sup>2</sup>
Peak 7:00 ~ 8:30	1.57	1.60	1.6	1.65	2.28	2.62
Off peak 8:30 ~ 10:00	1.53	1.87	0.66	0.88	1.35	1.66

As shown in Table 4-1, the large variation in passenger arrivals led to the employment of the negative binomial distribution. This Probability Density Function (PDF) may be characterized as having a variance higher than the mean whereas Poisson distribution requires a variance equal to the mean. The PDF of the negative binomial distribution for a random variable  $X$  can be calculated according to following equations (57,61):

$$P[X = x|r, p] = \binom{x+r-1}{r-1} p^r (1-p)^x \quad (4-4)$$

$$\mu = \frac{r(1-p)}{p} \quad (4-5)$$

$$s^2 = \frac{r(1-p)}{p^2} \quad (4-6)$$

where

$X$  = number of passenger arrival,

$r$  = number of success, and

$p$  = probability of success.

$\mu$  = sample mean

$s^2$  = sample variance

From Equation 4-5 and 4-6, the parameters  $p$  and  $r$  can be derived based on the mean and variance of the sample population as follows:

$$p = \frac{\mu}{s^2} \quad (4-7)$$

$$r = \frac{\mu^2}{s^2 - \mu} \quad (4-8)$$

The chi-square ( $\chi^2$ ) test, a goodness of fit test, was performed to evaluate the null hypothesis that the observation of passenger arrivals at each stop is drawn from assumed distribution (i.e. Poisson and negative binomial). Because the number of passenger arrivals during 5 minutes is a multinomial random variable, Pearson's chi-squared test was selected. As shown in Table 4-1, passenger arrival rates varied according to the time of day. The arrival rate during peak period was much higher than that during off peak period. In order to consider the variation of passenger arrival rate by time of day,

passenger arrivals are divided into two time-periods: peak (7:00 AM – 8:30 AM) and off-peak (8:30 AM – 10:00 AM). Table 4-2 gives the observed number of passenger arrivals and projected values from assumed distributions for each bus stop during the peak period. Mean Absolute Percentage Errors (MAPE) by Equation 4-9 are presented in the table. The Poisson distribution and the negative binomial distribution gave similar results. This was because the mean and variance during peak period were similar, which satisfies the assumption of the Poisson distribution (i.e. mean and variance are equal). Figure 4-1 also illustrated the observed data and projected values for stop A.

$$MAPE(\%) = \frac{1}{N} \sum \frac{|observed - projected|}{observed} \times 100 \quad (4-9)$$

where

$N$  = number of classes

**Table 4-2 Passenger arrivals with Poisson and negative binomial distribution during peak period (7:00~8:30 AM)**

Number of passenger arrival	STOP A			STOP B			STOP C		
	Obs.	Poisson	N.B.	Obs.	Poisson	N.B.	Obs.	Poisson	N.B.
0	19	18.6	18.9	16	18.2	19.1	8	9.1	11.6
1	30	29.3	29.3	35	29.1	29.2	27	20.9	22.2
2	21	23.1	22.9	21	23.3	22.7	25	23.9	22.7
3	12	12.2	12.0	79	12.4	12.0	12	18.2	16.4
4	6	4.8	4.8	5	5.0	4.8	8	10.4	9.5
5	2	2.0	2.1	4	2.1	2.2	4	4.8	4.6
6+	-	-	-	-	-	-	6	2.6	3.1
MAPE (%)	-	6.0	6.2	-	28.9	29.6	-	30.9	24.3

The observed and projected numbers of passenger arrivals during off peak period were given in Table 4-3 and Figure 4-2. The negative binomial distribution provided better projected estimates than Poisson distribution because the variance was larger than



the mean for all stops during the off peak period. However, the improvements by using the negative binomial distribution were not substantial.



Figure 4-1 Observed and predicted passenger arrival during peak period at stop A

Table 4-3 Passenger arrivals with Poisson and negative binomial distribution during off-peak period (8:30~10:00 AM)

Number of passenger arrival	STOP A			STOP B			STOP C		
	Obs.	Poisson	N.B.	Obs.	Poisson	N.B.	Obs.	Poisson	N.B.
0	24	19.4	22.5	49	46.2	51.5	25	23.6	26.9
1	29	29.8	28.3	27	30.8	25.1	35	31.8	29.7
2	17	22.8	20.3	11	10.3	9.2	16	21.5	19.1
3	10	11.7	10.9	1	2.3	2.5	9	9.7	9.3
4	6	4.5	4.9	2	0.4	1.3	3	3.3	3.9
5+	3	1.8	3.0	-	-	-	3	1.1	2.1
MAPE (%)	-	23.0	9.2	-	47.2	42.7	-	30.2	24.4



**Figure 4-2 Observed and predicted passenger arrival during off peak period at stop A**

A chi-square ( $\chi^2$ ) goodness of fit test was performed for each distribution. A significance level of 5 percent was used. This means that if the hypothesis that the passenger arrival distribution is Poisson distribution is rejected, there is a 5 percent chance that the data may, in fact, be Poisson distribution. The observed  $\chi^2$  value along with the test value was shown for each data set in Table 4-4.

It can be concluded that passenger arrivals during 5 minutes at each stop for both peak and off-peak period give no evidence of a statistical difference from either Poisson or negative binomial distribution. It can be seen that the calculated  $\chi^2$  values of both distributions during peak period did not show much difference. During the off peak period the negative binomial distribution always resulted in much lower calculated  $\chi^2$  values than Poisson distribution.

From the evaluation of projected passenger arrivals in Table 4-2 and 4-3 as well as the result of the goodness of fit test in Table 4-4, it can be concluded that the negative binomial distribution performs slightly better than the Poisson distribution for the stops in the study site of this dissertation.

**Table 4-4 Chi-square goodness-of-fit test for Poisson and negative binomial distributions**

Time of Day	Stop	Poisson		Negative Binomial	
		Chi-Square	Test Value	Chi-Square	Test Value
Peak Period	STOP A	0.52	9.49 ( 4 df )	0.47	7.81 ( 3 df )
	STOP B	4.26	9.49 ( 4 df )	4.06	7.81 ( 3 df )
	STOP C	9.06	11.1 ( 5 df )	6.60	9.49 ( 4 df )
Off Peak Period	STOP A	5.97	9.49 ( 4 df )	1.33	7.81 ( 3 df )
	STOP B	6.99	7.81 ( 3 df )	2.35	5.99 ( 2 df )
	STOP C	4.97	9.49 ( 4 df )	2.17	7.81 ( 3 df )

Although the negative binomial distribution resulted in lower  $\chi^2$  values than the Poisson distribution, there was no statistical evidence in favor of the negative binomial distribution because both distributions had not been rejected in any data set. The negative binomial distribution was selected as an appropriate descriptor for the number of passengers arriving at stop for a given time period because the underlying assumption of the Poisson distribution (i.e. equality of mean and variance) could not be held. With the assumption of stationary passenger arrivals, the negative binomial distribution can provide an expected number of passenger arrivals for various levels of bus headway. The details about this assumption can be found in Appendix C.

#### **4.1.3 Probability Distribution for the Number of Alighting Passengers**

In the case of independent alighting and steady-state demand conditions, a binomial distribution is known to be an appropriate representation for the number of alighting passenger (48,53). If the alighting proportion for a given bus stop is stationary, the distribution of the number of alighting passengers can be derived from the conditional probability as shown in Equation 4-10.

$$f(x) = P(N_a = x | L = l) \quad (4-10)$$

where

$N_a$  = number of passenger alighting ( $p$ ), and

$L$  = total number of passengers on the bus.

The conditional probability of ‘ $x$ ’ alighting passengers for a given passenger loads ‘ $L$ ’ has a binomial distribution. If the number of passengers on bus is known, for example, through an APC system, the probability distribution for alighting passengers is binomial  $Bi(L, p)$ .

$$P[\text{passenger alighting } N_a = x] = f(x) = \sum_{L=x}^{\infty} \binom{L}{x} p^x (1-p)^{L-x} \quad (4-11)$$

where

$p$  = probability of alighting for a randomly chosen passenger on bus.

In the probabilistic model for dwell time estimation, the number of passenger alighting at each stop will be assumed to follow the binomial distribution. The probability of alighting and passenger loads will be the parameters for the model.

#### 4.1.4 Marginal Alighting and Boarding Times

The marginal service time required for passengers alighting and boarding had been provided in Table 27-9 in the HCM 2000. For an articulated bus with two doors the values are 2.6 s for each boarding passenger and 1.0 s for each alighting passenger. Note that these values are quite different from the observed data. Because the values drawn from HCM indicate the typical time headways between successive alighting or boarding passengers, they exclude the delays caused by passenger’s retardation in alighting or boarding activity and in collecting the fare. Therefore, the actual alighting and boarding

time for each passenger including passenger retardation must be estimated from the observed dwell time data.

In order to estimate marginal passenger service time, a multiple linear regression (MLR) model was developed. The estimated coefficients of the MLR for the number of alighting and boarding passengers are shown in Equation 4-12.

$$t_d = 2.55 N_a + 6.07 N_b \quad (4-12)$$

where

$$\begin{aligned} t_d &= \text{bus dwell time (sec),} \\ N_a &= \text{alighting passengers per bus (p),} \\ N_b &= \text{boarding passengers per bus (p), and} \end{aligned}$$

The regression output revealed that the adjusted  $R^2$  value was 0.33, with parameters that are significant at the 95% level. The model indicated that each alighting passenger requires 2.55 second and an additional 6.07 seconds are consumed for each passenger boarding through both doors. Therefore, the marginal passenger alighting and boarding times were estimated as 2.55 s and 6.07 s, respectively.

#### 4.1.5 Estimation of Bus Dwell Time Using a Probabilistic Model

As discussed previously, the probabilistic model for dwell time estimation assumes that the number of alighting or boarding passenger are random variables. It was found that the Poisson and binomial distribution, respectively, were appropriate descriptors for boarding and alighting passengers at each stop. Based on the definition of the binomial distribution, the number of alighting passengers  $N_a$  in Equation 4-1 can be substituted by the production of the ‘conditional expectation given passenger load  $l$ ’ and ‘alighting probability  $p$ ’. The number of boarding passengers can also be expressed by the conditional expectation given arrival rate  $\lambda$  and bus headway  $h$ . Based on these substitutions, expected bus dwell time can be estimated using a model that assumes a

linear relationship between passenger demand and marginal passenger service time as follows:

$$E[t_d] = t_a \cdot E[N_a = a | L = l, P = p] + t_b \cdot E[N_b = b | \Lambda = \lambda, \Delta t = h] \quad (4-13)$$

$$t_d = t_a \cdot (p \cdot l) + t_b (\lambda \cdot h) \quad (4-14)$$

where

- $t_d$  = bus dwell time (s),
- $t_a$  = marginal passenger alighting time (sec),
- $p$  = alighting probability for passenger in bus,
- $l$  = passenger loads (p),
- $t_b$  = marginal passenger boarding time (sec/p),
- $h$  = bus time headway (min), and
- $\lambda$  = passenger arrival rate (p/min).

As discussed in Chapter III, the bus dwell time only was estimated for route #2 because the other routes do not provide service for all the stops. The alighting probability  $p$  and passenger arrival rate  $\lambda$  for each stop were estimated by Equation 4-15. Table 4-5 showed alighting probability and passenger arrival rate for each stop during the peak and off peak periods

$$p_k = \frac{1}{n} \sum \frac{\text{observed alighting of bus } i}{\text{observed passenger load of bus } i} \quad (4-15)$$

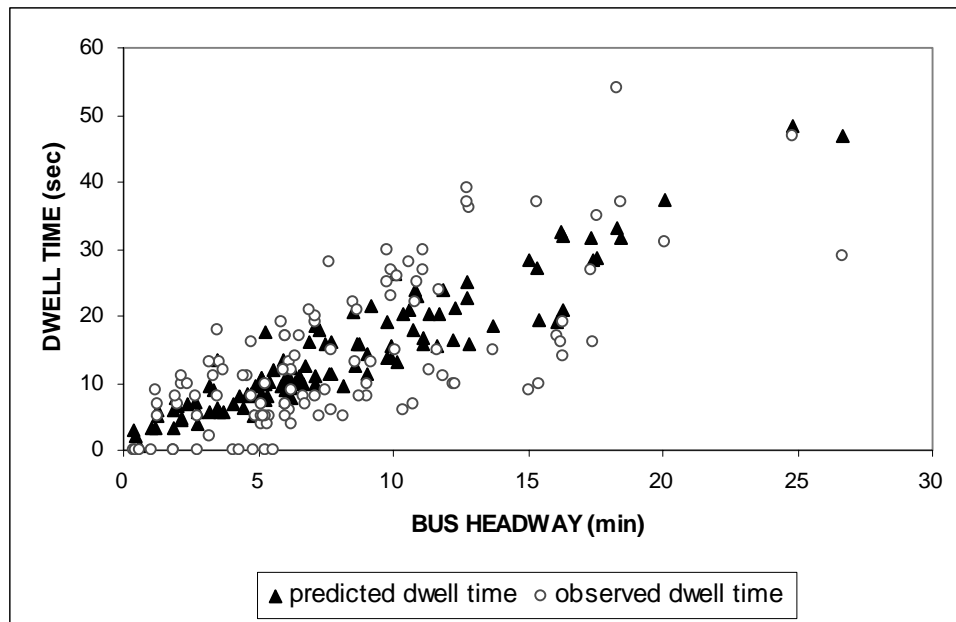
where

- $p_k$  = alighting probability at stop  $k$ ,
- $N_k$  = number of observed bus at stop  $k$ ,

**Table 4-5 Probability of alighting for passengers on buses at each stop (Route #2)**

	Stop A		Stop B		Stop C	
	Peak	Off-Peak	Peak	Off-Peak	Peak	Off-Peak
alighting probability (0~1.0)	0.071	0.131	0.065	0.040	0.125	0.171
arrival rate (passenger/minute)	0.169	0.238	0.169	0.111	0.411	0.313

The dwell times for stop A were plotted as a function of bus headway in Figure 4-3. For the purpose of the illustration, dwell times were arranged by bus headways (i.e. X axis) because dwell time data collected from the test bed showed a positive linear relationship with bus headway. The predicted dwell time showed a strong linear relation with bus headways and fluctuated moderately with variation in the number of alighting passengers. Because the dwell time itself has large variability caused by randomness in the passenger demand and passenger's service delay, large average absolute error (see Table 4-6) resulted. Same plots for stop B and C can be found in Figure D-1 and D-2 in Appendix D.

**Figure 4-3 Predicted and observed dwell time at stop A**

The average absolute error (AAE) of predicted dwell time was calculated by Equation 4-16. For all bus stops during peak and off peak period, AAE and average predicted dwell time are summarized in Table 4-6. The ratio of AAE to average predicted dwell time was also provided.

$$AAE_k = \frac{\sum_{i=1}^N |O_{ki} - P_{ki}|}{N_k} \quad (4-16)$$

where

- $AAE_k$  = average absolute error at stop  $k$  ( $k=1,2,3$ ),  
 $O_{ki}$  = observed dwell time for bus  $i$  at stop  $k$  ( $k=1,2,3$ ),  
 $P_{ki}$  = predicted dwell time for bus  $i$  at stop  $k$  ( $k=1,2,3$ ), and  
 $N_k$  = number of buses at stop  $k$  ( $k=1,2,3$ ).

**Table 4-6 Average absolute error and average predicted dwell time for all stops**

	Stop A		Stop B		Stop C	
	AAE (sec)	Average Dwell Time	AAE (sec)	Average Dwell Time	AAE (sec)	Average Dwell Time
Peak	5.46 (54%)	9.93	3.87 (39%)	9.82	7.84 (36%)	21.98
Off peak	7.63 (37%)	20.46	3.80 (44%)	8.62	9.98 (36%)	27.53
Overall	6.35 (44%)	14.24	3.84 (41%)	9.33	8.71 (36%)	24.24

Because of the large AAE values for dwell time, it was decided to conduct the diagnosis on the linear relationship between dwell time and its determinants such as alighting and boarding passengers. Through examining the significance of each determinant to dwell time, the probabilistic model proposed in this study will be evaluated and an alternative approach can be proposed, if necessary.



## 4.2 DETERMINANTS FOR DWELL TIME

The probabilistic model in section 4.1 was based on the assumption of a linear relationship between the number of alighting passengers and the number of passengers on the bus, and the number of boarding passengers and bus headways. These relations were presented in Equation 4-13. Therefore, the probabilistic model is valid only when a linear relationship exists between the determinants. In the following section, by using the analysis of coefficients of correlation and multiple linear regression model, the assumption of linear relationship between determinants will be examined. In addition, most statistically significant determinants of dwell time will be identified.

### 4.2.1 Analysis of Relations between Determinants and Dwell Time

#### 4.2.1.1 Analysis of coefficient of correlation

A linear relationship between two random variables can be measured by the correlation coefficient (62). The correlation coefficient is a measure of the degree of linear relationship between variables and it lies between -1 and 1, inclusive. High absolute value indicates strong relationship. The correlation coefficient of variable  $X$  and  $Y$  can be obtained using Equation 4-17.

$$\rho = \frac{n \sum x_i y_i - (\sum x_i)(\sum y_i)}{\sqrt{n \sum x_i^2 - (\sum x_i)^2} \sqrt{n \sum y_i^2 - (\sum y_i)^2}} \quad (4-17)$$

where

$\rho$  = correlation coefficient,  $-1 < \rho < 1$ ,

$x_i$  and  $y_i$  = random variables,  $i = 1, \dots, n$ , and

$n$  = number of sample population.

The correlation coefficients between the number of alighting (boarding) passenger and passenger loads (bus headways) were calculated to examine the linear

relationship. Figure 4-4 illustrates the relationship between the number of alighting passengers and passengers on the bus at stop A. No linear relationship was found and the value of correlation coefficient was 0.199. The number of alighting passengers and passenger loads at stop B and stop C also had no linear relationship as illustrated in Figure D-3 and D-4 in Appendix D. The correlation coefficients were 0.073 and 0.21 for stop B and stop C, respectively.

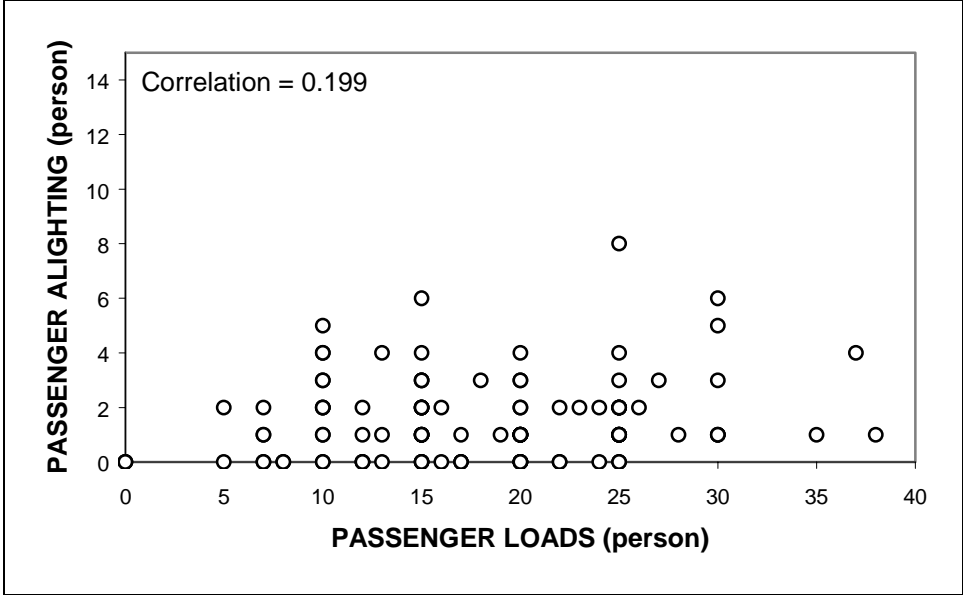
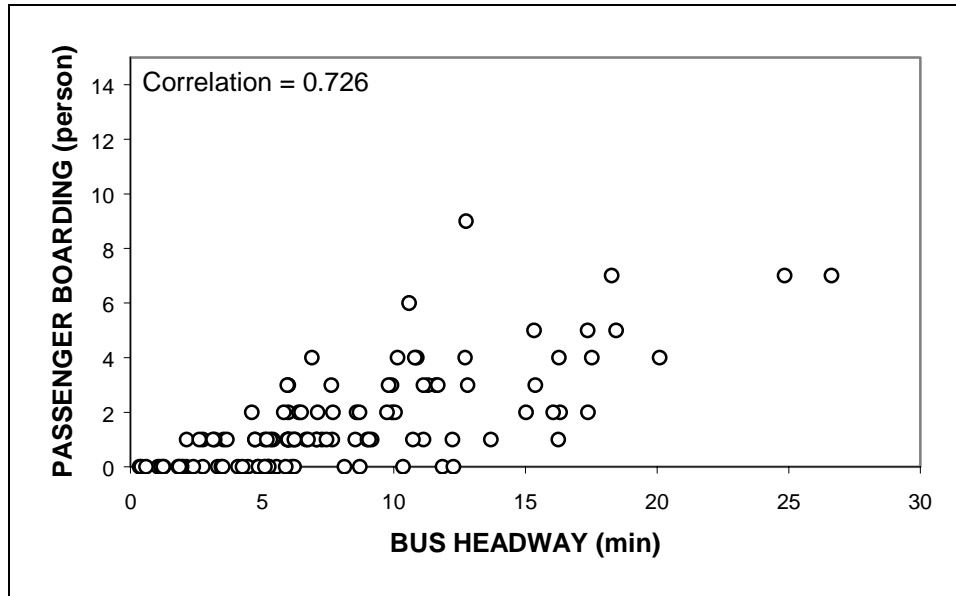


Figure 4-4 Relationship between passenger alighting and passenger loads at stop A

A visual examination of Figure 4-4 confirmed the correlation coefficients results. Base on these results, it can be concluded that no linear relationship exists between the number of alighting passengers and passengers on the buses at any of the stops. This is important because the probabilistic model is on the basis of the assumption of linear relation between alighting passengers and passenger loads.

The relationship between bus headway and the number of boarding passengers, is illustrated in Figure 4-5. It can be seen that there is a strong linear relationship as evidenced by the value of correlation coefficient. The correlation coefficients of 0.726,

0.496, and 0.702 for stops A, B, and stop C, respectively (The plots for stop B and C can be found in Figure D-5 and D-6 in Appendix D). Although the correlation coefficient for stop B indicated only a moderate linear relationship, it can be concluded that the number of boarding passengers and bus headways has a linear relationship, in general.



**Figure 4-5 Relationship between passenger boarding and bus headway at stop A**

The correlation coefficient analysis led to the conclusion that the number of boarding passengers has a linear relationship to the bus headway while the number of alighting passengers has no linear relationship to passengers on the bus for the stops in test bed. This conclusion indicates that an assumption of the probabilistic model was violated. Therefore, an alternative method was needed for estimating dwell time. The alternative methods do not guarantee better results than the probabilistic model. However, the alternatives can provide more reliable results if they satisfy underlying modeling assumptions.

#### 4.2.1.2 Analysis of coefficient of parameter in multiple regression model

Multiple linear regression models were developed in order to evaluate the relationships between determinants and dwell time. The determinants of dwell time at a specific bus stop could include passenger loads, bus headways, schedule adherence, time of day, dwell time at adjacent upstream stop, etc. In this dissertation three variables were considered in the model: schedule adherence, passenger loads, and bus headways. These determinants have been commonly used variables in the estimation of dwell time or bus travel time in previous studies (47,50,51,53). In addition, the preliminary analyses indicated that these were good candidates.

The regression model in Equation 4-18 was developed for each bus stop, and two sided t-tests at a 0.05 significance level were conducted to determine statistical significance. The test results of the models were summarized in Table 4-7. P-values and t-test statistics of the estimated coefficients of the parameters are shown in the table. Because the  $R^2$  value can only increase by adding more  $X$  variables, an adjusted  $R^2$  was employed. The adjusted  $R^2$  accounts for this phenomena and effectively allows models with different number of parameters to be compared.

$$Y_i = \beta_0 + \beta_1 X_{i1} + \beta_2 X_{i2} + \beta_3 X_{i3} + \varepsilon_i \quad (4-18)$$

where

$Y_i$  = bus dwell time of  $i$  th bus (sec),

$\beta$  = parameter,

$X_{i1}$  = schedule adherence (sec),

$X_{i2}$  = passenger loads (person),

$X_{i3}$  = bus headway (minutes), and

$\varepsilon_i$  = random error,  $N(0, \sigma^2)$ .

**Table 4-7 Summary of multiple regression models**

	STOP A		STOP B		STOP C	
	P-Value	t Stat	P-Value	t Stat	P-Value	t Stat
Schedule adherence	0.09	1.73	0.94	0.07	0.81	-0.23
Passenger loads	0.38	0.88	0.56	0.59	0.63	0.48
Bus headway	0.00	7.45*	0.000	5.16*	0.00	7.64*
Adjusted $R^2$	0.49		0.27		0.43	

Note:

\* indicates statistically significant at 0.05 level

The results of MLR analysis shown that the estimated coefficient of the parameter for passenger loads was high p-values (0.38~0.63) in all stops, which implies that passenger load is not a significant determinant in the model. This was confirmed by the t-statistic results. The schedule adherence was insignificant in the models for stop B and C. Low  $R^2$  values of the MLR models indicated that the observed data have large variation and the prediction with these models would results in large prediction errors.

#### 4.2.2 Simple Linear Regression Model

The MLR analysis concluded that the bus headways among three determinants have a linear relationship with bus dwell time but not schedule adherence nor passenger loads. Therefore a simple linear regression model was built for each bus stop. Figure 4-6 shows an estimated regression line for stop A.

The results are shown in Table 4-8. It can be seen that the estimated regression coefficients (i.e. parameters) were significant at the significance level,  $\alpha = 0.05$ . The adjusted  $R^2$  value for the simple regression model was 0.44 which is only 0.05 lower than that of a multiple linear regression model. The models for stops B and C had slightly higher adjusted  $R^2$  values to those of the multiple regression models. The regression models for stops B and C can be found in Figures D-7 and D-8, respectively, in Appendix D.

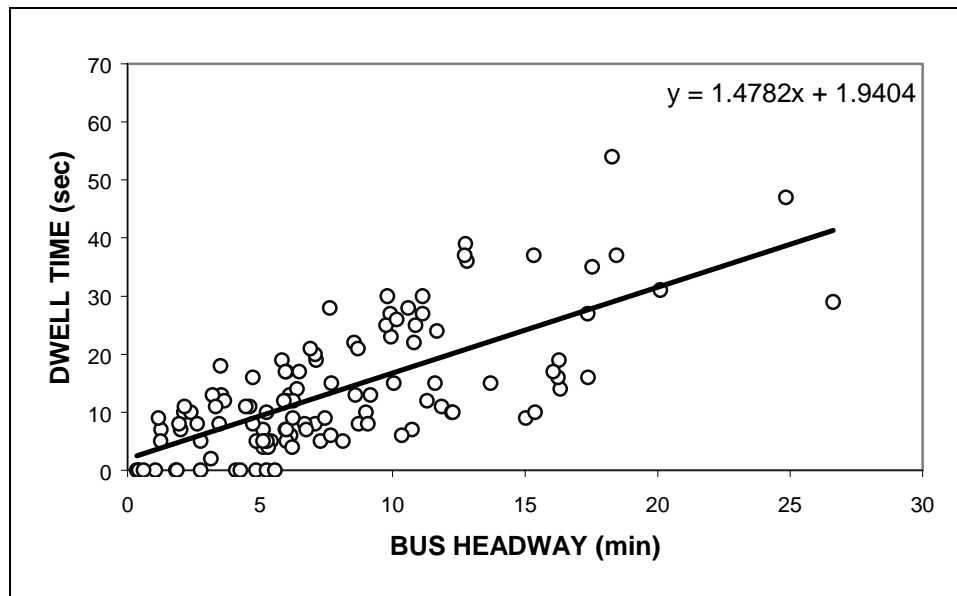


Figure 4-6 Estimated regression line at stop A

Table 4-8 Summary of simple regression models

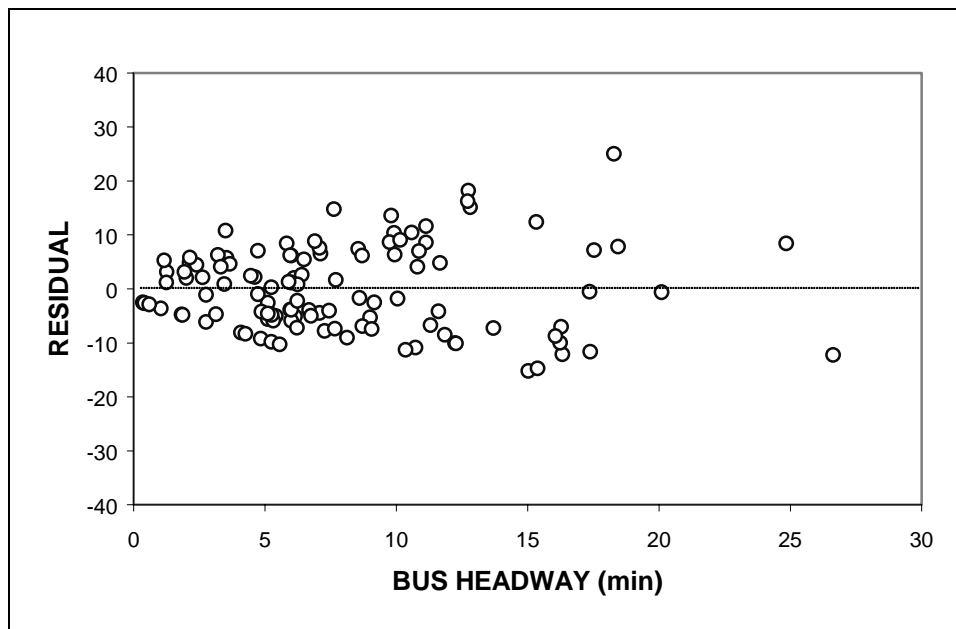
	STOP A		STOP B		STOP C	
	P-Value	t Stat	P-Value	t Stat	P-Value	t Stat
Bus headway	0.0001	9.42*	0.0001	6.72*	0.0001	9.42*
Intercept	0.0001	4.96*	0.0001	4.15*	0.0001	4.96*
Adjusted $R^2$	0.44		0.28		0.44	

Note:

\* indicates statistically significant at 0.05 level

Plots of the residuals against the predictor variable are not only helpful in determining whether a linear regression function is appropriate, but also in examining whether the variance of the error terms is constant. A common assumption underlying most process modeling methods, including linear least squares regression, is that the standard deviation of the error term, the residual, is constant over all values of the predictor variables (63). This assumption, however, clearly does not hold, even approximately, in every modeling application.

A residual plot against the predictor variable, bus headway, is shown in Figure 4-7. The plot suggests that the spread of the residuals increases as the predictor variable (i.e. bus headway) increases. Because the relation between dwell time and bus headways is positive, this suggests that the error variance is larger for longer bus headway than for shorter ones. The residual plots for stop B and C also were presented in Figure D-9 and D-10 in Appendix D, and also showed the funnel shaped variance over bus headways.



**Figure 4-7 Residual plot of the regression model for stop A**

#### **4.2.3 Tests for Constancy of Error Variance**

When a residual plot gives the impression that the variance may be increasing or decreasing in a systematic manner related to  $X$  or  $E\{Y\}$ , a statistical test such as the modified Levene test or the Breusch-Pagan test (63), is recommended to ascertain whether the error terms have non-constant variance. In this dissertation, the modified Levene test was performed as follows (63):

*Step 1:* Divide the 115 cases in order into two groups with approximately same population in each group (at 7 minutes of headway).

$$n_1 = 61, n_2 = 54$$

*Step 2:* Obtain the sample means of absolute deviations of the residuals around their group median

$$d_{i1} = |e_{i1} - \tilde{e}_1| \quad d_{i2} = |e_{i2} - \tilde{e}_2| \quad (4-19)$$

where

$d_{ik}$  = absolute deviation of the residual  $i$  in group  $k$ ,

$\tilde{e}_k$  = median of the residuals in group  $k$ , and

$e_{ik}$  = residual  $i$  in group  $k$ .

*Step 3:* Calculate the two-sample t test statistic by:

$$t_L^* = \frac{\bar{d}_1 - \bar{d}_2}{s \sqrt{\frac{1}{n_1} + \frac{1}{n_2}}} \quad (4-20)$$

$$s^2 = \frac{\sum (d_{i1} - \bar{d}_1)^2 + \sum (d_{i2} - \bar{d}_2)^2}{n - 2} \quad (4-21)$$

where

$t_L^*$  = test statistic for the modified Levene test,

$\bar{d}_k$  = sample mean of the  $d_{ik}$  in group  $k$ ,

$n$  = sample size,  $n = n_1 + n_2$ , and

$s^2$  = pooled variance.



*Step 4:* Compare the test statistic with the table value of  $t$  distribution with  $n - 2$  degree of freedom. If  $|t_L^*| > t_{1-\alpha/2, n-2}$ , it can be concluded the error variance is not constant. The tests were performed at 0.05 significance level.

The results of the modified Levene test are summarized in Table 4-9. The test statistics for all stops were greater than the table value (i.e. value of  $t$  distribution with 113 degree of freedom at 0.05 significance level). It can be concluded that the error variance of the dwell time is not constant and varies with the level of bus headways in all three bus stops.

**Table 4-9 Summary of the modified Levene test**

	$ t_L^* $	$t_{0.975,113}$	If test statistic is:	Error variance is:
Stop A	5.72	1.982	$ t_L^*  > t_{0.975,113}$	Not constant
Stop B	2.76	1.982	$ t_L^*  > t_{0.975,113}$	Not constant
Stop C	3.57	1.982	$ t_L^*  > t_{0.975,113}$	Not constant

The diagnosis of the residual plots and the modified Levene tests confirmed that the error variance is not constant and increases with bus headway. In situations like this, when it may not be reasonable to assume that every observation should be treated equally, weighted least squares can be used to maximize the efficiency of parameter estimation. This is done by attempting to give each data point its proper amount of influence over the parameter estimates.

### **4.3 WEIGHTED LEAST SQUARES REGRESSION**

Like all of the least squares regression method, weighted least squares (WLS) is an efficient method that makes good use of small data sets. It also shares the ability to

provide different types of easily interpretable statistical intervals for estimation, prediction, calibration and optimization. In addition, the main advantage that WLS enjoy over other methods is the ability to handle regression situations in which the variance of the data points are varying with the predictor variable. If the standard deviation of the random errors in the data is not constant across all levels of the explanatory variables, using weighted least squares with weights that are inversely proportional to the variance at each level of the explanatory variables yields the most precise parameter estimates possible.

In weighted least squares parameter estimation, as in regular least squares, the unknown values of the parameters in the regression function are estimated by finding the numerical values for the parameter estimates that minimize the sum of the squared deviations between the observed responses and the functional portion of the model. Unlike least squares, however, each term in the weighted least squares criterion includes an additional weight,  $w_i$ , that determines how much each observation in the data set influences the final parameter estimates.

#### **4.3.1 Weighted Least Squares Procedure**

The details about theoretical backgrounds of WLS can be found elsewhere (63,64,65). The general estimation process for WLS can be summarized as following:

- Step 1:* Fit the regression model by unweighted least squares and analyze the residuals.
- Step 2:* Estimate the variance function or the standard deviation function by regressing either the squared residuals or the absolute residuals on the appropriate predictor.
- Step 3:* Use the fitted values from the estimated variance or standard deviation function to obtain the weights  $w_i$ .

*Step 4:* Estimate the regression coefficients using these weights.

*Step 5:* If the estimated coefficients differ substantially from the estimated regression coefficients obtained by ordinary least squares, it is usually advisable to iterate the weighted least squares process by using the residuals from the weighted least squares fit to reestimate the variance or standard deviation function and then obtain revised weights.

A linear regression line for dwell time at stop A was fitted by unweighted least squares to conduct some preliminary analyses of the residual. The fitted regression function is:

$$\hat{Y} = 1.94 + 1.478h \quad (4-22)$$

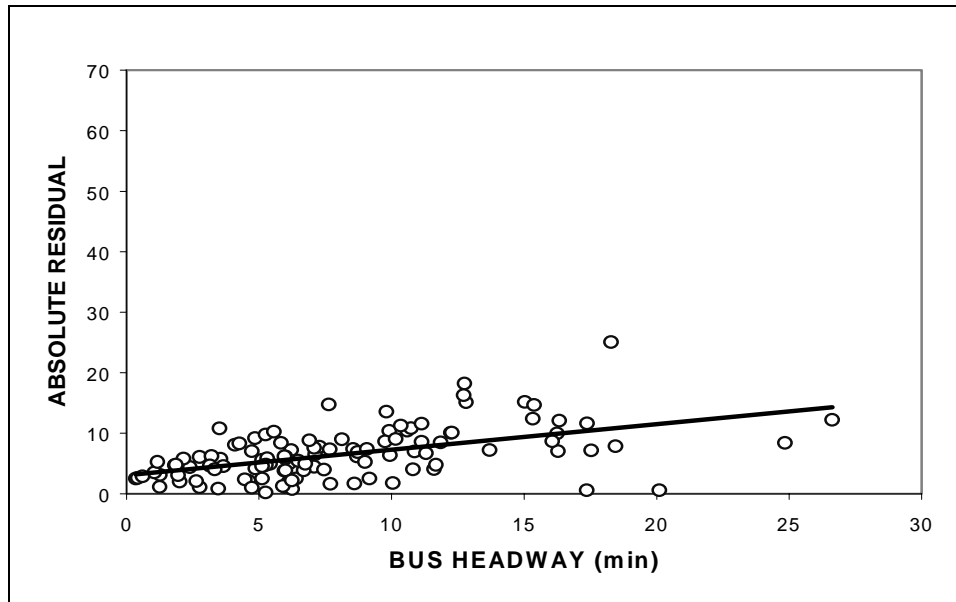
where

$$h = \text{bus headway (min)}$$

To obtain the standard deviation function, the absolute residuals were regressed against bus headways as shown in Figure 4-8. A standard deviation function for stop A was obtained as follows:

$$\hat{s} = 3.0955 + 0.4196h \quad (4-23)$$

The standard deviation functions for absolute residuals for stop B and stop C illustrated in D-11 and D-12 in Appendix D.



**Figure 4-8 Absolute residual plot and regression line for stop A**

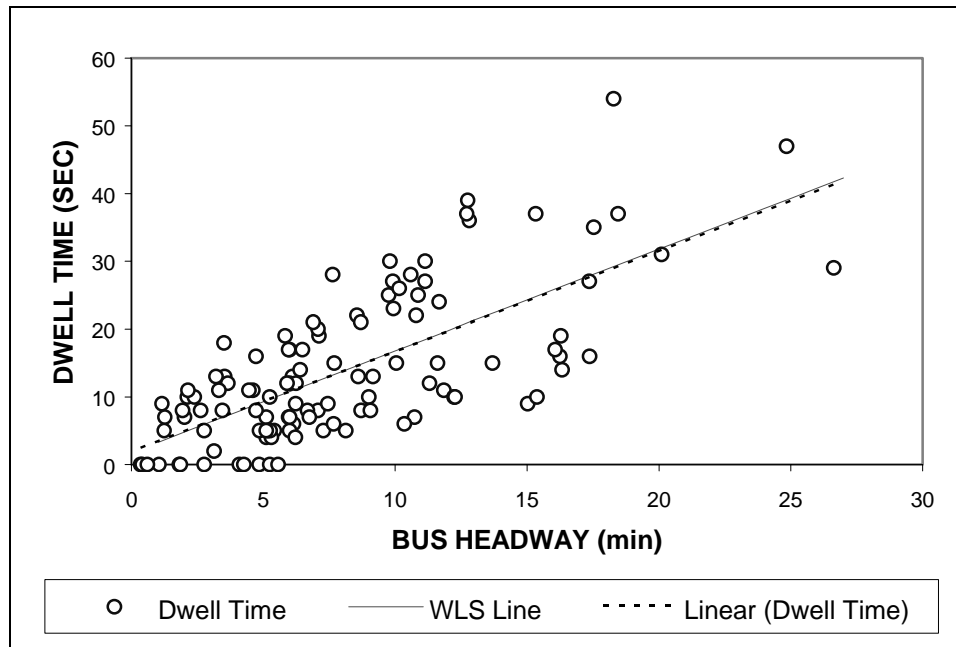
The weights are then obtained by standard deviation function shown in Equation 4-23. The weight for each data point is generally set to equal to the reciprocal of the sample variance (63,65).

$$w_i = \frac{1}{(\hat{s}_i)^2} \quad (4-24)$$

Using these weights, the following estimated regression function was obtained:

$$\hat{Y} = 1.7688 + 1.5h \quad (4-25)$$

Weighted regression functions for stop B and stop C can be found in Equations D-1 and D-2 of Appendix D. The estimated regression coefficients are not much different from those in Equation 4-25 obtained using unweighted least squares. Figure 4-9 illustrates two estimated regression lines for stop A: weighted and unweighted lines.



**Figure 4-9 Estimated weighted and unweighted lines for stop A**

It can be seen in Figure 4-9 that the estimated lines lie right on top of another over almost the entire range of the data. Even at the highest levels of bus headway, the models diverge slightly. This is fairly common result because WLS model shares the theoretical background of ordinary least squares regression model. The only difference between these models is non-constant variance over the predictor variable, which allows to calculate a prediction interval that varies according to the bus headways.

The average absolute error (AAE) of WLS regression model was calculated and compared with AAE of the probabilistic model for all the bus stops shown in Table 4-10. Even though WLS models were built based on one predictor variable, their performance was similar to the probabilistic model.

**Table 4-10 Comparison of AAE from probabilistic models and WLS models**

	Stop A	Stop B	Stop C
Probabilistic Model	6.35 sec.	3.84 sec.	8.71 sec.
WLS Regression Model	6.45 sec.	3.84 sec.	6.47 sec.

### 4.3.2 Prediction Interval of Dwell Time

The forecasting process, including the prediction model for dwell time, is itself subject to some prediction error. Therefore, interval estimations of the dwell time are more informative than point estimations of dwell time for the successful BSP implementation. The prediction interval of WLS regression model can be obtained by the definition of prediction interval in the linear regression model.

Let  $x_0$  denote a specified value of the independent variable  $x$ . Then, once the estimates  $\hat{\beta}_0$  and  $\hat{\beta}_1$  have been calculated,  $\hat{y}_0$  can be regarded as a prediction of  $Y$  value that will result from a single observation made when  $x = x_0$ . The prediction by itself gives no information concerning how precisely  $Y$  has been predicted. This can be remedied by developing a prediction interval for a single  $Y$  value. If  $\hat{\sigma}_i^2$  from standard deviation function is an unbiased estimator of  $\sigma^2$ , the variance of the error, a  $100(1-\alpha)\%$  prediction interval on a future observation  $Y_0$  at the value  $x_0$  is given by Equations 4-26 and 4-27.

$$\hat{y}_0 \pm t_{\alpha/2, n-2} \cdot \sqrt{\text{Var}\{Y_0 - (\hat{\beta}_0 + \hat{\beta}_1 x_0)\}} \quad (4-26)$$

$$= \hat{y}_0 \pm t_{\alpha/2, n-2} \cdot \hat{\sigma}_0 \sqrt{1 + \frac{1}{n} + \frac{n(x_0 - \bar{x})^2}{n \sum x_i^2 - (\sum x_i)^2}} \quad (4-27)$$

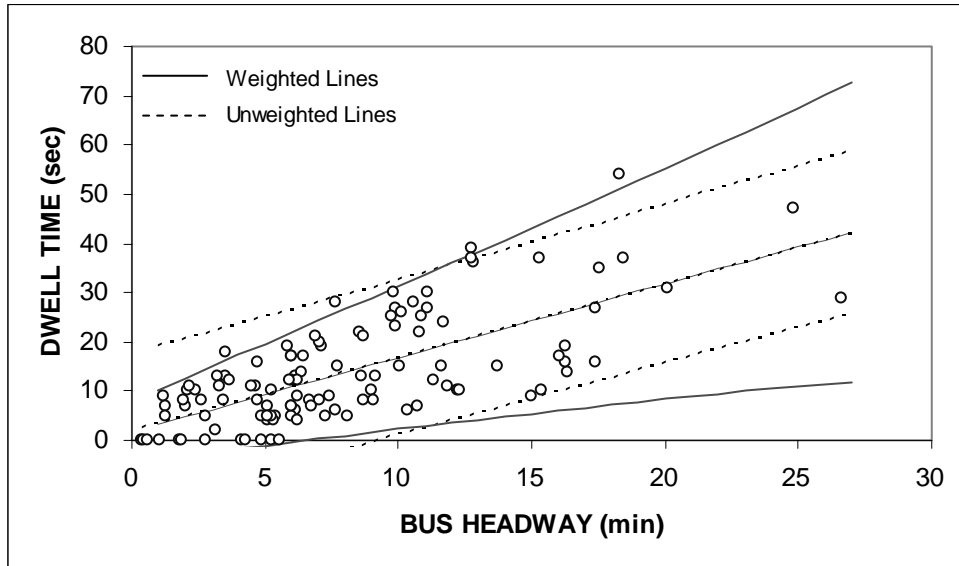
where

$t_{\alpha/2, n-2}$  = Appropriate point based on the  $T_{n-2}$  distribution, and

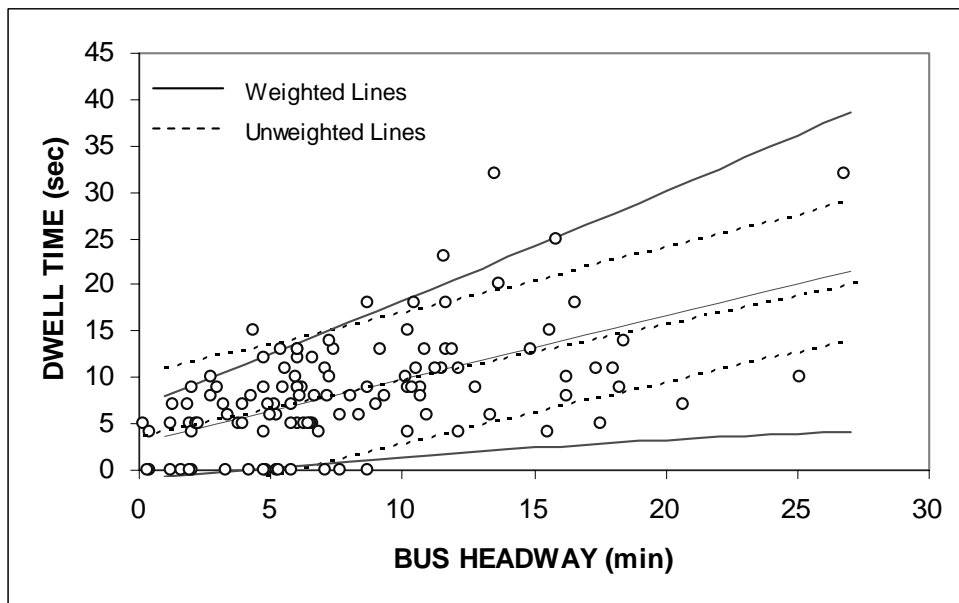
$\hat{\sigma}_0$  = Estimate from standard deviation function.

The 95% prediction intervals for unweighted regression model and WLS model are shown in Figures 4-10, 4-11, and 4-12. Because  $\hat{\sigma}_i^2$  of WLS model increased with bus headway, the prediction intervals also become wider as bus headway increases while

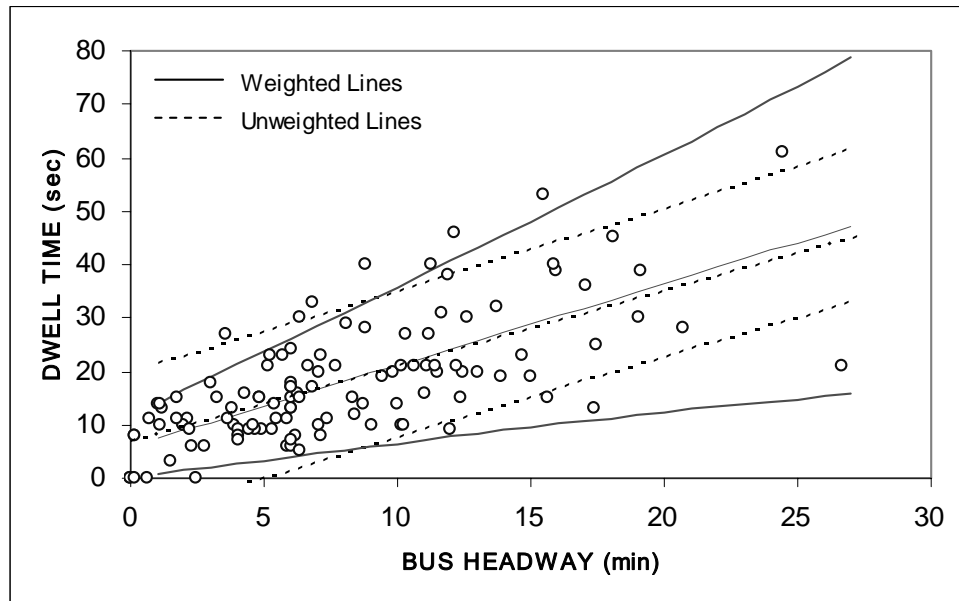
the unweighted models result in constant prediction intervals. It can be seen that unweighted models have the prediction interval that are much larger for low levels of bus headways and conversely for high levels.



**Figure 4-10 Prediction intervals and projected lines for stop A**



**Figure 4-11 Prediction intervals and projected lines for stop B**



**Figure 4-12 Prediction intervals and projected lines for stop C**

#### 4.6 CONCLUDING REMARKS

The models for forecasting the bus dwell time and prediction interval were developed in this chapter. A probabilistic model was developed and its related probability distributions were defined. A binomial distribution and a Poisson distribution were exploited for alighting and boarding passengers, respectively.

The probabilistic models are based on the linear relations between the number of alighting passengers and passenger loads, and the number of boarding passengers and bus headways. However, the observed data revealed that the number of alighting passengers is not correlated with the passenger loads. Several regression models were examined with different combination of independent variables such as bus headway, passenger loads on bus, and schedule adherence. The analysis concluded that a regression model with one independent variable, bus headway, had the best results. The residual analysis of the regression model revealed non-constant variance over bus headways, which violated the common assumption underlying regression modeling. The weighted least squares method, therefore, was employed in order to consider the non-



constant variance. Another advantage from WLS method can provide the prediction interval that varies according to the bus headway.

In Chapter V, a new bus signal priority algorithm will be developed. The prediction interval as well as the predicted dwell time from the WLS model will be utilized in the improved BSP strategies in order to accommodate the variability in dwell time.

## **CHAPTER V**

### **DEVELOPMENT OF IMPROVED BSP ALGORITHM**

#### **CONSIDERING DWELL TIME VARIABILITY**

In Chapter IV, a dwell time prediction model was developed based on weighted least squares regression model where the dependent variable was dwell time and the independent variable was bus headway. In addition, the prediction intervals, which vary according to the level of headway, were also developed. In this chapter, an improved BSP algorithm will be developed by modifying the signal logic from an existing BSP algorithm to take advantage of integration of the dwell time prediction interval into the BSP timing.

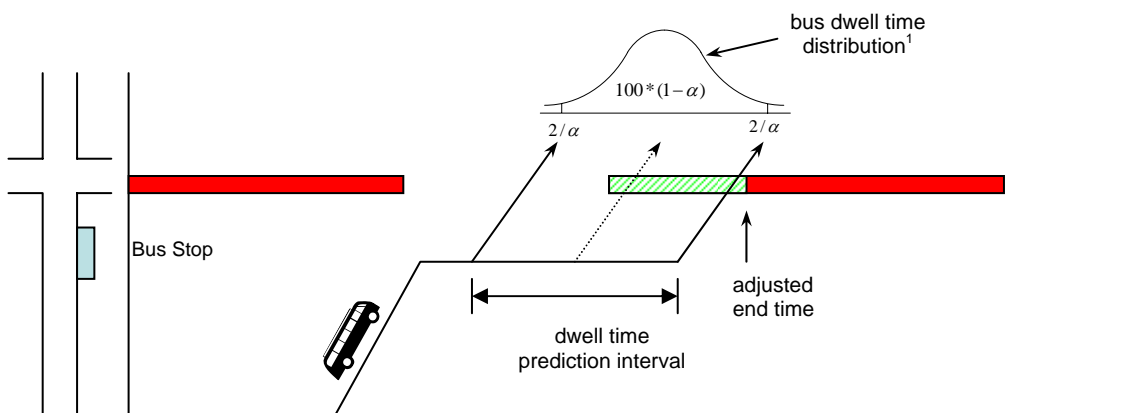
First, the concepts of the improved BSP algorithm will be introduced, which will explicitly address the needs of the required improvements in current BSP algorithm discussed in Chapters I and II. The algorithm makes use of the dwell time prediction model to obtain a prediction interval for when the bus will arrive at the intersection. The improved BSP algorithm will employ the existing priority signal timing methodology and incorporate the prediction interval of dwell time into the priority strategies. It is hypothesized that by including the prediction interval of dwell time in the BSP timing, more buses will arrive at the intersection during the green time and therefore bus delay will be improved. The second objective is to reduce the negative impact to the performance of the signal operation. The improved BSP algorithm will be designed not to disrupt the signal coordination. In addition, to reduce unnecessary delay to non-priority movements, the improved algorithm utilizes a restoring feature that restores unused priority green time back to non-priority phases. It is hypothesized that if this strategy is followed, the negative impact of BSP implementation will be reduced.

As discussed in Chapters III and IV, the test bed was an arterial section of Bellaire Boulevard in Houston, Texas. The BSP will be “implemented” on a VISSIM

simulation environment at two intersections that have nearside bus stops: Rookin at Bellaire and Hilcroft at Bellaire. Although the improved BSP algorithm is developed based on this specific test bed, the methodology developed in this dissertation can be applied to any intersection with nearside bus stops.

## 5.1 OVERVIEW OF THE IMPROVED BSP ALGORITHM

The variability in dwell time is taken into account by including the prediction interval of the dwell time when adjusting the signal timing plan. The basic idea of the improved BSP algorithm is to provide a priority phase wide enough to accommodate the prediction interval of dwell time at nearside stop. Figure 5-1 illustrates the concept of the improved BSP algorithm with the prediction interval and the BSP timing. Once a dwell time and its prediction interval are calculated using the dwell time prediction model developed in Chapter IV, the improved BSP system determines when in the cycle the bus will arrive at the intersection. Based on the predicted time interval of the bus arrival, an appropriate BSP strategy is selected so that the priority phase covers the prediction interval of the dwell time in order to ensure that the bus can traverse the intersection without stop delay.



Note:

<sup>1</sup> The distribution of dwell time is assumed as symmetric shape for the purpose of the illustration.

**Figure 5-1 Concept of the improved BSP algorithm**

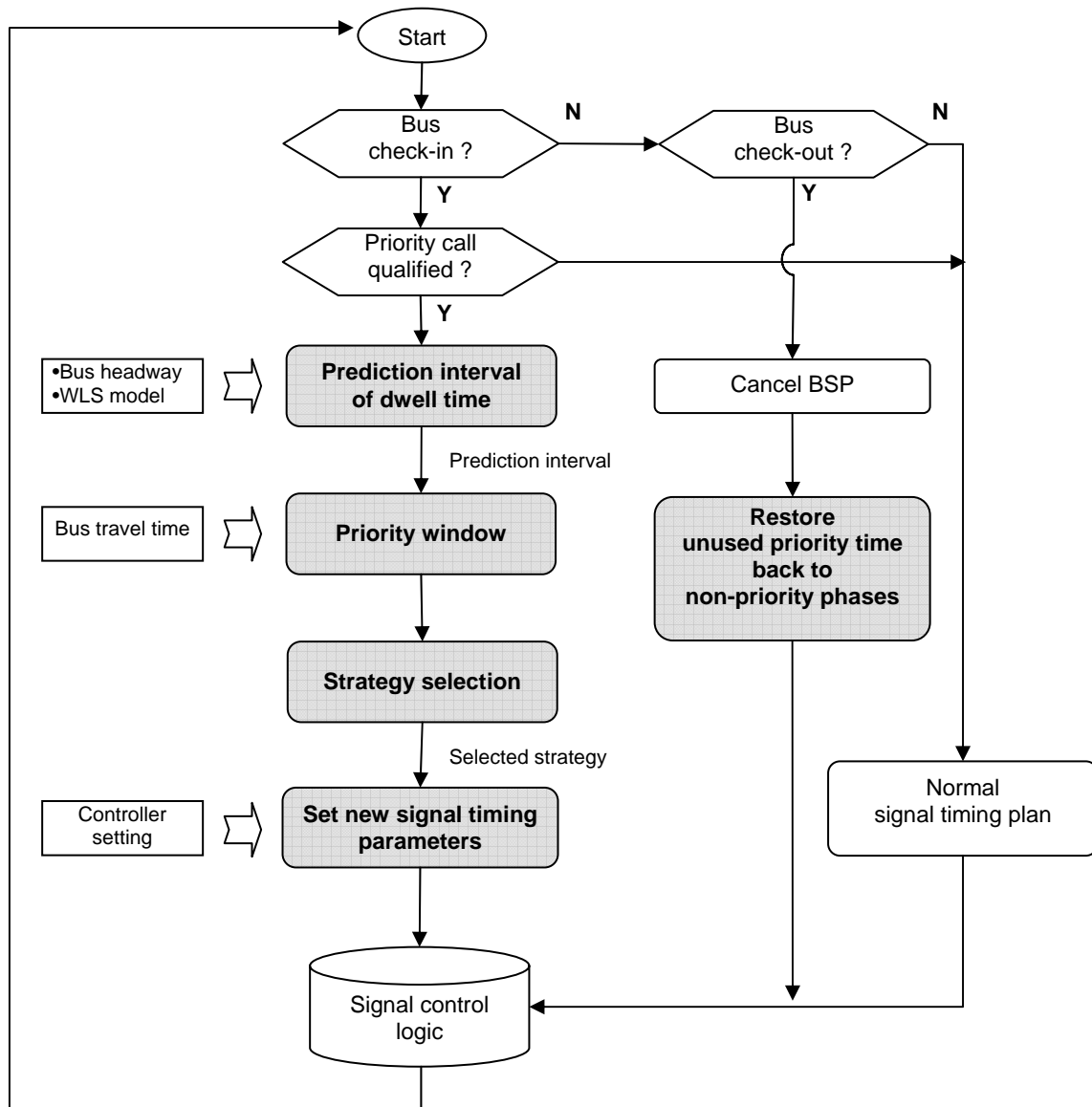
Figure 5-2 illustrates the functional diagram of the improved BSP algorithm. The first step in the algorithm is to update the status of the bus detectors every time step (assumed 1 second in this dissertation). When the check-out detector is activated, the algorithm terminates priority service and restores unused priority green phase back to non-priority phases. If the check-in detector is activated, the algorithm assesses the bus information (passenger loads) based on pre-defined criteria. If a bus satisfies the criteria, the signal priority service is initiated. Once priority service begins, the next step is to predict the time interval of the bus arrival in the cycle based on the prediction interval of the dwell time and the bus travel time from the check-in detector to the intersection. The algorithm then selects the most appropriate strategy for providing priority to the bus, given its predicted priority window. Based on the selected priority strategy, the force-off point for each phase will be adjusted to provide a green time to an approaching bus without disrupting the coordination. At the end of the algorithm, new force-off points are sent to the signal controller to implement the bus signal priority strategy. The specific logic of each of the shaded steps in Figure 5-2 will be discussed in the following sections.

### **5.1.1 Assumptions and Constraints**

The following assumptions and constraints were identified as affecting the development of the improved BSP algorithm.

- An optical bus detector is assumed to be the bus detector because intersections in the study site have already equipped the optical detection system for emergency vehicles. The receiver is mounted over the signal arm and senses any optical signal from the emitter mounted on the bus units. Two designated locations for bus detection are employed for sensing both the approaching and exiting bus. The check-in location is set upstream of the intersection to sense the approaching bus. The location is varied by the type of BSP system. The check-out location just past the stop line is set to sense when the bus exits the intersection. If the detection range is extended up to check-in location, the detector can sense the presence of the bus at check-in location once it receives the optical signal from the emitter.

When the optical signal is terminated, the detector assumes that the bus has reached the check-out location.



**Figure 5-2 Functional diagram of the improved BSP algorithm**

- An Automatic Passenger Count (APC) system with a global positioning system (GPS) is assumed to be on every bus. An APC system can accurately sense the passenger movements through doors and provide the number of passengers on the bus to the BSP algorithm.
- Communication systems are designed so that the passenger loads and signal timing information can be available to the various components of the algorithm. It was also assumed that communications failures will not exist and that all the information provided to the algorithm is correct and accurate.
- The improved BSP algorithm is developed to work with the signal controllers operating in an actuated-coordinated operations mode. This means that the coordinated phase (i.e. main street phase) must be activated during each cycle while other phases will be skipped if there is no vehicle actuation. However, under the priority mode, it was assumed that no phase skipping is allowed regardless of vehicle actuation. This assumption was made to reduce the complexities of the signal logic needed to implement the priority strategy.
- Pedestrian phasing requirements including a minimum walk and clearance interval are not considered in the development of the improved BSP algorithm. Although the pedestrian requirements are ignored for initial development and proof-of-testing purposes, in practice, they often control the minimum duration of a phase when pedestrian calls are placed. Consequently it would be expected that this assumption allow more flexible signal timing for providing a priority phase.
- The minimum phase requirements such as minimum green time, yellow change interval, and vehicle clearance time are required to be satisfied for each phase.
- It is assumed that the phases for the cross streets are not part of the signal progression. If the BSP strategy needs to account for the coordination systems for both the main street and cross streets simultaneously, the flexibility in adjusting signal timing for the priority will be extremely limited. Because the coordination system generally operates in the major arterial corridor, the coordination of the cross streets is ignored in this dissertation.

## **5.2 DEVELOPMENT OF BSP STRATEGIES**

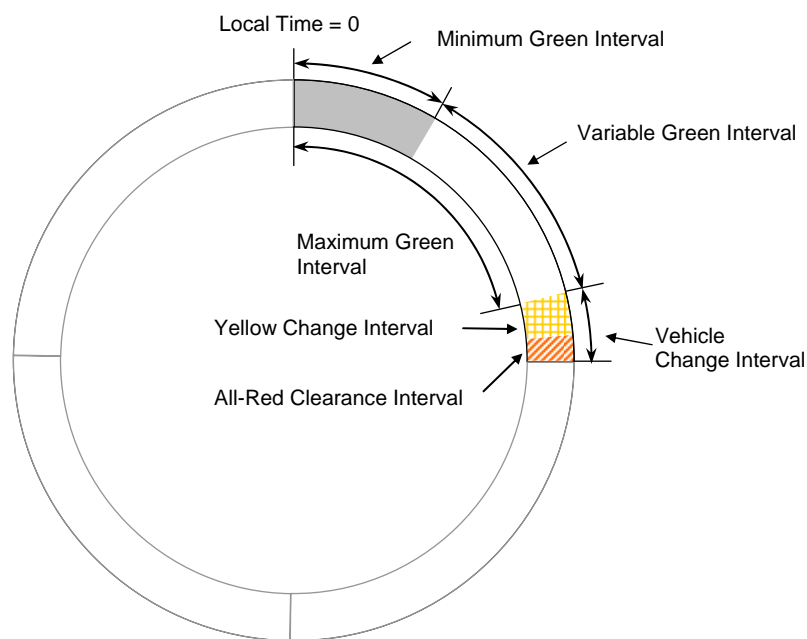
The current priority strategies (e.s. green extension, early green, and phase insertion) will be used to provide green time to the buses. Each current strategy is modified in order to include the prediction interval as a constraint in adjusting signal timing plan. The fundamentals of traffic signal operations with particular emphasis on actuated-coordinated operations mode, will be introduced in order to better understand the priority strategy logic.

### **5.2.1 Fundamentals of Traffic Signal Operations**

The purpose of traffic signal control is to reduce or eliminate conflicts at intersections. These conflicts exist because an intersection is an area shared among multiple traffic streams, and the role of the signal system is to manage the shared usage of the area. Signals accomplish this by controlling access to the intersection and allocating usage time among the various users. In traffic signal operations, specified combinations of movements receive right-of-way simultaneously.

Any discussion of signal timing usually provides the basic definitions of the common terms used to depict the various aspects of timing parameters. Figure 5-3 illustrates the signal timing intervals in a phase. A 'cycle' is the time required for one complete sequence of signal indications. A 'phase' is the portion of the signal cycle allocated to any combination of one or more traffic movements simultaneously receiving the right of way during one or more interval. Each phase is divided into 'intervals,' which are durations in which all signal indications remain unchanged. A phase is typically made up of three intervals: green, yellow, and all red. A phase fulfills all its intervals before moving to the next phase in the cycle. The order in which the phases are arranged is termed the 'phase sequence.' The green interval can be further divided into multiple subintervals. The first interval is referred to as the 'minimum green interval' that is the shortest time that a green indication can be displayed to drivers (66). The 'maximum green interval' represents the maximum time that a green indication can be displayed to drivers when a call is placed on a competing phase. In actuated control, the

maximum green time represents the maximum duration that a green indication can be displayed when there is demand on a serviceable opposing approach. The difference between the maximum green time and the minimum green time is referred to as the 'variable green time'. The MUTCD (66) requires that a vehicle change interval be displayed before the signal can service a different movement at an intersection. The vehicle change interval consists of two intervals: the yellow change interval and the all-red clearance interval.

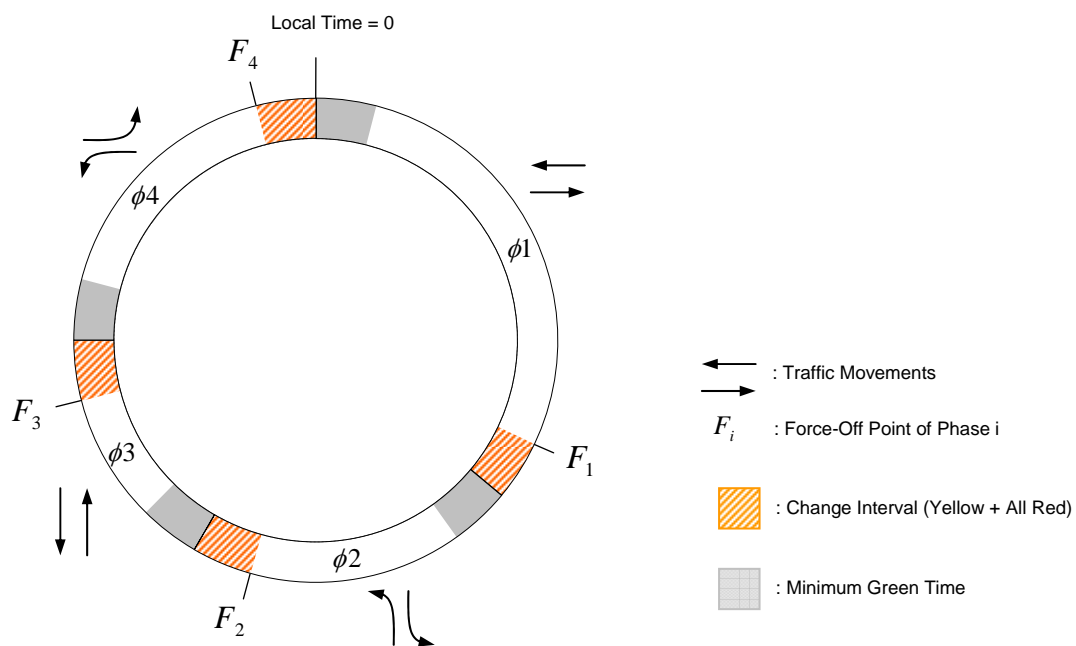


**Figure 5-3 Illustration of intervals in a phase**

Arterial coordination is a signal strategy that links the signals of adjacent intersections. The goal of such strategies is most often to provide progression through multiple intersections, allowing vehicles to move through successive signals without encountering a red signal. The timing of the signals can be set such that a vehicle traveling at a certain constant speed and departing at the appropriate time can obtain green lights at each intersection. The green times at the signals create a 'green band,' and vehicles whose trajectories fall within this band will be unimpeded by the signals. This



result is achieved by setting each signal at a different ‘offset,’ defined as the time difference between the start of the coordinated green interval and a system reference time. Coordination timing plan are generally entered as ‘split’ times (as opposed to phase time). A split is defined as a segment of the cycle length allocated to each phase or interval that may occur in the cycle. Arterial coordination under actuated control operates with fixed cycle lengths and offsets for the coordinated green intervals. Unlike pretimed signals, the non-coordinated phases (such as those for cross streets or for left turns from the arterial) can be skipped or extended based on demand. The coordinated phases, however, must always be green at a fixed time for a specified duration each cycle in order to maintain the green band for progression. In most traffic signal controllers, coordination is achieved by holding the controller in the coordinated phase until a specific point in the cycle and by forcing-off non-coordinated phases at predetermined points in the cycle as shown in Figure 5-4.



**Figure 5-4 Phase sequence and force-off points under coordination mode**

Forcing-off means that a change in phase will occur at a specified time within each cycle. The force-off point (referred to as  $F_i$ ) is the point in the cycle where the controller begins the vehicle change or clearance interval. If the specified time in the cycle is reached and a given phase is still green, this condition will force the signal to change to yellow in preparation for the next phase. In actuated-coordinated control, phases can be extended; however, the amount of this extension will be limited because coordination may require the next phase to start at a specified time in order to maintain the green band for arterial progression.

For the purposes of this dissertation, the signal timing parameters of the BSP strategies will be illustrated based on the coordinated four-phase signal plan. Figure 5-4 represents a phase sequence and force-off points for each phase. Phase  $\phi_1$  is the coordinated phase and it services the through movements on the main street. The cross-street left-turn, the cross street through, and the main street left-turn phases are referred to as the non-priority phases, and are presented as  $\phi_2$ ,  $\phi_3$ , and  $\phi_4$  respectively. The local cycle time is set to zero at the start of the coordinated phase (main street through phase). As discussed previously, the coordinated phase has to begin no later than cycle time 0 and continues until its force-off point,  $F_1$ .

### 5.2.2 Development of BSP Strategies

When a constant bus travel time from the check-in point to the intersection is assumed, the width of prediction interval of bus arrival time is identical to that of dwell time. For the purposes of this dissertation, the prediction interval in the cycle is referred to as a 'priority window.' It is a time interval in the cycle needed to ensure that a bus arrives during a green indication with  $100(1 - \alpha)\%$  confidence level. The width of the priority window is determined by the prediction interval of the dwell time, and the location of the priority window in the cycle is dependent on the bus travel time from the check-in location to the intersection (including a predicted dwell time at stop). The start point and end point of the priority window in the cycle are represented by the symbols  $\omega$  and  $\omega'$

respectively. Three priority strategies will be exploited in order to accommodate the priority window in BSP timing.

5.2.2.1 Green extension strategy

The green extension strategy is utilized to provide a signal priority when the priority window can be accommodated by extending the main street green. Figure 5-5 illustrates an example of green extension strategy when the predicted window of bus arrival time at the intersection starts during the green time for phase 1 but ends during the red time for phase 1. The leading and lagging phase sequence, which operates at the intersections in test bed, is assumed in the example. It can be seen that the priority window (i.e. prediction interval of dwell time) is accommodated by modified green extension strategy without disrupting the coordination.

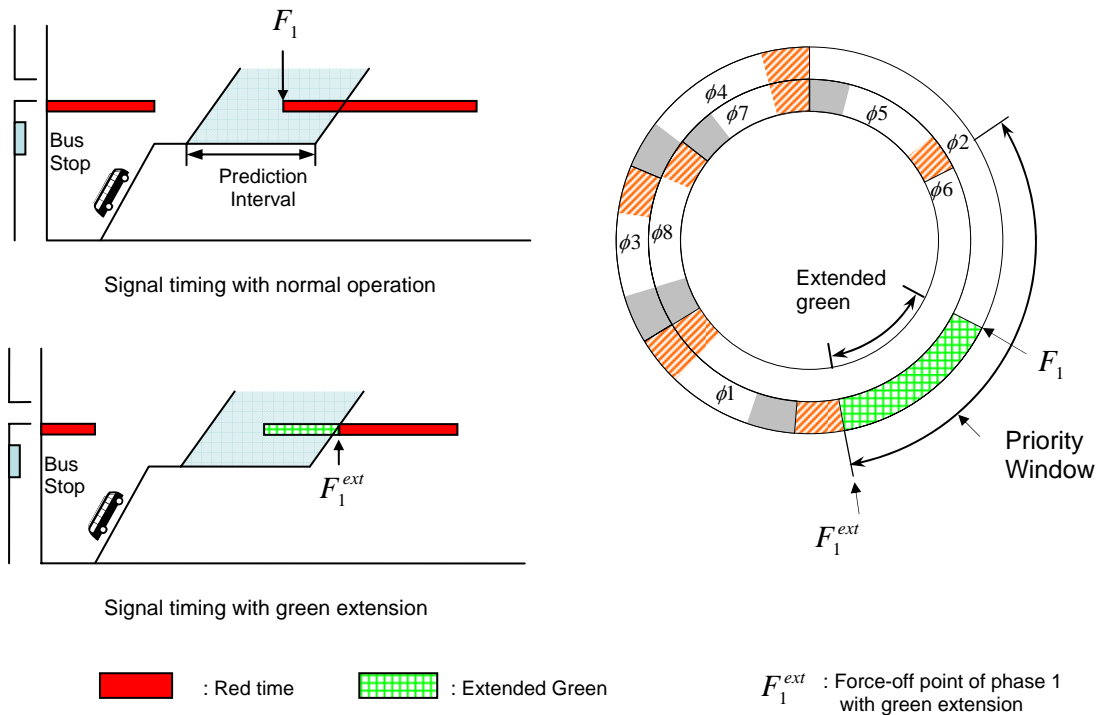


Figure 5-5 Example of green extension strategy under eight-phase signal operation

The maximum extension of the priority phase depends on the minimum requirements for non-priority phase and change interval of the priority phase as shown in Figure 5-6a. Note that every phase must be provided where each phase should have the minimum green time and change interval (yellow change and all red). As discussed in the previous section, the point in the cycle where a phase could begin its termination sequence is the force-off point. To hold the green phase until the priority window ends, the force-off point of the main street phase with the green extension strategy,  $F_1^{ext}$ , is set at the same point in the cycle to the upper bound of the priority window as shown in Figure 5-6b. Therefore the green extension strategy can provide the green time to the bus which arrives at the intersection during its prediction interval. The variable green time for non-priority phase is determined by the difference between maximum time of green extension and new force-off point of the priority phase as shown in Figure 5-6b. The maximum amount of time that the coordinated (main street) phase can be extended a function of the minimum green time and the change interval for all non-priority phases as well as phase length of the main street phase. This relationship can be formulated by a mathematical expression, Equation 5-1.

$$M_{ext} = C - G_1 - \left( \sum_{i=2}^n R_i + \sum_{i=1}^n I_i \right) \quad (5-1)$$

where

$M_{ext}$  = maximum amount that the priority phase ( $\phi_1$ ) can be extended (sec),

$n$  = number of phases in the cycle,

$C$  = cycle length,

$G_1$  = green time for phase 1,

$R_i$  = minimum green time for phase  $i$ , and

$I_i$  = change interval for phase  $i$ .

The last time in the cycle that the priority green phase can be extended is referred to the maximum extension,  $Z_{ext}$ , and is defined by Equation 5-2.

$$Z_{ext} = M_{ext} + F_1 \quad (5-2)$$

where

$$Z_{ext} = \text{last time in the cycle that the priority green phase can be extended.}$$

The maximum extension,  $Z_{ext}$ , is defined as an upper threshold for selecting the green extension strategy. When the end point of the priority window,  $\omega'$ , is located between  $Z_{ext}$  and  $F_1$ , a green extension strategy is selected. When  $\omega' = Z_{ext}$ , the main street green phase is extended to its maximum extension points and non-priority phases are reduced to their minimum phase lengths. In the situations where  $\omega'$  locates between  $Z_{ext}$  and  $F_1$ , the main street green is needed to be extended up to  $\omega'$  instead of  $Z_{ext}$ . The non-priority phases also have additional variable green time as well as the minimum phase length. The amount of the variable green time to be distributed to each non-priority phase is determined by Equation 5-3.

$$S_i^{ext} = R_i + I_i + \frac{(F_1 + M_{ext}) - \omega'}{n-1} \cdot w_i \quad (5-3)$$

$$\sum_{i=1}^{n-1} w_i = n-1 \quad (5-4)$$

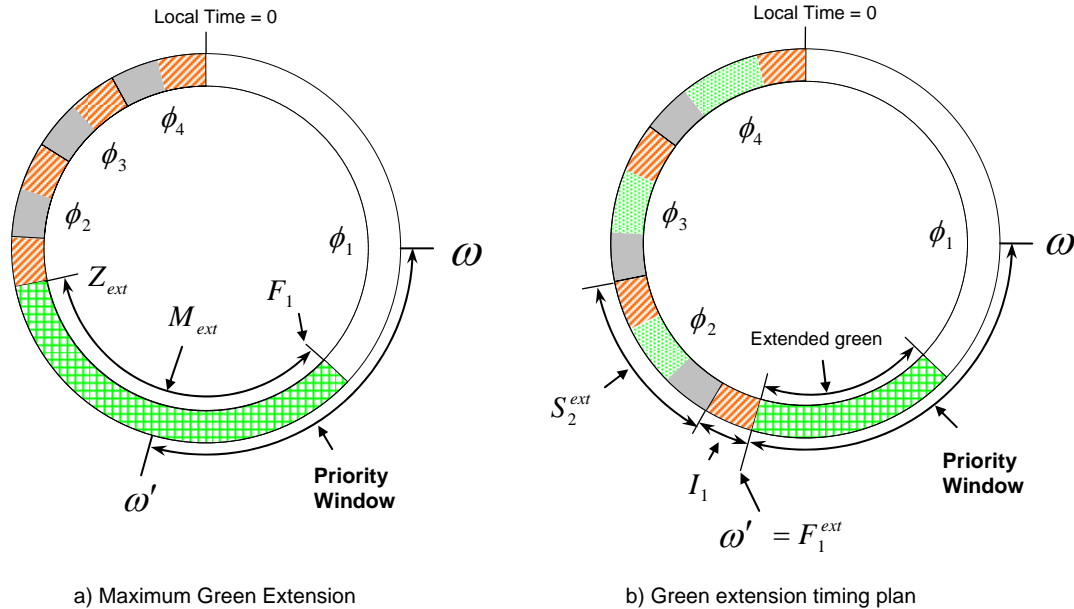
where

$S_i^{ext}$  = split of phase  $i$  with green extension strategy (sec),

$F_1$  = force-off point of priority phase  $I$ ,

$\omega'$  = end point (upper bound) of the priority window in the cycle (sec), and

$w_i$  = weight of phase  $i$ .



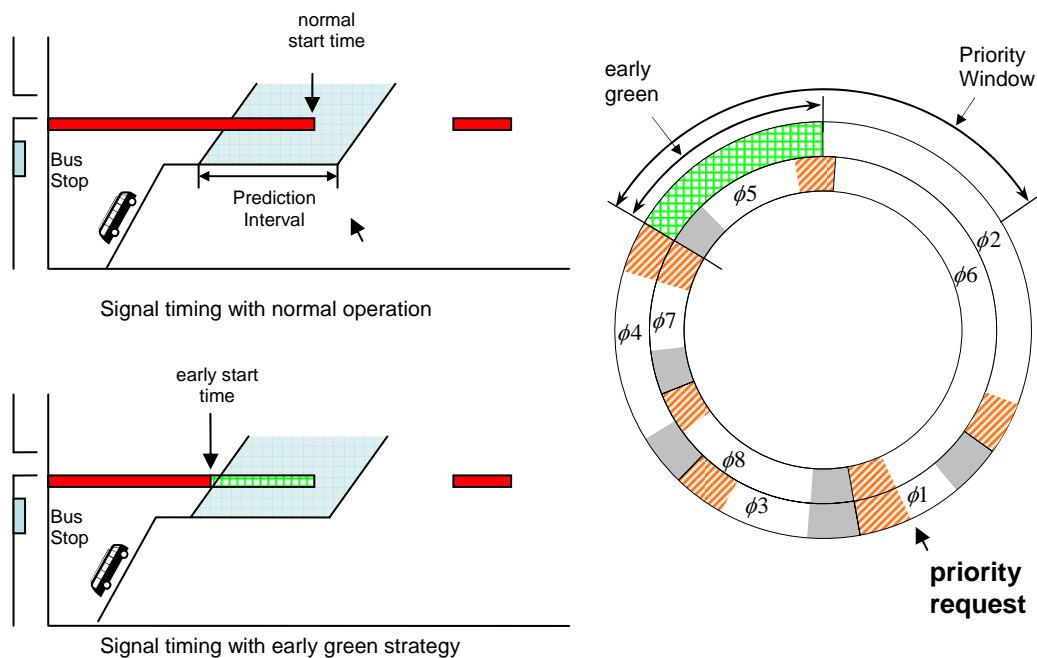
**Figure 5-6 Illustration of green extension strategy**

A weight,  $w_i$ , is introduced in order to consider the utilization of the phases in assigning variable green times to the non-priority phases. The utilization of the phases can be determined by either traffic demand for phases or phase durations (i.e. splits) in the normal signal plan. For example, a phase which has larger split in the normal signal plan may have greater weight than those with shorter splits. The weight for the phase of cross street through movements that have high demand may be greater than those for left-turn movements.

5.2.2.2 *Early green strategy*

The early green strategy truncates the green time of the non-priority phases in order to start the main street green phase earlier. If a bus is expected to arrive during the red

signal for phase 1 and the bus is due to receive a green in the next cycle, the non-priority phases can be shortened to allow the main street to receive a green earlier than normal. The amount of time available to start the main street phase early depends on where in the cycle the priority request is placed, and the minimum phase requirements for all of the non-priority phases. Figure 5-7 illustrates an example for the implementation of early green strategy under leading and lagging eight-phase signal operation.



**Figure 5-7 Example of early green strategy under eight-phase signal operation**

The maximum amount of time available to start the priority phase is dependent on the time in cycle the priority request occurs. When the request is made during the green time for phase 1, all the non-priority phases can be reduced to their minimum phase length and the priority phase can start as early as possible. However, with the priority request placed during the red time for the main street, the earliest possible start time of the priority phase is limited by the number of non-priority phases between the current phase and the main street phase. The current phase where the priority request is

placed is terminated and its change interval activated, only when the current phase fulfills the minimum green time. Therefore the maximum amount of time available to start the priority phase early is a function of the number of non-priority phases being reduced, the time of priority request in the current phase, and the minimum phase requirements. Figures 5-8 and 5-9 illustrate these situations. The maximum amount of time available to start the priority phase early is calculated using Equation 5-5. In the equation, the time and current phase when the priority request is placed are referred as  $\theta_c$  and  $k$ , respectively. The elapsed green time of the current phase,  $\tau_k$ , is another constraint in the calculation of the maximum early green time. The algorithm compares  $\tau_k$  and  $R_k$ , and choose bigger number for calculating  $M_{gm}$ . The elapsed green time,  $\tau_k$ , is calculated by Equation 5-6.

$$M_{gm} = C - \left\{ (G_1 + I_1) + \sum_{i=2}^{k-1} (G_i + I_i) + \max(R_k, \tau_k) + \sum_{i=k+1}^n (R_i + I_i) \right\} \quad (5-5)$$

$$\tau_k = \theta_c - F_{k-1} - I_{k-1} \quad (5-6)$$

where

- $M_{gm}$  = the maximum time available to service buses by returning early to the priority phase (sec),
- $k$  = current phase in which priority call is requested,  $k = 1 \cdots n$ ,
- $\tau_k$  = elapsed green time of phase  $k$  (sec), and
- $\theta_c$  = time point in the cycle when priority is requested.

The maximum early green time is seldom used in the implementation of the early green strategy unless the start point of the priority window,  $\omega$ , is equal to the earliest start point of the priority phase in the cycle. In most situations, the priority window can be accommodated by using a time earlier than the maximum early green time. Similar to



the green extension strategy, the splits for the non-priority phases are determined by the available time and the number of non-priority phases as shown in Equation 5-7.

$$S_i^{gm} = R_i + I_i + \frac{M^{gm} - (C - \omega)}{n - (k - \delta(\theta_c))} \cdot w_i, \quad i = (k - \delta(\theta_c)) \dots n \quad (5-7)$$

$$\delta(\theta_c) = \begin{cases} 0, & \text{when } \tau_k > R_k \\ 1, & \text{when } \tau_k < R_k \end{cases} \quad (5-8)$$

where

$S_i^{gm}$  = split of phase  $i$  with early green strategy (sec), and

$\delta(\theta_c)$  = dummy variable,  $\theta_c \leq C$ .

A dummy variable,  $\delta(\theta_c)$ , is introduced in order to take into account the situation where the minimum green is fulfilled for the phase which receives the priority call. If the elapsed green time of the current phase is less than the minimum green time, the current phase will be given the variable green time.

Two situations, that the priority request is placed during green time or red time period for phase 1, are shown in Figures 5-8 and 5-9, respectively. When the request occurs during green time period, the priority phase can start at earliest possible time. The split for non-priority phases is a function of the start point of the priority window and the maximum early green time. Figure 5-9 illustrates a situation when the request occurs in phase 3. Because the time of the priority request is such that the minimum green time of phase 3 has already been met, the controller would terminate phase 3 at next time step and reduce the phase 4 to its minimum length in order to calculate the maximum early green time. The split for phase 4 is determined by the priority window and available time for non-priority phase.

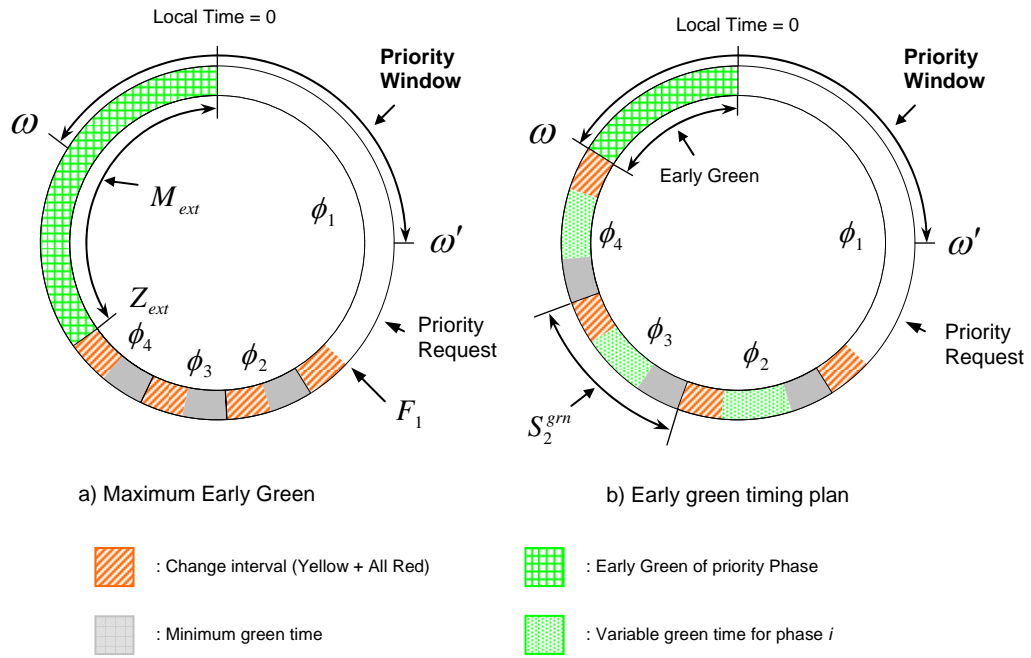


Figure 5-8 Illustration of early green strategy with priority request during green time

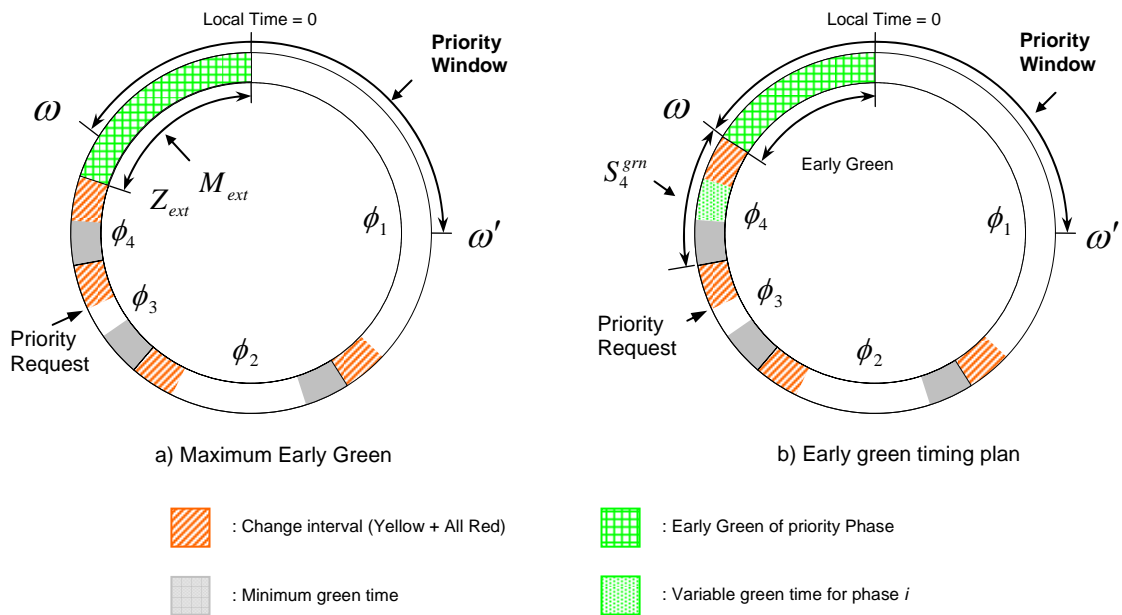
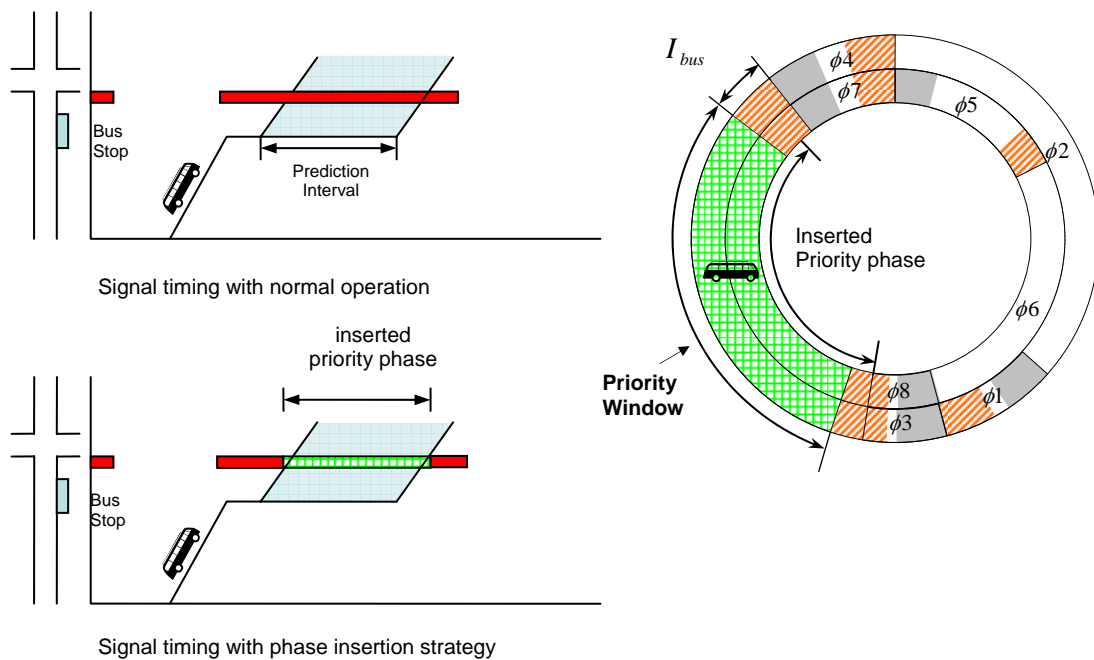


Figure 5-9 Illustration of early green strategy with priority request during red time

### 5.2.2.3 Phase insertion strategy

The phase insertion strategy inserts an additional phase into the normal phase sequence specifically for the bus. This strategy is used when a bus is expected to arrive at the intersection during the red phase for its approach and the priority window of the bus begins and ends within the red phase. Figure 5-10 illustrates an example of phase insertion strategy on eight-phase leading and lagging signal operation. The time-space diagram for the normal operation represents that the expected bus arrival and its prediction interval is located within red time for the bus approach.



**Figure 5-10 Example of phase insertion strategy under eight-phase signal operation**

The phase duration of the inserted priority phase is determined by the priority window and the change interval of the priority phase. This strategy can be used when the maximum amount of time available in red period for inserting the special phase is greater than the priority window. If the condition shown in Equation 5-11 is not satisfied, then the algorithm evaluates other possible strategies such as green extension and early

green strategy that can accommodate the priority window. Given that the condition shown in Equation 5-11 is satisfied, the phase insertion strategy determines where in the normal phase sequence the priority phase should be inserted. This is a function of the location of the priority window in the cycle and the minimum phase requirements for non-priority phases. Figure 5-11 illustrates an example in which an approaching bus is predicted to arrive during the red phase and its priority window is located within the red phase for the bus approach. The red period outside the priority window in the cycle is the available time for non-priority phases. The amount of red period before/after the priority window can be represented by Equations 5-9 and 5-10.

$$\rho = \omega - (F_1 + I_1) \quad (5-9)$$

$$\rho' = (F_n + I_n) - \omega' \quad (5-10)$$

where

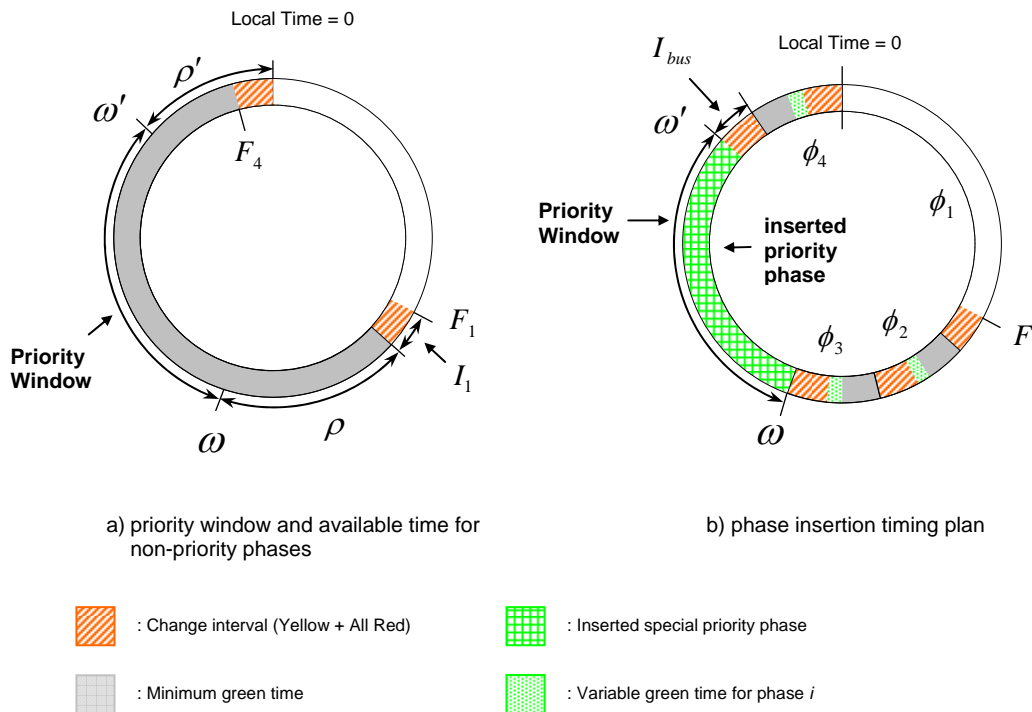
- $\rho$  = the amount of red period **before** the priority window (sec),
- $\rho'$  = the amount of red period **after** the priority window (sec), and
- $\phi_n$  = the last phase in the ring.

The amount of available time for non-priority phases,  $\rho$  and  $\rho'$ , should be greater than the amount of time required for all non-priority phases that satisfy the minimum phase requirements as shown in Equation 5-11.

$$\sum_{i=2}^n (G_i + I_i) - (\rho + \rho') \geq \sum_{i=2}^n (R_i + I_i) \quad (5-11)$$

If a four-phase signal operation is assumed, the priority phase can be inserted in between phase  $\phi_2$  and phase  $\phi_3$  or between phase  $\phi_3$  and phase  $\phi_4$ . In Figure 5-11, two non-priority phases are serviced before the priority phase because the  $\rho$  can hold up

to two non-priority phases with the minimum phase requirements. The last non-priority phase services after the priority phase because the  $\rho'$  can fit only one minimum phase. Therefore, the priority phase is inserted in between phase  $\phi_3$  and phase  $\phi_4$ .



**Figure 5-11 Illustration of phase insertion strategy**

Before adjusting the signal timing plan, the numbers of non-priority phases before and after the priority phase need to be defined. For the purposes of this dissertation, the number of phases before and after the priority phase are referred as  $N_b$  and  $N_a$ , respectively. Because traffic signals seldom operate more than four phases in each ring, the phase insertion strategy in this dissertation is developed based on the four-phase signal operation. The BSP algorithm first calculates  $\rho$  and  $\rho'$ , and then calculates the number of phases that can be fit into each red time period. If both red time periods are wide enough to accommodate two non-priority phases, the longer red time period services two non-priority phases.

Once the numbers of phases,  $N_a$  and  $N_b$ , that are serviced before/after the priority window are determined, the BSP algorithm calculates the splits of the non-priority phases. When the  $N_b$  is one, the split for phase 2 is equal to the  $\rho$ . For the  $N_a$ , the split is equal to  $\rho' - I_{bus}$  because the inserted priority phase also requires a phase changing interval. When the number of non-priority phases before or after the priority phase is two, the phase splits are determined by adding the variable green time to the minimum phase length as shown in Equation 5-12.

$$S_i^{\text{int}} = R_i + I_i + \frac{t_{red} - \sum_{j=s}^{s+1} (R_j + I_j)}{2} \cdot w_i \quad (5-12)$$

for phases before priority phase:  $t_{red} = \rho$ ,  $i = 2, 3$ ,  $s = 2$

for phases after priority phase:  $t_{red} = \rho' - I_{bus}$ ,  $i = 3, 4$ ,  $s = 3$

where

- $S_i^{\text{int}}$  = split of non-priority phase  $i$  with phase insertion strategy (sec),
- $t_{red}$  = the available time before/after priority window for non-priority phases (sec),
- $i$  = phase number, and
- $I_{bus}$  = change interval for inserted priority phase.

When both red time periods,  $\rho$  and  $\rho'$ , can accommodate only two non-priority phases (i.e. one phase for each red time period), the inserted priority phase needs to be reduced in order to service all three non-priority phases. The longer red time period services two non-priority phases with the minimum length and its associated bound of the priority phase is reduced. If either  $\rho$  or  $\rho'$  is less than the minimum phase length, the alternative strategy is implemented instead of the phase insertion strategy. When the time available for non-priority phase before the priority window is less than a minimum

phase length, the green extension strategy is selected to accommodate the priority window. When the  $\rho'$  is less than minimum phase length plus the change interval for the inserted priority phase, the early green strategy is selected.

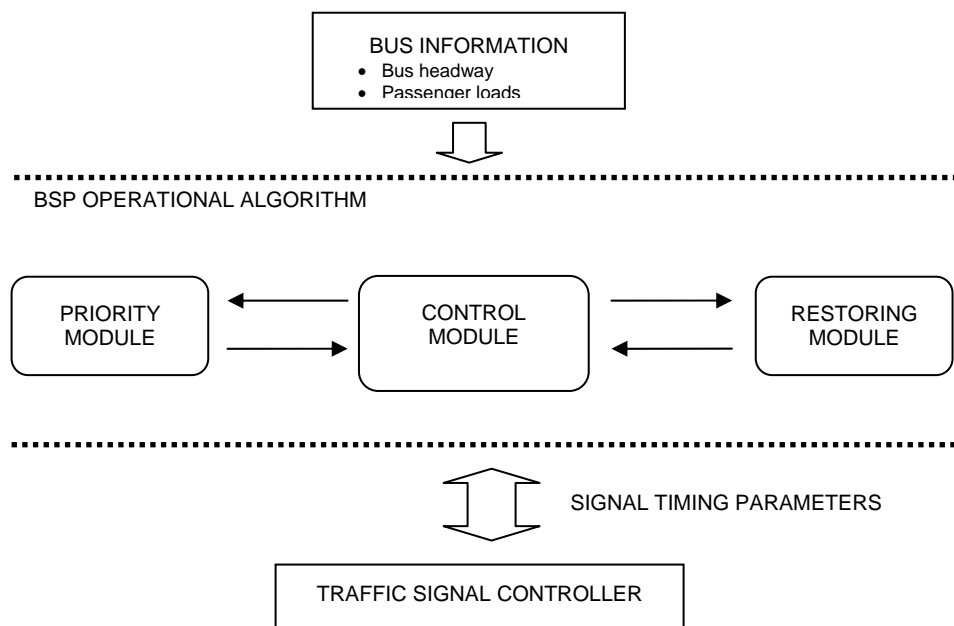
### **5.3 IMPLEMENTATION OF IMPROVED BSP STRATEGIES IN VISSIM OPERATIONAL ALGORITHM**

The BSP strategies developed in previous section are based on the premise that if the time window of the bus arrival at the intersection is known, the traffic signal timing could be adjusted to allow priority service while simultaneously preventing the signal from dropping out of coordination. The previous section described how the signal timing plan is adjusted in order to accommodate the priority window for each BSP strategy. In this section, the operational algorithm for the improved BSP strategies is developed, which focuses on the implementation of the improved BSP strategies in the traffic simulation model, VISSIM. The operational algorithm are developed using VAP programming code (56).

The operational algorithm is designed to reduce unnecessary delay to non-priority movements by restoring the remaining priority green time back to the non-priority phases once the bus has exited the intersection. In addition, the number of priority activations is limited to one per cycle in order to avoid undue delay to non-priority approaches. The second priority request received by the traffic signal control system does not result in any change to the signal indications. Once the priority service is initialized, no priority request can alter the priority service until the controller completes the priority service.

The architecture of the algorithm consists of three modules as shown in Figure 5-12: control module, priority module, and restoring module. The control module decides how the algorithm functions at current time step. The major task of this module is to 1) monitor the improved BSP system including the bus detectors and the implementation of BSP strategies, and 2) determines whether the signal timing parameters needs to be

adjusted. The priority module calculates the prediction interval of dwell time, identifies priority window, selects the appropriate strategy, and adjusts signal timing parameters. The restoring module adjusts the current signal timing parameters to restore the unused priority green time back to non-priority phases. In this section, a detailed description of the functions in each module provided.



**Figure 5-12 Architecture of improved BSP operational algorithm**

### 5.3.1 Control Module

#### 5.3.1.1 Signal control mode

The control mode in the improved algorithm is defined as the current status of the signal operation. In the improved BSP algorithm, the signal controller can service the normal, the priority, and restoring operations as described below.

##### *Normal mode*

The controller operates under normal mode (e.g. default signal timing parameters) when there is no bus on the approach of interest.



### *BSP mode*

When there is a bus between the check-in and check-out detectors and it is eligible for priority service, the controller operates under BSP mode. In BSP mode, the signal timing parameters are adjusted to provide the priority phase. The signal timing parameters for BSP mode are a function of the BSP strategy selected, the time in the cycle the priority request was received, and the width of the priority window.

### *Restoring mode*

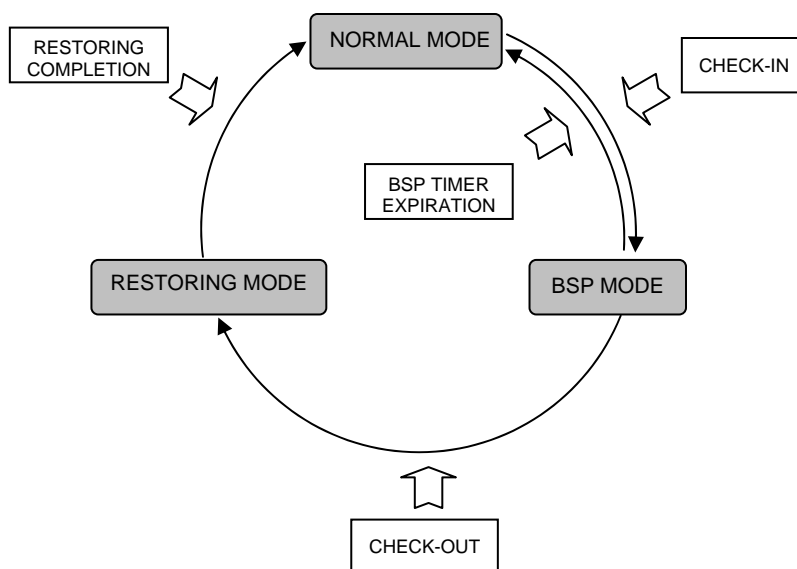
After the successful implementation of any priority strategy, if there is unused priority green time, the control mode is switched to the restoring mode. Similar to the BSP mode, a new set of signal timing parameters are achieved whenever the control mode is switched to the restoring mode. The restoring parameters are a function of the type of BSP strategy implemented and the amount of time not used by the priority phase. It should be noted that if another bus arrives at the check-in detector while the restoring module is active, it will not receive priority treatment.

#### *5.3.1.2 Mode transitions*

Figure 5-13 illustrates the relationship between control modes. The transitions in mode status take place when any of the four pre-defined condition are satisfied. The pre-defined conditions are 1) check-in call, 2) check-out call, 3) completion of the priority phase, and 4) completion of the restoring process. Therefore the control module continuously monitors the conditions and looks for changes. If no change is detected, the controller stays in the current control mode. When an eligible bus is sensed at the check-in detector, the algorithm switches the control mode from normal mode to BSP mode and obtains the new signal timing parameters. Once in BSP mode, the logic can be transferred to either the restoring or the normal mode. If the bus fails to pass through the intersection during the priority phase, the priority phase fulfills its full length and the control mode switches back to normal mode. When the bus passes the check-out detector during the priority phase, the logic is transferred to the restoring mode. In the restoring mode, the amount of time not used by the priority phase is calculated and the signal

timing parameters adjusted. The controller returns to normal mode from restoring mode when the traffic signal timing plan identified in the restoring mode are satisfied.

When the transition between modes occurs, the control mode is flagged in order to indicate that new signal parameter set need to be obtained for activating the control mode. For example, when the normal mode switches to the BSP mode, BSP mode is flagged and the algorithm calculates the new signal parameters for implementing signal priority. The flag is deleted next time step.



**Figure 5-13 Illustration of the changes in control mode and decision factors**

### 5.3.1.3 Control logic of control module

The functional diagram of the control module logic is represented in Figure 5-14. This control logic is performed every time step and the control mode for next time step is determined. The first step is to update the status of the bus detectors. If any change does not occur, the controller stays in current control mode. An implementation of the bus signal priority strategy requires the detection of buses upstream of the intersection in order to start any priority process. When a bus crosses a check-in detector, the algorithm

assesses the eligibility of the priority request. The eligibility of the bus for the priority is determined by assessing pre-defined criteria. The commonly used criteria include the schedule adherence, the headways between buses, and the occupancy level of the bus (29). In this dissertation the occupancy level, passenger loads, will be used as the criterion. If the bus is eligible for the priority, the algorithm considers the bus checked-in. Once detected at check-out detector, the bus is identified as checked-out.

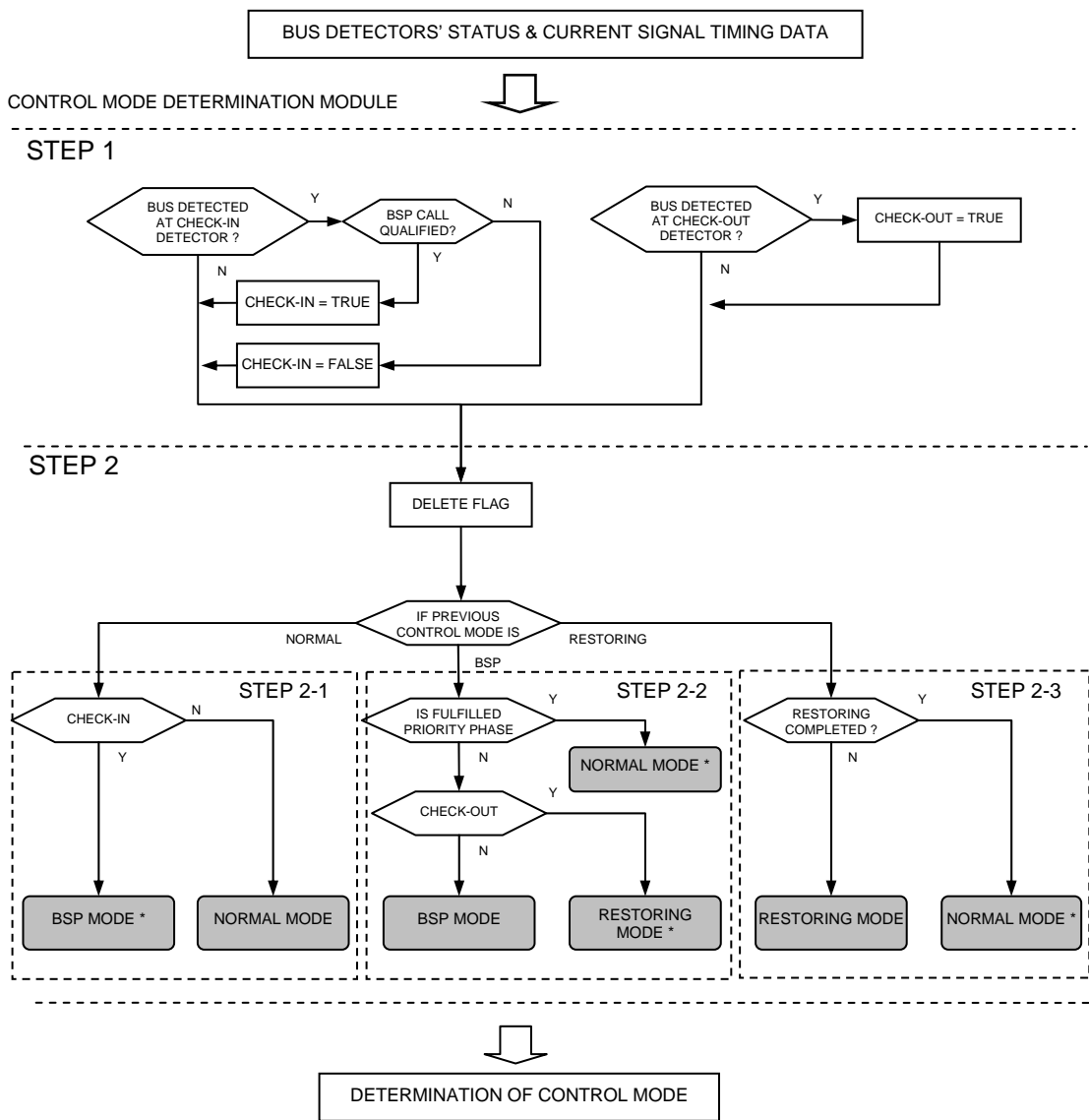


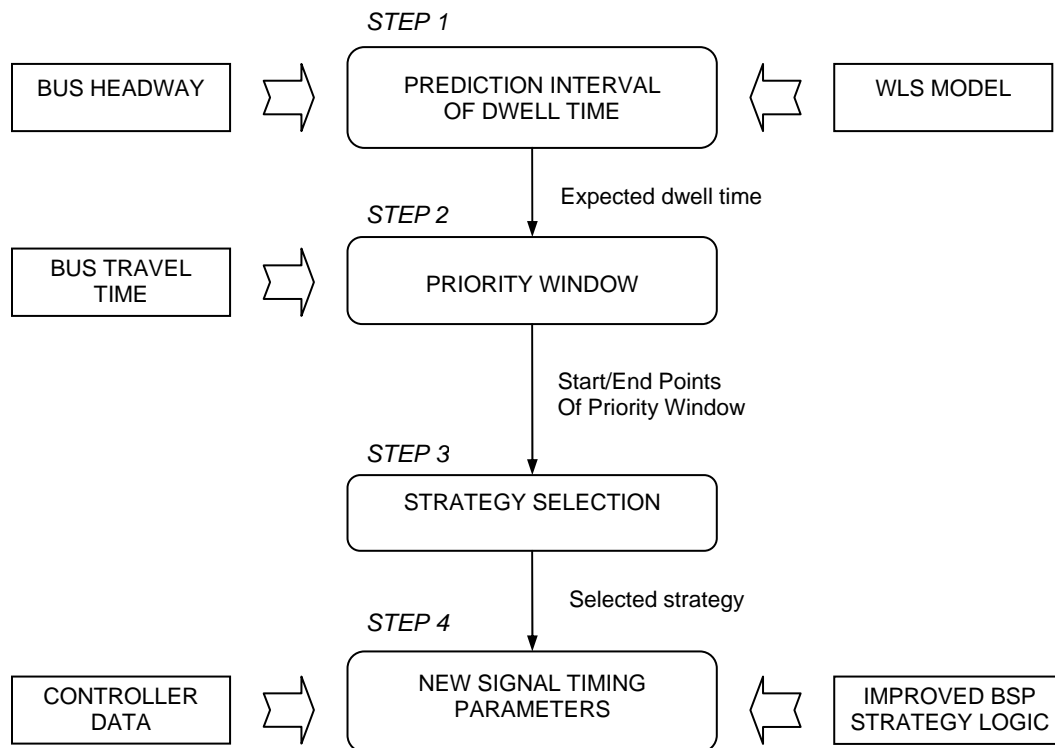
Figure 5-14 Functional logic of control module

Once a check-in detector is activated, the algorithm obtains the ridership information (e.g. the number of passenger on the bus) from on-board APC. The algorithm compares the passenger loads of the bus with pre-defined criteria. If the number of passenger on the bus is over a certain occupancy level (e.g. 20 passenger/bus), the bus is consider eligible for priority treatment.

In Step 2, the control mode for next time step is determined by the logic shown in Figure 5-14. The Step 2-1 represents that if the controller is in the normal mode, the control mode changes to BSP mode with the bus check-in, otherwise, it stays in the normal mode. Because the control mode is switched to the BSP mode, the BSP mode is flagged and the algorithm calculates the signal timing parameters for the priority. Step 2-2 illustrates the case when the current control mode is BSP mode. The normal mode is flagged if the controller fulfills the full length of the priority phase. The signal timing parameters for the normal mode will be obtained. If a bus passes the intersection during priority phase, the restoring mode is flagged otherwise the control mode stays in the BSP mode. When the current control mode is the restoring mode at shown in Step 2-3, the normal mode will be activated with the flag if the restoring process is completed; otherwise, the control mode stays in restoring mode. Through Step 1 and Step 2 in Figure 5-14, the control mode for next time step is determined and the algorithm obtains the signal parameter set according to the flagged control mode.

### **5.3.2 Priority Module**

When the control mode is flagged, the priority module is activated. The priority module then calculates new signal timing parameters that provide priority to the bus. As shown in Figure 5-15, the first step is to obtain a prediction interval of the dwell time. With the prediction interval and the bus travel time, the location of the priority window in the cycle is calculated. A priority strategy is selected by examining start and end points of the priority window. Once an appropriate BSP strategy is decided, a new set of signal timing parameters are obtained and returned to the control mode determination module. A detailed description for each task is discussed in the following sections.



**Figure 5-15 Functional diagram for the priority module**

#### 5.3.2.1 Prediction interval of dwell time (Step 1)

A prediction interval of dwell time for the approaching bus is calculated using the Weighted Least Square (WLS) regression model, discussed in Chapter IV. The WLS model provides the prediction of the dwell time as well as its prediction interval that varies according to the bus headway. Based on the bus headway that is achieved from the bus detector information, a  $(1 - \alpha) \cdot 100\%$  prediction interval is obtained. The WLS model provides three statistics: lower bound,  $(L_1)$ , upper bound  $(L_2)$ , and an expected dwell time  $(\hat{t}_d)$  for given bus.

### 5.3.2.2 Priority window (Step 2)

With the statistics obtained in step 1, the priority window is calculated based on the assumption of a constant bus travel time from the check-in detector to the bus stop and from the bus stop to the intersection. In practice, the bus travel time varies depending on the traffic conditions. However, because the bus travel time in this dissertation is a link travel time that excludes the intersection delay and the dwell time, the assumption of a constant travel time was deemed appropriate. The priority window in the cycle can be obtained by adding the bus travel time to both the lower bound and upper bound of the prediction interval. If the assumption of the constant bus travel time is valid, the bus detected at the check-in detector will arrive at the intersection during the priority window with the significance level of  $(1 - \alpha) \cdot 100\%$ . The lower bound and upper bound of the priority window are obtained from Equations 5-13 and 5-14.

$$\omega = t_c + T_b + L_1, \quad \omega = \omega - C, \text{ if } \omega > C \quad (5-13)$$

$$\omega' = t_c + T_b + L_2, \quad \omega' = \omega' - C, \text{ if } \omega' > C \quad (5-14)$$

where

$t_c$  = current cycle time (sec),

$T_b$  = bus travel time from check-in detector to stop line (sec),

$L_1$  = upper bound of the prediction interval for the dwell time (sec),

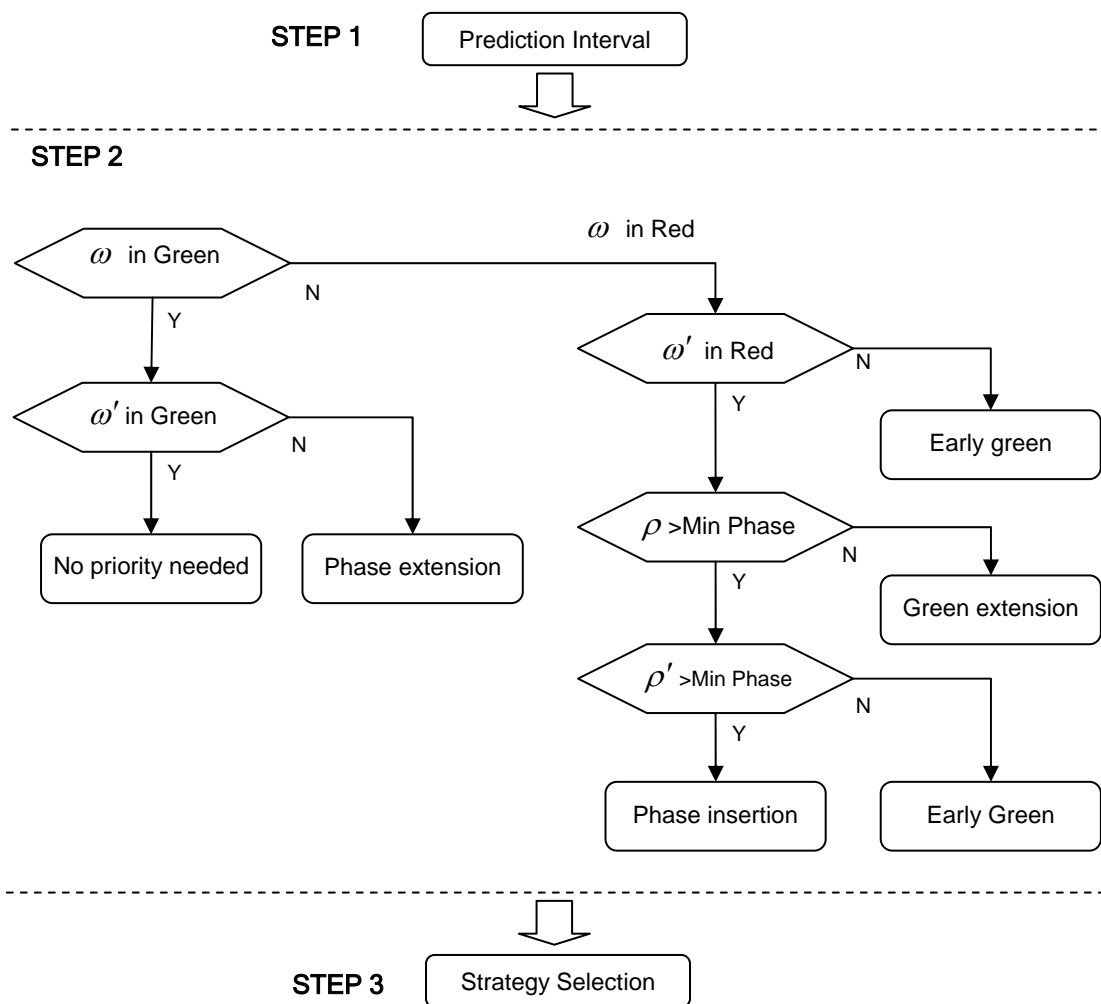
$L_2$  = lower bound of the prediction interval for the dwell time (sec), and

$C$  = cycle length (sec).

### 5.3.2.3 Strategy selection (Step 3)

The start and end points of the priority window that are calculated in step 2 are examined with respect to the background signal timing plan. The algorithm determines the signal phases in which the priority window starts and ends. An appropriate BSP strategy is selected by examining the phases that contains the start and end points of the priority

window as shown in Figure 5-16. When both the start and end points of the priority window,  $\omega$  and  $\omega'$ , locates in red period for the bus approach, there are three possible strategies. When the red time period before the priority window,  $\rho$ , is less than the minimum phase length (see Equation 5-11), the green extension strategy is selected as discussed in section 5.2.2.3. Similarly, the early green strategy is selected when the  $\rho'$  can not satisfy the condition in Equation 5-11; otherwise, the phase insertion strategy is selected.



**Figure 5-16** Logic flow for strategy selection

#### 5.3.2.4 New signal timing parameters (Step 4)

Once an appropriate priority strategy is determined, the signal timing plan is adjusted to provide the priority phase. The new signal timing plan is obtained by the logic of improved BSP strategies developed in section 5.2. The strategies modify the force-off points of the phases and the phase sequence in order to fit the priority window into the green phase for the bus approach. In adjusting the signal timing plan, the algorithm communicates with the signal controller to archive current signal timing data such as minimum green time for each phase, phase sequence, current phase being served, etc. Given the signal timing data, the algorithm obtains a new set of signal timing parameters tailored for the priority service, and returns them to the control module.

#### 5.3.3 Restoring Module

The improved BSP algorithm restores the remaining time not used by the priority phase back to non-priority phases. If the restoring mode is flagged (i.e. the control mode changes from the BSP mode to the restoring mode), the restoring module is initiated in order to calculate new set of signal timing parameters that assign unused priority green time to non-priority phases. The amount of time to be restored is decided by the difference between the force-off point of priority phase and check-out time of the bus as shown in Equation 5-15. The non-priority phases that are given the restoring green time will be a function of the BSP strategy implemented.

$$M_{rst} = \omega' - \theta_o \quad (5-15)$$

where

$M_{rst}$  = amount of time to be restored (sec), and

$\theta_o$  = time point in the cycle when a bus checks out (sec).



### 5.3.3.1 Green extension strategy

In this situation, all non-priority phases are eligible for the additional green time because the priority phase in the green extension strategy is provided before any non-priority phase. However when the bus crosses the check-out detector during a normal green period, the restoring process will not be activated because the control mode is switched to the normal mode. The restoring module is activated only when the current cycle timer is in the extended green period.

### 5.3.3.2 Early green strategy

The restoring options are quite limited for this strategy because all non-priority phases are implemented before providing the priority phase. The restoring process can be performed only when a bus checks out much earlier than the start of main street phase. In this case a non-priority phase can be inserted between the end of priority window and the start of main street phase. The number of non-priority phases that can be restored is determined by the amount of time available. In order to simplify the implementation, the cross street through phase is restored whenever the available time for the restoring is greater than the minimum phase length as shown in Equation 5-16. The minimum requirement includes the minimum green time and change interval for phase 4 as well as the change interval for priority phase (i.e. main street phase).

$$M_{rst} > (R_4 + I_4) + I_1 \quad (5-16)$$

### 5.3.3.3 Phase insertion strategy

The number of non-priority phases to be restored is a function of the phase sequence when the phase insertion strategy is implemented. Because the four-phase signal operation was assumed in the development of the phase insertion strategy, one or two non-priority phases occur after the priority phase. When one non-priority phase follows the priority phase, the available time for the restoring is assigned to this phase.

Figure 5-17 illustrates examples of restoring timing plans for the green extension strategy, early green strategy, and phase insertion strategy. The amount of green time to be restored back to each non-priority phase is a function of the BSP strategy, the amount of unused priority green time, and number of non-priority phases to be restored. Similar to the BSP strategies discussed in section 5.2.2, a weight is introduced for determining the amount of restored time to each phase as shown in Equation 5-17. Because the vehicles in the approach with high demand are expected to experience more delay due to the signal priority, the phase for the approach with high demand is given higher weight. In this dissertation, a weight of 1.5 is given to phases for through movements while the phases for turning movements are given a weight of 0.5.

$$S_i^{rst} = S_i^{BSP} + \frac{M_{rst}}{m} \cdot w_i \quad (5-17)$$

where

$S_i^{rst}$  = split of phase  $i$  in restoring mode (sec),

$S_i^{BSP}$  = split of phase  $i$  in BSP mode (sec), and

$m$  = number of non-priority phases being restored,  $1 \leq m \leq n - 1$ .

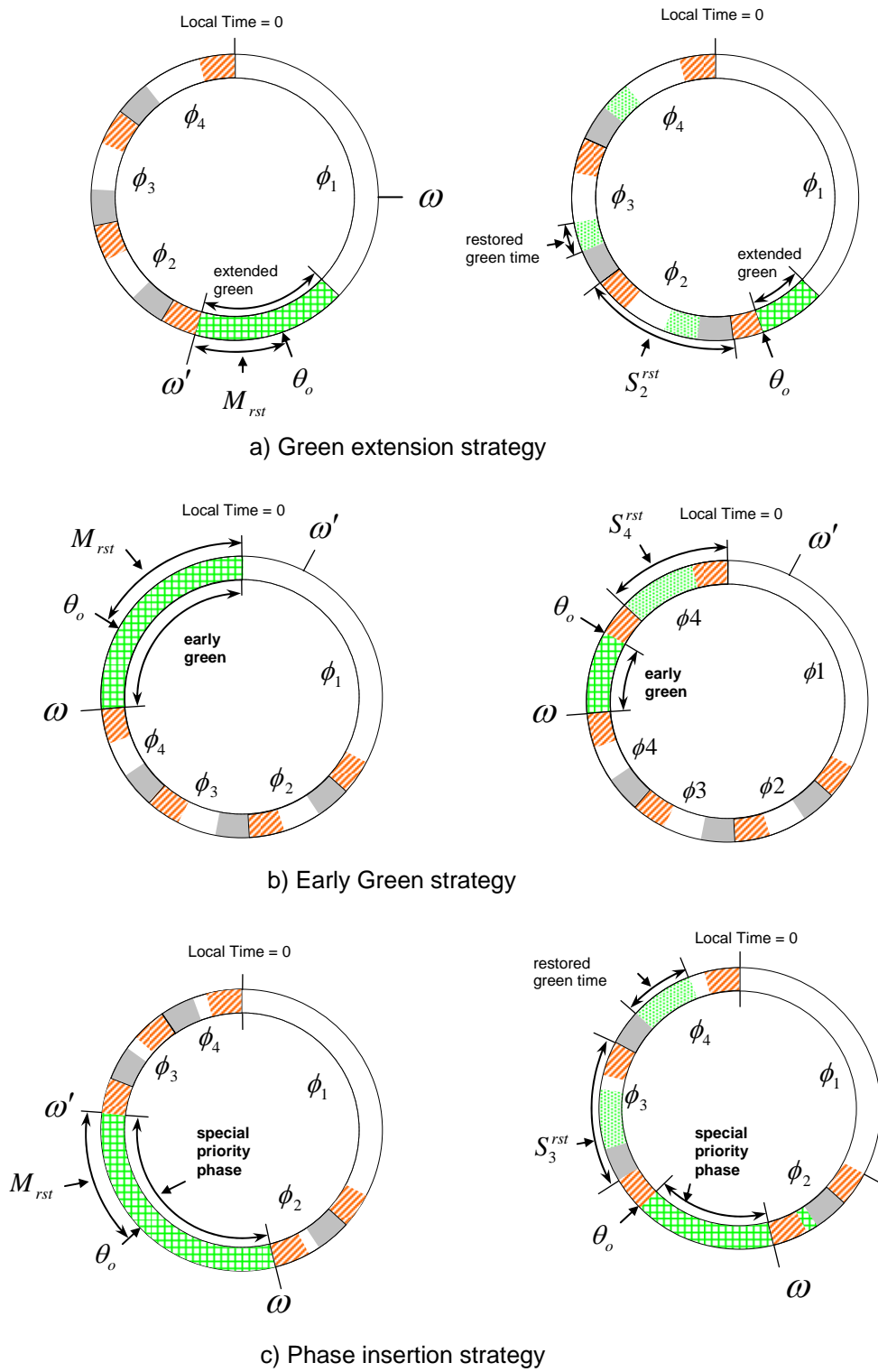


Figure 5-17 Examples of restoring for different BSP strategies

#### **5.4 CONCLUDING REMARKS**

Most current bus signal priority systems have been inefficient at intersections with nearside bus stops (5,9,28,29). Because of the variability in dwell time, the bus may fail to arrive at the intersection during the priority phase that is timed based on pre-defined bus travel time. The failure in the implementation of BSP aggravates the intersection delay of both buses and other traffic, which results in severe deterioration in the performance of signal operations.

In this chapter an improved BSP algorithm was developed to accommodate the variability of dwell time. The new prediction model and its prediction interval developed in Chapter IV were used as input to the improved BSP algorithm. The basic idea of the improved BSP algorithm is to provide a priority phase wide enough to accommodate the prediction interval of the bus dwell time. An operational algorithm was designed to implement the improved BSP strategy efficiently within the VISSIM simulation environment. The unused priority time is restored back to non-priority phases after the bus passes through the intersection during the priority phase.

The improved BSP strategies and operational algorithm were programmed using VAP in VISSIM. The improved BSP algorithm will be evaluated and a sensitivity analysis of the major parameters will be conducted using VISSIM simulation model in Chapter VII.

## CHAPTER VI

### CALIBRATION OF THE MICROSCOPIC SIMULATION MODEL

The calibration of microscopic simulation models has received widespread attention in the transportation and traffic engineering professions because of the increasing use of simulation models in operations and planning applications. The ability to accurately and efficiently model the traffic flow characteristics, drivers' behavior, and traffic control operation is critical for providing high fidelity simulation results. Because of the difficulty in collecting data in the field or lack of readily available procedures, the microscopic simulation model has often been used in analyses under default parameter values or "best guessed" values. With inappropriate parameters, the simulation model may produce unrealistic results

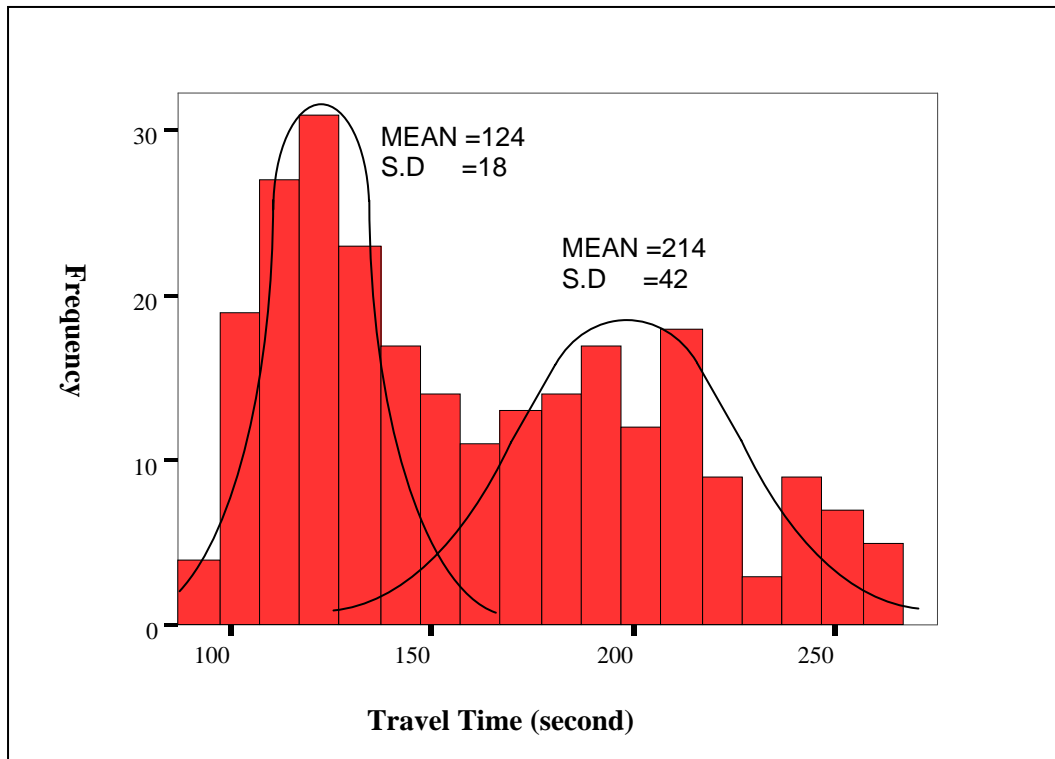
Calibration is the process of adjusting the value of model parameters based on observed data so that the model can realistically represent specific components of the system being modeled. Historically, calibration of traffic micro-simulation model has been considered to be a simple and non-automated procedure because of the lack of available data and the cost of iterative manual process. With recent growth in computational resources and ITS data, automated calibration methodologies for traffic microscopic simulation models have been proposed (67,68,69,70,71,72). The automated calibration procedures focused on finding the model parameters for an accurate representation of network performance through the use of optimization theory. These performance measures are utilized in determining how accurately the simulation model represents the real traffic system by comparing simulated performance measures to observed performance measures. An average travel time or total traffic volume have frequently been employed as performance measures (59,60,67,72). The calibration methodologies select the parameters that produce an average travel time that is closest to the observed average travel time. This selection is taken to be efficient if the difference

between variations (or dispersions) of two sample populations, that is the simulated and observed travel times, are minimized.

In this dissertation, the statistical testing procedure for testing the equality of two populations will be incorporated into the automated calibration methodology. A genetic algorithm (GA) automated calibration procedure is utilized to sample parameters from a specified range of values. Wilcoxon rank-sum test and Moses' test are introduced to test whether the median values and the dispersion of simulated travel times are statistically equal to those of the observed travel times. The use of statistical test to the automated calibration is a major contribution to this field.

## **6.1 STATISTICALLY BASED OBJECTIVE FUNCTION**

For the stable traffic condition such as traffic flow on the freeway section during off peak period, the single performance measure, such as average travel time or total traffic volume could be an adequate performance measure because the variability of travel time may be expected to be small. For an urban arterial section like the study site in this dissertation, however, a relatively large variability in travel time was expected because the test bed is a signalized arterial which operates under a coordinated control system. The observed travel times in the study site showed a bimodal distribution as shown in Figure 6-1. Travel time data was collected on October 16, 2003 during the AM peak period (7:30 AM ~ 8:30 AM). The average travel time was 164 seconds and the standard deviation was 54seconds. The vehicles in the first peak represent those which receive a green signal while those in the second peak represent vehicles that are stopped by a red signal. The average travel time in the first peak (i.e. travel time less than 160seconds) was 125 and their standard deviation was 18. In contrast, the average travel time in the second peak (i.e. travel time greater than 160seconds) was 214 and their standard deviation was 42. Intuitively, the vehicles in the first peak would have a smaller standard deviation than those in the second peak because the vehicles in the progression band tend to travel at a similar speed in order to stay in the progression band.



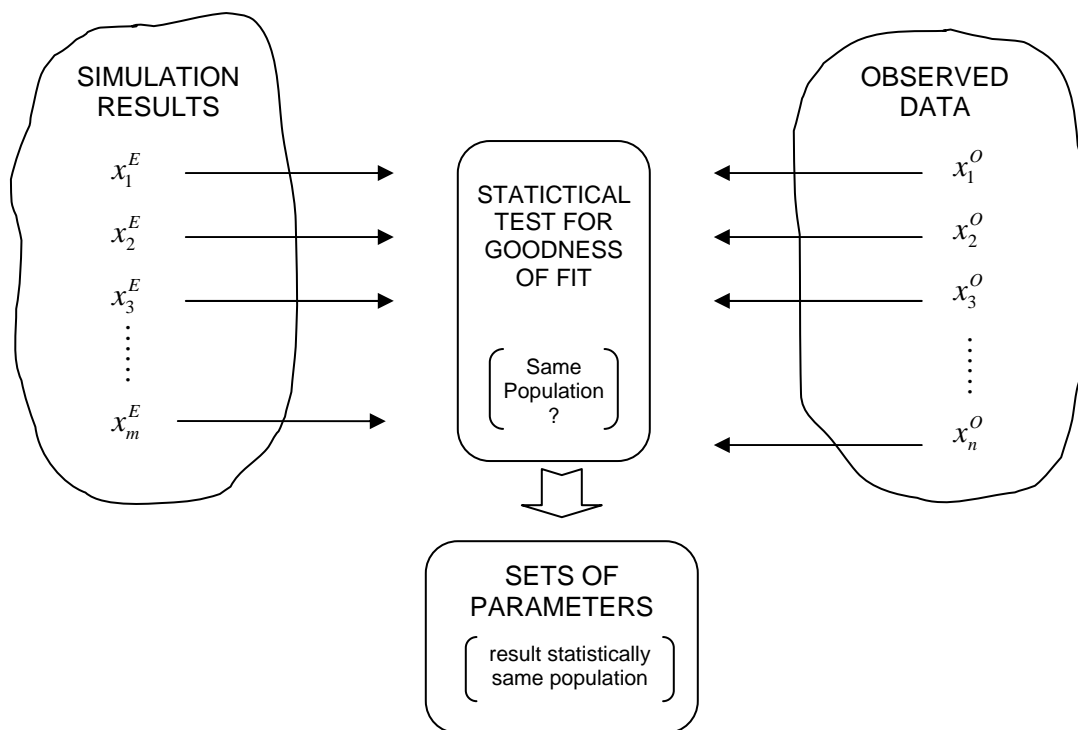
**Figure 6-1 Observed travel time distribution for arterial section with signalized intersections**

When the traffic conditions in a test bed have large variability and a highly non-normal distribution an aggregated performance measure, such as mean travel time, may not be the most appropriate measure of effectiveness. If the aggregated performance measure is used in the calibration process there is a danger that inappropriate parameter sets may be selected. To avoid this situation a statistically based approach, which is based on a more disaggregate form of the observed travel time, is used. Specifically, the “closeness” of the observed travel time distribution to that of the simulated travel time distribution is chosen as the objective function.

A conceptualization of the calibration process is shown in Figure 6-2. Note that because the process is statistically based there may be numerous parameter sets (or none) that match the observed data. When this occurs an alternative selection technique for identifying the “best” parameter set is required as will be discussed later.

There are numerous statistical methods for testing whether two samples are drawn from the same population (73). The more popular of these techniques focuses on testing the equality of the means or variance of the different distributions. The most popular methods are the student t-test for testing means and the F-test for testing variances. However, these tests do not examine the distribution of the metric which may be rather restrictive for many transportation applications. In this study the metric of interest is the travel time on a signalized arterial street and, for this situation, modeling the distribution of travel times would be important.

In these situations nonparametric or distribution-free methods for testing the difference between two sample populations are required. These techniques do not require *a priori* assumptions about the distribution of the underlying population other than that it is continuous. Two nonparametric tests are used to test the difference between two populations in this paper as will be discussed in the following sections.



**Figure 6-2 Conceptualization of disaggregated performance measure in calibration**



## **6.2 AUTOMATED CALIBRATION PROCEDURE**

The proposed automated calibration method employs a GA algorithm and nonparametric statistical testing methods. In this section, the fundamentals of the GA algorithm are introduced and the nonparametric statistical test procedures are presented. Finally, each step of the calibration procedure is explained briefly.

### **6.2.1 Genetic Algorithm Process**

A GA is a problem-solving algorithm that emulates biological evolutionary theories to solve problems of the field of optimization. In transportation engineering, GAs have been employed in optimizing traffic signal timing and calibrating traffic simulation models (59,67,68,69,70). While the detailed theory behind the GA can be found in the literature (74,75), a basic understanding of the GA methodology and logic is presented here to aid in comprehension of the simulation and calibration results, including the steps followed for this research.

The calibration parameters are encoded as strings of chromosomes that are uniquely mapped to each of the parameters. Then, the GA generates potential parameter sets until it satisfies certain stopping criteria. In each generation, the GA performs at least the following three operations: reproduction, crossover, and mutation. Reproduction starts with assigning a probability of being selected to each chromosome. The probabilities are calculated based on the fitness values obtained by a predetermined fitness function that evaluates the performance of the chromosome. The chromosomes with higher fitness value are more likely to be selected during reproduction than those with lower fitness value. After reproduction, the crossover operations are performed to create new offspring chromosomes from the parent chromosomes by exchanging genes. In essence, the chromosomes being selected in reproduction phase have a higher probability of sending their genes to the next generation. After crossover is finished, the mutation operation is performed to ensure that fresh solutions are considered. This process is relatively straightforward in that a particular location on the chromosome is identified and the value of the binary cell at that location is flipped. In both crossover

and mutation operations, each chromosome has the same chance of being selected for each operation and the probabilities of the operations are pre-defined.

Following the process of reproduction, crossover, and mutation, a newly derived population is generated and another new competition takes place where the weak candidates are discarded and only the strong survive. This entire process is continued until the stopping rules are met.

### **6.2.2 Statistical Test Procedures**

Numerous statistical methods for testing whether two samples are drawn from the same population have been developed. These focus on testing equality of population means or variance. The most well known methods are the student *t*-test for testing means and the *F*-test for testing variances and these tests are based on the assumption of normally distributed random variables. However, this rather restrictive assumption is not always reasonable in applications that include travel time distribution, which is the case in this dissertation.

Nonparametric or distribution-free methods for testing the difference between two sample populations are available, which require no assumptions about the distribution of the underlying population other than it is continuous. Two nonparametric tests are performed consecutively to test the difference between two populations with respect to distributional parameters such as central tendency and dispersion. At first the Moses' distribution free rank-like test is utilized for testing the equality of dispersion (76). This test is a good alternative when the medians are unknown. Wilcoxon rank-sum test is subsequently performed in order to check the equality of location for two populations if the underlying distributions of the populations have equal dispersion. The Wilcoxon test assumes that the distributions of two populations have the same shape and spread and differ only in their locations. The procedures for these tests are briefly summarized as follows:

### 6.2.2.1 Moses' distribution free rank-like test

This test constructs subsamples which are used to estimate dispersions that are similar to variance estimates, but are in fact just sums of squares. The Wilcoxon rank-sum test is used to compare the dispersions in the two groups.

*Step 1:* select a positive integer  $k \geq 2$ , and randomly divide the  $X$  and  $Y$  observations into  $m'$  and  $n'$  subgroups of size  $k$

*Step 2:* for  $i = 1, \dots, m'$ , define  $i$  th subgroup of  $X$  consisting of  $k$  observations by  $X_{i1}, \dots, X_{ik}$   
for  $i = 1, \dots, n'$ , define  $i$  th subgroup of  $Y$  consisting of  $k$  observations by  $Y_{i1}, \dots, Y_{ik}$

*Step 3:* define  $C_1, \dots, C_{m'}$  by:

$$C_i = \sum_{s=1}^k (X_{is} - \bar{X}_i)^2 \quad i = 1, \dots, m' \quad (6-1)$$

$$\bar{X}_i = k^{-1} \sum_{s=1}^k X_{is} \quad (6-2)$$

define  $D_1, \dots, D_{n'}$  by:

$$D_i = \sum_{s=1}^k (X_{is} - \bar{X}_i)^2 \quad i = 1, \dots, n' \quad (6-3)$$

$$\bar{X}_i = k^{-1} \sum_{s=1}^k X_{is} \quad (6-4)$$

*Step 4:* use Wilcoxon Rank-Sum test on the C and D values.

### 6.2.2.2 Wilcoxon rank-sum test

This test is the most widely used method for testing equality of location for two populations when the underlying distributions are nonnormal.

*Step 1:* define continuous random variables,  $X_1, \dots, X_m$  and  $Y_1, \dots, Y_n$ ,  $m \leq n$

*Step 2:*  $m + n$  observations are pooled to form a single sample with the group identity of each observation retained.

*Step 3:* the observations are ordered smallest to largest and ranked from 1 to  $N = m + n$

*Step 4:* obtain the test statistic  $W_m$ , sum of the ranks associated with the observations that originally constituted the smaller sample ( $X$  values). when the sample size  $m$  or  $n$  exceed the table values, a large sample normal approximation is used:

$$W^* = \frac{W_m - E(W_m)}{\sqrt{\text{Var } W_m}} \quad (6-5)$$

$$E(W_m) = \frac{n(m+n+1)}{2} \quad (6-6)$$

$$\text{Var } W_m = \frac{mn(m+n+1)}{12} \quad (6-7)$$

*Step 5:* compare the test statistics with critical values in Wilcoxon rank-sum table (or standard normal table for large sample approximation).

### 6.2.3 Calibration Procedure

Figure 6-3 provides an overview of the calibration procedure including the GA used in this dissertation. It may be seen that the procedure is essentially iterative in that a series of candidates are identified, simulation results of the candidates evaluated, and then a new population of candidates is generated. Based on the statistical test for the microscopic simulation output, parent chromosomes are identified and stored in the pool of accepted chromosomes. The process is repeated until a stopping criterion is met. As can be seen in Figure 6-3, there are five steps in the procedure, and each step is explained in the following subsections.

#### *Step 1: Initialize the GA parameters and a significant level for statistical test*

The first step in the calibration procedure is the initialization of the GA parameters including the population size ( $P$ ), mutation probability ( $P_m$ ), and the probability of crossover ( $P_c$ ). In addition, the maximum number of accepted chromosomes ( $N_t$ ) and the significance level ( $\alpha$ ) are identified along with a scheme of statistical tests. The parameters of microscopic simulation model that are to be calibrated are identified and represented in the format of binary strings. In this step, an initial population of parent chromosomes ( $P$ ) are created utilizing a random process.

#### *Step 2: Operation of microscopic simulation model*

Following initialization, the microscopic traffic simulation model is run with the input file where the parameters generated in the format of binary strings are translated into the appropriate format. The simulation is repeated for each of the  $N$  chromosomes. The number of iteration  $N$  is defined by the number of chromosomes that are created by the initialization or crossover/mutation operations. Note that  $N$  is constantly changing based on the number of offspring chromosomes.

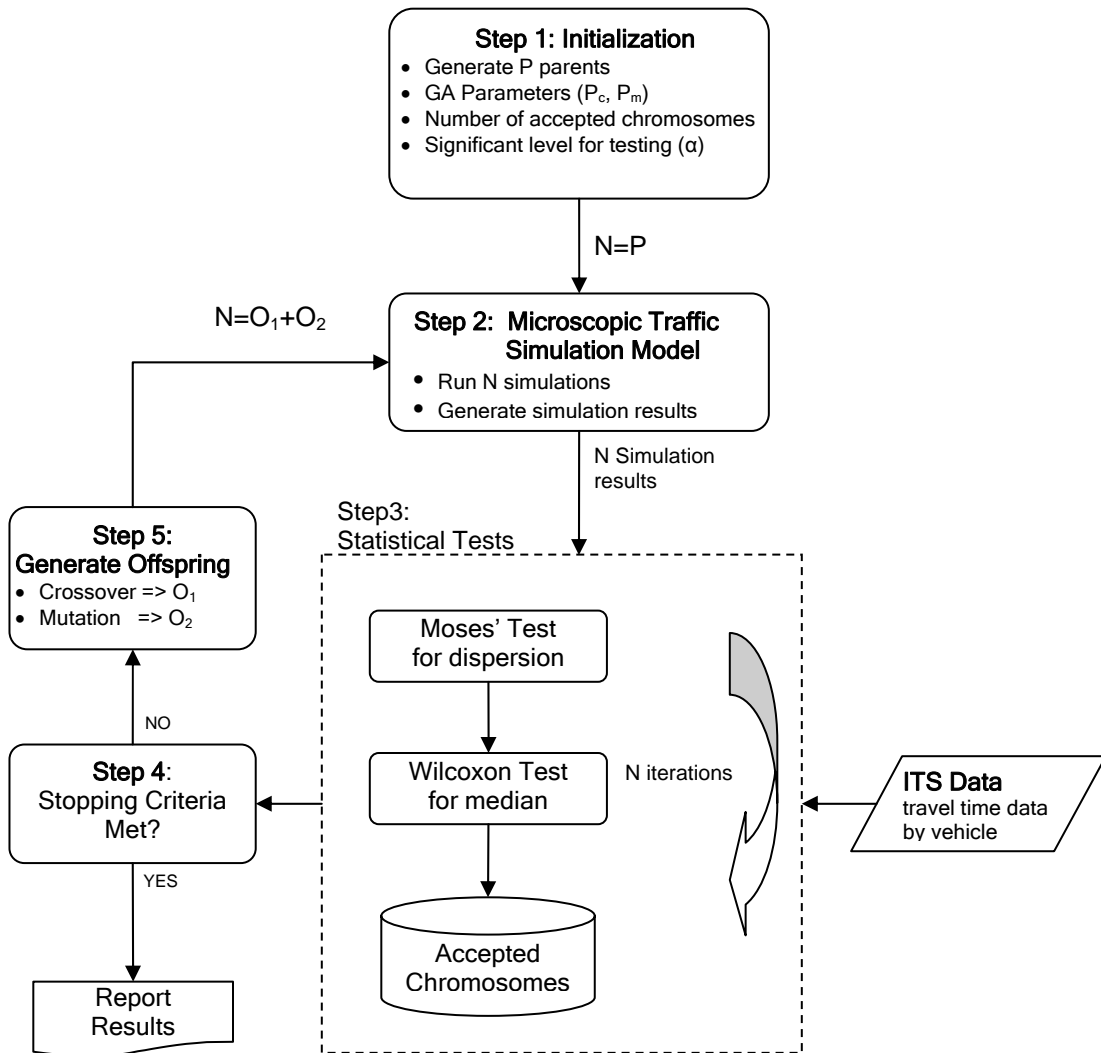


Figure 6-3 Overview of calibration procedure

*Step 3: Evaluate model output and select parameter set*

The evaluation of the model output and selection of the parameter set are some of components of this procedure that distinguish it from conventional calibration methods. The model output for each candidate (i.e. chromosome) is evaluated through the statistical tests for equality of the populations. As discussed previously, two descriptive statistics, median and dispersion, are tested using nonparametric testing methods. Moses' test is performed first to test the equality of dispersions, because the testing methods for equality of medians require a distributional assumption of same dispersions in two populations. Once the test of dispersions concludes, that is the two populations have statistically equal dispersion, the medians of two populations are tested using Wilcoxon rank-sum test. The chromosomes that are accepted by both tests are stored in the pool of accepted solutions that are used in forming the new set of parent chromosomes. Any candidate that is rejected by either test is discarded. The tests are repeated for each of the  $N$  chromosomes.

*Step 4: Check stopping rules*

After selecting parent chromosomes, the stopping rules established for the analysis are checked. In this dissertation, a maximum number of chromosomes is identified *a priori*. However, other stopping rules such as a maximum number of iterations can be used in conjunction with a maximum accepted chromosome value. If stopping rules are not met, the algorithm proceeds to Step 5 to generate offspring chromosomes.

*Step 5: Perform crossover and mutation operations*

Based on the probability of selection ( $P_m, P_c$ ), crossover and mutation operations are performed to generate new offspring chromosomes from the parent chromosomes that were selected in Step 3. The total number of offspring created in this step is the sum of operation results from crossover ( $O_1$ ) and mutation ( $O_2$ ). Following the generation of offspring, the algorithm proceeds to Step 2 to simulate the offspring chromosomes and the process continues.

At the end of the procedure, a number of parameter sets that are significant are reported as a result. These parameter sets produce the performance measures that are not statistically different. This result also allow additional analysis for selecting the significant parameters or defining the range of each parameter.

## **6.3 IMPLEMENTATION OF THE PROPOSED PROCEDURE**

### **6.3.1 VISSIM Background**

VISSIM, a German acronym for Traffic In Towns: SIMulation, is a microscopic, time-step and behavior based simulation model that has the ability to evaluate vehicular traffic, transit operations, and pedestrians. The traffic flow model in VISSIM is a discrete, stochastic, time step based microscopic model, with driver-vehicle-units as single entities. The model contains a psycho-physical car following model for longitudinal vehicle movement and a rule-based algorithm for lateral movements (77,78).

#### *6.3.1.1 Car-following model of VISSIM*

The psycho-physical driver behavior model developed by Wiedemann (77) is employed in order to capture both the physical and human components of traffic simulations. The basic concept of the psycho-physical car following model is that the driver of a faster moving vehicle is sensitive to a slower moving vehicle in front. The following driver perceives changes in distance and speed difference and reacts accordingly (79,80). Changes are only perceived if the physical impulse exceeds a certain minimum value, referred to as the threshold. In this case, the physical impulse is the observed size of vehicle in front. Perception of a change depends on how fast the image of the front vehicle changes, which is a function of difference in speed and distance.

Once the perception threshold for the realization of a difference of speed is exceeded, the following driver will chose to decelerate until he can no longer perceive any relative speed, and the threshold is not then re-exceeded. Because the driver cannot exactly determine the speed of the vehicle in front, the speed will fall below speed of the



front vehicle until driver starts to slightly accelerate again after reaching another perception threshold. This results in an iterative process of acceleration and deceleration. Besides the thresholds in the context of the difference of speeds, other thresholds were introduced to describe the distance between vehicles. The individual properties of these thresholds were first combined into a fully working simulation model by Wiedemann (77). The perception thresholds of the psycho-physical car-following model and their definitions can be found elsewhere (77,80)

#### *6.3.1.2 Lane changing model*

VISSIM uses a model of human lane changing behavior, which represents human decisional process concerning lane changing. Since vehicle movements are based on human decisions that are influenced by a perception of surrounding vehicles, the lane changing model has been defined in strong relation to the car following model (77,80).

On multi-lane links, a hierarchical set of rules is used to model lane changes. A driver tries to change lane if he is hindered by a slow leading vehicle. First, the driver checks whether he can improve his present situation by changing lanes. If so, he checks the possibility of finding acceptable gaps on neighboring lanes without generating a dangerous situation. For this maneuver, a driver takes into consideration up to six other vehicles. Lane changes are divided into four types of changes from a slower to a faster lane and two types of changes from a faster to a slower lane. Each type of lane change has a different set of parameters and rules.

#### **6.3.2 VISSIM Calibration Parameters**

VISSIM includes a variety of controllable parameters that allow users to calibrate the model to match existing traffic conditions. The VISSIM calibration parameters can be summarized into two general categories: 1) driver behavior parameters and 2) vehicle performance parameters. The base calibration parameters for VISSIM that have been considered in this dissertation are the driver behavior parameters, specifically the car-following parameters and the lane changing parameters. There are described as follows:

### 6.3.2.1 *Number of observed preceding vehicles*

The number of observed preceding vehicles affects how well vehicles in the network can anticipate other vehicles' movements and react accordingly. The default value in VISSIM is two vehicles. The simulation will run slower with higher values because of additional calculations for the car following behaviors of each driver.

### 6.3.2.2 *Look ahead distance*

The look ahead distance defines the distance that a vehicle can see forward in order to react to other vehicles either in front or to the side of it within the same link. Minimum and maximum values for this parameter can be entered in VISSIM. The default values in VISSIM are 0 and 250 meters, respectively.

### 6.3.2.3 *Average standstill distance (AX)*

Average standstill distance defines the average desired distance between stopped cars and also between cars and stop lines. The default value in VISSIM is 2.0 meters. With fixed vehicle length, this parameter determines the average length of roadway occupied by each queue position.

### 6.3.2.4 *Additive and multiplicative part of desired safety distance (BX\_Add, BX\_Mult)*

The additive part and multiplicative part of desired safety distance affects the computation of desired minimum following distance at low speed differences. The desired minimum following distance consists of the distance AX, safety distance BX, and the speed term as shown in Equations 6-8 and 6-9.

*BX\_Add* and *BX\_Mult* are both calibration parameters for the desired safety distance which can be adjusted by the field studies about car following behaviors. Note that the saturation flow rate is determined by these parameters because it is a function of the desired safety distance.

$$ABX = AX + BX \quad (6-8)$$

$$BX = (BX\_Add + BX\_Mult \cdot RND1_i) \cdot \sqrt{v} \quad (6-9)$$

where

- $ABX$  = desired minimum following distance,
- $AX$  = desired distance for standing vehicle
- $BX$  = desired safety distance,
- $BX\_Add$  = calibration parameter defining the range of variation,
- $BX\_Mult$  = calibration parameter defining the range of variation,
- $RND1_i$  = random number for vehicle  $i$  from distribution  $N(0.5,0.15)$ ,
- $v$  = speed of front vehicle for following process  
speed of following vehicle for free flow driving

### 6.3.2.5 Lane change distance

The lane change distance defines the distance at which vehicles will begin to attempt to change lanes. This parameter is used with the emergency stopping distance to model lane change behavior in order for cars to follow their route. The default value for this parameter in VISSIM is 200.0 meters. Acceptable values should be selected to ensure a vehicle has a reasonable distance to make a lane change before it reaches intersection.

The calibration parameters are outlined in Table 6-1 and the minimum and maximum allowable values utilized in the calibration procedure are also provided.

**Table 6-1 VISSIM calibration parameters**

Parameter ( $P_i$ )	Description	Units	Default value	Min Value	Max Value
$P_1$	Number of Observed Preceding Vehicles	Vehicle	2	0	4
$P_2$	Look Ahead Distance	Meter	250	0	400
$P_3$	Average Standstill Distance (AX)	Meter	2	1	4
$P_4$	Additive part of desired safety distance	N/A	2	1	10
$P_5$	Multiplicative part of desired safety distance	N/A	3	1	10
$P_6$	Lane Change Distance	meter	200	50	300

### 6.3.3 Analysis of Results

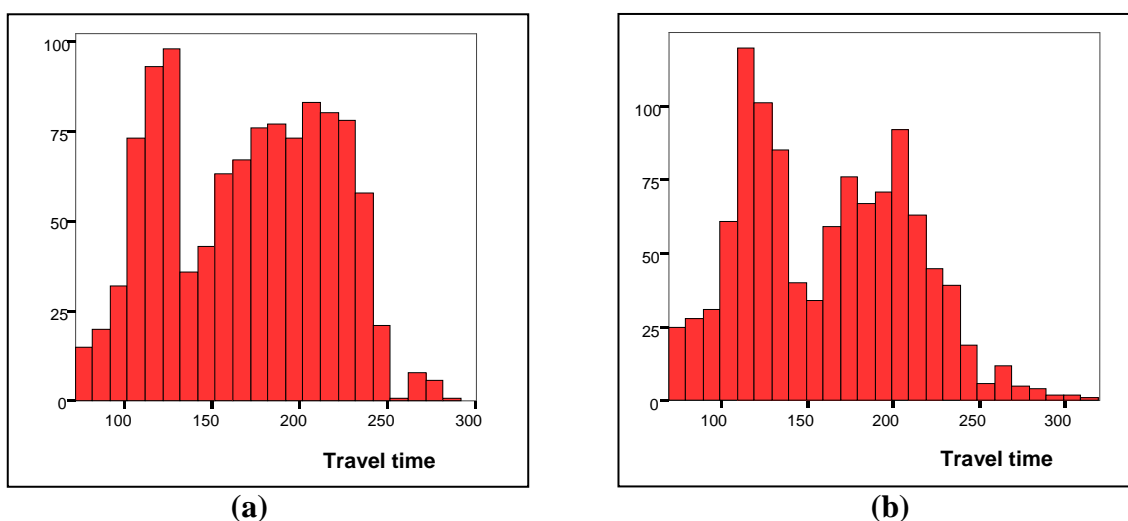
The proposed calibration procedure was performed to “fine tune” the microscopic simulation model to match existing traffic condition of the test bed. In particular, the travel time on the links in terms of median and dispersion were the closer performance measures. The accepted chromosomes of 100 were resulted with a 0.05 significance level. Table 6-2 shows a part of the accepted parameter sets with test statistics. It can be seen that accepted parameter sets always have low travel time Mean Absolute Error Ratio (MAER), which ranges from 0.002 (0.2%) to 0.062 (6.2%) while default parameter set results in a MAER of 21.5%. Because the accepted parameter sets produce simulated travel time distributions that are not statistically different from the observed travel time distribution, the difference between the means of the distributions is expected to be quite small.

**Table 6-2 Summary of accepted parameter sets**

No.	Calibrated Parameters						Mose's Test	Wilcoxon Test	MAER (error)
	$P_1$	$P_2$	$P_3$	$P_4$	$P_5$	$P_6$	p-value	p-value	
1	1	130	2	5	5	260	0.749	0.481	0.003
2	2	70	1	7	3	280	0.784	0.704	0.002
3	2	240	4	4	4	270	0.837	0.292	0.043
4	3	90	2	5	4	140	0.157	0.481	0.040
5	4	190	2	5	3	100	0.337	0.088	0.062
⋮	⋮	⋮	⋮	⋮	⋮	⋮	⋮	⋮	⋮
99	2	330	1	5	7	120	0.411	0.677	0.018
100	3	330	1	5	5	80	0.749	0.915	0.006

It is important to point out that MAERs in the 10<sup>th</sup> column in Table 6-2 does not represent any superiority or inferiority among accepted parameter sets. Any parameter set that has passed the statistical tests is considered as one of the solution sets for parameter calibration regardless of its MAER. The parameter sets that produce lower MAER than accepted sets can be rejected when they fail in testing equality of dispersions but pass Wilcoxon test for equal medians successfully. Figure 6-4 illustrates

the two travel time distributions resulting from the calibration process. The frequency histogram in Figure 6-4 (a) was drawn from results of the rejected parameter set with 1% of MAER. An example of an accepted parameter set with 1% of MAER is shown in Figure 6-4 (b). Although the rejected parameter set produces a same MAER, the shape of distribution is different from observed travel time distribution in Figure 6.1. However, the accepted parameter set results in bimodal distribution similar to the observed distribution.



**Figure 6-4 (a) Rejected set with 1% MAER and (b) accepted set with 1% MAER**

A proposed calibration procedure where the statistical tests are incorporated can avoid faulty selections that may be caused when MAER is solely employed as a performance measure. As discussed previously, low MAER can not always guarantee the most “fit” parameter set.

Once parameter sets that have equal distribution with observed data have been determined, the “best” parameter set may need to be selected in order to utilize the microscopic simulation model for the operation and planning applications. One might select the best solution among accepted parameter sets based on MAER or P-values. For the purposes of this dissertation, the parameter set that has lowest difference in bus travel times between stops has been selected because the simulation model is utilized in the

performance evaluation of the bus signal priority system. Each of the accepted parameter sets is coded into VISSIM input files and then the simulations are performed. MAER of the average bus travel time for each simulation run is recorded and then compared. The optimum parameter set was chosen by Equation 6-10.

$$\mathbf{P}_{bus}^* = \min \left\{ \sum_{k=1}^S |E_{ik} - O_{ik}| \right\} \quad (6-10)$$

where

- $\mathbf{P}_{bus}^*$  = optimum parameter set for buses,
- $E_{ik}$  = estimated bus travel time on link  $k$  for parameter set  $i$ ,  $i = 1..I$ ,  $k = 1..S$
- $O_{ik}$  = observed estimated bus travel time on link  $k$  for parameter set  $i$ ,
- $I$  = number of accepted parameter set, ( $I = 100$ ), and
- $S$  = number of the link between stops, ( $S = 3$ , in this study).

Table 6-3 shows a part of results for parameter selection for bus travel time. The MAER for passenger car travel time and bus travel time are compared in the table. The bus travel time MAER ranges from 0.155 to 0.35, which shows a 40% improvement in MAER comparing with that of default parameter set. The parameter set with lowest MAER for bus travel time was selected for this dissertation and it is shown on the first row in Table 6-3. The results indicate that MAER for passenger vehicles improves from 0.215 (value with default parameters) to 0.004, after employing the selected parameter set. The selected parameters are not substantially different from default parameter values except the additive part and multiplicative part of desired safety distance,  $P_4$  and  $P_5$ . As shown in Equation 6-9, the desired safety distance that affects the saturation flow is an additive function of these two parameters. Therefore, the sum of these two parameters can represent the sensitivity of the drivers to the distance from the vehicle in front. The sum of these parameters is 9 while the default setting is 4. The sum of these two parameters for the accepted parameter sets ranges between 8 and 12. It can be concluded that the value of each parameter which is selected lies within reasonable range.

**Table 6-3 Summary of bus and car MAER from accepted parameter set**

No.	Calibrated Parameters						Car MAER	Bus MAER
	$P_1$	$P_2$	$P_3$	$P_4$	$P_5$	$P_6$		
60	2	300	1	8	1	270	0.004	0.155
31	0	210	3	5	3	80	0.004	0.161
43	1	90	1	6	6	280	0.062	0.167
⋮	⋮	⋮	⋮	⋮	⋮	⋮	⋮	⋮
55	1	140	2	5	5	260	0.010	0.307
46	1	270	2	4	7	290	0.055	0.350

#### 6.4 CONCLUDING REMARKS

Recent advances in computational technology along with the development of microscopic simulation models such as VISSIM have led to increasing attention being focused for the calibration and validation of simulation models. The automated calibration procedures focus on finding the model parameters for an accurate representation of network performance through the use of optimization theory. In the evaluation of each candidate parameter set, aggregated measures, such as average travel time and total traffic volume are conventionally utilized. In this chapter, faulty selections that could potentially occur with aggregated measure, have been described. In order to utilize disaggregated measures, statistical tests that evaluate the equality of two populations (i.e. simulated and observed travel times) using individual vehicle information are integrated into the GA-based calibration procedure.

For the test bed, the proposed calibration procedure was successful in exploring the travel time distributions that are a bimodal mixture of two distributions produced due to the effects of signal progression. The travel time MAER was significantly improved for all accepted parameter sets that produce travel time distributions which are statistically equal to the observed distribution. Finally, the parameter set which yields lowest bus travel time MAER was chosen for simulation run in order to evaluate the performance of BSP systems.

## CHAPTER VII

### EVALUATION AND SENSITIVITY ANALYSIS

A new model for predicting bus dwell time and an improved bus signal priority algorithm were developed in Chapters IV and V. The predicted dwell time and its prediction interval were incorporated into an improved BSP algorithm as discussed in Chapter V. In Chapter VI, the traffic simulation model for the study site was calibrated. In this chapter two simulation studies will be conducted as parts of the evaluation of the performance of the improved BSP algorithm. The first simulation study compares the performance of the improved BSP algorithm with other BSP algorithms. The second study focuses on sensitivity analysis of the parameters, such as traffic demand, bus headways, and significance levels of the prediction interval.

#### 7.1 EXPERIMENTAL DESIGN

##### 7.1.1 Simulation Design

As discussed in Chapter III, four signal operations were tested: Normal operation without BSP, basic BSP, BSP with consideration of constant dwell time, and the improved BSP algorithm where user updated predicted dwell time and prediction intervals. All signal operation algorithms were coded using VAP in VISSIM. The detailed information for the algorithms can be found in Chapters III and V. For the purposes of this dissertation, these signal operation scenarios<sup>1</sup> are referred as Normal, BSP0, BSP1, and BSP2 scenario, respectively. Because it was hypothesized that the BSP2 scenario can reduce the bus delay at the intersection without significant deterioration in the performance of signal operation, the other scenarios were developed for the purpose of comparing measure of effectiveness (MOE).

---

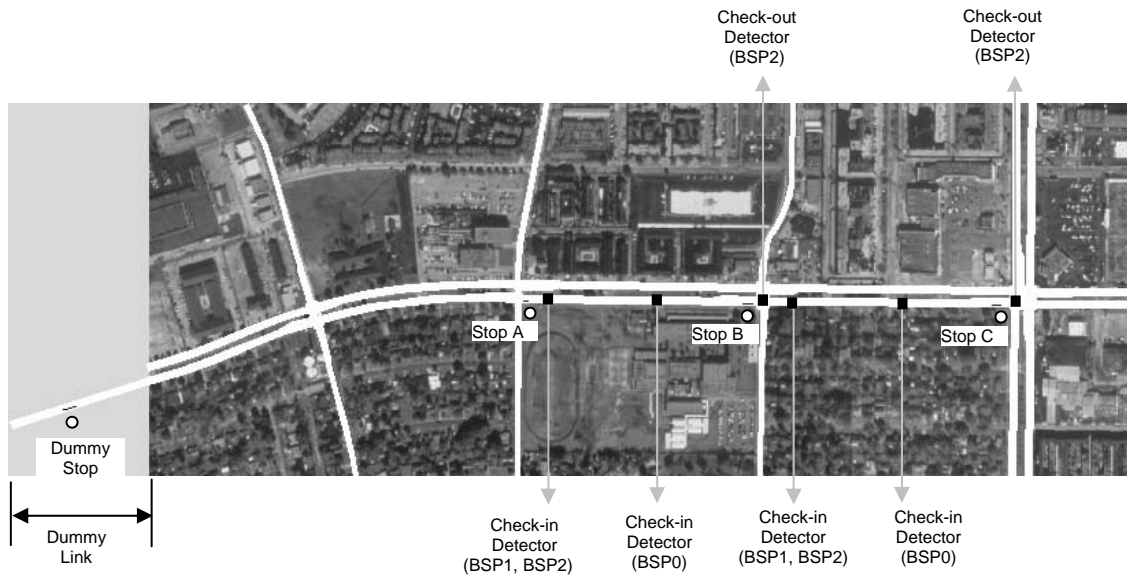
<sup>1</sup> Throughout this chapter the term of 'scenario' refers to the signal operation algorithm.



The study site consists of three signalized intersections and three bus stops including two nearside stops. The BSP scenarios were implemented at two intersections with nearside bus stops because the primary objective of this study is to develop a BSP algorithm for the intersections with nearside stops. In addition, the priority service was provided to the buses on the eastbound approaches for initial development and proof-of-testing purposes. During the morning peak period, which is the base period of this study, the eastbound approaches were congested with traffic commuting towards the downtown of Houston. Therefore, the reduction in the bus delay because of the BSP implementation was expected to be greater on the eastbound approaches than those on westbound approaches. Among the three bus routes operating at the study site, route #2 was selected as an eligible bus route for priority treatment because only route #2 services all bus stops.

Each BSP scenario requires a different setting of the bus detector. Figure 7-1 illustrates the simulation network in VISSIM. Detector settings for BSP operations and stop locations have also been depicted. The normal actuated scenario without BSP logic requires no bus detector. The BSP0 requires a check-in detector near the intersection because the priority process is initiated upon the detection of a bus. The check-in detector was set at a location 200 meters upstream of the intersection. The 'PT calling detector' was set at the same location for communicating with the signal controller. Note that PT (public transport) calling detector in VISSIM only senses transit vehicles that send out PT information. When buses are detected at a check-in detector the PT information, which would be passenger loads in this study, is sent to the signal controller for the assessment of the eligibility of priority requests. For BSP1 and BSP2, the check-in detectors were set 350 meters upstream from the intersections because these scenarios require a longer preparation period. For example, in these latter scenarios the phase splits and sequences are adjusted for providing the priority phase. Like the BSP0 scenario the PT calling detectors were installed at same location at the check-in detectors. The check-out detectors for the restoring feature of BSP2 were installed at the intersections of Rookin at Bellaire (intersection B) and Hilcroft at Bellaire (intersection C). When buses

are sensed at check-out detectors, a check-out call is sent to the signal controller. Once the controller receives the check-out call the restoring process is initiated.



**Figure 7-1 Detector settings and stop locations on simulation network**

As discussed in Chapter III, the simulation study was performed with four levels of bus headways because the VISSIM model cannot emulate the realistic variations in dwell time according to the change in the headway level. The dwell time distribution for each of the headway levels was obtained from the observed data and subsequently was input into VISSIM. The four headway levels that were employed are 2~5 minutes, 5~8 minutes, and 8~11 minutes, and 11~14 minutes. Note that headway levels exceeding 14 minutes were not considered because the scheduled headway during the morning peak period was 6 minutes and the number of observation was not enough to derive the cumulative distribution. In this simulation study, the buses were generated at constant bus headway and therefore a distribution needed to be imposed by other methods. As shown in Figure 7-1, a dummy stop was created on the dummy link. The dwell time was selected randomly from the normal distribution with a mean value of 90 seconds and a standard deviation of 30 seconds, in which the actual departure time at the dummy stop

would be normally distributed between 0 and 3 minutes. Therefore, the buses arrived at the simulated test section in the desired manner. A detailed procedure can be found in section 3.4.1 in this dissertation.

The improved BSP algorithm, BSP2 scenario, was developed with respect to two objectives. The primary objective was to improve the bus operations at the intersection. The impact of the BSP scenarios on the bus operations were assessed by measures of effectiveness related to bus delay. The second objective was to minimize the negative impacts of bus priority on the intersection performance and these impacts were evaluated on the basis of MOEs related to the intersection delay for non-transit vehicles. Table 7-1 gives a summary of the measures of effectiveness used to assess the impact of each scenario on bus, main street, and cross-street traffic operations.

**Table 7-1 Summary of measure of effectiveness used in the assessment of BSP scenarios**

Impacts on	Measure of effectiveness	Units	Notes
Bus operation	average control delay per bus on the main street	seconds per bus	MOE1
	average travel time of buses on the main street	seconds	MOE2
	bus arrival rate during green phase	percentage	MOE3
Non-transit Vehicles	average control delay per vehicle on non-priority approaches	seconds per vehicle	MOE4
	average control delay per vehicle for the intersection	seconds per vehicle (including buses)	MOE5

The Highway Capacity Manual (35) defines the control delay as the portion of the total delay attributed to traffic signal operation for signalized intersections. The control delay includes initial deceleration delay, queue move-up time, stopped delay, and final acceleration delay. A more detailed discussion of each measure is presented in the following sections.

#### *7.1.1.1 Average control delay per bus on the main street (MOE1)*

The average control delay per bus represents the bus delay experienced at the intersection. It is computed for every bus traversing the intersection by subtracting the theoretical travel time from the real travel time. The theoretical travel is the time that would be reached if there were no other vehicles and no signal controls. It is output directly by VISSIM. The improved BSP system was judged to be effective if significant reduction in bus delay is found in the comparison with the normal operation and other BSP operations.

#### *7.1.1.2 Average travel time of buses on the main street (MOE2)*

The average travel time of buses on the eastbound main street was the primary measure of effectiveness in assessing the impacts of using BSP scenarios on bus traffic. The measure was computed by averaging the travel time of all buses from the intersection of Bintiff and Bellaire to the intersection of Hilcroft and Bellaire for each simulation run. In VISSIM the average travel time including waiting or dwell times is determined by the difference between the times that a bus enters and exits the travel time section. This measure is obtained directly from VISSIM output. Because each scenario was examined under the same traffic conditions, any significant difference in the average bus travel time was attributed to the BSP implementation. The improved BSP algorithm was judged to be effective if the average travel time of buses was statistically less than that for other BSP scenarios.

#### *7.1.1.3 Bus arrival rate during green phase (MOE3)*

The bus arrival rate during the green phase was used to measure whether the BSP scenarios provide the priority phase in a timely manner. The successful implementation of the signal priority depends on the BSP scenario's capability of anticipating the bus arrival time and providing a green indication when buses reach the intersection. Because the improved BSP algorithm explicitly considers the variability in dwell time, these

measures were good representations of the improvement in performance resulting from the improved BSP algorithm. The bus arrival rate during green phase (i.e. success rate of priority) was obtained by counting the buses that pass through the intersection without stopping and the total number of priority services granted during the simulation run as shown in Equation 7-1. The bus arrival time at the intersection was obtained from a log VISSIM file that records bus identification code, position (i.e. location on the link), and the waiting time. The signal timing data was also provided directly from a VISSIM output file.

$$MOE3 = \frac{M_p}{N_s} \quad (7-1)$$

$$M_p = \{bus\ i\ satisfies\ \kappa_i < \omega_i'\}$$

where

- $N_s$  = the total number of buses generated during simulation run,
- $M_p$  = the number of buses arrived during their associated priority phase,
- $\kappa_i$  = arrival time of bus  $i$  at the intersection, and
- $\omega_i'$  = the end point of the priority window for bus  $i$ .

#### 7.1.1.4 Average control delay per vehicle for the intersection (MOE4)

In addition to the impacts on bus operations, the average control delay for the intersection was used to evaluate the intersection-wide impact of BSP scenarios. Average control delay was computed by dividing the total amount of delay experienced by all the vehicles (buses and cars) at the intersection by the total number of vehicles entering the intersection. It is computed in VISSIM and is obtained directly from VISSIM output file that contains delay data for all approaches of the network, independently of the vehicle types. This measure was intended to give a global view of how scenario impacts traffic operations at the intersection. The improved BSP algorithm

was judged to be effective if implementing the signal priority did not significantly increase the average control delay for the intersection.

#### *7.1.1.5 Average control delay per vehicle on non-priority approaches (MOE5)*

The delay experienced by non-priority movements were also used to gauge the effectiveness of the improved BSP algorithm. The non-priority movements for the test bed consisted of all approaches on the cross street and the left turn approaches on the main street. The algorithm was considered to be effective if it did not significantly increase the delay for any of these movements. The average control delay experienced by non-priority movements when the improved BSP algorithm was implemented were compared with those when the other scenarios were implemented. A significant increase in control delay was assumed to imply that the improved BSP algorithm had a detrimental impact on the non-priority movements.

All scenarios were simulated under the same traffic conditions such as traffic demand, bus headway, and dwell times. Each simulation was repeated 10 times with a different random seed in order to account for the stochastic nature of traffic simulation model. The MOEs from each of the scenarios were averaged and compared in order to evaluate the performance of the scenarios. A statistical testing method was employed in comparing the MOEs. The testing method used in this study will be introduced in the next section.

### **7.1.2 Statistical Testing**

The goal of the statistical testing was to determine whether the difference in the measures-of-effectiveness between the different scenarios were statistically significant. Duncan's multiple range test was used to test the different hypothesis (62). The null hypothesis was that there is no difference between the measure-of-effectiveness between one scenario and another. The null ( $H_0$ ) and alternative ( $H_a$ ) hypotheses are as follows:

$$\begin{aligned}
 H_0 : \mu_i &= \mu_j \\
 H_a : \mu_i &\neq \mu_j
 \end{aligned}
 \tag{7-2}$$

The Duncan's multiple range test uses multiple critical points for testing whether the sample means (e.g. MOEs) are significantly different. The critical point varies according to the span of the means in the ordered set of means. The detailed procedure of the test is explained as follows:

*Step 1:* Linearly order the  $k$  sample means ( $k = 4$  in this study).

*Step 2:* Find the value of the least significant "studentized range,"  $r_p$  (critical point), for each  $p = 2, 3, \dots, k$ . This value is given in Duncan's table (62) for  $\alpha$  levels of .1, .01 or .05. In this table  $r$  denotes the number of degrees of freedom associated with  $MS_E$ , the mean square error in the original analysis of variance. The  $MS_E$  is obtained by Equation 7-3.

$$\begin{aligned}
 MS_E &= \frac{SS_E}{N - k} \\
 SS_E &= \sum_{i=1}^k \sum_{j=1}^n (Y_{ij} - \bar{Y}_i)
 \end{aligned}
 \tag{7-3}$$

where

$MS_E$  = error mean squares,

$SS_E$  = error sum of squares,

$\bar{Y}_i$  = sample mean for the  $i$ th scenarios,

$n$  = sample size ( 10 in this dissertation), and

$N$  = total number of all responses.

*Step 3:* For each  $p = 2, 3, \dots, k$  find the shortest or least significant range,  $SSR_p$ . This value is given by Equation 7-4.

$$SSR_p = r_p \sqrt{\frac{MS_E}{n}} \quad (7-4)$$

*Step 4:* Consider any subset of  $p$  adjacent sample means. Let  $|\bar{Y}_i - \bar{Y}_j|$  denote the range of the means in this subgroup. The population means, of span  $p$ ,  $\mu_i$  and  $\mu_j$  are considered to be different if

$$|\bar{Y}_i - \bar{Y}_j| > SSR_p \quad (7-5)$$

*Step 5:* Perform  $\binom{k}{2}$  comparisons and summarize the results of all comparisons.

Duncan's multiple range test was performed on all 5 MOEs for all 4 scenarios. All tests were performed at a 0.05 significance level.

## 7.2 EVALUATION OF THE IMPROVED BSP ALGORITHM

The performance of the improved BSP algorithm was evaluated in this section. The evaluations were performed by comparing the MOEs of between the scenarios. This simulation study focused on measuring the improvement in the performance of the scenario by the BSP implementations under the current traffic conditions. The AM peak demand was the basis of the simulations. The bus headway level of 5~8 minutes was chosen for generating buses and associated dwell time distribution because the scheduled bus headway during AM peak period was 6 minutes. The improved BSP algorithm will be evaluated at various headway levels in the next section. The statistical tests were used to test whether or not the improved BSP algorithm improves MOEs over other scenarios.



## 7.2.1 Impacts on Bus Operations

### 7.2.1.1 Average control delay per bus at the main street approach (MOE1)

The results for MOE1 for the different scenarios are shown in Table 7-2. These intersection control delays of buses were computed from each simulation run for the intersections of Rookin and Bellaire, Hilcroft and Bellaire. As discussed previously, each simulation scenario was replicated 10 times with different random seed numbers in order to represent the stochastic nature of traffic simulation model.

**Table 7-2 Average control delay per bus on the main street approach, MOE1 (sec/bus)**

Intersection Simulation Run Number <sup>1</sup>	Rookin and Bellaire				Hilcroft and Bellaire			
	Normal <sup>2</sup>	BSP0 <sup>3</sup>	BSP1 <sup>4</sup>	BSP2 <sup>5</sup>	Normal	BSP0	BSP1	BSP2
1	28.0	17.6	13.3	12.5	58.4	66.6	31.9	22.6
2	24.6	19.3	17.3	15.6	85.0	36.0	47.4	17.7
3	28.5	23.7	16.3	13.5	81.0	55.9	45.0	21.4
4	27.0	22.2	15.7	9.9	64.7	49.8	43.0	28.2
5	22.6	15.2	17.7	15.4	65.6	52.9	27.9	23.4
6	18.9	16.4	13.9	15.0	56.9	42.5	25.0	48.7
7	30.7	23.7	18.4	16.9	44.8	46.7	47.0	37.7
8	29.5	14.6	15.6	17.3	51.4	57.7	42.2	34.0
9	24.1	13.1	13.9	15.2	50.6	36.6	24.4	18.8
10	21.2	23.2	15.0	16.7	78.7	58.8	46.2	26.5
Mean	25.5	18.9	15.7	14.8	63.7	50.3	38.0	27.9
S.D.	3.9	4.1	1.7	2.3	13.9	10.0	9.6	9.7
C.V.	15.1%	21.6%	11.0%	15.4%	21.8%	19.8%	25.1%	34.7%
Percentage Reduction In Mean <sup>6</sup>	-	-25.9%	-38.4%	-41.9%	-	-21.0%	-40.3%	-56.2%
	-	-	-16.9%	-21.7%	-	-	-24.5%	-44.6%
	-	-	-	-5.8%	-	-	-	-26.6%

Note:

<sup>1</sup> Simulation was repeated with different random seed.

<sup>2</sup> Normal actuated scenario

<sup>3</sup> BSP with green extension and early green (no consideration of dwell time)

<sup>4</sup> BSP with consideration of fixed dwell time in calculating bus travel time

<sup>5</sup> BSP using updated bus dwell time and prediction interval

<sup>6</sup> percentage change in MOE for given scenario in comparison to Normal, BSP0, and BSP1 scenario

From Table 7-2, it can be seen that all BSP scenarios had lowered MOE1 than the Normal scenario. The BSP2 scenario had lowest value of MOE1 than any other scenario at both the intersections. The BSP2 scenario had a 10.7 seconds and 35.8 seconds reduction in MOE1 at the intersections of Rookin and Bellaire, Hilcroft and Bellaire, respectively. This represents a 41.9 and 56.2 percent reduction in MOE1 as compared to the base case.

It can be seen that the standard deviation (S.D.) over the 10 runs varied from 1.7 to 13.9. The coefficient of variance (C.V.) also varied from 11% to 34.7%. This illustrates the importance of using multiple runs in traffic simulation models because a single run may lead to spurious results.

Tables 7-3 and 7-4 show the results of the Duncan test comparing MOE1 between the scenarios at both intersections. A 95 percent confidence level was used in the Duncan tests. From the results of the statistical test, two important observations can be made about the different scenarios.

The first was that the BSP scenarios all performed better than the Normal scenario with respect to MOE1. In addition, the BSP1 and BSP2 scenarios had statistically significant improvements in MOE1 in comparing to the basic BSP scenario (BSP0).

The second observation from the Duncan's tests was that the bus delays for the BSP1 and BSP2 scenarios at the intersection of Rookin and Bellaire were not significantly different from each other as shown in Table 7-3. Although the BSP2 resulted in slightly better performance, the difference was not statistically significant. This result can be attributed to two factors; 1) the amount of the variability in dwell time at nearside stop was small (about 11seconds) at the given headway level (5~8 minutes), and 2) queues from the traffic signal seldom prevent buses from reaching the nearside bus stop because the green time for the main street approach at the intersection of Rookin and Bellaire was long enough to avoid the excessive standing queues. In contrast, the difference between MOE1 for the BSP1 and BSP2 scenarios at the intersection of Hilcroft and Bellaire were found to be significantly different. This was attributed to the

greater congestion at this intersection. For example, with BSP1 scenario, the total bus stop time due to the queue at the intersection of Rookin and Bellaire was 12.7 seconds while this value for the intersection of Hilcroft and Bellaire was 77.6 seconds. As would be expected the BSP2 scenario performs better under congested conditions where there is more variability in traffic conditions.

**Table 7-3 Results of Duncan test between scenarios (average control delay per bus, MOE1, at the intersection of Rookin and Bellaire)**

Operation Comparison		Mean (sec/veh)		Test Statistic	Critical Value	Result
Operation 1	Operation 2	Operation 1	Operation 2			
BSP2	Normal	14.8	25.5	10.71	3.101	Reject $H_0$ <sup>1</sup>
BSP2	BSP0	14.8	18.9	4.10	3.006	Reject $H_0$
BSP2	BSP1	14.8	15.7	0.91	2.859	<b>Accept <math>H_0</math></b> <sup>2</sup>
BSP1	Normal	15.7	25.5	9.80	3.006	Reject $H_0$
BSP1	BSP0	15.7	18.9	3.19	2.859	Reject $H_0$
BSP0	Normal	18.9	25.5	6.61	2.859	Reject $H_0$

Note:

<sup>1</sup> Statistically significant difference between two means at 0.05 level of significance,  $\mu_1 \neq \mu_2$ .

<sup>2</sup> No statistically significant difference between two means,  $\mu_1 = \mu_2$ .

**Table 7-4 Results of Duncan test between scenarios (average control delay per bus, MOE1, at the intersection of Hilcroft and Bellaire)**

Operation Comparison		Mean (sec/veh)		Test Statistic	Critical Value	Result
Operation 1	Operation 2	Operation 1	Operation 2			
BSP2	Normal	27.9	63.7	35.81	10.770	Reject $H_0$
BSP2	BSP0	27.9	50.4	22.45	10.438	Reject $H_0$
BSP2	BSP1	27.9	38.0	10.10	9.930	Reject $H_0$
BSP1	Normal	38.0	63.7	25.71	10.438	Reject $H_0$
BSP1	BSP0	38.0	50.4	12.35	9.930	Reject $H_0$
BSP0	Normal	50.3	63.7	13.36	9.930	Reject $H_0$

### 7.2.1.2 Average bus travel time on the main street (MOE2)

The results for the comparison of the scenarios under AM peak demand were shown in Table 7-5. This table presents the average bus travel times on the eastbound main street for the buses (MOE2) from each simulation run. The BSP scenarios reduced the MOE2 from 8% to 21.1%. The BSP2 scenario resulted in the largest reduction in MOE2 (21.1 percent), and the BSP1 scenario had the second largest reduction (15.6 percent).

**Table 7-5 Average bus travel time on the eastbound main street, MOE2**

Simulation Run Number	Normal (seconds)	BSP0 (seconds)	BSP1 (seconds)	BSP2 (seconds)
1	214.5	218.8	175.7	176.6
2	247.5	191.6	197.7	163.1
3	247.3	211.1	188.9	161.3
4	223.2	208.1	190.7	160.8
5	219.8	200.9	177.3	167.0
6	204.0	193.2	164.6	190.9
7	198.6	196.1	203.0	187.5
8	212.1	204.6	186.2	182.1
9	202.1	177.2	175.3	167.4
10	228.1	209.7	194.2	173.8
Mean	219.72	201.13	185.36	173.05
S.D.	17.3	12.0	11.9	10.9
C.V.	7.9%	6.0%	6.4%	6.3%
Percentage Reduction In Mean <sup>1</sup>	-	-8.5%	-15.6%	-21.1%
	-	-	-7.8%	-14.0%
	-	-	-	-6.6%

Note:

<sup>1</sup> percentage change in MOE for given scenario in comparison to Normal, BSP0, and BSP1 scenario

The results of the Duncan tests for MOE2 are summarized in Table 7-6. The results indicated that the reductions in bus travel time shown in Table 7-5 for each scenario are statistically significant. In addition, the differences in average travel time for each of the BSP scenarios are also statistically significant. It was concluded that for

this test bed the implementation of any BSP scenario can improve MOE2, and the BSP2 scenario improves MOE2 more than any other BSP scenarios.

**Table 7-6 Results of Duncan test between scenarios (bus travel time on eastbound main street, MOE2)**

Operation Comparison		Mean		Test Statistic	Critical Value	Result
Operation 1	Operation 2	Operation 1	Operation 2			
BSP2	Normal	173.3	219.7	46.37	13.208	Reject $H_0$
BSP2	BSP0	173.3	201.1	27.78	12.801	Reject $H_0$
BSP2	BSP1	173.3	185.3	12.31	12.178	Reject $H_0$
BSP1	Normal	185.3	219.7	34.36	12.801	Reject $H_0$
BSP1	BSP0	185.3	201.1	15.77	12.178	Reject $H_0$
BSP0	Normal	201.1	219.7	18.59	12.178	Reject $H_0$

### *7.2.1.3 Bus arrival rate during green phase (MOE3)*

The rate of bus arrivals during green time (MOE3) are shown in Table 7-7 for each scenario. The MOE3 values were improved in comparison to the Normal scenario for all BSP scenarios at both intersections. Note that the largest improvement (102.8%) in MOE3 was found at the intersection of Hilcroft and Bellaire with the BSP2 scenario. It is hypothesized that because the BSP2 scenario provided the priority green time centering on the anticipated bus arrival time, more buses were able to reach the intersection during green time despite the variability in dwell time. At the intersection of Rookin and Bellaire, the BSP2 scenario showed better performance than the other BSP scenarios, however the difference were not as large.

**Table 7-7 Bus arrival rate during green phase, MOE3**

Intersection	Rookin and Bellaire				Hilcroft and Bellaire			
	Normal	BSP0	BSP1	BSP2	Normal	BSP0	BSP1	BSP2
Simulation Run Number								
1	0.44	0.89	1.00	1.00	0.44	0.33	0.78	0.89
2	0.56	0.89	0.89	1.00	0.33	0.67	0.44	1.00
3	0.78	0.78	1.00	1.00	0.44	0.44	0.33	1.00
4	0.89	0.89	1.00	1.00	0.44	0.44	0.44	0.67
5	0.89	0.89	0.89	0.89	0.22	0.67	0.78	1.00
6	0.89	0.78	1.00	1.00	0.33	0.78	0.44	0.67
7	0.44	0.78	1.00	0.89	0.67	0.56	0.56	0.78
8	0.44	0.89	0.89	1.00	0.56	0.78	0.89	0.89
9	0.78	1.00	1.00	1.00	0.44	0.67	0.56	0.89
10	0.78	0.67	0.89	1.00	0.33	0.56	0.56	0.78
Mean	0.689	0.844	0.956	0.978	0.422	0.589	0.578	0.856
S.D.	0.19	0.09	0.06	0.05	0.13	0.15	0.18	0.13
C.V.	28.2%	11.1%	6.0%	4.8%	29.9%	25.2%	31.1%	15.1%
Percentage Reduction In Mean <sup>1</sup>	-	22.6%	38.7%	41.9%	-	39.5%	36.8%	102.6%
	-	-	13.2%	15.8%	-	-	-1.9%	45.3%
	-	-	-	2.3%	-	-	-	48.1%

Note:

<sup>1</sup> percentage change in MOE for given scenario in comparison to Normal, BSP0, and BSP1 scenario

Tables 7-8 and 7-9 show the result of the Duncan tests for MOE3 for the intersections of Rookin and Bellaire, Hilcroft and Bellaire, respectively. It can be seen in Table 7-8 that the improvements in MOE3 by BSP scenarios in comparison to Normal scenario all were statistically significant. In addition, the BSP2 scenario resulted in better MOE3 values than Normal or BSP0 scenarios, and the improvements were significant. However, the difference between BSP2 and BSP1 was not statistically significant. As discussed in Section 7.2.1.1, the BSP1 scenario resulted in comparable intersection performances with the BSP2 scenario under the given traffic conditions. However, the BSP2 scenario had statistically better MOE3 values than any other scenario at the intersection of Hilcroft and Bellaire. This was attributed to the greater

congestion. Interestingly, the BSP1 and BSP0 scenarios had statistically similar results. This indicates that having better travel time estimates does not necessarily lead to better bus performance. That is, it is important to consider both the mean and variability in traffic operations.

**Table 7-8 Results of Duncan test between scenarios (bus arrival rate during green phase, MOE3, at the intersection of Rookin and Bellaire)**

Operation Comparison		Mean		Test Statistic	Critical Value	Result
Operation 1	Operation 2	Operation 1	Operation 2			
BSP2	Normal	0.978	0.689	0.289	0.112	Reject $H_0$
BSP2	BSP0	0.978	0.844	0.133	0.109	Reject $H_0$
BSP2	BSP1	0.978	0.956	0.022	0.104	<b>Accept <math>H_0</math></b>
BSP1	Normal	0.956	0.689	0.267	0.109	Reject $H_0$
BSP1	BSP0	0.956	0.844	0.111	0.104	Reject $H_0$
BSP0	Normal	0.844	0.689	0.156	0.104	Reject $H_0$

**Table 7-9 Results of Duncan test between scenarios (bus arrival rate during green phase, MOE3, at the intersection of Hilcroft and Bellaire)**

Operation Comparison		Mean		Test Statistic	Critical Value	Result
Operation 1	Operation 2	Operation 1	Operation 2			
BSP2	Normal	0.856	0.422	0.433	0.145	Reject $H_0$
BSP2	BSP0	0.856	0.589	0.267	0.141	Reject $H_0$
BSP2	BSP1	0.856	0.578	0.278	0.134	Reject $H_0$
BSP1	Normal	0.578	0.422	0.156	0.141	Reject $H_0$
BSP1	BSP0	0.578	0.589	0.011	0.134	<b>Accept <math>H_0</math></b>
BSP0	Normal	0.589	0.422	0.167	0.134	Reject $H_0$

## 7.2.2 Impacts on Non-transit Vehicles

### 7.2.2.1 Average control delay per vehicle on the non-priority approaches (MOE4)

The average control delays per vehicle on non-priority approaches (MOE4) results are summarized in Table 7-10. The table shows the comparison between MOE4 for each of

the scenarios. As would be expected the implementation of any BSP scenario increases MOE4. For the intersection of Rookin and Bellaire these increases are relatively small and ranged from 1.5 to 12.5 percent. However, for the more congested intersection of Hilcroft and Bellaire, the increase was considerably larger and ranged from 25.4 to 29.9 percent.

**Table 7-10 Average control delay per vehicle on non-priority approaches, MOE4 (sec/veh)**

Intersection	Rookin and Bellaire				Hilcroft and Bellaire			
	Normal	BSP0	BSP1	BSP2	Normal	BSP0	BSP1	BSP2
1	26.1	28.2	28.3	27.1	44.8	52.7	53.7	66.1
2	26.9	30.1	26.5	24.5	44.4	73.2	60.7	62.3
3	25.7	27.4	27.6	27.5	51.8	54.7	50.4	61.8
4	23.9	27.1	24.8	26.4	45.6	52.5	56.3	63.9
5	27.1	29.6	28.8	27.7	48.4	79.9	60.2	53.9
6	24.5	29.5	27.4	26.4	46.9	67.5	65.7	51.8
7	26.6	29.2	26.8	26.5	44.0	52.0	55.9	60.2
8	24.9	31.0	28.7	24.0	45.7	71.2	49.3	52.7
9	26.4	30.0	25.7	26.6	45.9	53.3	64.0	69.0
10	26.3	28.7	25.8	25.7	50.9	51.4	71.1	59.1
Average	25.84	29.08	27.04	26.24	46.84	60.84	58.73	60.08
S.D.	1.07	1.23	1.36	1.20	2.70	10.88	6.94	5.78
C.V.	4.1%	4.2%	5.0%	4.6%	5.8%	17.9%	11.8%	9.6%
Percentage Reduction In Mean <sup>1</sup>	-	12.5%	4.6%	1.5%	-	29.9%	25.4%	28.3%
	-	-	-7.0%	-9.8%	-	-	-3.5%	-1.2%
	-	-	-	-3.0%	-	-	-	2.3%

Note:

<sup>1</sup> percentage change in MOE for given scenario in comparison to Normal, BSP0, and BSP1 scenario

The results of the Duncan tests for the intersections are shown in Tables 7-11 and 7-12. It can be seen that only BSP2 scenario had statistically same MOE4 as the Normal



scenario at the intersection of Rookin and Bellaire. Increases in MOE4 by other BSP scenarios were statistically significant. From the Table 7-12, it can be seen that all BSP scenarios significantly increased the MOE4 at the intersection of Hilcroft and Bellaire. However, the differences in MOE4 between the BSP scenarios were not statistically different. It indicates that all BSP scenarios at the intersection Hilcroft and Bellaire have similar effect on the vehicles on non-priority approaches.

**Table 7-11 Results of Duncan test between scenarios (average control delay per vehicle on non-priority approaches, MOE4, at the intersection of Rookin and Bellaire)**

Operation Comparison		Mean		Test Statistic	Critical Value	Result
Operation 1	Operation 2	Operation 1	Operation 2			
BSP2	Normal	26.24	25.84	0.40	1.109	<b>Accept H<sub>0</sub></b>
BSP2	BSP0	26.24	29.08	2.84	1.166	Reject H <sub>0</sub>
BSP2	BSP1	26.24	27.04	0.80	1.109	<b>Accept H<sub>0</sub></b>
BSP1	Normal	27.04	25.84	1.20	1.166	Reject H <sub>0</sub>
BSP1	BSP0	27.04	29.37	2.04	1.109	Reject H <sub>0</sub>
BSP0	Normal	29.37	27.34	3.24	1.203	Reject H <sub>0</sub>

**Table 7-12 Results of Duncan test between scenarios (average control delay per vehicle on non-priority approaches, MOE4, at the intersection of Hilcroft and Bellaire)**

Operation Comparison		Mean		Test Statistic	Critical Value	Result
Operation 1	Operation 2	Operation 1	Operation 2			
BSP2	Normal	60.08	46.84	13.24	6.872	Reject H <sub>0</sub>
BSP2	BSP0	60.08	60.84	0.76	6.538	<b>Accept H<sub>0</sub></b>
BSP2	BSP1	60.08	58.73	1.35	6.538	<b>Accept H<sub>0</sub></b>
BSP1	Normal	58.73	46.84	11.89	6.538	Reject H <sub>0</sub>
BSP1	BSP0	58.73	60.84	2.11	6.872	<b>Accept H<sub>0</sub></b>
BSP0	Normal	60.84	46.84	14.00	7.091	Reject H <sub>0</sub>

#### *7.2.2.2 Average control delay per vehicle for the intersection (MOE5)*

Average control delay per vehicle for the intersection (MOE5) was another measure of effectiveness used to determine the overall impact of BSP scenarios on traffic operations at the intersection. The MOE5 results for the scenarios are shown in Table 7-13. From the table, it can be seen that the amount of increase in the MOE5 by BSP scenarios was not considerably large in either of the two intersections. Note that at the intersection of Hilcroft and Bellaire the BSP2 scenario reduced MOE5 by 0.2 percent (0.4 second). These results can be attributed to the higher demands on the main street approaches. The implementation of signal priority means that additional green time is given to the phases for the main street approach, which benefits the vehicles on the main streets. The reduction in delay on the main street traffic negated the increase in delay at the non-priority approaches.

The results of the Duncan tests for the intersections are shown in Tables 7-14 and 7-15. From the results for the intersection of Rookin and Bellaire (see Table 7-14), it was found that all BSP scenarios increased MOE5 as compared to the Normal scenario, and the differences were statistically significant. However, the MOE5 between BSP scenarios was not statistically different, which means that any of the three BSP scenarios would have the same effect on MOE5 at this intersection.

It was noted that MOE5 for all scenarios at the intersection of Hilcroft and Bellaire were not significantly different. Implementing any BSP scenario did not result any significant increase in MOE5. It was concluded that under current traffic conditions, the BSP2 scenario can improve the bus operations without any significant impact upon the performance of scenario. This is important because when traffic conditions are congested the BSP2 scenario improved bus operations but did not affect on other vehicles' delay.

**Table 7-13 Average control delay per vehicle at the intersections, MOE5**

Intersection	Rookin and Bellaire				Hilcroft and Bellaire			
Simulation Run Number	Normal	BSP0	BSP1	BSP2	Normal	BSP0	BSP1	BSP2
1	14.6	14.7	14.9	16.2	37.6	37.9	40.0	41.2
2	15.2	15.8	15.9	15.9	43.2	46.8	41.9	42.6
3	14.7	15.1	15.1	15.1	44.9	42.2	37.1	40.6
4	15.5	16.4	14.9	15.5	39.6	37.0	41.1	41.6
5	15.0	15.8	15.0	15.2	39.1	52.0	40.7	38.0
6	13.5	16.0	15.9	15.7	36.8	48.4	40.2	35.8
7	14.1	16.0	15.1	15.3	38.9	39.8	40.3	40.2
8	14.2	15.6	14.6	14.7	39.4	52.1	36.5	38.3
9	14.7	15.7	16.2	16.1	38.3	36.4	41.2	42.8
10	14.0	15.1	15.4	15.7	43.6	40.8	46.3	39.6
Mean	14.55	15.62	15.30	15.54	40.14	43.34	40.53	40.07
S.D.	0.61	0.51	0.53	0.47	2.76	6.03	2.68	2.20
C.V.	4.2%	3.3%	3.5%	3.0%	6.9%	13.9%	6.6%	5.5%
Percentage Reduction In Mean <sup>1</sup>	-	7.4%	5.2%	6.8%	-	8.0%	1.0%	-0.2%
	-	-	-2.0	-0.5%	-	-	-6.5%	-7.5%
	-	-	-	1.6%	-	-	-	-1.1%

Note:

<sup>1</sup> percentage change in MOE for given scenario in comparison to Normal, BSP0, and BSP1 scenario

**Table 7-14 Results of Duncan test between scenarios (average control delay per vehicle, MOE5, at the intersection of Rookin and Bellaire)**

Operation Comparison		Mean		Test Statistic	Critical Value	Result
Operation 1	Operation 2	Operation 1	Operation 2			
BSP2	Normal	15.54	14.55	0.99	0.508	Reject $H_0$
BSP2	BSP0	15.54	15.62	0.08	0.483	Accept $H_0$
BSP2	BSP1	15.54	15.3	0.24	0.483	Accept $H_0$
BSP1	Normal	15.3	14.55	0.75	0.483	Reject $H_0$
BSP1	BSP0	15.3	15.62	0.32	0.508	Accept $H_0$
BSP0	Normal	15.62	14.55	1.07	0.524	Reject $H_0$

**Table 7-15 Results of Duncan test between scenarios (average control delay per vehicle, MOE5, at the intersection of Hilcroft and Bellaire)**

Operation Comparison		Mean		Test Statistic	Critical Value	Result
Operation 1	Operation 2	Operation 1	Operation 2			
BSP2	Normal	40.07	40.14	0.07	3.399	Accept $H_0$
BSP2	BSP0	40.07	43.34	3.27	3.687	Accept $H_0$
BSP2	BSP1	40.07	40.53	0.46	3.573	Accept $H_0$
BSP1	Normal	40.53	40.14	0.39	3.399	Accept $H_0$
BSP1	BSP0	40.53	43.34	2.81	3.399	Accept $H_0$
BSP0	Normal	43.34	40.14	3.20	3.573	Accept $H_0$

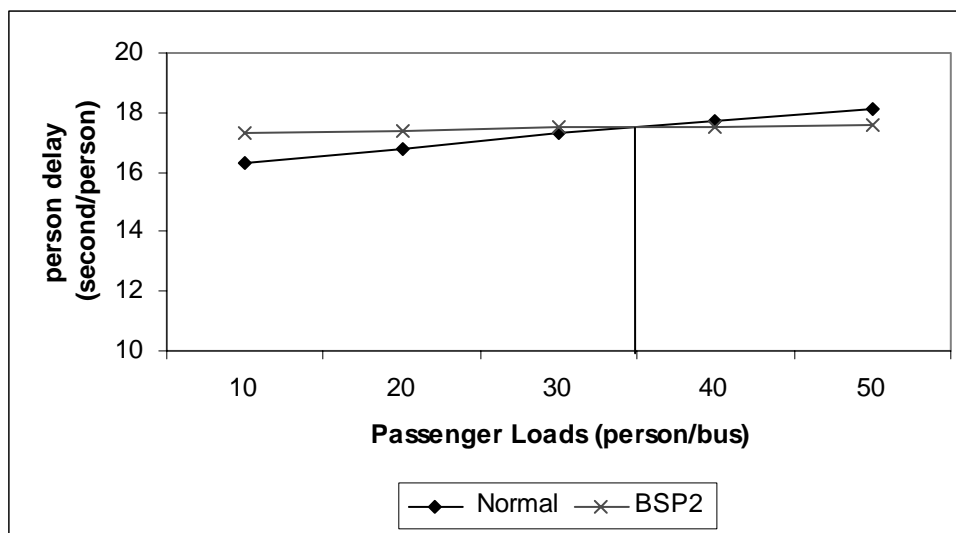
### 7.2.2.3 Average person delay for the intersection

As a part of intersection delay analysis, the average person delay for the intersection was evaluated for the Normal and BSP2 scenarios. The BSP system is generally known to be effective in improving the person delay while the vehicle delay may increase by the implementation of BSP strategy. The five levels of passenger loads were considered in this analysis. Table 7-16 shows the average vehicle delay and the average person delay for each intersection. It can be seen that the person delays by the BSP2 scenario have smaller variation than those by the Normal scenario for the both intersections. It is because the bus delay has been reduced by the BSP implementations. Note that at the intersection of Rookin and Bellaire the person delays for BSP2 are less than those for Normal at the passenger loads of 40 and 50 while the vehicle delays are adverse. Figure

7-2 emphasizes these results. The person delays by the Normal and BSP2 scenarios are same at the passenger loads of 35. If the passenger loads are greater than 35, the BSP2 scenario performs better than the Normal scenario in terms of average person delay at the intersection of Rookin and Bellaire. For the intersection of Hilcroft and Bellaire, the BSP2 scenario results in lower average person delay at all levels of passenger loads.

**Table 7-16 Comparison of average person delay at the intersections**

Passenger loads	Rookin and Bellaire				Hilcroft and Bellaire			
	Normal		BSP2		Normal		BSP2	
	Vehicle delay	Person delay	Vehicle delay	Person delay	Vehicle delay	Person delay	Vehicle delay	Person delay
10	15.9	16.3	17.2	17.3	41.7	42.0	40.1	40.1
20	15.9	16.8	17.2	17.4	41.7	42.4	40.1	40.1
30	15.9	17.3	17.2	17.5	41.7	42.7	40.1	40.0
40	15.9	17.7	17.2	17.5	41.7	43.0	40.1	40.0
50	15.9	18.1	17.2	17.6	41.7	43.3	40.1	39.9



**Figure 7-2 Average person delays at the intersection of Rookin and Bellaire**

### 7.2.3 Summary of Findings

The MOE1, average control delay per bus, have been lowered by all BSP scenarios compared to the Normal scenario. The BSP2 scenario had lowest value of MOE1 than any other scenario at both the intersections.

The average bus travel times on the eastbound main street for the buses, MOE2, was reduced by all BSP scenarios from 8% to 21.1%. The BSP2 scenario resulted in the largest reduction in MOE2 (21.1 percent), and the BSP1 scenario had the second largest reduction (15.6 percent).

The MOE3, rate of bus arrivals during green time, was improved in comparison to the Normal scenario for all BSP scenarios at both intersections. Note that the largest improvement (102.8%) in MOE3 was found at the intersection of Hilcroft and Bellaire with the BSP2 scenario.

The implementation of any BSP scenario increases MOE4, the average control delays per vehicle on non-priority approaches. For the intersection of Rookin and Bellaire these increases are relatively small and ranged from 1.5 to 12.5 percent. However, for the more congested intersection of Hilcroft and Bellaire, the increases were considerably larger and ranged from 25.4 to 29.9 percent.

Average control delay per vehicle for the intersection, MOE5, was not considerably increased by any BSP scenario in either of the two intersections. Note that at the intersection of Hilcroft and Bellaire the BSP2 scenario reduced MOE5 by 0.2 percent (0.4 second). The average person delays by the BSP2 scenario were less than those by the Normal scenario when the passenger loads is greater than 35, while the vehicle delays by BSP2 were greater.

It was concluded that BSP scenarios improved bus operations without a severe deterioration in intersection performance. In particular, the BSP2 scenario showed greater benefit than any other BSP scenarios under congested traffic conditions, and had no significant impact on other traffic.

The summary of Duncan test for each MOE used in this section is shown in Table 7-16. The improvements in MOE1, MOE2, and MOE3 by the BSP2 scenario

were statistically significant compared to the Normal scenario. For MOE4 and MOE5, the BSP2 scenario had statistically similar increases to the Normal scenario or other BSP scenarios.

**Table 7-17 A summary of statistical test results for all MOEs used**

MOE	Rookin and Bellaire	Hilcroft and Bellaire
MOE1	BSP2 <sup>1</sup> ≥BPS1> <sup>2</sup> BSP0>Normal	BSP2>BPS1>BSP0>Normal
MOE2	BSP2>BPS1>BSP0>Normal	
MOE3	BSP2≥BPS1>BSP0>Normal	BSP2>BPS1≥BSP0>Normal
MOE4	BSP0>BPS1≥BSP2≥Normal BPS1>Normal	BSP0≥BPS2≥BSP1>Normal BSP0≥BSP1
MOE5	BSP0≥BPS2≥BSP1>Normal BPS0≥BSP1	BSP0≥BPS1≥ Normal≥BSP2 BSP0≥BSP2

Note:

<sup>1</sup> no statistical difference between two scenarios, and

<sup>2</sup> statistical difference between two scenarios.

### 7.3 SENSITIVITY ANALYSIS

In this section, the performance of the improved BSP algorithm was analyzed under various simulation scenarios that include five levels of significance for the prediction interval, four headway levels for buses, and seven traffic demand levels. This simulation study focused on the assessments of changes in the MOEs with the improved BSP algorithm according to various simulation parameters. Unlike the evaluation of the BSP2 scenario in section 7.2, the comparisons between BSP scenarios were not performed because the purpose of this simulation study was to determine whether the performances of the BSP2 scenario differ with traffic parameters (or algorithm parameters). The evaluations were performed based on two or three MOEs, instead of the five MOEs that were used in section 7.2, which best suited the particular analysis. The MOEs for each of the analysis were selected in order to better represent the impacts of the changes in the parameters on the performance of the BSP2 scenario. The statistical tests were performed to determine whether there is a significant difference in the MOEs of the BSP2 algorithm when implemented under different conditions.

### 7.3.1 Sensitivity Analysis of Prediction Interval

The inclusion of the prediction interval of the dwell time into the BSP logic was a feature of the BSP2 scenario. For a given dwell time distributions, the length of the prediction interval was determined by the significance level used in the calculation of the interval in the weighted least squares regression model (as discussed in Chapter IV). The significance level  $\alpha$  varied from 0.3 to 0.01, equivalent to 70% ~ 99% prediction intervals. Low significant levels resulted in wide prediction intervals. The BSP2 scenario was evaluated at various significance levels to determine how the level of significance affects the performance of the bus and non-transit vehicles. A headway level of 5~8 minutes and AM peak period demand were used as current traffic conditions. Three MOEs were selected for assessing the impact of the BSP2 scenario. For bus operations, the average bus travel time (MOE2) and arrival rate during green phase (MOE3) were selected. The average control delay for the intersection (MOE5) was selected for the impact of BSP operations on general traffic.

The simulation was repeated 10 times for each significance level. The average width of the prediction interval is listed for each significance level in Table 7-18. The stop B near the intersection of Rookin and Bellaire has shorter intervals because average dwell time was lower than that of stop C near the intersection of Hilcroft and Bellaire.

**Table 7-18 Width of the prediction interval for each significance level (second)**

Stop (Intersection)	Significance Levels of Prediction Interval				
	0.30 (70%)	0.20 (80%)	0.10 (90%)	0.05 (95%)	0.01 (99%)
Stop B (Rookin and Bellaire)	7.2	8.9	11.5	13.7	18.1
Stop C (Hilcroft and Bellaire)	12.0	14.9	19.2	23.0	30.3

#### 7.3.1.1 Average bus travel time (MOE2)

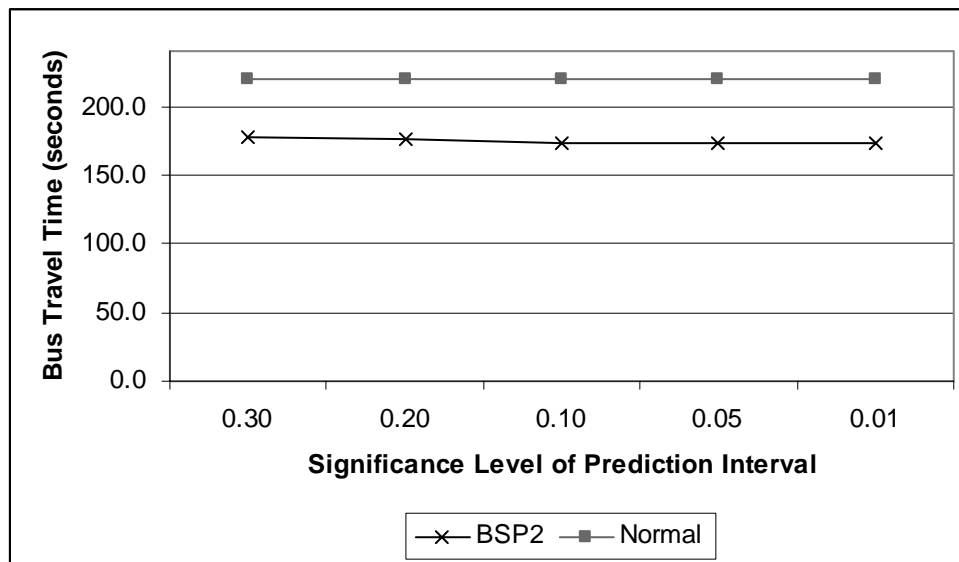
The results for average bus travel times along the eastbound main street for each of the significant levels are shown in Table 7-19. The values in the table are averages of 10 simulation runs. It can be seen that as the significance value decreased so to did MOE2.



This would be expected because a lower significance level means larger prediction interval and priority phase. Consequently the buses were provided with more priority green time and therefore the buses have a greater probability of reaching the intersection during the green phase. The MOE2 was reduced with lowering significant level, but as shown in Figure 7-3, the amount of reduction was not noticeable. The MOE2 with Normal scenario was presented for reference purposes.

**Table 7-19 Average bus travel time on the eastbound main street, MOE2**

	Normal	Significance Levels of Prediction Interval				
		0.30 (70%)	0.20 (80%)	0.10 (90%)	0.05 (95%)	0.01 (99%)
Average Bus Travel Time (sec)	219.72	177.6	176.5	173.4	173.4	172.7



**Figure 7-3 Changes in average bus travel time, MOE2, with significance levels**

The Duncan test results are summarized in Table 7-20. The values of MOE2 for each significance level were compared with each other. None of the pair-wise comparison resulted in the rejection of the null hypothesis that the means were the same.

Therefore it was concluded that while the significance level of the prediction interval in BSP2 scenario affected the average bus travel time, there was no evidence found that these differences were statistically significant.

**Table 7-20 Results of Duncan test between average bus travel times, MOE2, under various significance levels**

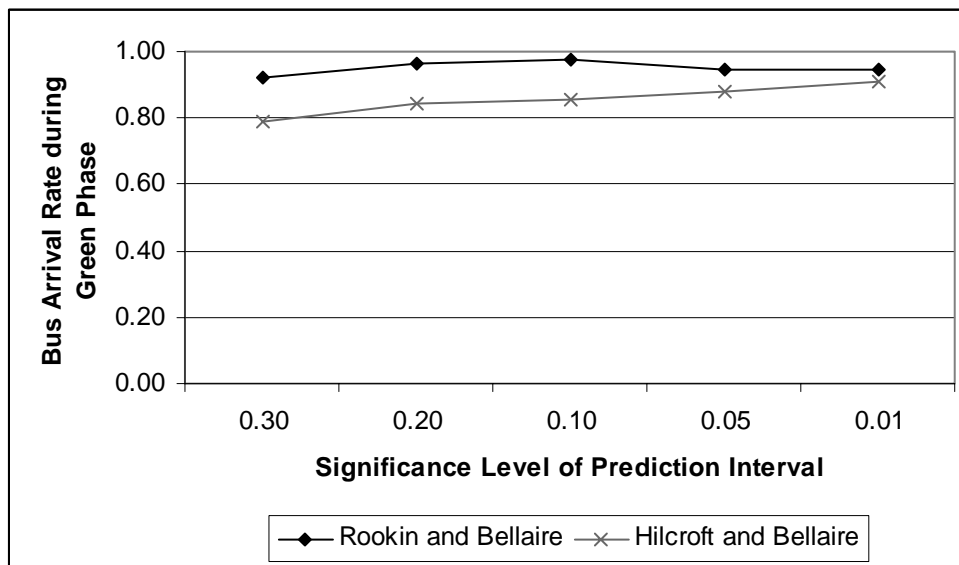
Significance Level Comparison		Mean		Test Statistic	Critical Value	Result
Significance Level 1	Significance Level 2	Significance Level 1	Significance Level 2			
0.30	0.20	177.61	176.45	1.160	8.557	Accept $H_0$
0.30	0.10	177.61	173.36	4.250	9.001	Accept $H_0$
0.30	0.05	177.61	173.40	4.260	9.295	Accept $H_0$
0.30	0.01	177.61	172.65	4.960	9.506	Accept $H_0$
0.20	0.10	176.45	173.36	3.090	8.557	Accept $H_0$
0.20	0.05	176.45	173.35	3.100	9.001	Accept $H_0$
0.20	0.01	176.45	172.65	3.800	9.295	Accept $H_0$
0.10	0.05	173.36	173.35	0.010	8.557	Accept $H_0$
0.10	0.01	173.36	172.65	0.710	9.001	Accept $H_0$
0.05	0.01	173.35	172.65	0.700	8.557	Accept $H_0$

### 7.3.1.2 Bus arrival rate during green phase (MOE3)

Table 7-21 shows the MOE3 results. It can be seen that MOE3 at the intersection of Hilcroft and Bellaire increased as the significance level increased. Note that no such pattern was found at the intersection of Rookin and Bellaire. It should also be noted that the range of values is relatively small. For example, the range for the intersection of Rookin and Bellaire was 0.92 to 0.98 while for the intersection of Hilcroft and Bellaire it was 0.79 to 0.91. As discussed previously, because the queues that prohibit the buses from reaching the stop were frequently built at the intersection of Hilcroft and Bellaire, a longer prediction interval was beneficial to clearing the queues before buses arrive at the nearside stop. Figure 7-4 shows the changes in MOE3 according to the significance levels for both intersections.

**Table 7-21 Bus arrival rate during green phase, MOE3, under various significance levels**

	Intersection	Significance Level of Prediction Interval				
		0.30	0.20	0.10	0.05	0.01
Bus Arrival Rate during Green Phase	Rookin and Bellaire	0.92	0.97	0.98	0.94	0.94
	Hilcroft and Bellaire	0.79	0.84	0.86	0.88	0.91

**Figure 7-4 Changes in bus arrival rate during green phase, MOE3, with significance levels**

The results of the Duncan test for MOE3 were summarized in Tables 7-22 and 7-23 for both intersections. From the Table 7-21, it can be seen that the differences in MOE3 by different significance levels were not statistically significant the intersection of Rookin and Bellaire. The results of the test at the intersection of Hilcroft and Bellaire in Table 7-23 indicate that the BSP2 scenario was mostly insensitive to the changes in level of significance of the prediction interval. A statistical difference was shown between significance levels of 0.3 and 0.01. These two significance levels represent the widest difference in the significance levels. Therefore, it was concluded that, from a

practical perspective, the MOE3 results from the BSP2 scenario were not sensitive to the level of the significance.

**Table 7-22 Results of Duncan test between bus arrival rate during green phase, MOE3, under various significance levels at the intersection of Rookin and Bellaire**

Significance Level Comparison		Mean		Test Statistic	Critical Value	Result
Significance Level 1	Significance Level 2	Significance Level 1	Significance Level 2			
0.30	0.20	0.92	0.97	0.044	0.060	Accept H <sub>0</sub>
0.30	0.10	0.92	0.98	0.056	0.062	Accept H <sub>0</sub>
0.30	0.05	0.92	0.90	0.022	0.056	Accept H <sub>0</sub>
0.30	0.01	0.92	0.94	0.022	0.058	Accept H <sub>0</sub>
0.20	0.10	0.97	0.98	0.011	0.056	Accept H <sub>0</sub>
0.20	0.05	0.97	0.94	0.022	0.058	Accept H <sub>0</sub>
0.20	0.01	0.97	0.94	0.022	0.056	Accept H <sub>0</sub>
0.10	0.05	0.98	0.94	0.033	0.060	Accept H <sub>0</sub>
0.10	0.01	0.98	0.94	0.033	0.058	Accept H <sub>0</sub>
0.05	0.01	0.94	0.94	0.000	0.056	Accept H <sub>0</sub>

**Table 7-23 Results of Duncan test between bus arrival rate during green phase, MOE3, under various significant levels at the intersection of Hilcroft and Bellaire**

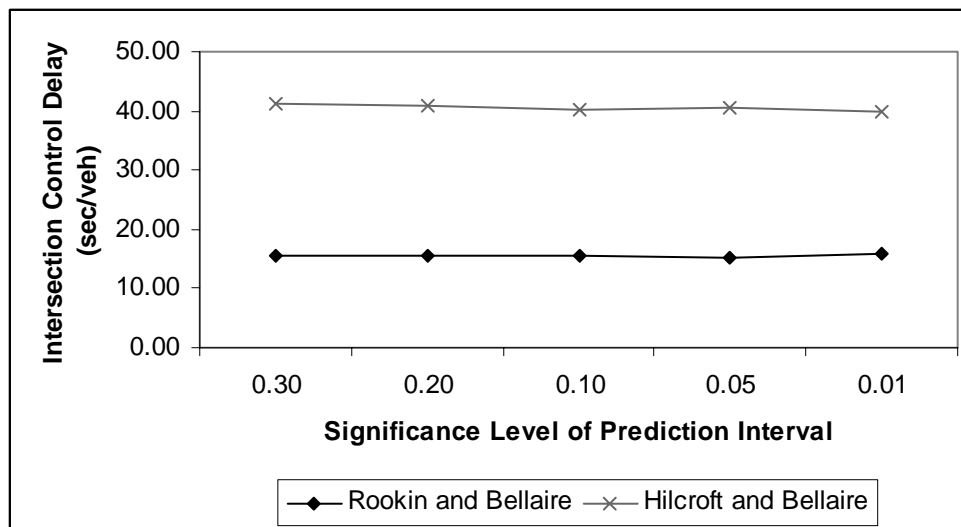
Significance Level Comparison		Mean		Test Statistic	Critical Value	Result
Significance Level 1	Significance Level 2	Significance Level 1	Significance Level 2			
0.30	0.20	0.79	0.84	0.056	0.090	Accept H <sub>0</sub>
0.30	0.10	0.79	0.86	0.067	0.095	Accept H <sub>0</sub>
0.30	0.05	0.79	0.90	0.089	0.098	Accept H <sub>0</sub>
0.30	0.01	0.79	0.91	0.122	0.100	Reject H <sub>0</sub>
0.20	0.10	0.84	0.86	0.011	0.090	Accept H <sub>0</sub>
0.20	0.05	0.84	0.88	0.033	0.095	Accept H <sub>0</sub>
0.20	0.01	0.84	0.91	0.067	0.098	Accept H <sub>0</sub>
0.10	0.05	0.86	0.88	0.022	0.090	Accept H <sub>0</sub>
0.10	0.01	0.86	0.91	0.056	0.095	Accept H <sub>0</sub>
0.05	0.01	0.88	0.91	0.033	0.090	Accept H <sub>0</sub>

### 7.3.1.3 Average control delay per vehicle for the intersection (MOE5)

It was shown that the significance level did not have a statistically significant effect upon the bus operations. The MOE5, average control delay per vehicle for the intersection, represents the impacts by the significance level to non-transit vehicles and the results are shown in Table 7-24. It can be seen that the MOE5 for the intersection of Rookin and Bellaire did not change by more than 0.5 second. The difference in MOE5 at the intersection of Hilcroft and Bellaire was also not considerable (less than 1.5 seconds). Figure 7-5 represents the changes in MOE5 according to the different significance levels.

**Table 7-24 Average control delay per vehicle for the intersection, MOE5, under various levels of significance**

	Intersection	Significance Level of Prediction Interval				
		0.30	0.20	0.10	0.05	0.01
Average Control Delay per Vehicle for Intersection	Rookin and Bellaire	15.6	15.5	15.5	15.3	15.7
	Hilcroft and Bellaire	41.3	40.9	40.1	40.5	39.9



**Figure 7-5 Changes in average control delay per vehicle at the intersections, MOE5, with significance levels**

The results of Duncan tests are shown in Tables 7-25 and 7-26. It can be seen that the significance level did not have any significant impact on MOE5 for either intersection. In conclusion, the MOE5 was not sensitive to the significance level, in other words, widening the prediction interval in the BSP2 scenario did not cause any significant increase in intersection control delay per vehicle.

**Table 7-25 Results of Duncan test between average control delay per vehicle, MOE5, under various Significance levels at the intersection of Rookin and Bellaire**

Significance Level Comparison		Mean		Test Statistic	Critical Value	Result
Significance Level 1	Significance Level 2	Significance Level 1	Significance Level 2			
0.30	0.20	15.64	15.52	0.120	0.501	Accept $H_0$
0.30	0.10	15.64	15.54	0.100	0.476	Accept $H_0$
0.30	0.05	15.64	15.30	0.340	0.517	Accept $H_0$
0.30	0.01	15.64	15.78	0.140	0.476	Accept $H_0$
0.20	0.10	15.52	15.54	0.020	0.476	Accept $H_0$
0.20	0.05	15.52	15.30	0.220	0.476	Accept $H_0$
0.20	0.01	15.52	15.78	0.260	0.517	Accept $H_0$
0.10	0.05	15.54	15.30	0.240	0.501	Accept $H_0$
0.10	0.01	15.54	15.78	0.240	0.501	Accept $H_0$
0.05	0.01	15.30	15.78	0.480	0.529	Accept $H_0$

**Table 7-26 Results of Duncan test between average control delay per vehicle, MOE5, under various significance levels at the intersection of Hilcroft and Bellaire**

Significance Level Comparison		Mean		Test Statistic	Critical Value	Result
Significance Level 1	Significance Level 2	Significance Level 1	Significance Level 2			
0.30	0.20	41.29	40.85	0.440	2.671	Accept $H_0$
0.30	0.10	41.29	40.07	1.220	2.901	Accept $H_0$
0.30	0.05	41.29	40.50	0.780	2.810	Accept $H_0$
0.30	0.01	41.29	39.90	1.390	2.967	Accept $H_0$
0.20	0.10	40.85	40.07	0.780	2.810	Accept $H_0$
0.20	0.05	40.85	40.51	0.340	2.671	Accept $H_0$
0.20	0.01	40.85	39.90	0.950	2.901	Accept $H_0$
0.10	0.05	40.07	40.51	0.440	2.671	Accept $H_0$
0.10	0.01	40.07	39.90	0.170	2.671	Accept $H_0$
0.05	0.01	40.51	39.90	0.610	2.810	Accept $H_0$

### 7.3.2 Sensitivity Analysis of Bus Headway

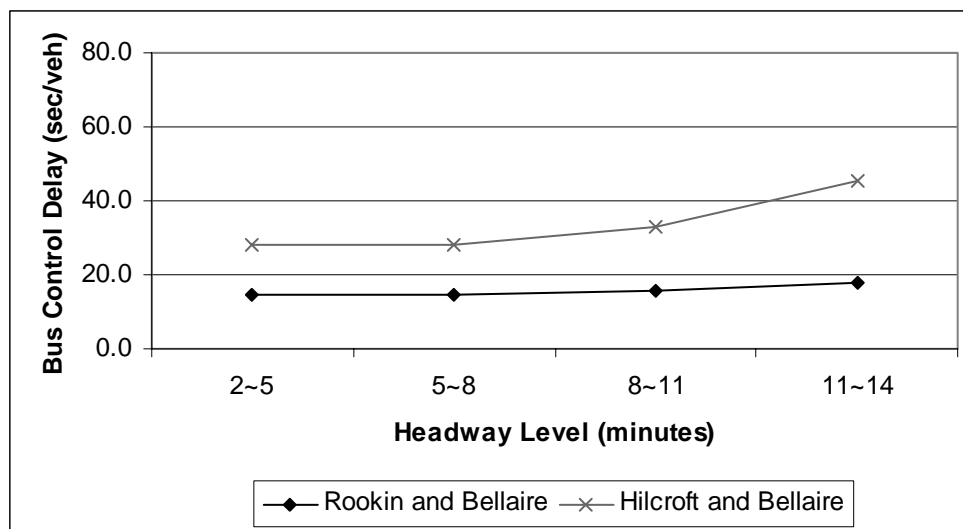
A sensitivity analysis of the BSP2 scenario to the value of bus headways were conducted next. As discussed previously in Chapter III, four levels of bus headway were utilized in this study: 2~5 minutes, 5~8 minutes, 8~11 minutes, and 11~14 minutes. The effects of bus headway were evaluated only for the bus operations. The MOEs used in measuring the effects of the bus headways on the bus operations were the average control delay per bus (MOE1) and bus arrival rate during green phase (MOE3). The average control delay for the intersection (MOE5) was selected for the impact of BSP operations on general traffic. Each of the headway levels were simulated under AM peak traffic demand and 90% prediction interval.

#### 7.3.2.1 Average control delay per bus at intersection (MOE1)

When the headway increases (i.e. the bus is behind schedule), the dwell time, as well as its variability, also increases. Intuitively, this will reduce the performance of the BSP2 scenario. The average control delay that was experienced by each bus was summarized, for each intersection, in Table 7-27. The MOE1 for other scenarios were shown for reference purposes. It can be seen that the MOE1 for the BSP2 scenario increased as the headway levels varied between 5~8 and 11~14 minutes for both intersections. The pattern of increase in the MOE1 was more noticeable at the intersection of Hilcroft and Bellaire where the main street bus approach experienced greater traffic congestion. At headway levels of 2~5 and 5~8 minutes, the changes in MOE1 by the BSP2 scenario were relatively small. Figure 7-6 illustrates the changing patterns of MOE1 at both intersections.

**Table 7-27 Average control delay per bus, MOE1, at the intersections with various headway levels**

Intersection	Rookin and Bellaire				Hilcroft and Bellaire			
	Normal	BSP0	BSP1	BSP2	Normal	BSP0	BSP1	BSP2
2~5	25.2	20.3	15.5	14.8	77.0	52.9	37.6	28.2
5~8	30.6	18.9	15.7	14.7	60.8	50.4	38.0	27.9
8~11	30.7	18.6	17.4	15.8	65.1	53.4	50.1	33.1
11~14	31.4	20.4	19.6	17.8	65.2	58.8	55.6	45.5



**Figure 7-6 Changes in average control delay per bus, MOE1, at the intersections with headway levels**

Tables 7-28 and 7-29 show the Duncan test results for various bus headway levels used in the sensitivity analysis. It can be seen that the MOE1 for different headway levels did not show any significant difference at the intersection of Rookin and Bellaire. At the intersection of Hilcroft and Bellaire the headway level of 11~14 resulted in significantly different MOE1 from other headway levels. However, any significant difference in MOE1 was not found between headway levels of 2~5, 5~8, and 8~11 minutes. It was concluded that the MOE1 for the BSP2 scenario was not affected by the



bus headways at the intersection of Rookin and Bellaire. In addition, a longer headway level that produces a wider prediction interval resulted in a significant increase in MOE1 under congested traffic conditions.

**Table 7-28 Results of Duncan test between average control delay per bus, MOE1, under various headway levels at the intersection of Rookin and Bellaire**

Headway Level Comparison		Mean		Test Statistic	Critical Value	Result
Headway Level 1	Headway Level 2	Headway Level 1	Headway Level 2			
11~14	8~11	17.75	15.82	1.930	2.959	Accept $H_0$
11~14	5~8	17.75	14.72	3.030	3.209	Accept $H_0$
11~14	2~5	17.75	14.80	2.950	2.959	Accept $H_0$
8~11	5~8	15.82	14.72	1.100	3.110	Accept $H_0$
8~11	2~5	15.82	14.80	1.020	2.959	Accept $H_0$
5~8	2~5	14.72	14.80	0.080	2.959	Accept $H_0$

**Table 7-29 Results of Duncan test between average control delay per bus, MOE1, under various headway levels at the intersection of Hilcroft and Bellaire**

Headway Level Comparison		Mean		Test Statistic	Critical Value	Result
Headway Level 1	Headway Level 2	Headway Level 1	Headway Level 2			
11~14	8~11	45.52	33.09	12.430	12.285	Reject $H_0$
11~14	5~8	45.52	27.90	17.620	13.324	Reject $H_0$
11~14	2~5	45.52	28.20	17.350	12.914	Reject $H_0$
8~11	5~8	33.09	27.90	5.190	12.914	Accept $H_0$
8~11	2~5	33.09	28.17	4.920	12.285	Accept $H_0$
5~8	2~5	27.90	28.17	0.270	12.285	Accept $H_0$

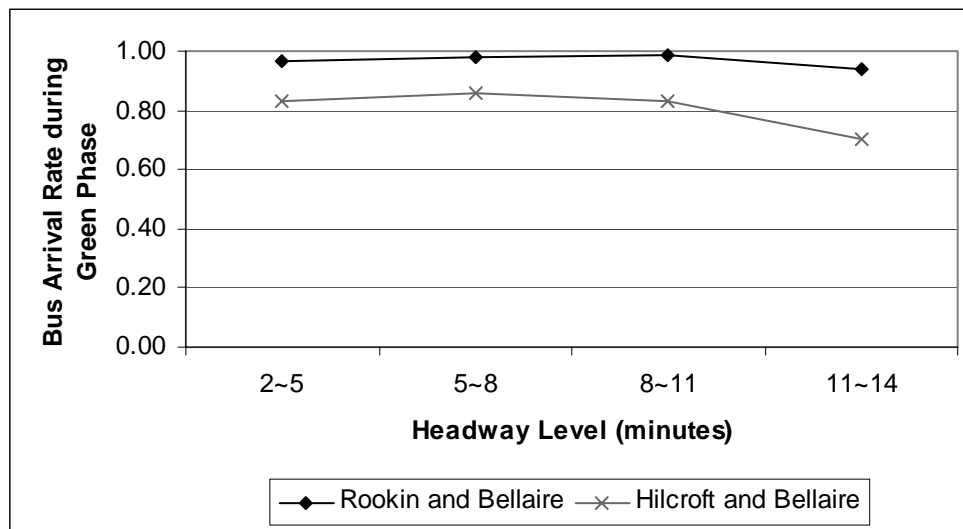
### 7.3.2.2 Bus arrival rate during green phase (MOE3)

The MOE3 for different headway levels are summarized for each intersection in Table 7-30. Note that the differences in MOE3 for different headway levels were relatively small

at the intersection of Rookin and Bellaire. It can be seen that the reduction in MOE3 with the headway level of 11~14 minutes at the intersection of Hilcroft and Bellaire was noticeable while other headway levels resulted in similar values of MOE3. In addition the BSP2 scenario always resulted in significantly better performance than any other BSP scenario at the both intersections. Figure 7-7 illustrates the changes in MOE3 according to the headway levels.

**Table 7-30 Bus arrival rate during green phase, MOE3, under various headway levels**

Intersection Headway Levels (minutes)	Rookin and Bellaire				Hilcroft and Bellaire			
	Normal	BSP0	BSP1	BSP2	Normal	BSP0	BSP1	BSP2
2~5	0.74	0.86	0.93	0.97	0.37	0.66	0.66	0.83
5~8	0.67	0.86	0.96	0.98	0.40	0.59	0.58	0.86
8~11	0.60	0.88	0.93	0.98	0.40	0.55	0.58	0.83
11~14	0.56	0.78	0.90	0.94	0.30	0.38	0.44	0.70



**Figure 7-7 Changes in bus arrival rate during green phase, MOE3, with headway levels**

The results of Duncan tests for the intersection of Rookin and Bellaire are shown in Table 7-31. There was no statistical difference in the MOE3 between headway levels

found. Table 7-32 shows the results of the Duncan tests for the intersection of Hilcroft and Bellaire. It can be seen that no headway level results in a significant reduction in MOE3. While there was a comparative large reduction in MOE3 for the 11~14 level this was not shown to be statistically significant. Because of the relative large variation in MOE3 among the simulation replicates, the critical values in the test are much greater than those in Table 7-32. This variation was also caused by the traffic congestion that was experienced by the bus in the main street at the intersection of Hilcroft and Bellaire.

**Table 7-31 Results of Duncan test between bus arrival rate during green phase, MOE3, under various headway levels at the intersection of Rookin and Bellaire**

Headway Level Comparison		Mean		Test Statistic	Critical Value	Result
Headway Level 1	Headway Level 2	Headway Level 1	Headway Level 2			
11~14	8~11	0.94	0.98	0.043	0.063	Accept $H_0$
11~14	5~8	0.94	0.98	0.038	0.061	Accept $H_0$
11~14	2~5	0.94	0.97	0.029	0.058	Accept $H_0$
8~11	5~8	0.98	0.98	0.006	0.058	Accept $H_0$
8~11	2~5	0.98	0.97	0.014	0.061	Accept $H_0$
5~8	2~5	0.98	0.97	0.009	0.058	Accept $H_0$

**Table 7-32 Results of Duncan test between bus arrival rate during green phase, MOE3, under various headway levels at the intersection of Hilcroft and Bellaire**

Headway Level Comparison		Mean		Test Statistic	Critical Value	Result
Headway Level 1	Headway Level 2	Headway Level 1	Headway Level 2			
11~14	8~11	0.70	0.83	0.133	0.152	Accept $H_0$
11~14	5~8	0.70	0.86	0.156	0.164	Accept $H_0$
11~14	2~5	0.70	0.83	0.134	0.159	Accept $H_0$
8~11	5~8	0.83	0.86	0.022	0.159	Accept $H_0$
8~11	2~5	0.83	0.83	0.001	0.152	Accept $H_0$
5~8	2~5	0.86	0.83	0.021	0.152	Accept $H_0$

### 7.3.2.3 Average control delay per vehicle for the intersection (MOE5)

The results of the MOE5 for different headway levels are shown in Table 7-33, for each intersection. Because changing the bus headway may affect the delay to non-transit vehicles, the percentage change to the Normal scenario is used as an alternative measure for MOE5. This can separate the delay change by the BSP2 scenario from the changes by the headway level. It can be seen that the percentage changes in MOE5 for the both intersections are relatively small and have narrow range of variations. In particular, the percentage changes for the intersection of Hilcroft and Bellaire ranges from -0.2 to 1.4 percent. This result was attributed to the congestion on the main street approaches, and consequently the delay reduction of the vehicles on the main street approaches negates the delay increase on non-priority approaches. Figure 7-8 shows the change pattern of the MOE5 for each intersection.

The Duncan test results for the percentage change in MOE5 are summarized in Tables 7-34 and 7-35, for each intersection. It can be seen that any headway level did not change significantly the percentage change for either intersection. This result allows the conclusion that the headway level has no significant impact on average control delay per vehicle at both intersections. In addition the effect of the headway level diminishes at congested traffic conditions, such as the intersection of Hilcroft and Bellaire.

**Table 7-33 Average control delay per vehicle at the intersections, MOE5, under various headway levels**

Intersection	Rookin and Bellaire			Hilcroft and Bellaire		
	Normal	BSP2	Percentage Change to Normal	Normal	BSP2	Percentage Change to Normal
2~5	14.7	15.9	8.7%	42.7	43.3	1.4%
5~8	14.6	15.5	6.8%	40.1	40.1	-0.2%
8~11	14.7	16.1	9.1%	40.2	40.4	0.6%
11~14	14.6	16.0	10.0%	38.5	38.7	0.4%

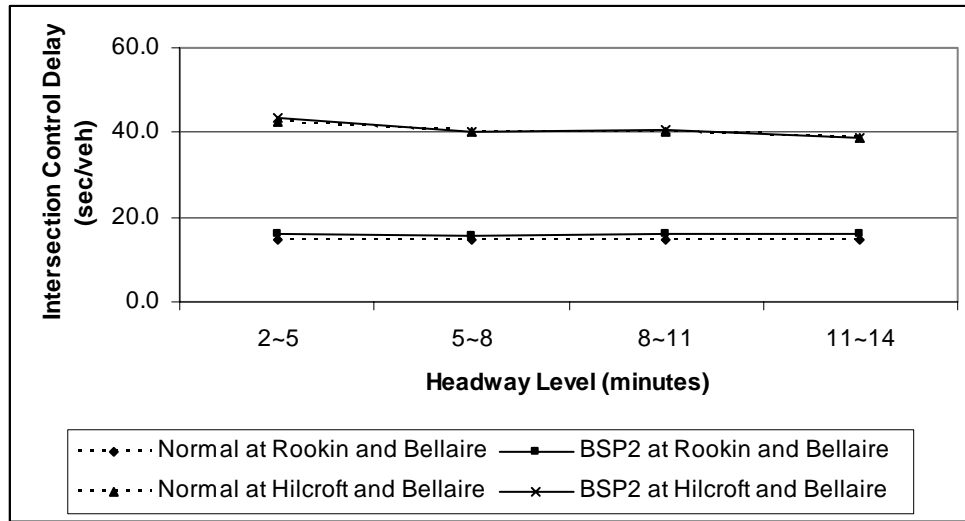


Figure 7-8 Changes in average control delay per vehicle at the intersections, MOE5, with headway levels

Table 7-34 Results of Duncan test for percentage change in MOE5 under various headway levels at the intersection of Rookin and Bellaire

Headway Level Comparison		Mean		Test Statistic	Critical Value	Result
Headway Level 1	Headway Level 2	Headway Level 1	Headway Level 2			
11~14	8~11	10.01	9.10	0.910	5.487	Accept H <sub>0</sub>
11~14	5~8	10.01	6.80	3.210	5.951	Accept H <sub>0</sub>
11~14	2~5	10.01	8.70	1.357	5.768	Accept H <sub>0</sub>
8~11	5~8	9.10	6.80	2.299	5.768	Accept H <sub>0</sub>
8~11	2~5	9.10	8.66	0.446	5.487	Accept H <sub>0</sub>
5~8	2~5	6.80	8.66	1.853	5.487	Accept H <sub>0</sub>

**Table 7-35 Results of Duncan test for percentage change in MOE5 under various headway levels at the intersection of Hilcroft and Bellaire**

Headway Level Comparison		Mean		Test Statistic	Critical Value	Result
Headway Level 1	Headway Level 2	Headway Level 1	Headway Level 2			
11~14	8~11	-0.17	0.60	0.772	11.227	Accept $H_0$
11~14	5~8	-0.17	0.39	0.564	10.680	Accept $H_0$
11~14	2~5	-0.17	1.40	1.555	11.584	Accept $H_0$
8~11	5~8	0.60	0.39	0.208	10.680	Accept $H_0$
8~11	2~5	0.60	1.38	0.783	10.680	Accept $H_0$
5~8	2~5	0.39	1.38	0.991	11.227	Accept $H_0$

### 7.3.3 Sensitivity Analysis of Demand

The effect of the increase in demand was tested by running seven demand scenarios. These are 70% (degree of saturation = 0.60 for eastbound main street), 80% (0.69), 90% (0.77), 100% (0.86), 110% (0.94), 120% (1.02), 130% (1.11) of the AM peak-hour demand. The MOE3, bus arrival rate during green phase, was employed to measure the impacts of demand levels on the bus operations. This MOE3 measures the effectiveness of BSP implementation by counting the buses that pass through the intersection during their priority phases. The MOE5, average control delay per vehicle for the intersection, was used for measuring impacts on the non-transit vehicles by demand levels. Each of the levels of demand was simulated under a headway of 5~8 minutes and a prediction interval of 90%.

#### 7.3.3.1 Bus arrival rate during green phase (MOE3)

The bus arrival rates during green phase under various demand level scenarios were summarized by intersection in Table 7-36. It can be seen that for demand levels less than 100 percent the MOE3 results are approximately same. However, when the demand level was 110% the MOE3 started to decrease. For the intersection of Rookin and Bellaire, the MOE3 dropped at the demand level of 130%. Note that the relative drop at

the 130% demand level was large for both intersections. This was because a spillback occurred on the eastbound main street for a demand level of 120%.

Figure 7-9 shows the changes in MOE3 as a function of demand levels at both intersections. The MOE3 for the Normal scenario is shown for reference purposes. It can be seen that the improvements of the BSP2 over the Normal scenario diminish at the 120% and 130% demand levels at the intersection of Hilcroft and Bellaire. Because the signal operation at the intersection of Rookin and Bellaire favored the main street movements, MOE3 was always higher at this intersection than that at the intersection of Hilcroft and Bellaire. The changes in MOE3 between levels of demand 120% and 130% are clearly noticeable as shown in Figure 7-9.

**Table 7-36 Average bus arrival rate during green phase for various demand levels**

Intersection Demand Level	Rookin and Bellaire				Hilcroft and Bellaire			
	Normal	BSP0	BSP1	BSP2	Normal	BSP0	BSP1	BSP2
70%	0.71	0.91	0.94	0.93	0.46	0.63	0.68	0.86
80%	0.66	0.79	0.93	0.98	0.49	0.69	0.70	0.83
90%	0.76	0.87	0.94	0.98	0.40	0.69	0.70	0.88
100%	0.73	0.88	0.97	0.97	0.32	0.58	0.57	0.83
110%	0.76	0.82	0.94	0.97	0.32	0.54	0.60	0.75
120%	0.70	0.84	0.91	0.92	0.25	0.29	0.36	0.50
130%	0.41	0.51	0.53	0.69	0.00	0.00	0.04	0.11

The results of Duncan tests are shown in Tables 7-37 and 7-38, for each intersection. Note that the MOE3 at 130% demand level is statistically different from other demand levels at the intersection of Rookin and Bellaire. At the intersection of Hilcroft and Bellaire, the MOE3 at demand levels of 120% and 130% is statistically different from other levels of demand. No significant difference was found at levels of demand less than 110% for either intersection. It can be concluded that the MOE3 for BSP2 scenario is significantly decreased under congested traffic conditions, such as 120% (1.03) and 130% (1.11) demand levels. In addition, the impacts on the bus

operations by the demand level are statistically same at 100% or less demand levels for the both intersections on the test bed.

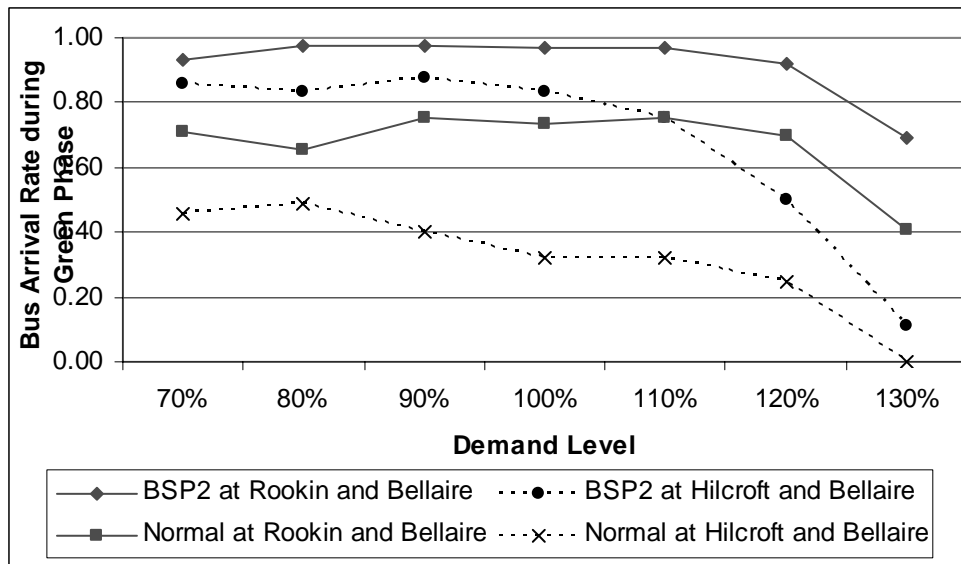


Figure 7-9 Changes in bus arrival rate during green phase, MOE3, with demand levels

Table 7-37 Results of Duncan test between bus arrival rate during green phase, MOE3, under various demand levels at the intersection of Rookin and Bellaire

Demand Level Comparison		Mean		Test Statistic	Critical Value	Result
Demand Level 1	Demand Level 2	Demand Level 1	Demand Level 2			
70%	80%	0.93	0.98	0.044	0.147	Accept H <sub>0</sub>
80%	90%	0.98	0.98	0.000	0.147	Accept H <sub>0</sub>
90%	100%	0.98	0.97	0.011	0.147	Accept H <sub>0</sub>
100%	110%	0.97	0.97	0.000	0.147	Accept H <sub>0</sub>
110%	120%	0.97	0.97	0.044	0.147	Accept H <sub>0</sub>
120%	130%	0.92	0.69	0.233	0.147	Reject H <sub>0</sub>



**Table 7-38 Results of Duncan test between bus arrival rate during green phase, MOE3, under various demand levels at the intersection of Hilcroft and Bellaire**

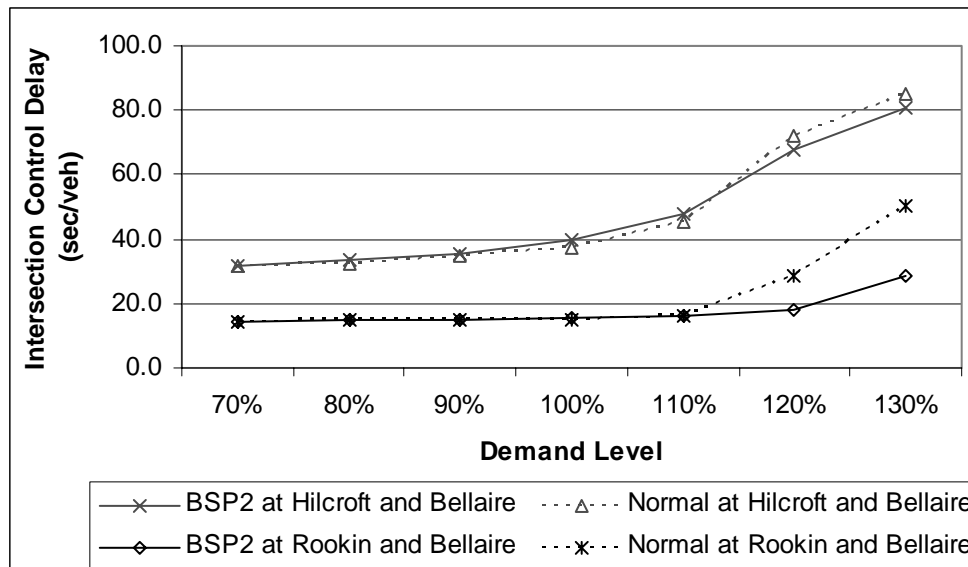
Demand Level Comparison		Mean		Test Statistic	Critical Value	Result
Demand Level 1	Demand Level 2	Demand Level 1	Demand Level 2			
70%	80%	0.86	0.83	0.030	0.139	Accept $H_0$
80%	90%	0.83	0.88	0.048	0.139	Accept $H_0$
90%	100%	0.88	0.83	0.048	0.139	Accept $H_0$
100%	110%	0.83	0.75	0.075	0.139	Accept $H_0$
110%	120%	0.75	0.50	0.254	0.139	Reject $H_0$
120%	130%	0.50	0.11	0.391	0.139	Reject $H_0$

### 7.3.3.2 Average control delay per vehicle for the intersection (MOE5)

The MOE5 results for different demand levels are shown in Table 7-39, for each intersection. As the demand level increases, the MOE5 also increases regardless of BSP implementation. Therefore, it is hard to capture the impacts of the demand levels on non-transit vehicles directly from the MOE5. The percentage change to the Normal scenario is used as an alternative measure for MOE5. It can be seen that the percentage increases in MOE5 at the 100% or less demand levels are relatively small for the both intersections. However, the BSP2 scenario has less delay than the Normal scenario at 110% or greater demand levels. These results are attributed to spillbacks occurred along eastbound of the main street and subsequently the considerable increase in delay. The simulation results indicated that the implementation of all BSP scenarios improved all delay measures for buses and non-transit vehicles when spillbacks occur. Because the BSP operations assigned more green time to the main street approach, a considerable amount of spillback was eliminated by implementing BSP scenario. This was an incidental result at the particular traffic conditions. It cannot be considered as the general performance of the BSP scenario. Figure 7-10 shows the change pattern of the MOE5 for each intersection. Note that the changes in MOE5 at the 100% or less demand levels are relatively small.

**Table 7-39 Average control delay per vehicle at the intersections, MOE5, for various demand levels**

Intersection	Rookin and Bellaire			Hilcroft and Bellaire		
	Normal	BSP2	Percentage Change to Normal	Normal	BSP2	Percentage Change to Normal
70%	14.0	14.2	1.6%	31.7	31.8	0.4%
80%	14.7	15.2	3.3%	32.4	33.6	3.6%
90%	14.7	15.2	3.1%	34.7	35.5	2.2%
100%	15.0	15.4	3.1%	37.1	40.0	7.8%
110%	16.4	16.2	-1.5%	45.5	48.1	5.8%
120%	28.7	17.9	-37.7%	72.0	67.5	-6.3%
130%	50.2	28.7	-42.9%	85.3	80.9	-5.1%



**Figure 7-10 Changes in average control delay per vehicle for the intersection, MOE5, with demand levels**

The results of the Duncan tests for various demand level are shown in Tables 7-40 and 7-41. It can be seen that the percentage change in MOE5 do not show any significant difference at any demand level at the intersection of Rookin and Bellaire. It

means that there is no statistical evidence that the demand level has significant impact on MOE5. For the intersection of Hilcroft and Bellaire it can be seen that the demand levels of 120% and 130% had statistically significant difference in the percentage change from other demand levels. However, these results are attributed to the specific traffic conditions of the test bed. From the analysis of the percentage change in MOE5, it can be concluded that the BSP2 scenario does not cause any statistically significant increase in MOE5 at all demand levels for the both intersections.

**Table 7-40 Results of Duncan test for percentage changes in MOE5 under various demand levels at the intersection of Rookin and Bellaire**

Demand Level Comparison		Mean		Test Statistic	Critical Value	Result
Demand Level 1	Demand Level 2	Demand Level 1	Demand Level 2			
70%	80%	0.44	3.58	3.134	16.942	Accept $H_0$
80%	90%	3.58	2.22	1.358	16.105	Accept $H_0$
90%	100%	2.22	7.84	5.626	17.494	Accept $H_0$
100%	110%	7.84	5.80	2.039	16.105	Accept $H_0$
110%	120%	5.80	-6.27	12.072	18.058	Accept $H_0$
120%	130%	-6.27	-5.14	1.131	16.105	Accept $H_0$

**Table 7-41 Results of Duncan test for percentage changes in MOE5 under various demand levels at the intersection of Hilcroft and Bellaire**

Demand Level Comparison		Mean		Test Statistic	Critical Value	Result
Demand Level 1	Demand Level 2	Demand Level 1	Demand Level 2			
70%	80%	1.64	3.27	1.623	23.733	Accept $H_0$
80%	90%	3.27	3.07	0.195	21.848	Accept $H_0$
90%	100%	3.07	3.1	0.012	21.848	Accept $H_0$
100%	110%	3.1	-1.52	4.582	22.984	Accept $H_0$
110%	120%	-1.52	-37.73	36.206	21.848	Reject $H_0$
120%	130%	-37.73	-42.89	5.159	21.848	Accept $H_0$

### 7.3.4 Summary of Findings

The BSP2 scenario showed similar performances regardless of the significance levels of the prediction interval. At the level of significance 0.01 (99% prediction interval), the bus travel time reduced by 3% from the significance level of 0.3 (70% prediction interval). The change in bus arrival rate during green phase was not significant at any significance level except a pair of significant level of 0.01 and 0.3. The intersection delay per vehicle was not sensitive to the significance level of the prediction interval. It was concluded that the performance of the BSP2 scenario is not sensitive to the change in the significance level of the prediction interval. Regardless of the level of significance, the BSP2 scenario always performed better than other BSP scenarios.

When the performances of the BSP2 scenario were evaluated for various bus headway levels, it was observed that the 11~14 minutes level resulted in the largest bus delays and lowest bus arrival rate during the green phase. The headway level didn't have significant impacts on the bus delay at the intersection of Rookin and Bellaire. However at the intersection of Hilcroft and Bellaire the 11~14 minutes level had significantly different bus delay from other headway levels. The bus arrival rates during green phase were lowest at the headway level of 11~14 minutes at both intersections, that is, 0.94 and 0.70, respectively. It was also found that the headway level has no significant impact on the BSP2 performance in terms of overall intersection delay.

When the level of traffic demand varied from 70% to 130% of the AM peak demand, the bus arrival rates during green phase decreased significantly in congested traffic conditions. At the intersection of Rookin and Bellaire the rate dropped to 0.69 at 130% demand level which is significantly different from other demand levels. At the intersection of Hilcroft and Bellaire the rate decreased significantly at the demand levels higher than 110%. The rates dropped to 0.5 at 120% and 0.11 at 130% levels of demand. The average intersection delay was reduced by the BSP2 scenario at the 120% and 130% demand levels at the both intersections. These results are attributed to spillbacks occurred along eastbound of the main street and subsequently the considerable increase

in delay. Because the BSP operations assigned more green time to the main street approach, a considerable amount of spillback and delay was eliminated by implementing BSP scenario. This was an incidental result at the particular traffic conditions. It cannot be considered as the general performance of the BSP scenario. It was concluded, from a practical prospect, that the BSP2 scenario does not perform well in congested traffic conditions, specifically with saturation rate over 1.0.

#### **7.4 CONCLUDING REMARKS**

It was found that all the MOEs used in the evaluation were improved with the BSP2 scenario. In addition, the BSP2 scenario performed better than other BSP scenarios. There was no significant evidence for rejecting the hypothesis of that the BSP2 scenario can improve the bus operations without significant impact on non-transit vehicles. In particular the impacts on other vehicles were minimized when the traffic conditions on the main street are congested. At the intersection of Hilcroft and Bellaire, the BSP2 scenario reduced the bus intersection delay by 56 percent without any increase in the intersection delay.

The BSP2 scenario resulted in similar MOEs for all significance levels of the prediction interval. It was concluded that the width of prediction interval is not important to the performance of the BSP2 scenario. Incorporating the prediction interval into the BSP strategy is essential to the improvements in BSP operations. It was also found that the headway level has no significant impact on the BSP2 performance. The sensitivity analysis of demand level indicated that the performance of the BSP2 scenario significantly decreases under congested traffic conditions, specifically oversaturated conditions.

## **CHAPTER VIII**

### **CONCLUSIONS**

In this dissertation, the development and evaluation of the improved bus signal priority algorithm for providing priority at traffic signals to buses traveling on arterial streets. An algorithm was developed to overcome inefficient operations of existing bus priority system when the intersection includes nearside bus stops. This section contains a summary of the results and the conclusions from the evaluation of the algorithm. Recommendations for future research and enhancements of the algorithm are also provided.

#### **8.1 SUMMARY**

##### **8.1.1 Bus Dwell Time Prediction**

A probabilistic model and the Weighted Least Squares (WLS) regression model were developed to predict the bus dwell time at specific bus stop. Although the probabilistic model showed the strength in representing the determinants of dwell time as random variables, the observed data did not support the model assumption of the linear correlation between the number of alighting passengers and the passenger loads. The determinants of the bus dwell time were analyzed in order to measure the significance of each determinant to the dwell time. The analysis concluded that the bus headway is most significant determinant and a regression model with the bus headway has the best results. The residual analysis of the regression model also revealed non-constant variance over bus headways, which violated the common assumption underlying regression modeling. The weighted least squares method, therefore, was employed in order to consider the non-constant variance. Another advantage from WLS method can provide the prediction interval that varies according to the bus headway.

### **8.1.2 The Improved Bus Signal Priority Algorithm**

Because of the variability in dwell time, most current bus signal priority systems have been inefficient at intersections with nearside bus stops. In this dissertation an improved BSP algorithm was developed to incorporate the variability of dwell time into BSP signal timing plan. The new prediction model and its prediction interval developed in this dissertation were used as input to the improved BSP algorithm. The basic idea of the improved BSP algorithm is to provide a priority phase wide enough to accommodate the prediction interval of the bus dwell time. An operational algorithm was designed to implement the improved BSP strategy efficiently within the VISSIM simulation environment. The unused priority time is restored back to non-priority phases after the bus passes through the intersection during the priority phase.

## **8.2 CONCLUSIONS**

On the test bed, the implementation of the improved BSP algorithm is found to be beneficial in reducing bus delay, providing buses with average travel time savings of up to 21% over the normal case of no priority implementation. Impacts on other traffic are insignificant at the intersection of Rookin St. and Bellaire Blvd. where the traffic conditions are less congested. However, at the congested intersection of Hilcroft Ave. and Bellaire Blvd., the vehicles on non-priority approaches experience an increase in delay of 28%. Other BSP algorithms resulted in similar increases in delay. The most significant benefit from implementing the improved BSP algorithm is the improvement of the mobility of the bus at the intersection and it is measured by the bus arrival rate during green time. This benefit is significant, providing increase of up to 100 % for current traffic conditions.

The improved BSP algorithm is found to be most beneficial in congested conditions, where queues at signals cause significant delay in the absence of priority. Under less congested conditions, signal delay may not be large enough to justify the priority implementation.

The simulation for sensitivity analysis demonstrates that the benefit obtained from the improved BSP algorithm can be affected by factors such as traffic demands, bus headways, and significance levels of the prediction interval. When the traffic demand increases, the bus arrival rates during green phase decreased significantly in congested traffic conditions. The decrease is more evident at the intersection of Hilcroft and Bellaire where the traffic experiences the congestion. At the intersection of Rookin and Bellaire, less congested condition, the rate does not change until the 130% demand level where the rate dropped to 0.69 from 0.97. The average intersection delay rather decreases by the BSP2 scenario at the 120% and 130% demand levels at the both intersections. These results are attributed to spillbacks occurred along eastbound of the main street and subsequently the considerable increase in delay. The BSP implementation eliminates a considerable amount of spillback and delay. These results are very site- and condition- specific. Therefore, it may not necessary apply in other conditions or sites. It was concluded, from a practical prospect, that the BSP2 scenario does not perform well in congested traffic conditions, specifically with saturation rate over 1.0.

When the performances of the BSP2 scenario were evaluated for various bus headway levels, it was observed that the headway level does not have significant impacts on the bus delay at the intersection of Rookin and Bellaire. However at the intersection of Hilcroft and Bellaire the 11~14 minutes level had significantly different bus delay from other headway levels. The bus arrival rates during green phase were not affected by the headway level. It was also found that the headway level has no significant impact on the BSP2 performance in terms of overall intersection delay.

It was noted that the BSP2 scenario showed similar performances regardless of the significance levels of the prediction interval. The bus arrival rate during green phase was not significantly affected by the significance level. The intersection delay per vehicle was also not sensitive to the significance level of the prediction interval. It was concluded that the performance of the BSP2 scenario is not sensitive to the change in the



significance level of the prediction interval. Incorporating the prediction interval into the BSP strategy is essential to the benefit from BSP operations.

Conclusions from the sensitivity analysis are that the benefit to bus operations from BSP2 algorithm is significantly diminished under congested traffic conditions and large bus headway situations. However, the benefit is not affected by the width of the prediction interval.

### **8.3 FUTURE RESEARCH**

Further sensitivity analyses are required to evaluate the optimum location for advancing bus detector. Longer distance provides flexibility in adjusting signal timing but large error is generally expected in the arrival time prediction. It is also required to evaluate how the underlying signal setting, such as cycle length and splits, affects the benefit of the improved BSP algorithm. Because the proposed algorithm utilizes the priority window within the main street green time, the effectiveness of the algorithm will be limited by the cycle length and splits.

An evaluation of longer bus corridors would allow studies about the recovery of schedule adherence and the bus behavior such as bus bunching. The network including multiple bus routes would also allow the modeling of simultaneous priority calls on conflicting signal groups.

This dissertation is based on the results of the simulations for evaluating the effects of the improved bus signal priority algorithm. Although the study was designed to be applicable into conventional traffic controller, such as ATC 2070 controller, which is currently used in the study site, field studies need to be performed to guarantee the benefits of the improved BSP algorithm.

## GLOSSARY

*Alighting time:*

The time required for a passenger to leave a transit vehicle, expressed as time per passenger or total time for all passengers.

*All-red clearance interval:*

An optional interval immediately following the yellow change interval during which all signals display a red indication.

*AM peak period:*

The period in the morning when additional services are provided to handle higher passenger volumes. The period begins when normal scheduled headways are reduced.

*Boarding time:*

The time for a passenger to board a transit vehicle, expressed as time per passenger or total time for all passengers.

*BSP0:*

The basic BSP logic that utilizes a check-in detector for sensing approaching buses upstream from the stop line. The green extension and early green strategies are used to provide the signal priority.

*BSP1:*

The BSP logic with consideration of average dwell time. This BSP logic incorporates the dwell time into the BSP timing plan through the addition of average dwell time in the calculation of the bus travel time from the check-in detector to the stop line.

*BSP2:*

The improved BSP logic developed in this dissertation. The prediction interval of dwell time is accommodated in adjusting BSP signal timing plan.

*BSP mode:*

A type of the controller mode proposed in this dissertation. The BSP mode is activated, when there is a bus between the check-in and check-out detectors and it is eligible for priority service.

*Bus:*

A transit mode comprised of rubber tired passenger vehicles operating on fixed routes and schedules over roadways. Vehicles are powered by diesel, gasoline, battery or alternative fuel engines contained within the vehicle.

*Bus change interval:*

The yellow plus all-red interval that is used to clear traffic using the priority phase.

*Bus stop:*

The buildings and shelters with all attached fixtures used as transit passenger station facilities. Additional passenger services are frequently available in these stations, (e.g. ticket/token/pass sales, transit malls, transfer facilities, intermodal terminals, depots, terminals and high occupancy vehicle facilities). This covers major terminals, wayside stations, passenger shelters, benches and stop signs along a route.

*Calibration:*

The process of tuning model parameters with real-world data to ensure that the model realistically represents the traffic environment. The objective is to minimize the discrepancy between model result and measurements or observations.

*Check-in:*

Check-in is accomplished when BSP eligible bus is entering in the detection zone or detected at the check-in detector.

*Check-out:*

Check-out is accomplished when BSP eligible bus is exiting from the detection zone or detected at the check-out detector.

*Clearance time:*

The time loss at a transit stop, not including passenger dwell times. This parameter can be the minimum time between one transit vehicle leaving a stop and the following vehicle entering and can include any delay waiting for a sufficient gap in traffic to allow the transit vehicle to reenter the travel lane.

*Control delay:*

The component of delay that results when a control signal causes a lane group to reduce speed or to stop; it is measured by comparison with the uncontrolled condition.

*Coordination:*

The operation of controller units in a manner to provide a relationship between specific green indications at adjacent intersections in accordance with a time schedule to permit continuous operation of groups of vehicles along the street at a planned speed.

*Coordination phase:*

The phase in which coordination is provided. The coordinated phase is usually the main street green phase.

*Cycle:*

A complete sequence of signal indications.

*Detection zone:*

A section of the approach that transit vehicles are detected typically using onboard detector equipment. The detection zone consists of the check-in point and the check-out point.

*Dwell time:*

The time a transit unit (vehicle or train) spends at a station or a stop to serve passengers at the busiest door, plus the time required to open and close the doors.

*Force-off point:*

The point in the cycle where the controller begins terminating (i.e. begin timing the vehicle change interval) a phase.

*Headway*

The time interval between vehicles moving in the same direction on a particular route.

*Interval:*

A period of time in which all traffic signal indications remain constant.

*Maximum green interval:*

The maximum time that a green indication can be displayed to drivers.

*Minimum green interval:*

The shortest time that a green indication can be displayed to drivers.

*Non-priority phase:*

A phase in the background cycle plan that cannot be used to move buses. For the purpose of this dissertation, these phases include the cross-street left-turn phase, the cross-street through phase, and the main street left-turn phase.

*Normal:*

The current coordinated-actuated signal logic operating in the test bed.

*Normal mode:*

A type of the controller mode proposed in this dissertation. The controller operates under normal mode (e.g. default signal timing parameters) when there is no bus on the approach of interest.

*Offset:*

The difference, in seconds, between the start of green time at the two signalized intersections of a diamond interchange for through traffic on the internal link or the time between the start of individual green times and a specified time datum in a system of signalized intersections.

*Passenger service time:*

The time required for a passenger to board or alight from a transit vehicle, in seconds per passenger.

*PDF (probability density function):*

A function used to calculate probabilities and to specify the probability distribution of a continuous random variable.

*Phase:*

The part of the signal cycle allocated to any combination of traffic movements receiving the right-of-way simultaneously during one or more intervals.

*Phase sequence:*

The order in which the phases are arranged in the cycle.

*PMF (probability mass function):*

A function that provides probabilities for the values in the range of a discrete random variable.

*Prediction interval:*

The interval between a set of upper and lower limits associated with a predicted value designed to show on a probability basis the range of error associated with the prediction.

*Priority phase:*

The green interval of the priority phase.

*Priority window:*

The prediction interval of bus arrival time at the intersection. It is a time interval in the cycle needed to ensure that a bus arrives during a green indication with  $100(1 - \alpha)$  % confidence level.

*PT calling detector:*

The PT (public transport) calling detector provided in VISSIM only senses transit vehicles that send out PT information. When buses are detected at a check-in detector the PT information, which would be passenger loads in this study, is sent to the signal controller for the assessment of the eligibility of priority requests.

*Public transportation:*

As defined in the Federal Transit Act, transportation by bus or rail, or other conveyance, either publicly or privately owned, providing to the public general or special service (but not including school buses or charter or sightseeing service) on a regular and continuing basis. Public transportation is also synonymous with the terms mass transportation and transit.

*Restoring mode:*

A type of the controller mode proposed in this dissertation. The control mode is switched to the restoring mode, after the successful implementation of any priority strategy, if there is unused priority green time.

*Split:*

A segment of the cycle length allocated to each phase or interval that may occur in a cycle.

*Variable green time:*

The difference between the maximum green time and the minimum green time for a phase.

*Vehicle change interval:*

The yellow plus all-red interval that occurs between phases of a traffic signal to provide for clearance of the intersection before conflicting movements are released.

*Yellow change interval:*

The first interval following the green interval in which the signal indication for the phase is yellow.

*Zone detector:*

The zone detectors sense the presence of transit vehicles at a designated zone on the approach to an intersection. Typically these system only know that a vehicle is somewhere on the approach.

## NOTATION

$A$	= number of passenger alighting (p),
$a$	= departure time of previous bus,
$ABX$	= desired minimum following distance,
$AX$	= desired distance for standing vehicle,
$B$	= number of passenger arrivals during preceding headway (p),
$b$	= arrival time of current bus,
$BX$	= desired safety distance,
$BX\_Add$	= calibration parameter defining the range of variation,
$BX\_Mult$	= calibration parameter defining the range of variation,
$C$	= cycle length,
$d_{ik}$	= absolute deviation of the residual $i$ in group $k$ ,
$\bar{d}_k$	= sample mean of the $d_{ik}$ in group $k$ ,
$E_{ik}$	= estimated bus travel time on link $k$ for parameter set $i$ , $i = 1 \dots I, \quad k = 1 \dots S$ ,
$\tilde{e}_k$	= median of the residuals in group $k$ ,
$e_{ik}$	= residual $i$ in group $k$ ,
$F_i$	= force-off point of phase $i$ ,
$G_i$	= green time for phase $i$ ,
$h$	= bus headway (min),
$I$	= number of accepted parameter set, ( $I = 100$ ),
$I_{bus}$	= change interval for inserted priority phase,
$I_i$	= change interval for phase $i$ ,
$i$	= phase number,
$k$	= current phase in which priority call is requested, $k = 1 \dots n$ ,
$L$	= total number of passengers on the bus,



$L_1$	=	lower bound of the prediction interval for the dwell time (sec),
$L_2$	=	upper bound of the prediction interval for the dwell time (sec),
$l$	=	passenger loads (p),
$M_{ext}$	=	maximum amount of time that the priority phase ( $\phi_1$ ) can be extended (sec),
$M_{grn}$	=	the maximum time available to service buses by returning early to the priority phase (sec),
$M_p$	=	the number of buses arrived during their associated priority phase,
$M_{rst}$	=	amount of time to be restored (sec),
$m$	=	number of non-priority phases being restored, $1 \leq m \leq n - 1$ ,
$MS_E$	=	error mean squares,
$N$	=	total number of all responses,
$N_a$	=	alighting passengers per bus (p),
$N_b$	=	boarding passengers per bus (p),
$N_k$	=	number of observed bus at stop $k$ ,
$N_s$	=	the total number of buses generated during simulation run,
$n$	=	sample size, $n = n_1 + n_2$ ,
$O_{ik}$	=	observed estimated bus travel time on link $k$ for parameter set $i$ ,
$p$	=	probability of alighting for a randomly chosen passenger on bus,
$P_a$	=	alighting passengers through busiest door during peak 15 min (p),
$P_b$	=	boarding passengers through busiest door during peak 15 min (p),
$p_k$	=	alighting probability at stop $k$ ,
$\mathbf{P}_{bus}^*$	=	optimum parameter set for buses,
$R_i$	=	minimum green time for phase $i$ ,
$r$	=	number of success,
$RND1_i$	=	random number for vehicle $i$ from distribution $N(0.5,0.15)$ ,
$S$	=	number of the link between stops, ( $S = 3$ , in this study),

$S_i^{BSP}$	=	split of phase $i$ in BSP mode (sec),
$S_i^{ext}$	=	split of phase $i$ with green extension strategy (sec),
$S_i^{gm}$	=	split of phase $i$ with early green strategy (sec),
$S_i^{int}$	=	split of non-priority phase $i$ with phase insertion strategy (sec),
$S_i^{rst}$	=	split of phase $i$ in restoring mode (sec),
$SS_E$	=	error sum of squares,
$s^2$	=	pooled variance,
$T_b$	=	total bus travel time from check-in detector to stop line (sec),
$t_a$	=	marginal passenger alighting time (sec/p),
$t_b$	=	marginal passenger boarding time (sec/p),
$t_c$	=	current cycle time (sec),
$t_d$	=	bus dwell time (sec),
$t_{oc}$	=	door opening and closing time (sec),
$t_{red}$	=	the available time before/after priority window for non-priority phases (sec),
$t_{\alpha/2, n-2}$	=	appropriate point based on the $T_{n-2}$ distribution,
$t_L^*$	=	test statistic for the modified Levene test,
$v$	=	speed of front vehicle for following process, speed of following vehicle for free flow driving,
$w_i$	=	weight of phase $i$ ,
$X$	=	number of passenger arrival,
$X_{i1}$	=	schedule adherence (sec),
$X_{i2}$	=	passenger loads (person),
$X_{i3}$	=	bus headway (minutes),
$Y_i$	=	bus dwell time of $i$ th bus (sec),
$\bar{Y}_i$	=	sample mean for the $i$ th scenarios,

$Z_{ext}$	= last time in the cycle that the priority green phase can be extended,
$\beta$	= parameter,
$\delta(\theta_c)$	= dummy variable, $\theta_c \leq C$ ,
$\varphi$	= correlation coefficient, $-1 < \varphi < 1$ ,
$\varepsilon_i$	= random error, $N(0, \sigma^2)$ ,
$\theta$	= time point in the cycle when priority is requested,
$\theta_c$	= time point in the cycle when priority is requested,
$\theta_o$	= time point in the cycle when a bus checks out (sec),
$\kappa_i$	= arrival time of bus $i$ at the intersection,
$\lambda(t)$	= passenger arrival intensity (p/sec), for stationary arrival $m = \lambda(b - a)$ ,
$\mu$	= sample mean,
$\rho$	= the amount of red period <b>before</b> the priority window (sec),
$\rho'$	= the amount of red period <b>after</b> the priority window (sec),
$\sigma_0$	= estimate from standard deviation function,
$\tau_k$	= elapsed green time of phase $k$ (sec),
$\phi_i$	= signal phase $i$ ,
$\phi n$	= the last phase in the ring,
$\omega$	= start point of the priority window in the cycle, and
$\omega'$	= end point of the priority window in the cycle.

## REFERENCES

1. Werner, J., Houston Metro Plans to Deploy a More Intelligent Transit Priority Scheme. *Newsletter of the ITS Cooperative Deployment Network*, National Associations Working Group for ITS, December 2002. Available: [www.nawgits.com/icdn/ivoms\\_tp.html](http://www.nawgits.com/icdn/ivoms_tp.html).
2. Khasnabis, S., G. V. Reddy, and S. K. Hoda. Evaluation of the Operating Cost Consequences of Signal Preemption as an IVHS Strategy. In *Transportation Research Record 1390*, TRB, National Research Council, Washington, D.C., 1993, pp. 3-9.
3. Sunkari, S. R., P. S. Beasley, T. Urbanik II, and D. B. Fambro. A Model to Evaluate the Impact of Bus Priority on Signalized Intersection. In *Transportation Research Record 1494*, TRB, National Research Council, Washington, D.C., 1995, pp. 117-123.
4. Urbanik II, T. Priority Treatment of Buses at Traffic Signals. *Transportation Engineering*, Vol. 47, No. 11, Washington, D.C., November 1977, pp.31-33.
5. Intelligent Transportation Society of America. *An Overview of Transit Signal Priority*. ITS America, Washington, D.C., 2003.
6. Urbanik, T. and R.W. Holder. *Evaluation of Priority Techniques for High Occupancy Vehicles on Arterial Streets*. Research Report 205-5. Texas Transportation Institute, Texas A&M University, College Station, Texas, 1977.
7. Skabardonis, A. Control Strategies for Transit Priority. Presented at 79th Annual Meeting of the Transportation Research Board, Washington, D.C., 2000.
8. Balke, K., C. Dudek, and T. Urbanik. Development and Evaluation of Intelligent Bus Priority Concept. In *Transportation Research Record 1727*, TRB, National Research Council, Washington, D.C., 2000, pp. 12-19.
9. Gardner System. *Improved Traffic Signal Priority for Transit*. Interim Report, TCRP A-16, FTA, U.S. Department of Transportation, Washington, D.C., 1998.
10. Ova, K and A. Smadi. Evaluation of Transit Signal Priority Strategies for Small-Medium Cities. Presented at 82nd Annual Meeting of the Transportation Research Board, Washington, D.C., 2001.

11. Niittymaki, J. and M. Maenpaa. The Role of Fuzzy Logic Public Transportation Priority in Traffic Signal Control. *Traffic Engineering and Control*, Vol. 42, No. 1, January 2001, pp. 22-26.
12. Mirchandani, P., H. Larry, A. Knyazyan, and W. Wu. An Approach Towards The Integration of Bus Priority and Traffic Adaptive Signal Control. Presented at 80th Annual Meeting of the Transportation Research Board, Washington, D.C., 2001.
13. Newell, G. F. The Rolling Horizon Scheme of Traffic Signal Control. *Transportation Research*, Vol. 32A, No. 1, 1998, pp. 39-44.
14. Yagar, S. Efficient Transit Priority at Intersections. In *Transportation Research Record 1390*, TRB, National Research Council, Washington, D.C., 1994, pp.10-15.
15. Yagar, S. and B. Han. A Procedure for Real-Time Signal Control That Considers Transit Interference and Priority. *Transportation Research*, Vol. 28B, No.4, 1993, pp. 315-331.
16. Conrad, M., F. Dion, and S. Yagar. Real-Time Traffic Signal Optimization with Transit Priority. In *Transportation Research Record 1634*, TRB, National Research Council, Washington, D.C., 1998, pp. 100-109.
17. Dion, F. and B. Hellinga. A Rule-Based Real-Time Traffic Responsive Signal Control System with Transit Priority: application to an Isolated Intersection. *Transportation Research*. Vol. 36B, No. 1, 2002, pp. 325-343.
18. Chang, G., M. Vasudevan, and C. Su. Bus-Preemption under Adaptive Signal Control Environments. In *Transportation Research Record 1494*, TRB, National Research Council, Washington, D.C., 1995, pp.146-154.
19. Chang, G., M. Vasudevan, and C. Su. Modeling and Evaluation of Adaptive Bus-Preemption Control with and without Automatic Vehicle Location Systems. *Transportation Research*, Vol. 30A, No.4, 1996, pp. 251-268.
20. Vasudevan, M. and G. Chang. Design Framework for Integrating Real-Time Bus Priority Control with Robust Arterial Signal Progression. Presented at 80th Annual Meeting of the Transportation Research Board, Washington, D.C., 2001.
21. Lin, G. S., P. Liang, P. Schenfeld, and R. Larson. *Adaptive Control of Transit Operation*. Report MD-26-7002, FTA, U.S. Department of Transportation, Washington, DC, 1995.
22. Wood, K. and R. T. Baker. Using SCOOT Weightings to Benefit Strategic Routes. *Traffic Engineering and Control*. Vol. 33, No 4, 1992, pp. 226-235.

23. Robertson, D. I. and R. D. Bretherton. Optimizing Networks of Traffic Signals in Real-Time: The SCOOT Method. *IEEE Transactions on Vehicular Technology*, Vol. 40, No. 1, 1991, pp. 11-15.
24. Mauru, V. and D. Taranto. UTOPIA. *Proceedings of 6th IFAC-IFIP-IFORS Symposium on Control Computers and Communications in Transportation*, Oxford, UK, 1990, pp. 245-252.
25. Henry, J. J., and J. L. Farges. PT Priority and PRODYN, *Proceedings of the First World Congress on Applications of Transport Telematics and Intelligent Vehicle Highway Systems*, Vol. 6, Paris, France, 1994, pp. 3086-3096.
26. Cornwell, P. R., J. T. K. Luk, and B. J. Negus. Tram Priority in SCATS. *Traffic Engineering and Control*. Vol. 27, No. 11, 1986, pp. 561-565.
27. Duerr, P. A. Dynamic Right-of-Way for Transit Vehicles: An Integrated Modeling Approach for Optimizing Signal Control on Mixed Traffic Arterials. In *Transportation Research Record 1731*, TRB, National Research Council, Washington, D.C., 2000, pp.31-39.
28. Ngan, V. A Comprehensive Strategy for Transit Signal Priority. *ITE Journal*, November 2003, pp. 28-32.
29. Balke, K. *Development and Laboratory Testing of an Intelligent Approach for Providing Priority to Buses at Traffic Signalized Intersection*. Ph.D. dissertation, Texas A&M University, College Station, Texas, 1998.
30. Koonce, P., J. Ringer, T. Urbanik, W. Rotich, and B. Kloos. Detection Range Setting Methodology for Signal Priority. *Journal of Public Transportation*, Vol. 5, No. 2, 2002, pp. 115-135.
31. Wadjas, Y., and P. Firth. Transit Signal Priority along an Arterial Using Advanced Detection. In *Transportation Research Record 1856*, TRB, National Research Council, Washington, D.C., 2003, pp.220-230.
32. Chada, S. and R. Newland. *Effectiveness of Bus Signal Priority Final Report*. National Center for Transit Research, University of South Florida, Tampa, Florida, 2002.
33. Bishop, C. *Transit Priority Traffic Control Systems: European Experience*. Canadian Urban Transit Association STRP Report 9-1, Toronto, Canada, 1994.

34. MacGowan, C. J. and I. J. Fullerton. Development and Testing of Advanced Control Strategies in the Urban Traffic Control System. *Public Roads*, Vol. 43, No. 3, Washington, D.C., 1979, pp. 97-105
35. Tarnoff, P. J. The Results of FHWA Urban Traffic Control Research: An Interim Report. *Traffic Engineering*, Vol. 45, No. 4, 1975, pp. 27-35.
36. Hu, K., S. Skehan, and R. Gephart. Implementation A Smart Transit Priority System for Metro Rapid Bus in Los Angeles. Presented at 80th Annual Meeting of the Transportation Research Board, Washington, D.C., 2001.
37. Kloos, W. C., A. R. Danaher, and K. M. Hunter-Zaworski. Bus Priority at Traffic Signals in Portland: The Powell Boulevard Pilot Project. In *1994 Compendium of Technical Papers*. Institute of Transportation Engineering, Washington, D.C., 1994.
38. King County Department of Transportation and City of Seattle Transportation. *Transit Signal Priority System Assessment Study: Rainier Avenue South Field Evaluation Draft Report*. Seattle, Washington, 2000.
39. Vahidi, H. Transit Signal Priority: A Comparison of Recent and Future Implementations. Presented at 70th Annual Meeting of Institute of Transportation Engineers, Nashville, Tennessee, 2000.
40. Cooper, B. R., R. A. Vincent, and K. Wood. Bus-Actuated Traffic Signals-Initial Assessment of Part of the Swansea Bus Priority Scheme. *TRRL Laboratory Report 925*, Transport and Road Research Laboratory, 1980, pp. 1-17.
41. Transportation Research Board, *Highway Capacity Manual*, National Research Council, Washington D.C., 2000.
42. Kraft, W. H. and H. Deutschman. Bus Passenger Service-Time Distributions. In *Transportation Research Record 625*, TRB, National Research Council, Washington, D.C., 1977, pp. 37-43.
43. Adamski, A., Probabilistic Model of Passenger Service Processes at Bus Stops. *Transportation Research*, Vol. 26B, No. 4, 1992, pp. 253-259.
44. Guenther, R. P. and K. Harmat. Transit Dwell Time Under Complex Fare Structure. *Journal of Transportation Engineering*, Vol. 114, No. 3, ASCE, 1988, pp.367-379.
45. Levinson, H. S. Analyzing Transit Travel Time Performance. In *Transportation Research Record 915*, TRB, National Research Council, Washington, D.C., 1983, pp. 1-6.

46. Maloney, M. and D. Boyle. Components of Travel Time on the Glendale Beeline Bus Network. In *Transportation Research Record 1666*, TRB, National Research Council, Washington, D.C., 1999, pp. 23-27.
47. Rajbhandari, R., S. Chien, and J. Daniel. Estimation of Bus Dwell Times with Automatic Passenger Counter Information. Presented at 82nd Annual Meeting of the Transportation Research Board, Washington, D.C., 2003.
48. Kraft, W. and T. Bergen. Evaluation of Passenger Service Times for Street Transit Systems. In *Transportation Research Board 505*, TRB, National Research Council, Washington, D.C., 1974, pp. 13-20.
49. Lin, T. M. and N. H. M. Wilson. Dwell Time Relationships for Light Rail Systems. In *Transportation Research Record 1361*, TRB, National Research Council, Washington, D.C., 1992, pp. 287-295.
50. Kimpel, T., J. Strathman, S. Callas, D. Griffin, and R. Gerhart. Automatic Passenger Counter Evaluation: Implications for National Transit Database Reporting. In *Transportation Research Record 1835*, TRB, National Research Council, Washington, D.C., 2003, pp. 109-119.
51. Dueker, K. J., T. J. Kimpel, and J. G. Strathman. Determinants of Bus Dwell Time. *Journal of Public Transportation*, Vol. 7, No. 1, 2004, pp. 21-40.
52. Bertini, R. L. and A. M. El-Geneidy. Modeling Transit Trip Time Using Archived Bus Dispatch System Data. *Journal of Transportation Engineering*, Vol. 130, No. 1, 2004, pp. 56-67.
53. Powell, W. and Y. Sheffi. A Probabilistic Model of Bus Route Performance. *Transportation Science*, Vol. 17, No. 4, 1983, pp. 376-404.
54. Chien, S. I., S. M. Chowdhury, K. C. Mouskos, and Y. Ding. Enhancements of CORSIM Model in Simulation Transit Operations. *Journal of Transportation Engineering*, Vol. 126, No. 5, 2000, pp. 396-404.
55. Chien, S. I., Y. Ding, and C. Wei. Dynamic Bus Arrival Time Prediction with Artificial Neural Networks. *Journal of Transportation Engineering*, Vol. 128, No. 5, 2002, pp. 429-438.
56. *VISSIM User's Manual, Version 3.7*. PTV Planung Transport Verkehr AG., Karlsruhe, Germany, January 2003.




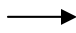




57. Guenther, R. P. and K. C. Shinha. Modeling Bus Delays due to Passenger Boardings and Alightings. In *Transportation Research Record 915*, TRB, National Research Council, Washington, D.C., 1983, pp. 7-13.
58. Kim, K. *Optimization Methodology for the Calibration of Transportation Network Micro-Simulation Models*. Ph.D. dissertation, Texas A&M University, College Station, 2002.
59. Kim, K. and L. R. Rilett. Genetic-Algorithm-Based Approach for Calibrating Microscopic Simulation Models. *Proceedings of IEEE Intelligent Transportation Systems*, Institute of Electrical and Electronics Engineers, Oakland, California, 2001, pp. 698–704
60. Schultz, G. and L. Rilett. An Analysis of the Distribution and Calibration of Car-Following Sensitivity Parameters in Microscopic Traffic Simulation Models. Presented at 83rd Annual Meeting of the Transportation Research Board, Washington, D.C., 2004.
61. Casella, G. and R. L. Berger, *Statistical Inference*. Duxbury Press, Pacific Grove, California, 1990.
62. Milton, J. S. and J. C. Arnold. *Introduction to Probability and Statistics: Principles and Applications for Engineering and the Computing Sciences*. 3rd ed. McGraw-Hill International Editions, New York, 1995.
63. Neter, J., M. H. Kutner, C. J. Nachtsheim, and W. Wasserman. *Applied Linear Statistical Models*. 4th ed. McGraw-Hill/Irwin, New York, 1996.
64. Carroll, R.J. and D. Ruppert. *Transformation and Weighting in Regression*. Chapman and Hall, New York, 1988.
65. *NIST/SEMATECH e-Handbook of Statistical Methods*, National Institute of Standards and Technology, 2004. Available: <http://www.itl.nist.gov/div898/>.
66. *Manual on Uniform Traffic Control Devices*. FHWA, U.S. Department of Transportation, Washington, D.C., 2003.
67. Cheu, R. L., X. Jin, K. C. Ng, Y. L. Ng, and D. Srinivasan. Calibration of FREESIM for Singapore Expressway Using Genetic Algorithm. *Journal of Transportation Engineering*, Vol. 124, No. 6, 1998, pp. 526-535.
68. Park, B., C. J. Messer, and T. Urbanik II. Enhanced Genetic Algorithm for Signal-Timing Optimization of Oversaturated Intersections. In *Transportation Research Record 1727*, TRB, National Research Council, Washington, D.C., 2000, pp. 32-41.

69. Yin, Y. Genetic-Algorithms-Based Approach for Bilevel Programming Models. *Journal of Transportation Engineering*, Vol. 126, No. 2, 2000, pp. 115-120.
70. Ma, T., and B. Abdulhai. Genetic Algorithm-Based Optimization Approach and Generic Tool for Calibrating Traffic Microscopic Simulation Parameters. In *Transportation Research Record 1800*, TRB, National Research Council, Washington, D.C., 2002, pp. 6-15.
71. Brockfeld, E., R. D. Kühne, and P. Wagner. Calibration and Validation of Microscopic Traffic Flow Models. Presented at 83rd Annual Meeting of the Transportation Research Board, Washington, D.C., 2004.
72. Park, B. and J. D. Schneeberger. Microscopic Simulation Model Calibration and Validation: A Case Study of VISSIM for a Coordinated Actuated Signal System. In *Transportation Research Record 1856*, TRB, National Research Council, Washington, D.C., 2003, pp. 185-192.
73. Devore, J. L. *Probability and Statistics for Engineering and the Sciences*, 4th ed. Duxbury Press, Pacific Grove, California, 1995.
74. Goldberg, D. E. *Genetic Algorithms in Search*. Addison-Wesley, Reading, Massachusetts, 1989.
75. Chambers, L. *Practical Handbook of Genetic Algorithms: Applications*, Volume I. CRC Press. Boca Raton, Florida, 1995.
76. Sheskin, D. J. *The Handbook of Parametric and Nonparametric Statistical Procedures*, 2nd ed. Chapman & Hall/CRC, New York, 2000.
77. Wiedemann, R. and U. Reiter. *Microscopic Traffic Simulation: The Simulation System MISSION, Background and Actual State*. CEC Project ICARUS (V1052), Final Report, Vol. 2, CEC, Brussels, Belgium, 1992.
78. Fellendorf, M. VISSIM: A Microscopic Simulation Tool to Evaluate Actuated Signal Control Including Bus Priority. Presented at 64th Annual Meeting of the Institute of Transportation Engineers, Dallas, 1994.
79. Brackstone, M. and M. McDonald. Car-Following: A Historical Review. *Transportation Research* Vol. 2F, No. 4, 1999, pp. 181-196.
80. Fritzsche, H., A Model for Traffic Simulation. *Traffic Engineering and Control*. Vol. 35, No. 5, 1994, pp. 317-321.

**APPENDIX A**

**SIGNAL CONTROL VARIABLES**

**Table A-1 Signal control variables at the intersection of Bintiff and Bellaire**

Movement	WB LT 	EB TH 	SB TH 	EB LT 	WB TH 	NB TH 
Phase	$\phi 1$	$\phi 2$	$\phi 4$	$\phi 5$	$\phi 6$	$\phi 8$
Minimum Green	5	25	10	5	25	10
Passage time	2.5	3.0	2.5	2.5	3.0	2.5
Yellow Change	3.6	3.6	3.2	3.6	3.6	3.2
Red Clearance	1.2	1.2	2.8	1.2	1.2	2.8
Split <sup>1</sup>	15	80	25	25	70	25
Minimum Recall <sup>2</sup>		x			x	
Hold <sup>3</sup>		x			x	
Variable Yield <sup>4</sup>		x			x	

Note:

Cycle length : 120

Offset value : 115

Variable yield : 10

(Variable yield defines the size of the permissive window during which the coordinated phases may terminate.)

<sup>1</sup> Coordination splits include the yellow and all red intervals


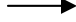


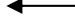

<sup>2</sup> Continuous phase call (phase can not be skipped)

<sup>3</sup> hold until minimum split

<sup>4</sup> with hold defines coordinated phase

Note: all values in table are expressed in seconds.

**Table A-2 Signal control variables at the intersection of Rookin and Bellaire**

Movement	WB LT 	EB TH 	SB TH 	EB LT 	WB TH 	NB TH 
Phase	$\phi 1$	$\phi 2$	$\phi 4$	$\phi 5$	$\phi 6$	$\phi 8$
Minimum Green	10	25	10	10	25	10
Passage time	2.5	3.0	2.5	2.5	3.0	2.5
Yellow Change	3.6	3.6	3.2	3.6	3.6	3.2
Red Clearance	1.2	1.2	2.7	1.2	1.2	2.7
Split <sup>1</sup>	20	67	33	20	67	33
Minimum Recall <sup>2</sup>		x			x	
Hold <sup>3</sup>		x			x	
Variable Yield <sup>4</sup>		x			x	

Note:

Cycle length : 120

Offset value : 45

Variable yield : 10

(Variable yield defines the size of the permissive window during which the coordinated phases may terminate.)

<sup>1</sup> Coordination splits include the yellow and all red intervals









<sup>2</sup> Continuous phase call (phase can not be skipped)

<sup>3</sup> hold until minimum split

<sup>4</sup> with hold defines coordinated phase

Note: all values in table are expressed in seconds.

**Table A-3 Signal control variables at the intersection of Hilcroft and Bellaire**

Movement	WB LT 	EB TH 	NB LT 	SB TH 	EB LT 	WB TH 	SB LT 	NB TH 
Phase	$\phi 1$	$\phi 2$	$\phi 3$	$\phi 4$	$\phi 5$	$\phi 6$	$\phi 7$	$\phi 8$
Minimum Green	1	1	0	1	1	1	0	1
Maximum Green	26	80	15	28	18	80	16	28
Passage time	0.5	3.0	0.5	2.5	0.5	3.0	0.5	2.5
Yellow Change	3.6	3.6	3.6	3.6	3.6	3.6	3.6	3.6
Red Clearance	1.7	1.7	2.2	2.2	1.7	1.7	2.2	2.2
Split <sup>1</sup>	27	41	22	28	30	40	19	31
Minimum Recall <sup>2</sup>		x				x		
Hold <sup>3</sup>		x				x		
Variable Yield <sup>4</sup>		x				x		

Note:

Cycle length : 120

Offset value : 75

Variable yield : 10

(Variable yield defines the size of the permissive window during which the coordinated phases may terminate.)

<sup>1</sup> Coordination splits include the yellow and all red intervals

<sup>2</sup> Continuous phase call (phase can not be skipped)

<sup>3</sup> hold until minimum split

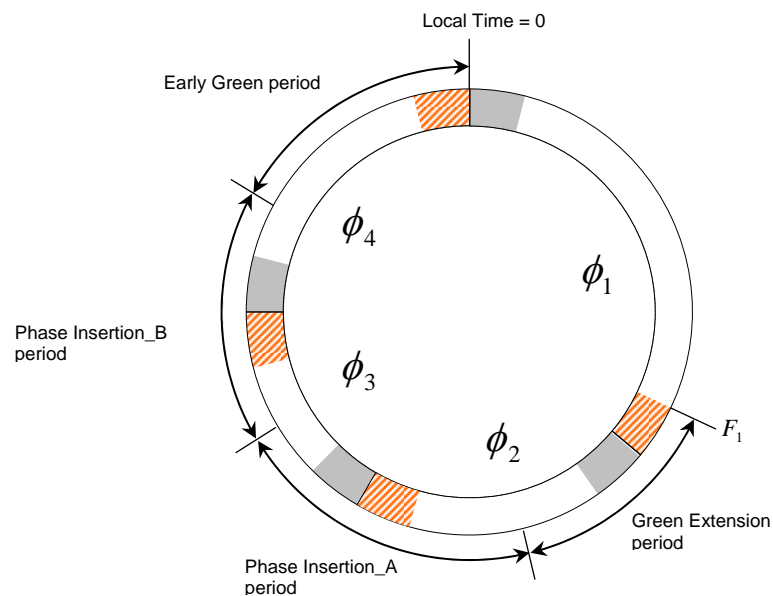
<sup>4</sup> with hold defines coordinated phase

Note: all values in table are expressed in seconds.

**APPENDIX B**

**BUS SIGNAL PRIORITY STRATEGY FOR CONSIDERATION OF  
AVERAGE DWELL TIME AT THE NEAR SIDE BUS STOPS**

In the BSP1 algorithm, dwell time will be incorporated in BSP timing plan through adding an average dwell time in calculating bus arrival time at the stop line (i.e. bus travel time from check-in detector to stop line). Once a bus has been detected at check-in detector, the algorithm assesses whether a priority service is granted through evaluating pre-defined criteria (i.e. number of passengers on the bus). If the bus satisfies the criterion, an adequate priority is implemented depending on when in the cycle the bus arrives at the intersection. The strategies used to provide priority include green extension, early green, and phase insertion strategy. Based on the bus arrival time in the cycle, multiple strategies possibly can be used to service the bus. The algorithm examines which strategy can accommodate the approaching bus with a minimum change in the background signal plan. The traffic signal cycle can be divided into regions that define where the different strategies can be used to service arriving buses. In order to simplify the strategy selection procedure, the regions were defined not to overlap each others. At any specific time point in the cycle, only one strategy is available to be implemented. Figure B-1 shows the periods of each of the strategies in a four-phase traffic signal.



**Figure B-1** Periods in the cycle for selecting different priority strategies



Each region for strategy selection determined as follows.

*Green extension strategy*

When a bus is expected to arrive at the intersection just after the end of the green time on the main-street, the normal end points of the main-street green is extended. The lower bound of the green extension strategy is the normal force-off point for the main-street phase. Buses predicted to arrive before this time in the cycle are serviced during the normal main-street phase so no priority service is required. The amount of extended green is determined by the variable green time in phase 2 as shown in Figure B-2a. The other non-priority phases (i.e. phase 3 and 4) are not reduced to minimize the change of phase durations. Therefore, the upper bound for the green extension strategy is defined by Equation B-1.

$$\pi = F_2 - R_2 - I_1 \quad (\text{B-1})$$

*Phase Insertion\_A strategy*

If any bus is expected to arrive at the stop line during the mid of red phase for its approach, a special bus phase is provided between non-priority phases. A special bus phase between phase 2 and 3 (referred here phase insertion\_A strategy) is provided when a bus is predicted to arrive after the upper bound of the green extension strategy but no later than the force-off point of phase 3. A range for phase insertion\_A strategy was illustrated in Figure B-2b. The lower bound for phase insertion\_A strategy was the same point in the cycle to the upper bound of the green extension strategy. The upper bound was determined by the variable green time in phase 3. This point can be obtained by subtracting minimum green time from force-off point of phase 3.

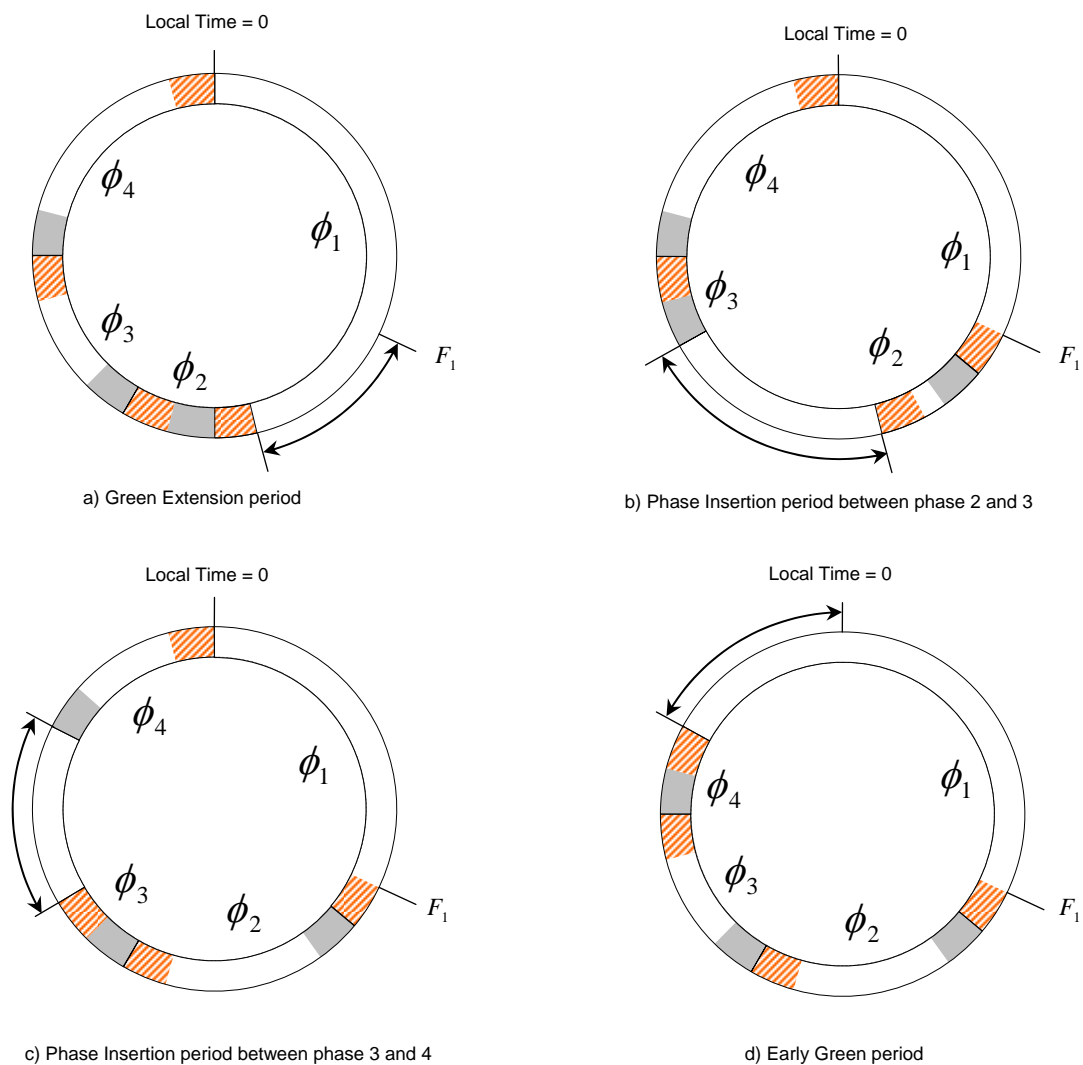
*Phase Insertion\_B strategy*

The range for phase insertion between phase 3 and 4 (phase insertion\_B) starts at the end of phase 3 that fulfills only its minimum green and change interval. Therefore the lower bound can be obtained by adding minimum requirement of phase 3 and change interval

of phase 2 to force-off point of phase 2. The upper bound was the lower bound for the early green strategy.

### *Early green strategy*

The lower bound of the early green strategy is immediately after phase 4 has provided its minimum green time and change interval. This point in the cycle can be obtained by adding minimum requirement of phase 4 and change interval of phase 3 to force-off point of phase 3.



**Figure B-2 Determination of Bounds for Implementing Each Priority Strategy**

## **APPENDIX C**

### **ESTIMATING PASSENGER ARRIVALS USING NEGATIVE BINOMIAL DISTRIBUTION**

Let the random variable  $X$  denote the number of passenger arrivals with parameter  $r$  and  $p$ .

$$P[X = x|r, p] = \binom{x+r-1}{r-1} p^r (1-p)^x \quad (\text{C-1})$$

$$\mu = \frac{r(1-p)}{p} \quad (\text{C-2})$$

$$s^2 = \frac{r(1-p)}{p^2} \quad (\text{C-3})$$

where

$X$  = number of passenger arrival,

$r$  = number of success, and

$p$  = probability of success.

$\mu$  = sample mean

$s^2$  = sample variance

From Equation C-3, the parameters  $p$  can be derived as follows:

$$p = \frac{\mu}{s^2} \quad (\text{C-4})$$

The parameter  $r$  can be defined from Equation C-2 and C-4.

$$r = \frac{\mu^2}{s^2 - \mu} \quad (\text{C-5})$$

With headway of 5 minutes, one can expect that the number of passengers waiting for bus is equal to the mean. For the situation where the headway is not greater or less than 5 minutes, the expectation of number of passengers can also be obtained from the negative binomial distribution.

Let  $X_1$  and  $X_2$  are Negative Binomial random variables with parameters  $p_1$ ,  $r_1$  and  $p_2$ ,  $r_2$ . As shown Equation C-4, parameter  $p$  indicates the relationship between mean and variance. If this relationship is assumed constant for each data set, the random variables can be written as follows:

$$\begin{aligned} X_1 &\sim N.B.(r_1, p) \\ X_2 &\sim N.B.(r_2, p) \end{aligned} \tag{C-6}$$

The expectation of random variable  $X_1 + X_2$  can be expressed through the Moment Generation Function (MGF). Let  $X_1 + X_2$  be a negative binomial random variable. The MGF of negative binomial random variable  $X$  is shown in Equation C-7.

$$m_X(t) = E(e^{tX}) = \frac{(pe^t)^r}{(1-qe^t)^r} \tag{C-7}$$

Then, MGF for  $X_1 + X_2$  is given by

$$m_{X_1+X_2}(t) = E(e^{tX_1+tX_2}) = E(e^{tX_1} e^{tX_2}) \tag{C-8}$$

$$= \frac{(pe^t)^{r_1}}{(1-qe^t)^{r_1}} \cdot \frac{(pe^t)^{r_2}}{(1-qe^t)^{r_2}} = \frac{(pe^t)^{(r_1+r_2)}}{(1-qe^t)^{(r_1+r_2)}} \tag{C-9}$$

It can be concluded that  $X_1 + X_2$  is a negative binomial random variable with parameters  $r_1 + r_2$  and  $p$ .

$$X_1 + X_2 \sim N.B.(r_1 + r_2, p) \tag{C-10}$$

The expectation of random  $X_1 + X_2$  can be estimated from means of random variables  $X_1$  and  $X_2$  as follows:

$$\mu_{x_1+x_2} = (r_1 + r_2) \frac{(1-p)}{p} = r_1 \frac{(1-p)}{p} + r_2 \frac{(1-p)}{p} = \mu_{x_1} + \mu_{x_2} \quad (\text{C-11})$$

Like Poisson distribution, the number of passengers waiting bus at stop with  $\Delta t$  headway can be simplified as follows:

$$\text{passengers waiting at stop} = \mu \cdot (\text{departure time of bus } v - 1 - \text{arrival time of bus } v) \quad (\text{C-12})$$

**APPENDIX D**

**ANALYSIS OF BUS DWELL TIME FOR STOP B AND STOP C**

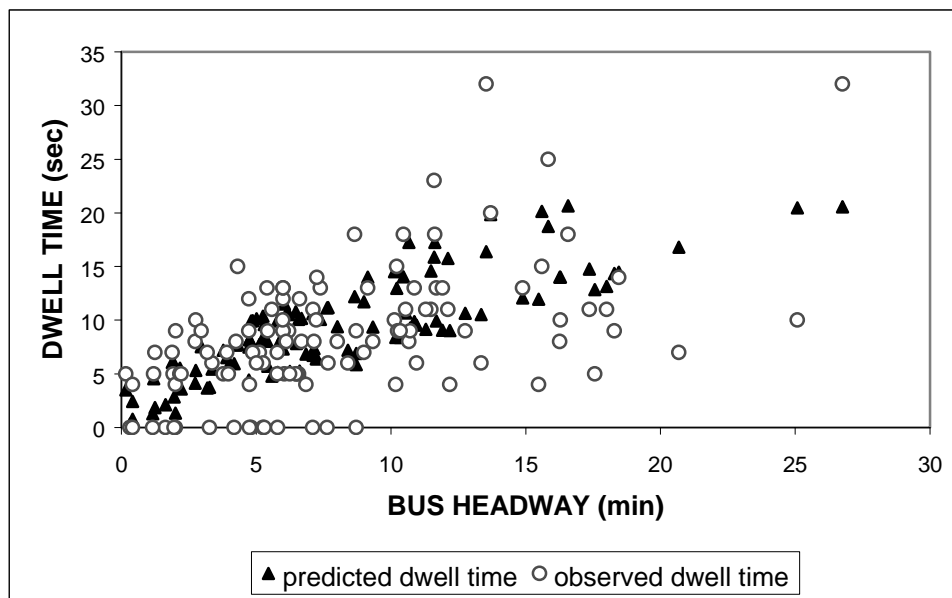


Figure D-1 Predicted and observed dwell time at stop B

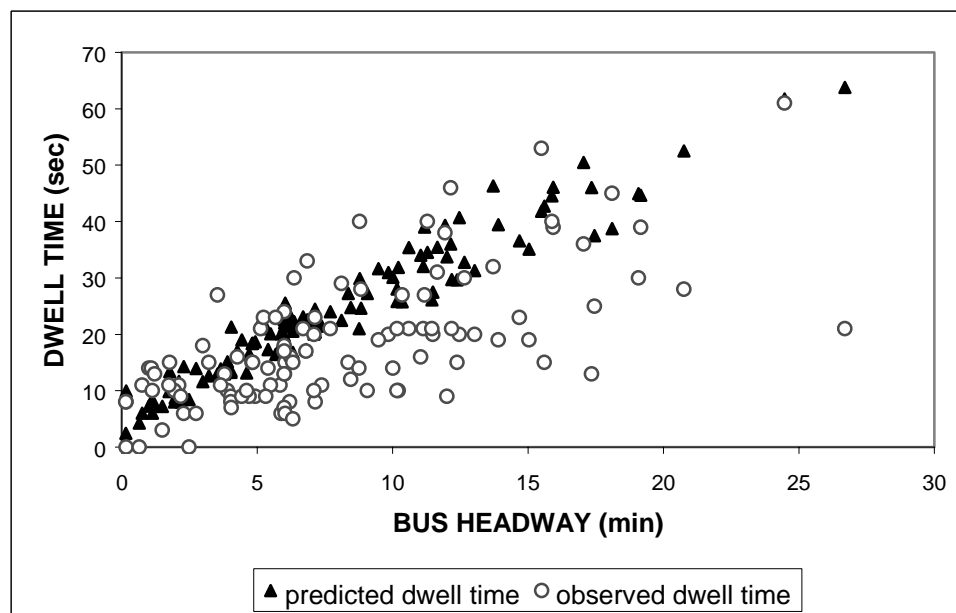


Figure D-2 Predicted and observed dwell time at stop C



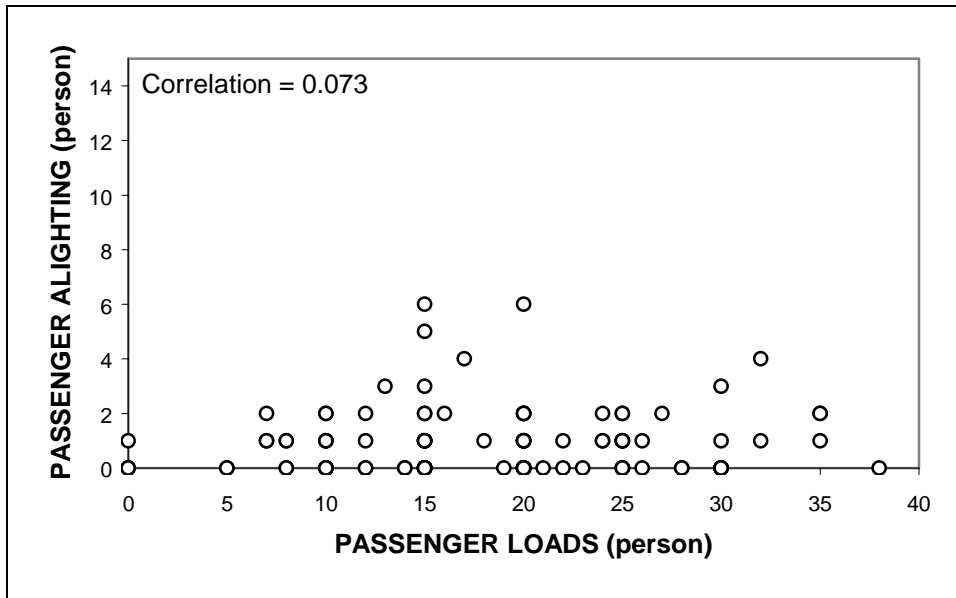


Figure D-3 Relationship between passenger alighting and passenger loads at stop B

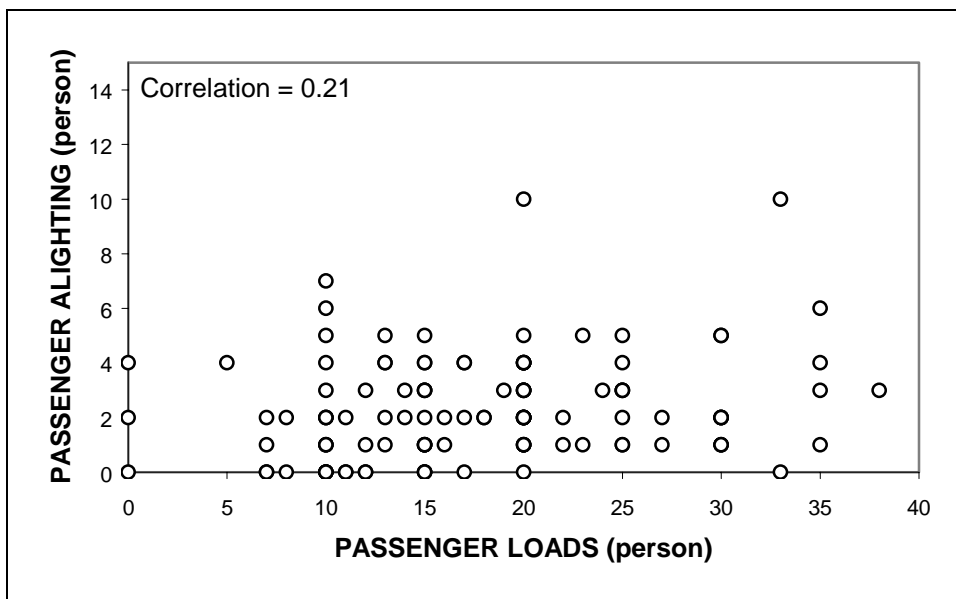


Figure D-4 Relationship between passenger alighting and passenger loads at stop C

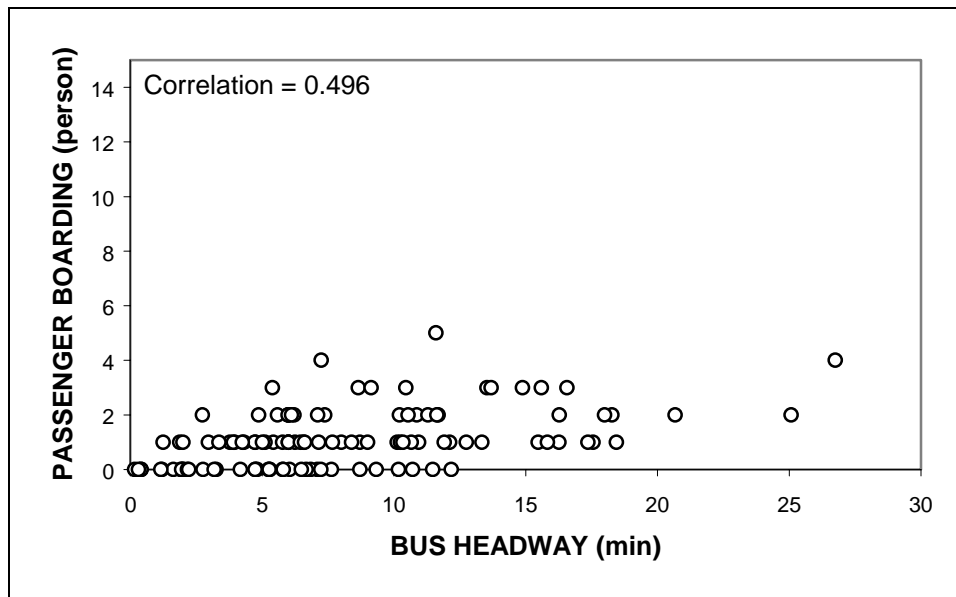


Figure D-5 Relationship between passenger boarding and bus headway at stop B

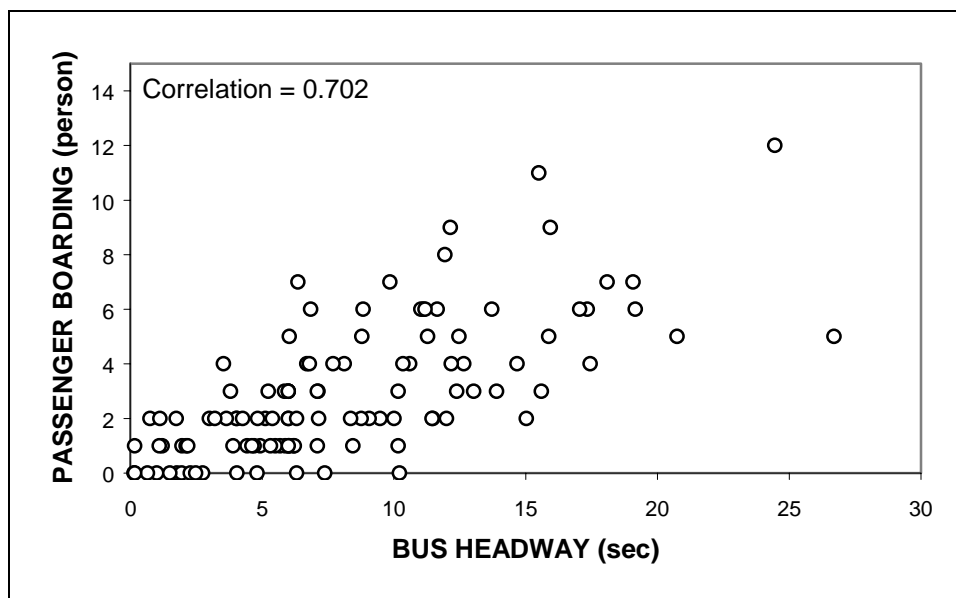


Figure D-6 Relationship between passenger boarding and bus headway at stop C

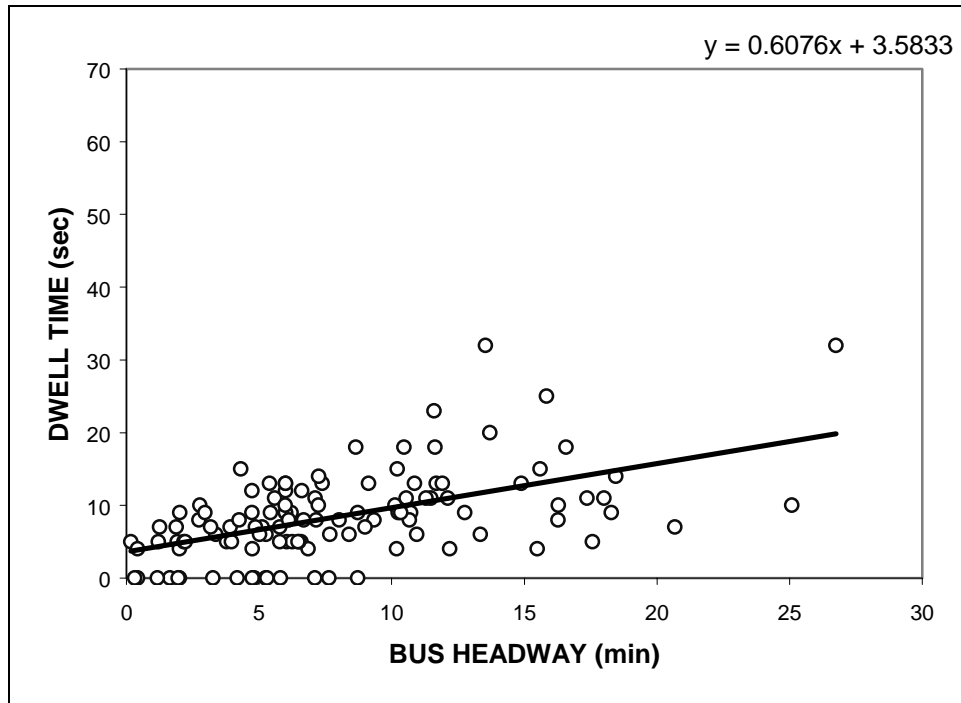


Figure D-7 Estimated regression line at stop B

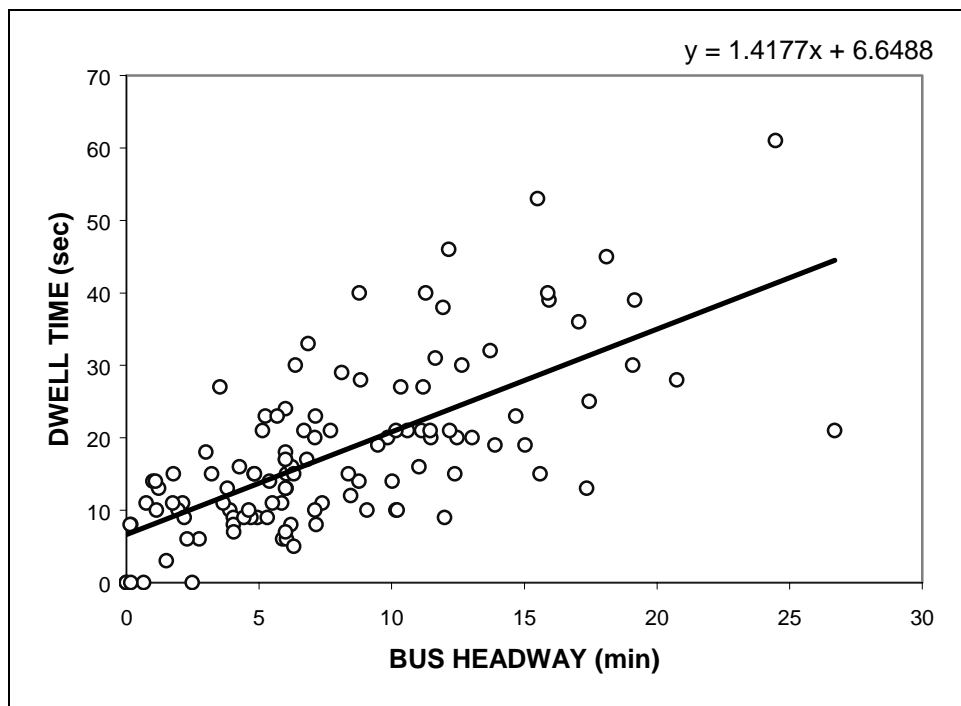


Figure D-8 Estimated regression line at stop C

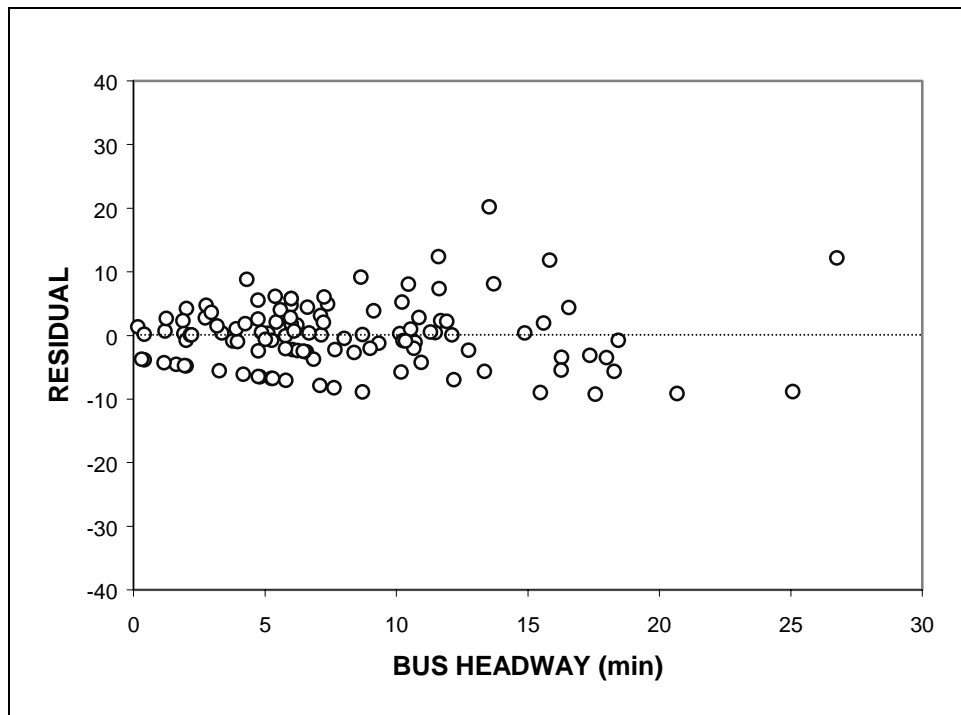


Figure D-9 Residual plot of the regression model for stop B

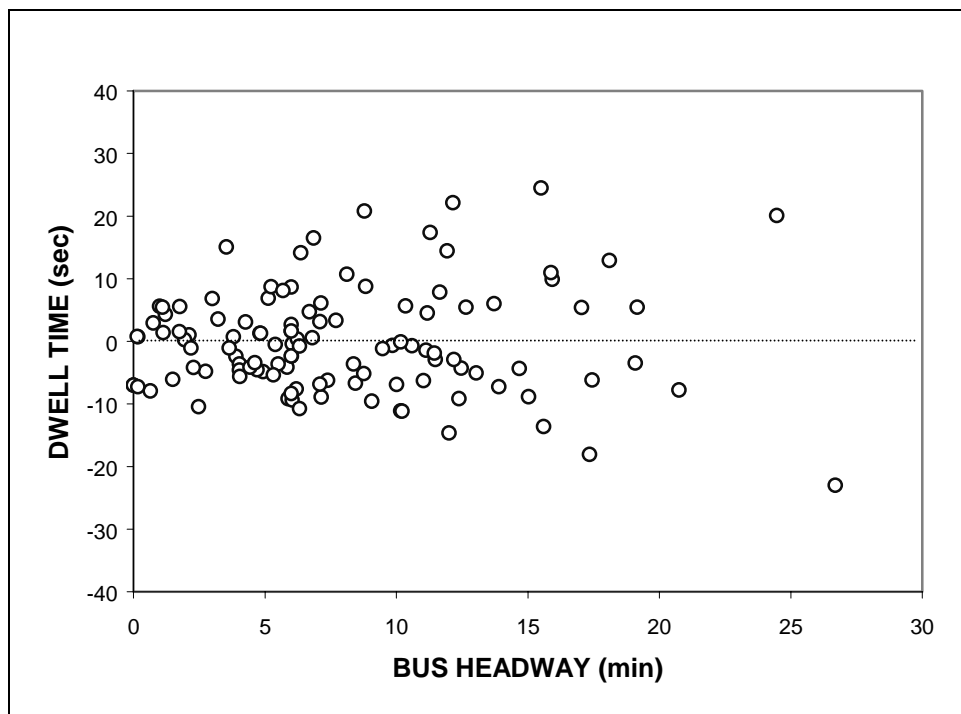


Figure D-10 Residual plot of the regression model for stop C

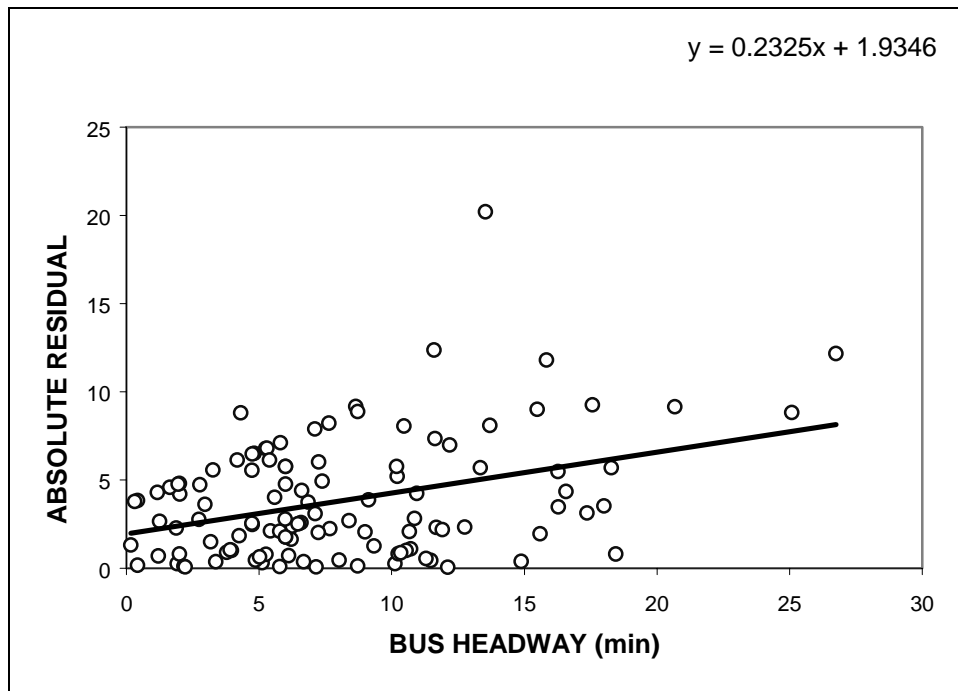


Figure D-11 Absolute residual plot and regression line for stop B

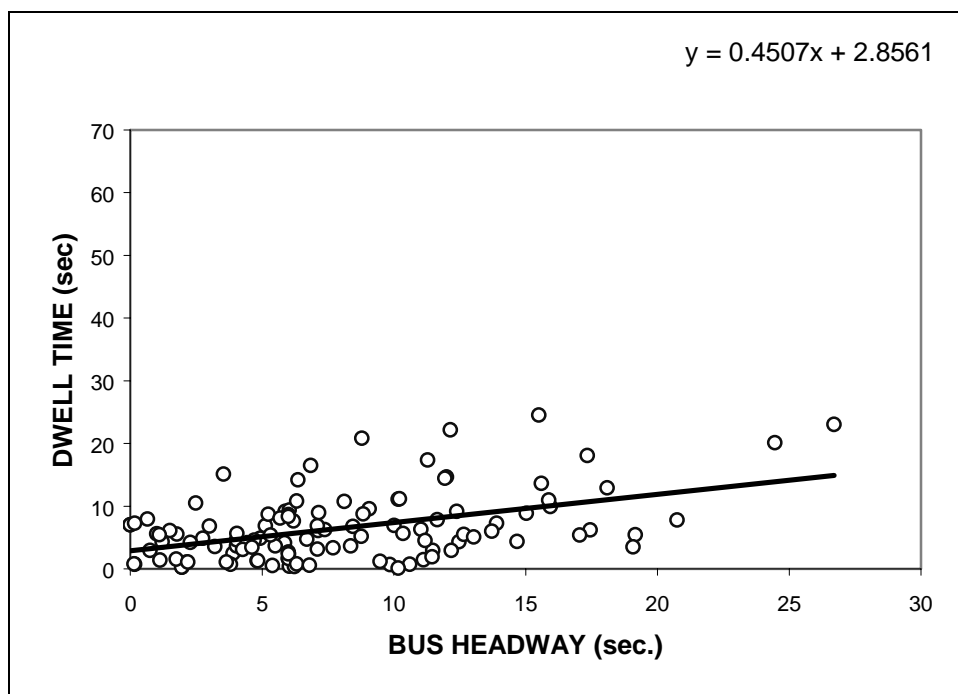


Figure D-12 Absolute residual plot and regression line for stop C

WLS regression function for stop B was obtained:

$$\hat{Y} = 3.051 + 0.681h \quad (\text{D-1})$$

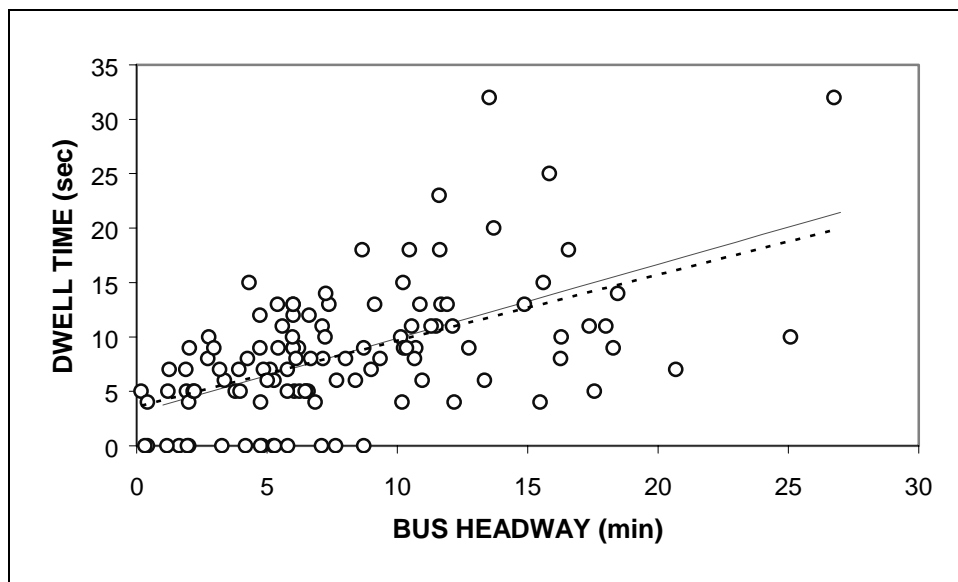


Figure D-13 Estimated weighted and unweighted lines for stop B

WLS regression function for stop C was obtained:

$$\hat{Y} = 5.808 + 1.54h \quad (\text{D-2})$$

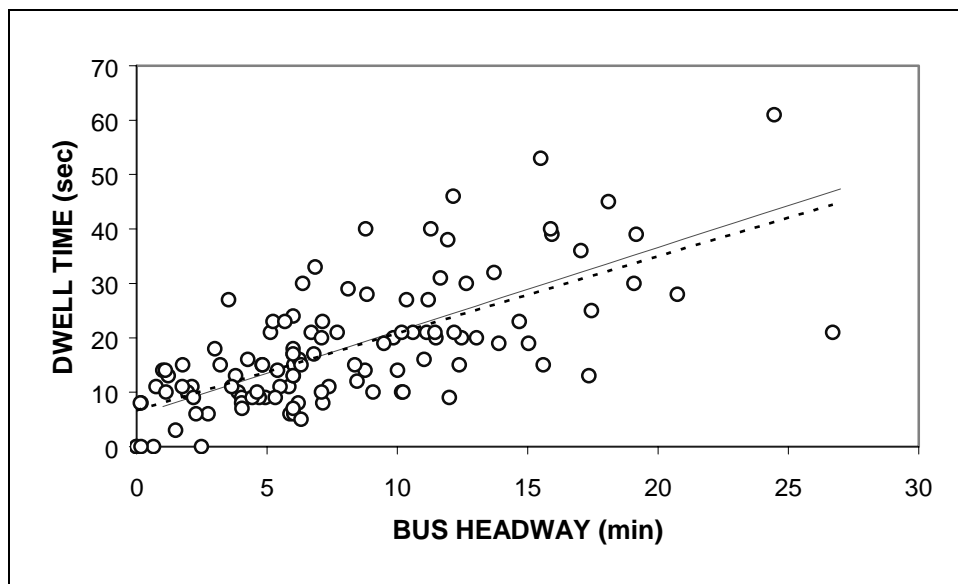


Figure D-14 Estimated weighted and unweighted lines for stop C

## VITA

### WONHO KIM

University of Nebraska at Lincoln  
Mid-America Transportation Center  
W337 Nebraska Hall  
Lincoln, NE 68588

#### Education

Ph.D., Civil Engineering, Texas A&M University, December 2004  
M.C.P., City Planning, Seoul National University, February 1997  
B.S., Urban Engineering, ChungBuk National University, February 1995

#### Academic Awards

Rotary Foundation Ambassadorial Scholarship, Rotary International, 1998-1999  
Study Abroad Scholarship, ChungBuk National University Foundation, 1998

#### Research Experience

Graduate Student Researcher, Texas Transportation Institute, June 1999 to August 2004  
Researcher, Seoul Development Institute, September 1996 - June 1998

#### Publications/Presentations

- Kim, S., W. Kim, and L. R. Rilett. Calibration of Micro-Simulation Models Using Non-Parametric Statistical Techniques. In *Transportation Research Record*, Washington, D.C., 2004, in press.
- Kim, W. and R. Rilett. New Bus Signal Priority System for Networks with Near-side Bus Stops. In *Transportation Research Record*, Washington, D.C., 2004, submitted.
- Kim, W. and K. Kim. A Study on Passenger's Time Saving Effects by Introducing Express Subway Systems. *Proceedings of Korean Society for Railway*, Seoul, Korea, 1998, pp.
- Kim, K., K. Son, J. Ko, and W. Kim. *A Study on Efficient Inter-Modal Connection Methods in Transportation System*. SDI 98-R-08, Seoul Development Institute, Seoul, Korea, 1998.
- Kim, W. and K. Kim. A Development of a Traffic Assignment Model: Reflecting the Effect of Signal Progression. *Proceedings of the 4th Annual World Congress on Intelligent Transport System*, Berlin, Germany, 1997.
- Kim, K., K. Son, W. Kim, and M. Park. *A Study on Integrated Development of Railroads in Seoul*. SDI 97-R-14-1, Seoul Development Institute, Seoul, Korea, 1997.